Experimental Design, Monitoring, and Assessment of Bioretention Systems for Urban Stormwater Management

Nailah Altuwairgi

THIS THESIS IS SUBMITTED IN PARTIAL FULFILMENT OF THE REQUIREMENTS FOR THE DEGREE OF DOCTOR OF PHILOSOPHY (PhD) IN ENGINEERING

Cardiff University

February 2025

Acknowledgements

I would like to begin by expressing my deepest gratitude to my supervisors, Prof Reza Ahmadian and Prof Devin Sapsford, for their invaluable guidance and continuous support throughout my PhD studies.

This research was funded by the Saudi Ministry of Education and made possible through the support of Cardiff Council, who granted permission to conduct field assessments on bioretention sites.

I am also sincerely grateful to the lab technicians at the School of Engineering for their assistance in generating the empirical evidence that formed the foundation of this project. In particular, I extend my thanks to Mr. Jeffery Rowlands for his expertise in chemical analysis, his assistance in processing large quantities of samples, and for providing essential laboratory training. I am also thankful to Ms. Amanda Kitching and Mr. Gary Shipley for their technical guidance in laboratory procedures. Additionally, I would like to thank Mr. Steven Rankmore for his construction of the SuDS lab, and assistance with fieldwork.

I extend my appreciation to the Postgraduate Research Office, Doctoral Academy, and Student Wellbeing for providing helpful guidance and resources throughout my studies. A special thanks to Ms. Aderyn Reid and Ms. Nikki Brough for their unwavering support, prompt responses to my queries, and invaluable assistance in navigating challenges, which made my PhD journey much smoother.

I am also grateful to my friends and colleagues at Cardiff University for lending specialised equipment, their expert advice, and words of encouragement throughout my studies, particularly Dr Hossein Amini, Mr. Raymond Ariho, Dr Fei Jin, Dr Pallavee Srivastava, Dr Yaowen Xu, Dr Arif Mohammad, Dr Evan Ricketts, Dr Eqbal Alenezi, Dr Man Lam, Dr Michael Harbottle, Dr Riccardo Maddalena, and Dr Duncan Muir.

Finally, I would like to express my heartfelt appreciation to my family and friends for their unwavering support and encouragement, especially during difficult times. Without them, this work would not have been possible.

Abstract

Climate change and urbanisation exacerbate urban flooding and stormwater pollution, causing significant environmental and socio-economic impacts. Bioretention systems provide decentralised solutions to these challenges; however, their effectiveness and longevity are dependent on optimised design and proactive maintenance, both of which are hindered by a lack of performance and monitoring data, particularly in a UK context. This research provides the first empirical evidence to support the design of UK-specific bioretention configurations through performance evaluation, and to inform maintenance strategies through the analysis of contaminant accumulation.

The research comprised integrated laboratory and field studies. A series of column experiments was conducted in this study to evaluate the influence of two key design variables: vegetation and biochar amendments, on bioretention performance under simulated rainfall conditions representative of Cardiff, UK, with accelerated heavy metal loading. All designs consistently achieved high removal efficiencies (80-99%) for suspended solids and heavy metals. In contrast, phosphorus removal was more variable, ranging from 53% removal to significant net leaching, depending on the specific design configuration. Vegetation was critical for sustaining hydraulic function, effectively preventing clogging observed in non-vegetated systems, while providing secondary treatment benefits. Performance was species-dependent, with *Carex pendula* identified as the most effective for combined treatment and hydraulic performance. Biochar amendments, while beneficial for dissolved zinc removal, reduced suspended solids and particulate lead retention and were a net source of dissolved phosphorus, leaching up to 1.36 mg/L. The results emphasise that biochar amendments must be selectively optimised and validated for specific stormwater treatment objectives.

Analysis of filter media profiles revealed that, the majority of heavy metals were captured in the top 0-3 cm layer, reaching potentially toxic concentrations. The investigation into heavy metal accumulation was further advanced through a field-scale study at two established bioretention sites in Cardiff. Traditional sampling and portable X-ray fluorescence (pXRF) were employed to map the spatial distribution of heavy metals and identify contamination hotspots. Concentrations in the surface layer (0-3 cm) ranged as follows: Cu: 15-69, Pb: 18-340, Zn: 69-583, and Cr: 13-95 mg/kg, with accumulation levels increasing with system age and decreasing with depth. While most metal concentrations fell well below screening levels, centralised inlets created hotspots approaching these limits for Pb and Cr. Therefore, prioritising diffuse inlets in design to promote a more uniform distribution, complemented by pXRF monitoring, enables targeted maintenance to keep all concentrations below screening levels indefinitely.

Table of Contents

List of Figures

List of Tables

Chapter 1. Introduction

1.1 Urban stormwater challenges

Urbanisation and climate change are two interconnected factors significantly exacerbating urban flooding and straining stormwater management systems (Eckart et al. 2017). Urbanisation increases the area of impermeable surfaces, such as paved roads and rooftops, which alters natural hydrological processes (Pitt et al. 1999; Berndtsson 2010). In urbanised catchments, the presence of smooth, impermeable land surfaces increases peak runoff flow rates by 30% to over 100% compared to non-urbanised catchments (Jacobson 2011). This alteration in runoff volume stresses existing stormwater infrastructure beyond its design capacity, and heightens the risk of sewer flooding, as overloaded systems may discharge wastewater through Combined Sewer Overflows (CSOs), and degrades water quality, as accelerated urban runoff scours and mobilises pollutants from urban surfaces, transporting rapidly into receiving lands and water bodies with minimal natural attenuation (Pitt et al. 1999; Berndtsson 2010; Zhou 2014).

Climate change further intensifies these challenges by increasing the frequency and severity of precipitation events. This creates a dual pressure on urban water systems: impervious surfaces amplify runoff volumes and speeds, while extreme weather events deliver larger quantities of water in shorter timeframes (Miller and Hutchins 2017; Lashford et al. 2019). Studies indicate that design rainfall intensities could increase by 20% to 80% depending on the region, posing significant challenges to drainage systems designed for historical climate conditions (Zhou 2014).

Urban development often encroaches on floodplains and natural drainage systems, replacing them with grey infrastructure such as curbs, gutters, and sewers to rapidly convey water away from urban areas. While these systems aim to mitigate flood risks, they are increasingly inadequate in handling the growing pressures of urbanisation, population growth, and climate change (Eckart et al. 2017; Lashford et al. 2019). For instance, in the UK, the winter storms of 2013-2014 and 2015-2016, caused widespread flooding resulted in damages exceeding £5 billion (Miller and Hutchins 2017; Lashford et al. 2019).

Major UK cities, including London, Cardiff, and Edinburgh, have experienced significant pluvial and fluvial flooding in recent years, with over 5.5 million properties currently at risk of flooding in the future (Environment Agency 2024).

Urban stormwater runoff is also a significant conveyer of diffuse pollution, including heavy metals, nutrients, hydrocarbons, and microplastics, which pose substantial risks to the natural environment (Pitt et al. 1999; Berndtsson 2010; Zhou 2014). These pollutants—often originating from urban, industrial, and agricultural activities—accumulate on impermeable surfaces and are transported into water systems during rainfall events (Pitt et al. 1999; Nyenje et al. 2010).

While climate change is a critical factor influencing water quality, broader global changes, such as land use evolution, deforestation, urban expansion, and surface waterproofing, also play significant roles in deteriorating water quality (Delpla et al. 2009). Human activities remain a primary driver of water pollution, with urban and agricultural runoff being major sources of diffuse pollution (Lamprea and Ruban 2011; Hwang et al. 2016; Yang and Toor 2017). Climate change exacerbates these challenges by altering key determinants of water quality, such as ambient air temperature and the frequency of extreme hydrological events (Delpla et al. 2009).

These interconnected issues highlight the complexity of managing urban stormwater in the face of both anthropogenic and climatic pressures. With the urban population in developed countries projected to increase from 75% in 2000 to 83% by 2030 (Jacobson 2011), and the escalating impacts of climate change, sustainable water management solutions are essential for socio-economic growth (Lashford et al. 2019). Current drainage systems are increasingly overwhelmed, leading to more frequent and severe urban flooding, particularly in densely populated areas. (Eckart et al. 2017). Future drainage designs must account for these changes to mitigate the risks of system overloading and maintain acceptable performance levels (Zhou 2014).

These challenges in stormwater management have been addressed and codified into legislation in many regions, including the European Union (EU) and the United Kingdom (UK). The EU Water Framework Directive (WFD) (2000/60/CE) is a key legislative framework aimed at achieving "good ecological and chemical status" for all European water

bodies by 2027 (European Commission [no date]). Its primary objectives include reducing pollution, ensuring sustainable water quantity, and protecting aquatic ecosystems through integrated river basin management, addressing both point and diffuse pollution sources (European Commission [no date]). The WFD emphasises public participation and regional adaptability, promoting the adoption of sustainable, nature-based solutions for water management and urban drainage (Delpla et al. 2009; Lamprea and Ruban 2011; European Commission [no date]).

1.2 Sustainable Drainage Systems

A recent paradigm in urban drainage is the concept of Sustainable Drainage Systems (SuDS), which aims to restore natural drainage processes by reducing impermeable surfaces and enhancing infiltration (Woods-Ballard et al. 2015). SuDS offer an alternative to traditional piped drainage systems and have emerged as a response to the environmental and socio-economic limitations of conventional drainage systems (Lashford et al. 2019). SuDS encompass a variety of design components engineered to fulfil multiple objectives and site-specific needs. These components include bioretention systems, green roofs, permeable pavements, constructed wetlands, and stormwater harvesting systems (Woods-Ballard et al. 2015).

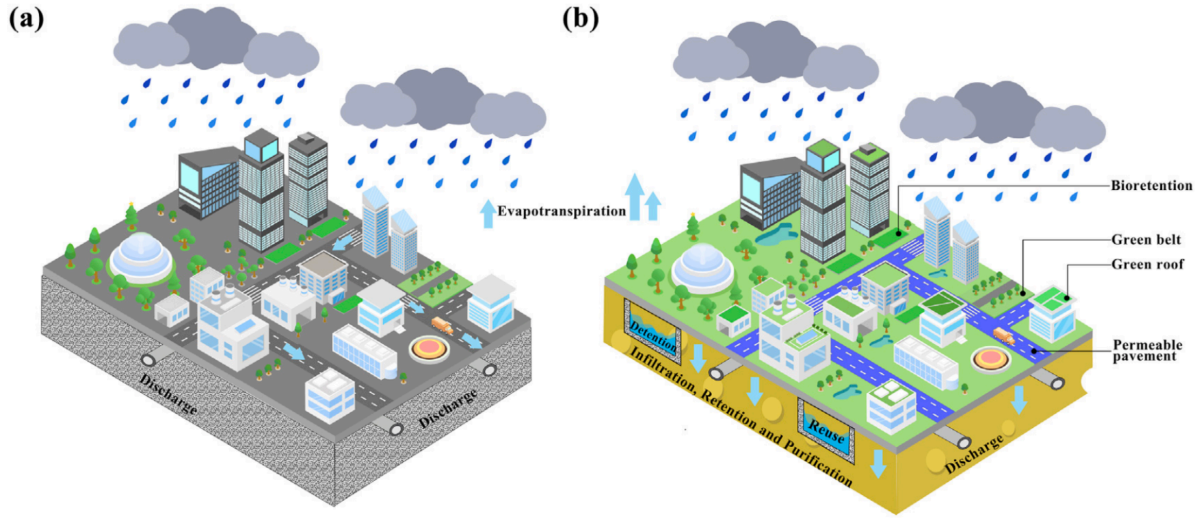

Figure 1.1 Difference in hydrological processes in urban stormwater management a) conventional grey drainage, b) SuDS (image: Yin et al.).

Beyond managing runoff, SuDS provide additional benefits, such as improved water quality, enhanced biodiversity, and increased aesthetic and amenity value (Zhou 2014; LeFevre et al. 2015; Eckart et al. 2017). In 2019, the Welsh Government mandated the inclusion of SuDS in new developments under Schedule 3 of the Flood and Water Management Act 2010. This made Wales the first nation globally to enact statutory SuDS laws, establishing SuDS Approving Bodies (SABs) within local authorities. These bodies are responsible for evaluating, approving, and maintaining drainage systems that meet national SuDS standards before construction begins (Ellis and Lundy 2016; Welsh Government 2019; James 2023). The statutory implementation of SuDS in Wales highlights the growing recognition of sustainable solutions in urban stormwater management and emphasises the need for research to ensure effective system performance and management.

1.3 Bioretention systems

One of the most adaptable SuDS design components in urban settings includes bioretention systems, colloquially known as rain gardens, due to their flexible scalability and integration into urban stormwater management frameworks (Clar et al. 2012; Woods-Ballard et al. 2015). Bioretention systems are small depressions in the urban landscape (Figure 1.2), designed to receive stormwater runoff from nearby impermeable surfaces and temporarily hold it through slow infiltration processes involving vegetation and soil layers (Dietz 2007). By mimicking pre-industrial hydrological processes, this technology offers decentralised solutions to challenges posed by urban flooding and climate change (Zhou 2014).

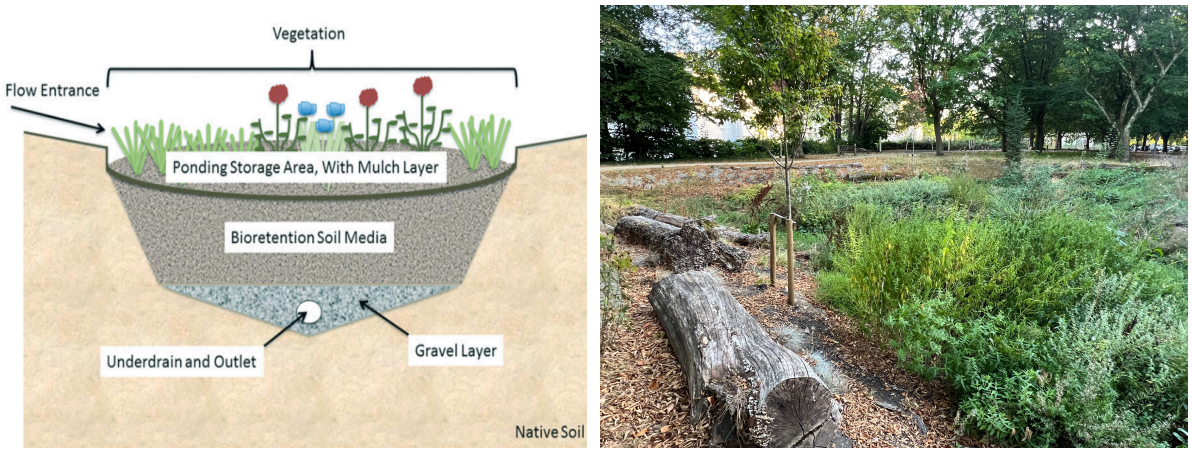

(a) (b)

Figure 1.2 Typical bioretention design. (a) cross section illustration (image: Muerdter et al.) (b) a bioretention system in Cardiff, UK.

Their functionality extends beyond peak flow attenuation, as they also significantly improve the quality of stormwater runoff through several physicochemical processes, including filtration, sedimentation, adsorption, plant uptake and ion exchange (Davis et al. 2003; Dietz and Clausen 2005; Hatt et al. 2007a; Bratieres et al. 2008). Findings reported in the literature show that bioretention systems can remove 67-99% of heavy metals (Read et al. 2008; Jacklin et al. 2021b), 50-77% of nutrients (Bratieres et al. 2008), 97% of organic contaminants (Pritchard et al. 2018), and >99% of microplastics (Kuoppamäki et al. 2021).

Moreover, bioretention systems have been shown to produce the lowest greenhouse gas emissions among stormwater management solutions and can significantly reduce eutrophication (Alyaseri et al. 2017). Bioretention systems are valuable assets in stormwater management, as they are cost-effective, easy to install, and provide aesthetic appeal (LeFevre et al. 2015). Other co-benefits include noise reduction, thermal comfort, biodiversity enhancement, and groundwater recharge (Siwiec et al. 2018).

Despite their multi-functional benefits, the effectiveness and operational lifespan of bioretention systems are critically dependent on (1) the initial design optimisation of key components, and (2) proactive maintenance strategies informed by long-term performance data.

In recent years, several jurisdictions worldwide have developed design manuals and best practices for bioretention systems to ensure optimal performance and return on investment. Examples include the Wisconsin Department of Natural Resources bioretention design guidelines (2006), in the US, the Facility for Advancing Water Biofiltration (FAWB, 2009) guidelines in Australia, and the Construction Industry Research and Information Association (CIRIA, 2015) SuDS manual in the UK (Atchison et al. 2006; FAWB 2009; Woods-Ballard et al. 2015). These manuals provide recommendations and design criteria for bioretention systems, including plant and filter media selection, drainage layout, and maintenance checklists, to optimise system performance. However, despite being founded on extensive global and regional research, these recommendations are often limited by a fragmented understanding of the complex interactions and dynamic processes occurring at the plant/soil/water interface in bioretention systems.

1.3.1 Component design

Significant knowledge gaps remain in understanding the nuanced role each design element plays in system performance. For example, vegetation functionality is evaluated on multiple levels, including enhancing hydrological and treatment performance, providing biodiversity and habitats, and improving aesthetic value (Muerdter et al. 2018; Vijayaraghavan et al. 2021). Yet, design manuals tend to overlook the significant contribution, or lack thereof, of certain plant species in the water treatment aspect of bioretention design and its interconnection with hydrological performance. Instead, they rely on general criteria for plant selection, such as desirable morphological traits, drought/flood tolerance, and the inclusion of native species (Dagenais et al. 2018; Vijayaraghavan et al. 2021). This approach may lead to suboptimal treatment efficiency, particularly under varying climatic conditions (Vijayaraghavan et al. 2021).

Studies have shown considerable variations among plant species in pollutant removal performance (Read et al. 2008). Some species perform poorly compared to non-vegetated systems, and in some cases, such as nutrient removal, certain species contribute to the net production of nutrients, causing the system to act as a source rather than a sink for stormwater pollution (Bratieres et al. 2008). According to design manuals, the use of dense-root species enhances infiltration rates and prevents system failure due to clogging (Muerdter et al. 2018). However, dense-root systems can also form preferential flow paths, which reduce pollutant removal efficiency. This phenomenon is heavily influenced by wetting and drying cycles, which are typical field conditions for bioretention systems (FAWB 2009; Woods-Ballard et al. 2015). This trade-off between infiltration enhancement and pollutant removal remains poorly researched, especially for UK-native plants operating in UK conditions.

Another design element integral to effective bioretention performance is the selection of substrate media. Current design guidelines recommend the use of well-graded loamy sand to sandy loam due to its affordability, local availability, and proven effectiveness in removing stormwater pollutants, particularly sediment-bound pollutants (FAWB 2009; Woods-Ballard et al. 2015). Mechanical filtration and sedimentation are the primary removal mechanisms of sand-based media (Hatt et al. 2007a; Read et al. 2008). However, their performance is less efficient for dissolved pollutants, which constitute a significant proportion of urban runoff

(LeFevre et al. 2015). Over the past two decades, research has evolved to engineer new materials that can be used wholly, or partially as amendments, to create substrates with optimised pollutant removal and water retention capacities. One such amendment is biochar, a carbon-rich material derived from the pyrolysis of plant-based or waste biomass. Biochar demonstrates significant potential as a filter medium in stormwater treatment due to its high porosity and adsorption capacity, especially for dissolved pollutants (Boehm et al. 2020; Biswal et al. 2022).

Depending on production properties such as pyrolysis temperature and feedstock type, biochar has been shown to effectively remove a wide range of pollutants, including heavy metals, nutrients, organic contaminants, and microplastics (Agrafioti et al. 2013; Mohanty et al. 2018). However, some studies have reported that biochar can leach significant amounts of nutrients into infiltrated water (Yao et al. 2012; Iqbal et al. 2015). The application of biochar in bioretention systems is a relatively new field, and knowledge is scarce regarding its performance under unsaturated conditions, and stormwater pollutant interactions. Further studies are required to optimise its practical application (Tirpak et al. 2021; Vijayaraghavan et al. 2021).

1.3.2 Monitoring and maintenance

Maintenance activities outlined in bioretention manuals typically focus on aesthetic upkeep, such as litter removal, pruning, mowing, and mulch scraping (Davis et al. 2009). However, the long-term performance of bioretention systems and their aging effects are poorly understood due to a lack of monitoring data. Research suggests that heavy metals in bioretention systems tend to accumulate primarily in the upper 10-30cm of the filter media, with the highest concentrations likely near the system's inlets (Jones and Davis 2013; Johnson and Hunt 2016). This accumulation indicates that surface layers play a crucial role in pollutant retention, as observed in multiple studies (Hatt et al. 2008; Davis et al. 2009; Al-Ameri et al. 2018).

Although studies have highlighted that clogging due to compaction and fine sediment accumulation is the primary cause of bioretention failure—likely occurring before the system exhausts its pollutant retention capacity—these sediments can accumulate to toxic levels over extended periods of operation (Hatt et al. 2008; Hatt et al. 2011). Over time, they may be re-

mobilised in infiltrated runoff or redeposited on roadsides, posing ecological and human health risks. This is particularly concerning for heavy metals, which do not degrade over time (Li and Davis 2008b; Johnson and Hunt 2016). Since heavy metals are primarily trapped in the top layer of bioretention systems, which can be accessible through direct human contact, their accumulation may violate regulatory guidelines and soil screening levels. Therefore, monitoring this accumulation is essential for long-term maintenance and risk assessment.

However, conventional laboratory-intensive methods, such as Atomic Absorption Spectrophotometry (AAS) and Inductively Coupled Plasma Mass Spectrometry (ICP-MS), are constrained by high costs and logistical challenges, particularly for large-scale monitoring. In-situ monitoring techniques using portable X-ray fluorescence (pXRF) analysers offer a rapid, non-invasive, and cost-effective alternative for heavy metal mapping in the field, enabling real-time decision-making for preliminary risk assessments (Venvik and Boogaard 2020; Boogaard et al. 2024). While pXRF is widely used in urban, mining, and landfill studies, its application in bioretention substrates is rarely explored (Kalnicky and Singhvi 2001; Lenormand et al. 2022; Boogaard et al. 2024). pXRF facilitates high-resolution contamination mapping, providing insights into heavy metals distribution which can support targeted remediation efforts and regulatory compliance (Radu and Diamond 2009). However, its accuracy depends on soil matrix characteristics, necessitating tailored methodologies and calibration protocols (Kalnicky and Singhvi 2001; Lenormand et al. 2022).

1.4 Scope of thesis

This research aims to enhance the design and maintenance of bioretention systems by evaluating design configurations using native plants and biochar amendments for improved performance, and by generating new insights into long-term heavy metal accumulation patterns to inform targeted maintenance strategies.

The methodological approach integrated laboratory experiments and field-scale validation, with each component tailored to isolate specific variables and answer a core part of the research aim. The investigation into design components was conducted through two targeted column studies. The influence of vegetation on bioretention performance was evaluated using a large-scale column experiment, a setup chosen to accommodate mature root systems and approximate field conditions. Concurrently, the performance of biochar amendments was

investigated under highly controlled conditions using a bench-scale column setup. This separate approach was essential to precisely isolate the removal mechanisms of the biochar itself, free from the confounding biological variables present in the vegetated systems. This strategy also provided a resource-efficient method to screen biochar efficiency before any potential future investigation into more complex interactions.

The long-term accumulation and distribution of heavy metals, a critical consequence of effective pollutant capture, addressed the maintenance aspect of the investigation. This was achieved through analysing the used filter media from the large column experiments, which served as aged biofilters for the study of accumulation depth profiles. This was complemented by a field study of operational bioretention systems in urban areas, which was necessary to investigate accumulation patterns under real-world conditions and to evaluate the influence of system-specific factors such as age and inlet design. The application of in-situ pXRF analysis was integral to this phase, providing a rapid method for mapping heavy metal distribution.

Collectively, the empirical evidence presented herein will support researchers and practitioners in establishing improved design, and maintenance practices that enhance the efficiency and long-term reliability of bioretention systems.

1.5 Thesis outline

This thesis is divided into seven chapters, including this introduction. Below is a summary of the content and contribution of each chapter to the overall thesis aim:

- Chapter 1: establishes the research context by presenting the challenge of urban stormwater pollution and the role of bioretention systems. It identifies key knowledge gaps in design and maintenance leading to the research scope and aim.
- Chapter 2: presents a critical review of urban stormwater pollution, and the design, performance, and maintenance of bioretention systems. The review identifies specific research gaps concerning the role of key design elements (vegetation, and biochar amendments), and the long-term fate of captured pollutants, which inform this study's objectives.
- Chapter 3: this chapter details the methodological approach developed to address the research objectives. It describes the design and implementation of two complementary

laboratory column experiments: a large-scale setup to investigate the effects of mature vegetation, and a bench-scale setup to isolate and examine the mechanistic role of biochar amendments. The chapter also outlines the protocols for synthetic stormwater preparation, sampling, and analytical techniques.

- Chapter 4: Presents experimental findings on the role of UK-native vegetation. It quantifies their impact on pollutant removal and hydrological performance and analyses the resulting heavy metal accumulation within the filter media.
- Chapter 5: focusing on media composition, this chapter evaluates the efficiency of biochar amendment for enhancing pollutant removal. It provides a mechanistic understanding of the dominant adsorption and filtration processes.
- Chapter 6: bridges lab and field by assessing heavy metal accumulation in operational bioretention systems. It evaluates the impact of system age and inlet design using ex-situ and in-situ (pXRF) techniques to inform maintenance strategies.
- Chapter 7: summarises the research findings and implications for bioretention design and maintenance. The chapter acknowledges limitations and provides recommendations for future research.

Chapter 2. Literature Review

2.1 Urban stormwater pollution

Urban stormwater pollution has become an increasingly pressing issue as water managers strive to comply with the European standards under the Water Framework Directive (WFD). The directive aims to achieve "good ecological and chemical status" for surface and groundwater by 2027 (Lenormand et al. 2022). This involves addressing pollutants from stormwater runoff, managing urbanisation and climate change effects, and adopting sustainable solutions like Sustainable Drainage Systems (SuDS) for stormwater management. Despite progress, implementation challenges remain due to variability in local regulations, evolving storm patterns, and the need for holistic solutions integrating water quality and urban planning frameworks (Lamprea and Ruban 2011).

The WFD mandates all EU member states establish monitoring programmes to evaluate the chemical and ecological status of their aquatic environments (European Commission [no date]). The aim is to reduce pollution from identified "Priority Substances" (PSs) or "Priority Hazardous Substances" (PHSs), also known as priority pollutants, to levels that comply with the established Environmental Quality Standards (EQSs) (European Commission 2009; Birch et al. 2011). Key aspects include addressing point and non-point sources of pollution, protecting aquatic ecosystems, and engaging public participation to ensure effective implementation of the WFD objectives. (European Commission 2003; European Commission 2009).

2.1.1 Identifying priority pollutants

To effectively address stormwater pollution challenges, identifying priority pollutants—those posing the greatest risks to ecosystems and human health—is critical. Early monitoring initiatives, such as the U.S. Nationwide Urban Runoff Program (NURP), laid the groundwork by cataloguing hundreds of pollutants in urban runoff, many of which were rarely documented or poorly understood (Cole et al. 1984; Müller et al. 2020). Building on this, frameworks such as the Chemical Hazard Identification and Assessment Tool (CHIAT)

developed by Eriksson et al., (2004), systematised the selection of priority pollutants through risk assessments and expert consultations, which can be regarded as “indicator parameters” to facilitate the monitoring process. The CHIAT framework, part of the DayWater project, produced the Selected Stormwater Priority Pollutants (SSPP) list, which includes 25 parameters such as metals (e.g. Cd, Cr, Cu, Ni, Pb, Zn), Polycyclic Aromatic Hydrocarbons (PAHs, e.g. naphthalene, pyrene), herbicides (e.g. glyphosate, terbutylazine), and industrial compounds (e.g. nonylphenol ethoxylates, pentachlorophenol) (Eriksson et al. 2004; Eriksson et al. 2007). This list aligns with the European WFD and guides monitoring and treatment strategies. A summary of the main priority pollutants identified in the UK and EU are presented in Table 2.1.

Subsequent programs, such as the ESPRIT project, further refined priority pollutant identification by analysing stormwater in urban catchments, focusing on 41 substances across combined and separate sewer systems (Bertrand-Krajewski et al. 2008). These efforts highlight key pollutants such as heavy metals, nutrients, pesticides, PAHs, and chlorides from road salts, which exhibit high groundwater contamination potential (Pitt et al. 1999). Notably, pollutants like dissolved copper and low molecular weight PAHs are increasingly recognised for their bioavailability and ecological impact, even at low concentrations (LeFevre et al. 2015). The distinction between dissolved and particle-bound pollutants is vital, as dissolved fractions (e.g., phosphorus, zinc) often bypass stormwater treatment systems, demanding advanced mitigation approaches (LeFevre et al. 2015).

Tools like CHIAT and ESPRIT, alongside databases from NURP, enable stakeholders to prioritise high-risk pollutants and tailor management strategies, balancing regulatory compliance with environmental protection. By narrowing focus to these priority substances, urban stormwater management can more effectively mitigate risks to water quality and ecosystem and human health.

Table 2.1 List of frequently detected pollutants in urban runoff, and their priority in the UK and EU stormwater management frameworks.

Category	Parameters	Detection Frequency (%)[a]	Priority (UK)[b]	Priority (EU)[c]	Category	Parameters	Detection Frequency (%)	Priority (UK)	Priority (EU)
Basic Parameters	pH	-	×	✓	Metals	Copper (Cu)	96%	✓	✓
	Temperature	-	×	✓		Lead (Pb)	96%	✓	✓
	Biological Oxygen Demand (BOD)	-	✓	✓		Zinc (Zn)	95%	✓	✓
	Chemical Oxygen Demand (COD)	-	✓	✓		Cadmium (Cd)	55%	✓	✓
	Total Suspended Solids (TSS)	-	✓	✓		Chromium (Cr)	57%	✓	✓
Nutrients	Nitrogen (N)	-	✓	✓		Iron (Fe)	-	✓	×
	Phosphorus (P)	-	✓	✓		Nickle (Ni)	48%	✓	✓
	Nitrate (NO_3^-)	-	×	×		Platinum (Pt)	-	×	✓
	Nitrite (NO_2^-)	-	×	×		Mercury (Hg)	16%	✓	×
	Ammonia (NH_3)	-	×	×		Arsenic (As)	58%	×	×
	Ammonium (NH_4^+)	-	✓	×	Organic Compounds	Oil and Grease	-	✓	×
	Orthophosphate (PO_4^{3-})	-	×	×		Polychlorinated biphenyl 28 (PCB 28)	Not detected	×	✓
	Total Kjheldahl-Nitrogen (TKN)	-	✓	✓					

a (Cole et al. 1984): preliminary data of the Nation-wide Urban Runoff Program (detection frequency: the percentage of runoff samples in which the pollutant was detected, (-): not available).
b (Mitchell 2005).
c (Eriksson et al. 2007)

2.1.2 Sources and characteristics of pollution

Human activities, ranging from traffic emissions to waste generation, inject diverse pollutants into urban environments, creating multifaceted pollution pathways that challenge water quality management (Brown and Peake 2006; Müller et al. 2020). To preserve the quality of aquatic environments in urban catchments, it is essential to identify pollution sources to enable the strategic and sustainable planning and management of urban drainage and pollution control measures.

The origins of stormwater pollution can be classified into two categories: point sources, such as wastewater treatment plants and industrial discharges, and non-point sources (NPS), which lack a single origin and are diffuse, spatially variable, and difficult to trace. Key NPS pollution contributors include atmospheric deposition, vehicular emissions, construction activities, and urban landscaping practices (Stuart et al. 2011; Carey et al. 2013). While point sources have long been regulated, non-point source (NPS) pollution has become a primary challenge in urban stormwater management. Stormwater runoff serves as the main transport mechanism for NPS pollution, which is particularly difficult to control due to its widespread nature and complex mitigation requirements (Tsihrintzis and Hamid 1997; Müller et al. 2020).

2.1.2.1 Non-point source pollution

NPS pollution arises from dispersed activities and land uses, making it difficult to trace and control (Göbel et al. 2007; Carey et al. 2013). Atmospheric deposition, for instance, transfers pollutants via precipitation (wet deposition) or particle settling (dry deposition), with vehicular traffic and industrial emissions contributing nitrogen oxides (NO_x) and heavy metals (Göbel et al. 2007; Carey et al. 2013). Construction sites exacerbate sediment transport, while pet waste and lawn fertilisers introduce nutrients like nitrogen (N) and phosphorus (P) into runoff (Carey et al. 2013). Even seemingly benign surfaces, such as metal roofs or roads, leach pollutants like copper (Cu) and zinc (Zn) through corrosion and abrasion.

The ecological consequences of NPS pollution are profound and have been documented in several studies in urban catchments (Lee and Bang 2000; Brown and Peake 2006; Göbel et al. 2007; Holvoet et al. 2007). For example, excessive nutrient loading from urban runoff drives eutrophication, fostering toxic algal blooms that deplete oxygen, reduce water clarity, and harm aquatic ecosystems (Nyenje et al. 2010). Despite advances in tracing pollutants through

stable isotope analysis, distinguishing sources such as fertilisers, wastewater, or atmospheric inputs remains challenging (Carey et al. 2013). Furthermore, climate change intensifies these risks by altering precipitation patterns and nutrient cycling, potentially increasing leaching rates and groundwater contamination (Stuart et al. 2011).

2.1.2.2 Heavy metal pollution

Heavy metals are a critical group of pollutants in urban stormwater due to their persistence, toxicity, and complex interactions within aquatic systems. In stormwater management, the term "heavy metals", also known as "trace metals", refers to metals that have a relatively high density of more than $5 g/cm^3$, and are toxic at high concentrations. Heavy metals such as zinc (Zn), copper (Cu), and lead (Pb) are ubiquitous in urban runoff, originating from both natural processes and anthropogenic activities (Odobašić et al. 2019). While Zn and Cu are essential micronutrients at low concentrations, they become toxic at elevated levels, whereas non-essential metals like Pb, cadmium (Cd), arsenic (As), and mercury (Hg) pose significant risks even in trace amounts due to bioaccumulation (Maniquiz-Redillas and Kim 2016; Kurup et al. 2017; Zhang et al. 2018).

Heavy metals pollution in the environment comes from natural and anthropogenic sources (Kurup et al. 2017). Natural sources include volcano eruptions, acid rock drainage, forest fires, and soil erosion (Lamprea and Ruban 2011; Odobašić et al. 2019), while anthropogenic sources include vehicular emission, industrial activities, landfills, and domestic activities. Although anthropogenic sources of heavy metals are documented more in terms of air pollution than stormwater runoff, the subsequent atmospheric deposition processes on roads and roofs surfaces aggravate the amount of heavy metals that is washed off by stormwater runoff (Petrucci et al. 2014). Heavy metals concentration levels are greater in catchments with heavy industrial activities, traffic emissions, coal-burning plant smelters, and domestic activities (Luo et al. 2012; Odobašić et al. 2019).

Studies on urban stormwater management have reported that heavy metals are present in almost every sample of runoff (Lee and Jones-Lee 2004). Among these, Zn, Cu and Pb are the most prevalent with ≥ 95% detection frequency (Cole et al. 1984), and have the most significant negative impacts on receiving water bodies (Jang et al. 2005).

2.1.2.2.1 Zinc

Zn-coated roofs and rain gutters are major sources of Zn in urban runoff. According to Petrucci et al. (2014), the emission of Zn from construction materials accounted for 70% of the total emissions in urban catchments, and the remaining 30% accounted for industrial-related emissions. Hwang et al. (2016) reported that approximately 50% of Zn in urban runoff was in dissolved state, and the total Zn concentrations exceeded the water quality limits. Research on urban runoff established strong correlation between Zn and sediments from various cities around the world, and the amount of fuel sold in those cities, which also correlated with the increasing number of travel distances over the past decades, indicating that wear of tires and brake pads were a major source for Zn (Göbel et al. 2007; LeFevre et al. 2015; Hwang et al. 2016).

2.1.2.2.2 Copper

Aryal et al. (2006) found that the presence of Cu in sediments was closely correlated with the presence of Zn, indicating possible common sources. A significant proportion of Cu is deposited as dust on road surfaces and nearby soils due to the abrasion and tearing of brake pads (Aryal et al. 2006; Petrucci et al. 2014; Hwang et al. 2016). Following the discontinuation of leaded petrol, Cu emerged as a major contaminant threatening aquatic life in urban waterways. It now ranks among the most harmful pollutants for aquatic organisms due to its widespread use in urban settings and its toxicity to aquatic ecosystems (Hwang et al. 2016).

2.1.2.2.3 Lead

Lead pollution, which is considered as the leading pollutant in the environment (Odobašić et al. 2019), primarily comes from anthropogenic activities such as the burning of fossil fuels, that releases lead into the atmosphere (Kurup et al. 2017), and industrial processes which release Pb-contaminated waste into the surrounding environment. Landfills also discharge Pb through leaching and fires, while agricultural activities contribute to Pb pollution through the use of phosphate-based fertilisers and pesticides (Odobašić et al. 2019). Pb can also find its way in drinking water due its historic use in plumping (Kurup et al. 2017). In urban environments, vehicle exhaust, particularly from older engines and leaded fuels can aggravate pollution. Once released, Pb can persist in the environment as sulphates, sulphides and carbonates which are highly toxic to organisms (Odobašić et al. 2019).

2.1.2.2.4 Partitioning and mobility of heavy metals

Heavy metals occur in stormwater runoff either in dissolved state (<0.45µm) or particulate state (>0.45µm) (Huber et al. 2016). Particulate, or sedimentary, metals tend to bound to suspended particles, while dissolved metals occur as free metal-ions. Heavy metals in both states interact with each other and react differently to environmental conditions such as temperature, pH, flow regime and redox conditions (Maniquiz-Redillas and Kim 2016). For example, dissolved metals can change to particle state through agglomeration and flocculation, while particulate metals are soluble in low pH conditions which can increase their re-mobility and leaching potential (LeFevre et al. 2015; Zhang et al. 2018).

The partitioning between dissolved and particle states has a great influence on the toxicity, mobility, bioavailability, and removal mechanisms of heavy metals in natural soils, and bioretention systems (LeFevre et al. 2015). Effective stormwater management must therefore account for dynamic partitioning mechanisms, and prioritise source control to mitigate bioavailability and long-term ecological risks (LeFevre et al., 2015; Zhang et al., 2018).

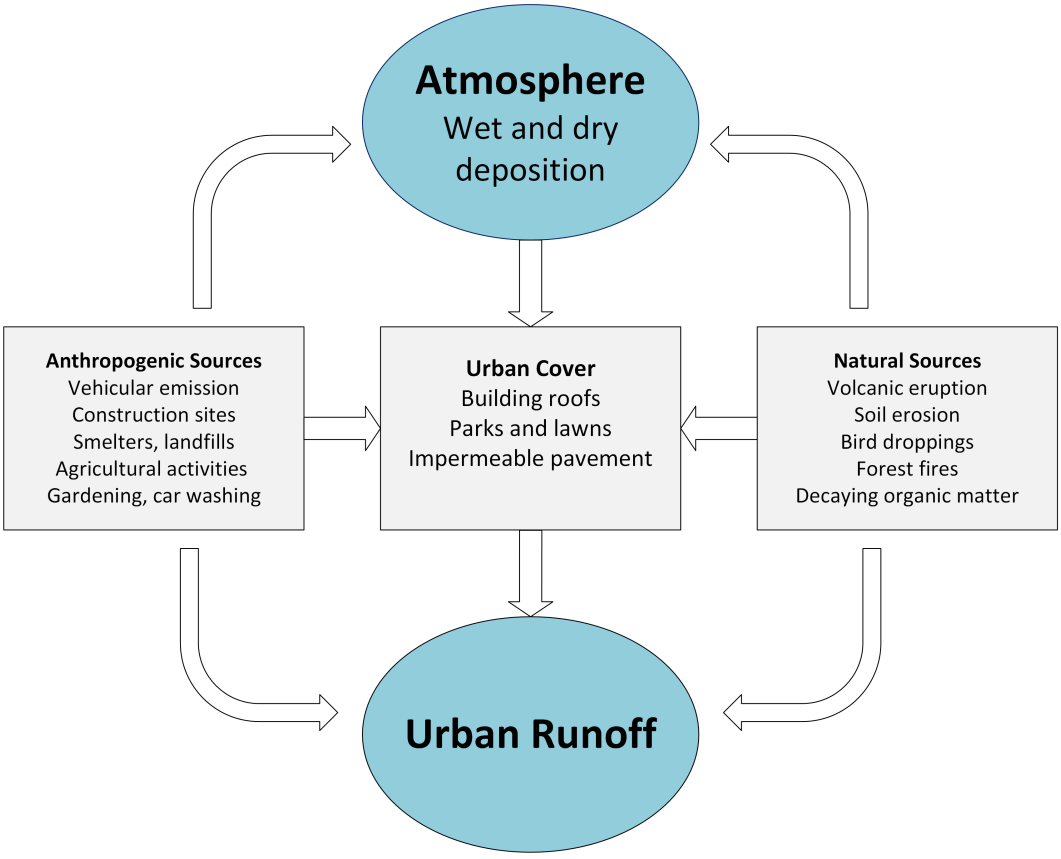

Figure 2.1 Urban stormwater pollution sources. Arrows represent pollution transport pathways.

2.1.2.3 Nutrient pollution

Nutrients such as nitrogen (N) and phosphorus (P) are essential elements for the survival of aquatic life, yet the accumulated loading of nutrients into lakes and rivers from point and non-point sources poses one of the most critical water quality issues in surface water bodies today (Badruzzaman et al. 2012). While most ecosystems can tolerate moderate increases, exceeding a critical nutrient loading threshold can trigger dramatic changes such as harmful algal bloom, oxygen depletion and shifts in species composition and ecosystem functions (Verhoeven et al. 2006). These changes can lead to a new stable state known as eutrophication—a process in which water bodies become excessively enriched with nutrients, leading to excessive plant biomass growth (e.g. phytoplankton and macrophyte). This results in development of toxic and non-toxic algal bloom (Carey et al. 2013), depletion of oxygen levels and death of aquatic life (Nyenje et al. 2010; Badruzzaman et al. 2012).

Eutrophication's harmful environmental effects also impact human health, as studies indicated correlation between eutrophication and various diseases. Excess nutrients in water bodies can promote harmful algal blooms, releasing toxins that contaminate drinking water, cause respiratory issues, or lead to neurological conditions upon exposure or ingestion (Nyenje et al. 2010; Badruzzaman et al. 2012; EPA [no date]). Nitrogen and phosphorus are regarded as priority pollutants in the CHIAT framework and are frequently detected in urban runoff samples.

2.1.2.3.1 Nitrogen

Nitrogen loading in waterways are usually greater than phosphorus loading as nitrogen occurs naturally both in the atmosphere and in the earth's soil (Pitt et al. 1999). Nitrogen exists in a variety of forms, organic and inorganic, dissolved and particulate, such as nitrate (NO_3^-), ammonium (NH_4^+), and oxidised nitrogen (NO_x), causing a range of environmental concerns (Lucke et al. 2018). For example, nitrate from naturally occurring nitrogen in soils is one of the most frequently detected pollutants in groundwater (Pitt et al. 1999), and is considered a major cause of groundwater contamination in the UK (Stuart et al. 2011). Nitrogen enters stormwater through diverse pathways, including atmospheric deposition and organic decomposition. Precipitation introduces nitrogen in the form of either nitrate or ammonium, with atmospheric nitrate primarily produced through combustion processes in power plants, large industrial facilities, and vehicle exhaust, while atmospheric ammonium

arises from the volatilisation of ammonia released by soils, fertilisers, animal waste, and vegetation, particularly in agricultural areas (Pitt et al. 1999). Both forms contribute to air pollution by reacting with other particles in the atmosphere, affecting air quality and potentially impacting human health and ecosystems. Additionally, organic nitrogen sources, such as proteins in leaf litter and grass clippings, undergo decomposition into inorganic species like ammonium and nitrate. Atmospheric deposition also introduces NO_x from fossil fuel combustion and ammonia (NH_3) from agricultural volatilisation (Pitt et al. 1999; Carey et al. 2013). Vehicles further complicate this dynamic: catalytic converters emit ammonia (NH_3) as a byproduct of NO_x reduction, creating localised deposition hotspots along highways (Carey et al. 2013).

2.1.2.3.2 Phosphorus

Similarly, phosphorus can occur in organic and inorganic forms, either dissolved such as orthophosphate (PO_4^{3-}), or bound to particles. Likely natural sources of phosphorus include animal droppings, dead insects, and intercepted dry deposition from tree canopies in residential areas (Yang and Toor 2017). Phosphorus is often assumed to be predominantly particulate-bound, however, in some cases the dissolved fraction can constitute up to 90% of stormwater runoff (LeFevre et al. 2015). Orthophosphate, a soluble form of phosphorous, is one of the most readily available nutrients in the environment (Sample et al. 2012). In its soluble form, orthophosphate can either precipitate directly or adsorb chemically to soil surfaces through interactions with exposed iron, aluminium, or calcium present on soil particles (Pitt et al. 1999). Orthophosphate binds to soil particles or dissolves as soluble reactive phosphorus (SRP), directly fuelling algal growth (LeFevre et al. 2015).

Land use critically influences nutrient exports, with distinct patterns across development types. Construction sites generate sediment loads ten times greater than residential areas, while fertilised lawns and impervious surfaces significantly increase dissolved nitrogen and phosphorus fluxes (Carey et al. 2013). In residential zones, fertiliser application accounts for a substantial portion of nutrient loading (Badruzzaman et al. 2012). Agricultural areas and green spaces contribute to urban nutrient pollution through stormwater runoff containing fertiliser residues and animal waste. Point sources present additional challenges, as wastewater from sewage treatment plants and septic systems—when inadequately treated for nitrogen and phosphorus—can directly trigger waterway eutrophication (Pitt et al. 1999;

Nyenje et al. 2010). Effective mitigation strategies must account for both source variability (diffuse vs. point sources) and nutrient speciation, coupled with improved fertiliser management practices such as controlled-release formulations and seasonal application timing (Carey et al. 2013).

2.1.3 Pollution mitigation strategies

Conventional grey infrastructure, such as sewers and gutters, prioritises rapid runoff conveyance but neglects essential water quality remediation, leaving ecosystems vulnerable to pollutant overload, eutrophication, and groundwater contamination. These systems struggle to adapt to increasing urban runoff volumes and climate-driven extremes, which exacerbate pollutant mobilisation and strain drainage networks. As traditional approaches become increasingly overwhelmed, there is growing urgency to reimagine urban stormwater management through resilient, multifunctional solutions that integrate hydrological control, pollution mitigation, and ecological restoration.

2.1.3.1 Sustainable Drainage Systems

Sustainable Drainage Systems (SuDS), also known as Low Impact Development (LID), Best Management Practices (BMPs), Green Infrastructure (GI), or Water Sensitive Urban Design (WSUD), represent a paradigm shift in urban stormwater management. These systems employ a decentralised approach to mitigate climate change and non-point source pollution impacts by restoring natural hydrological processes, and emulating pre-development water cycles (LeFevre et al. 2015; Eckart et al. 2017). As climate change leads to more frequent and extreme weather events, SuDS provide a flexible and adaptive approach to stormwater management. Unlike conventional drainage systems, which focus on "end-of-pipe" solutions and an "out of sight, out of mind" mentality, the SuDS approach relies on small-scale, decentralised techniques to manage urban surface water runoff locally. This approach integrates water into the urban landscape as a valuable resource rather than treating it as a waste product (Zhou 2014; Woods-Ballard et al. 2015; Eckart et al. 2017).

A SuDS scheme can include a combination of design components that can be tailored to fit the specific site characteristics, this versatility allows it to be applied and retrofitted anywhere to meet the design objectives. In highly urbanised areas, retrofitting existing infrastructure, such as car parks, footpaths, and buildings, may be the most practical approach (Woods-

Ballard et al. 2015). Additionally, existing permeable spaces, including parks, lawns, and gardens, can offer further opportunities for infiltration, contingent on site-specific conditions. SuDS can typically be integrated into these public areas without disrupting their primary functions (Woods-Ballard et al. 2015).

The philosophy of SuDS embodies four main objectives (Woods-Ballard et al. 2015):

1. Controlling water quantity by attenuating runoff to reduce flood risks.
2. Improving water quality by filtering pollutants like heavy metals and nutrients from runoff to protect aquatic ecosystems.
3. Enhancing urban spaces by creating attractive, water-integrated landscapes that benefit communities.
4. Supporting biodiversity through native planting and habitat creation, countering urban ecological decline.

Together, these benefits demonstrate the role of SuDS in sustainable water management.

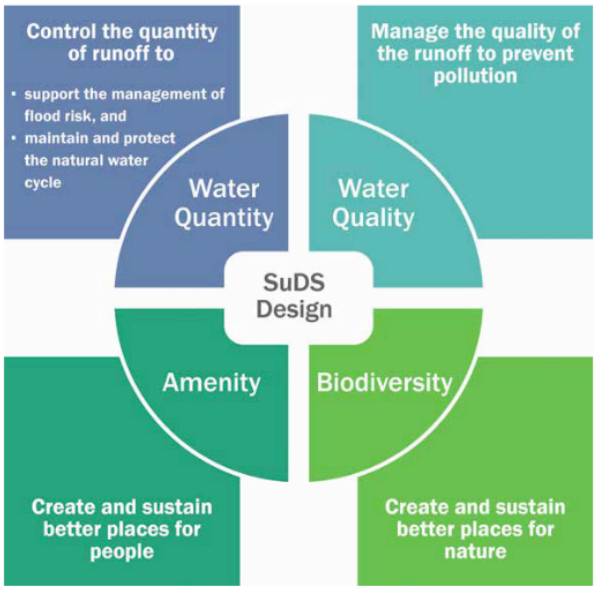

Figure 2.2 The four objectives of SuDS design in the SuDS manual (image: Woods-Ballard et al.).

While SuDS encompass a range of techniques (e.g., bioretention systems, green roofs, permeable pavements, constructed wetlands, ponds), this review focuses specifically on bioretention systems due to their widespread application, versatility in urban settings, and direct relevance to the research objectives of this thesis.

Table 2.2 Primary sources of stormwater runoff pollutants.

Parameters	Sources	Parameters	Sources
Sediments	**Residential:** soil erosion, littering, plastic bags, tire wear, road marking paints, microfibres. **Agricultural:** agricultural plastic mulching and films from sludge utilised to farmland. **Industrial:** Construction activities, drainage channel erosion, mismanaged landfill causing plastic windborne debris, leading to the formation of microplastic form weathering processes.	**Heavy metals**	**Residential:** wear of motor vehicle parts, such as brake pads and tires, and metal-coated roofs. **Industrial:** manufacturing activities smelters, mining, landfills.
Nutrients	**Residential:** dry deposition from tree canopies in residential areas, leaves and grass clippings decomposition, decaying organic matter on roof surfaces, residential lawn fertiliser applications. **Natural**: bird droppings, insects, debris, decomposition of organic matter **Industrial**: combustion from industrial and automobile activities, volatilization of ammonia from soils, fertilisers, animal wastes.	**Organic compounds**	**Residential**: lawns and gardens, landscaping, animal wastes **Industrial**: sewage sludge and organic wastes, and surfactants. **Agricultural:** pesticides and burning residuals. **Natural**: volcano eruption, forest fires, decaying organic matter.

2.2 Introduction to bioretention systems

Bioretention or biofiltration systems, commonly referred to as rain gardens, are shallow depressions in urban landscapes, designed to manage and treat stormwater runoff from impervious surfaces from roofs, car parks, and highways (Figure 2.3). These systems typically consist of engineered soil media, vegetation such as native shrubs, perennials, trees, and mulch layers, to capture runoff pollutants and infiltrate rainwater (Dietz 2007; Bąk and Barjenbruch 2022). Bioretention systems are a key component within the broader framework of SuDS and are located strategically in the urban stormwater management train to intercept runoff upstream, allowing it to temporarily pond on the surface before filtering through the vegetation and soil layers. This process aims to attenuate surface runoff, mitigating the risk of urban flooding, and improve water quality by filtering out pollutants such as sediments (Barrett et al. 2013; Søberg et al. 2020), nutrients (Bratieres et al. 2008; Bratieres et al. 2008), and heavy metals (Hatt et al. 2007b; Read et al. 2009; Wang et al. 2017).

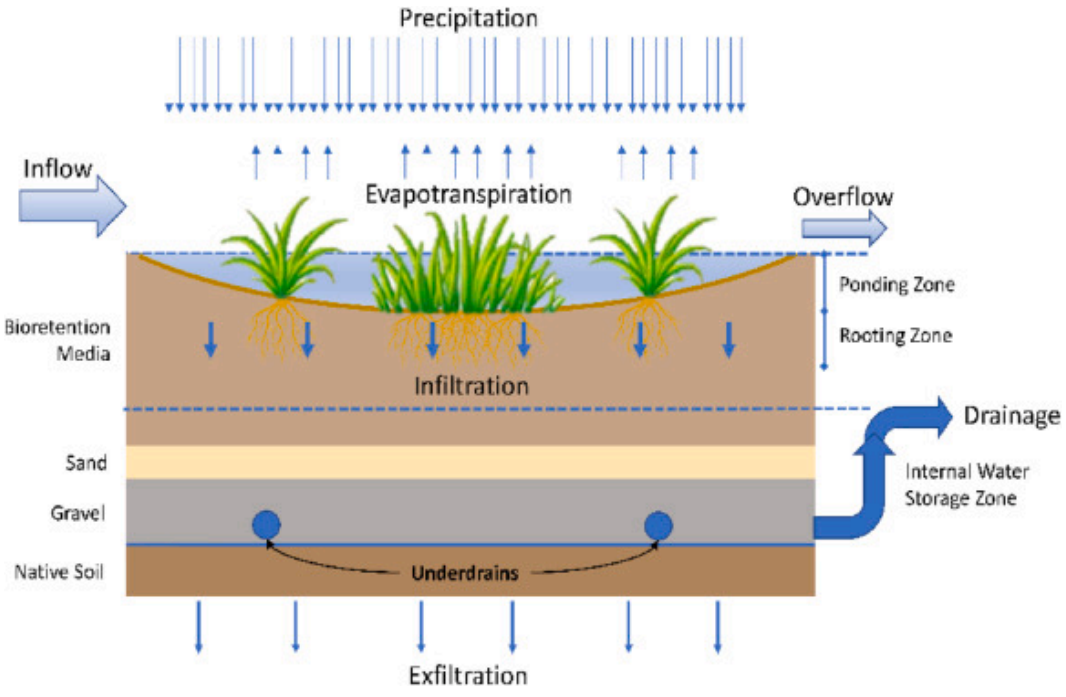

Figure 2.3 Illustration of a typical bioretention system design with an internal water storage zone (saturated zone). The hydrological pathways are indicated by blue arrows (image: Lisenbee et al.).

Bioretention systems also promote groundwater recharge and offer ecological and aesthetic benefits, including enhanced biodiversity, habitat creation, and micro-climate cooling through evapotranspiration (LeFevre et al. 2015; Woods-Ballard et al. 2015). Their flexibility in design allows them to be integrated into various landscapes, from low-density residential areas with soft edges to high-density urban settings with hard edges, addressing multiple urban stormwater challenges at the source (Woods-Ballard et al. 2015; Eckart et al. 2017). The main features of bioretention systems include their layered structure, which typically consists of a surface layer of vegetation and mulch underlying an engineered soil mix for filtration, and an optional underdrain system for controlled discharge into surface water bodies (Figure 2.3), while other designs allow slow percolation into groundwater, often termed “bio-infiltration” (LeFevre et al. 2015). The engineered soil filter supports plant growth and enhances pollutant removal through physical, and chemical processes, while the vegetation aids in biological uptake, evapotranspiration and prevents clogging of the filter media (Vijayaraghavan et al. 2021).

Bioretention systems are designed to operate in unsaturated conditions with frequent wetting and drying periods. Some designs incorporate an internal water storage zone that is permanently saturated, known as a saturated or submerged zone (SZ) created by upturned underdrain elbows (Figure 2.3), typically located at the bottom of the system, to improve pollutant removal, particularly for nutrients and bacteria (Blecken et al. 2010; Zhang et al. 2011; Chandrasena et al. 2014; Payne et al. 2014b). Bioretention systems are particularly effective for managing frequent, small rainfall events, though they can be designed with overflow mechanisms to handle larger storms (LeFevre et al. 2015; Woods-Ballard et al. 2015).

2.3 Key design factors influencing bioretention performance

While bioretention systems can offer numerous benefits for stormwater management, their hydrological and treatment performance critically depends on design elements that balance hydraulic efficiency, pollutant removal, and long-term resilience. Key design factors include vegetation selection, substrate media composition and depth, saturated zone configuration, catchment-to-system sizing ratios, and wetting-drying dynamics. These factors are interdependent, creating synergistic effects that influence overall system performance.

This review examines three key structural design elements: vegetation, saturated zones, and substrate media, synthesising research to clarify their roles, interdependencies, and operational trade-offs in achieving robust bioretention performance. The aim is to identify research gaps in optimising bioretention designs across diverse environmental conditions.

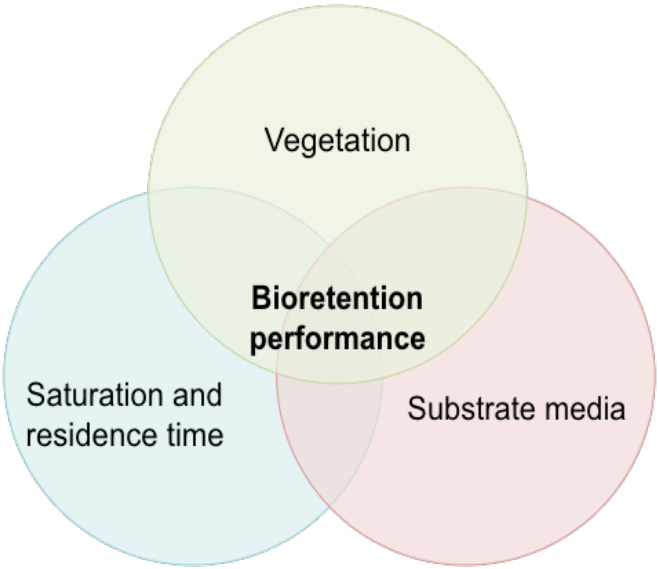

Figure 2.4 Venn diagram of key design components affecting bioretention performance discussed in this review.

2.3.1 Vegetation

Vegetation is an essential component in the design of bioretention systems, offering functional benefits that extends beyond its aesthetical value. It can significantly impact both hydrological performance and pollutant removal mechanisms. In terms of the hydrological benefits, vegetation intercepts surface runoff, prevents scouring of the bioretention surface caused by water influx, improves the hydraulic conductivity of the soil media, prevents clogging over time, and contributes to runoff volume reduction through transpiration (Woods-Ballard et al. 2015; Muerdter et al. 2018; Yang et al. 2022). Simultaneously, vegetation plays a key role in pollutant removal through mechanisms such as nutrient and metal uptake and assimilation, degradation of organic pollutants through phytodegradation, and microbial transformations facilitated by root zone activities (Mohanty et al. 2018).

2.3.1.1 Hydrological processes

Vegetation contributes to the hydrological performance of bioretention systems through evapotranspiration and stormwater filtration processes (Figure 2.5). These processes occur above, at, and below the media surface (Muerdter et al. 2018). Evapotranspiration (ET), the combined process of transpiration from vegetation and evaporation from soil, plays a critical role in bioretention systems by reducing stormwater volume, restoring water storage capacity, and mitigating urban heat island effects through evaporative cooling (Vijayaraghavan et al. 2021). Vegetation can further enhance stormwater infiltration and hydraulic conductivity, while mitigating clogging by creating macropores and root channels that enhance stormwater infiltration (Peng et al. 2016; Yang et al. 2022).

Hydraulic conductivity, the rate at which water moves through porous media, is critical for effective bioretention performance. However, clogging can significantly reduce hydraulic conductivity (Le Coustumer et al. 2012), impairing the treatment efficiency of bioretention systems. Clogging arises through various mechanical, biological, and chemical mechanisms, including media compaction, fine particle deposition, microbial growth within pores, root development, and organic matter swelling, all of which block pore spaces (Bratieres et al. 2008; Li and Davis 2008b; Li et al. 2020). Its severity depends on sediment influx, composition and the hydraulic conditions of incoming flows (Li and Davis 2008b; Lim et al. 2015; Muerdter et al. 2018).

Clogging has several adverse effects on bioretention performance. Firstly, it reduces infiltration rates, leading to prolonged ponding of untreated water, promoting mosquito breeding and overflowing (Muerdter et al. 2018; Vijayaraghavan et al. 2021). Secondly, it can lead to the formation of a polluted surface layer (cake layer) which may pose environmental and health risks (Li and Davis 2008b; Le Coustumer et al. 2012). Design manuals such as the SuDS manual and FAWB guidelines specify a maximum ponding depth of 100-300 mm, and planting vegetation to mitigate these issues (FAWB 2009; Woods-Ballard et al. 2015).

Several studies revealed that vegetation significantly influences the hydraulic conductivity of bioretention systems (Hatt et al. 2009; Le Coustumer et al. 2012; Virahsawmy et al. 2014). Hatt et al. (2009) studied bioretention plants native to Australia in the field and highlighted the important role of root zones in maintaining the hydraulic conductivity of the substrates, as significant increases in infiltration rates were observed with vigorous vegetation growth.

Another large-scale Australian study by Le Coustumer et al. (2012) demonstrated that vegetation, particularly species with thick and extensive root systems such as *Melaleuca ericifolia*, an Australian native plant, improved hydraulic conductivity and infiltration rates of biofilters from 155 mm/hr to 295 mm/h after 60 weeks of experimenting. Conversely, the study showed that the hydraulic conductivity decreased in unvegetated controls from 199 mm/hr to 53 mm/hr. Le Coustumer et al. (2012) also highlights the importance of species selection as other species with finer and denser roots such as *Carex appresa* did not perform significantly differently form unvegetated controls in terms of hydraulic conductivity.

While vegetation generally enhances infiltration, some studies report conflicting results. For example, Chandrasena et al. (2014) observed that vegetated systems with a saturated zone (SZ) had lower infiltration rates than those without. Similarly, species with higher *E. coli* removal efficiencies exhibited lower infiltration rates, suggesting a trade-off between hydraulic performance and pollutant removal (Chandrasena et al. 2014). On the other hand, pollutant removal can be negatively impacted by the presence of vegetation as root growth may induce channelling and preferential flow paths, especially in plants with dense root systems, which reduces the retention of TSS and particulate-bound pollutants (Virahsawmy et al. 2014; Li et al. 2020; Yang et al. 2022).

Design considerations, such as the ratio of root depth to media depth, must account for plant species, climate, and the presence of SZ, which can inhibit root growth (Muerdter et al. 2018; Yang et al. 2022). Results remain context-dependent, influenced by plant species, root morphology, seasonal changes, and experimental design. Large long-term studies are required to refine understanding of vegetation's role in bioretention systems, particularly across varying climates and designs. Further research should quantify these effects and optimise species selection (Dagenais et al. 2018; Vijayaraghavan et al. 2021; Yang et al. 2022).

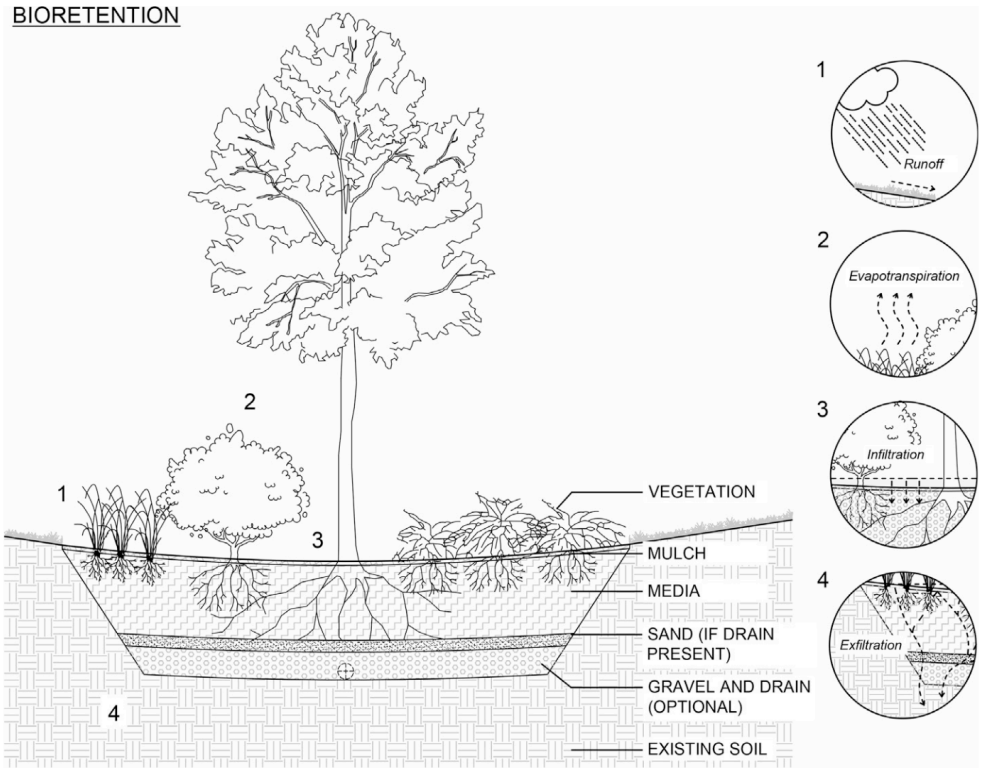

Figure 2.5 Schematic of bioretention structure and key hydrological processes (Image: Dagenais et al.).

2.3.1.2 Pollutant removal

Stormwater management manuals and design standards for bioretention systems such as the SuDS manual and FAWB guidelines often prioritise the hydrological functionality, alongside the ecological benefits, aesthetic appeal, and resilience to harsh climatic conditions of using native or regionally adapted plants (FAWB 2009; Bray et al. 2012; Woods-Ballard et al. 2015). However, these guidelines frequently overlook the rigorous evaluation of the role of vegetation in pollutant removal performance, relying instead on general criteria about plant selection and recommend desirable vegetation traits, such as root structure, growth rates, and tolerance to bioretention conditions, which influence plant growth and overall system performance (Vijayaraghavan 2016; Dagenais et al. 2018; Muerdter et al. 2018).

This approach might lead to suboptimal removal efficiency of certain pollutants, particularly when comparing the performance of bioretention systems across different climatic conditions and weather patterns, as regionally native plants may not perform effectively in different geographical areas, sometimes resulting in failures to meet desired effluent quality standards (Vijayaraghavan et al. 2021). Significant gaps remain in understanding the specific

contributions of plants to the removal of pollutants with high efficiency, due to the abundant speciation of plants and the synergistic and dynamic ways in which they interact with water and soil media (Dagenais et al. 2018; Vijayaraghavan et al. 2021).

For example, as mentioned earlier soil penetration by plant roots, especially dense-root systems can cause large crack formation and preferential flow paths for suspended particles to bypass filtration, impairing the systems treatment efficiency as pointed by Li et al. (2020) and Zinger et al. (2021). This can also reduce the removal efficiency of heavy metals and phosphorus, as a significant portion of these elements in urban stormwater exist in particulate form (Guo et al. 2021). Studies have also found a strong correlation between total suspended solids (TSS) and metal removal efficiency (Xiong et al. 2022).

Similarly, a study by Kuoppamäki et al. (2021) on the fate of microplastics (MPs) in bioretention system revealed that MPs were heavily concentrated along the root channels, and travelled deeper in the substrates of vegetated systems compared to non-vegetated systems. Despite that, no MPs were detected in the influent given the substantial removal efficiency (96-100%) of TSS in all systems (Kuoppamäki et al. 2021). Moreover, the study was conducted over a 17-week period, with MPs analysis carried out during the last 5 weeks of the experiment. Research on the effect of vegetation on MPs transport and deposition in bioretention systems, particularly regarding long-term performance, is still in its infancy (Han et al. 2024).

While vegetation is widely regarded as a critical component of bioretention systems, its specific mechanisms and contributions to pollutant removal remain poorly understood, especially in comparison to non-vegetated systems (Dagenais et al. 2018). Even in the absence of plants, non-vegetated systems can partially achieve their water quality objectives through physical and chemical processes such as filtration, sedimentation, adsorption, and precipitation, as well as microbial activity in bare soil media (Dagenais et al. 2018).

2.3.1.2.1 Heavy metal removal

The role of vegetation in the removal of heavy metals within bioretention systems has been widely studied, yet findings remain inconsistent (Vijayaraghavan et al. 2021). For instance, a comparison study between vegetated and non-vegetated systems by Read et al. (2008) revealed significant variation in effluent metal concentrations among plant species, with some species even releasing higher levels of Zn, Pb, Al, and Ni compared to non-vegetated controls. The effectiveness of vegetation in metal removal appears to depend on factors such as plant species, metal bioavailability, and environmental conditions such as pH levels.

For example, the study showed that species such as *Carex* and *Melaleuca* achieved over 70% metal removal, while *Juncus* species were less effective for lead, despite exhibiting relatively high retention capacity for nitrogen and phosphorus. On average, the study revealed no significant differences in metal removal between vegetated and non-vegetated systems. The authors speculated rapid sedimentation, adsorption, and precipitation in the soil media to dominate metal removal, particularly in pH-neutral soils, with vegetation playing a secondary role (Read et al. 2008).

Plants contribute to metal removal through phytoremediation mechanisms, such as phytoextraction, rhizofiltration, and phytostabilisation, as well as through adsorption and complexation with organic constituents. Certain plant species exhibit hyperaccumulative properties, enabling them to absorb and store high concentrations of specific metals in their shoots and leaves. Harvesting this biomass can permanently remove metals from the system, preventing re-mobilisation and extending the system's service life (Vijayaraghavan et al. 2021; Yang et al. 2022). However, whether harvesting significantly impacts metal removal remains largely uncertain.

An investigation by Sun and Davis (2007) on the accumulation of dissolved metals in bioretention media planted with three different species revealed that metal uptake was only 0.2-3.3%, largely observed in roots and to a lesser extent in shoots, compared to 88-97% by the soil media, which was explained by the low plant biomass yields throughout the duration of the experiment. The authors suggested that the use of vegetation with higher biomass was necessary to achieve considerable metal uptake where harvesting might be a viable option to impact accumulation levels.

A more recent study by Beral et al. (2023) reported that apart from Zn and Mn, metal concentrations were largely below the detection limits for Pb, Cr, Cu and Ni in plant tissues, supporting the notion that plants play a supplementary role in metal uptake. Interestingly, the authors observed higher accumulation levels of Zn and Mn in leaves of *Juncus* species than the total amount in the influent added throughout the experiment. The surplus Zn and Mn levels, according to the authors, might have originated from the substrate. Given the higher biomass of *Juncus* plants, the study concluded that above-ground harvesting at the end of the growing season could contribute to metal removal.

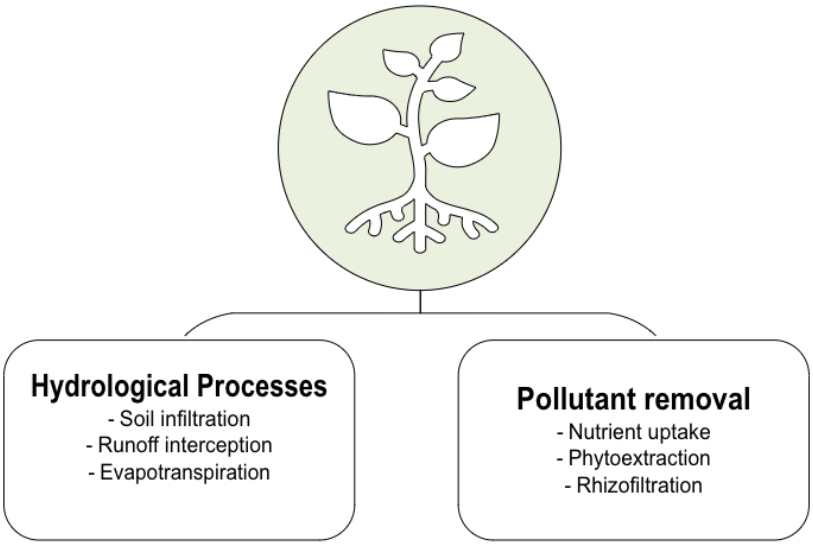

Figure 2.6 Plant-related processes in bioretention systems.

2.3.1.2.2 Phosphorus removal

Studies often yield conflicting results with phosphorus removal, with some highlighting the benefits of plants in enhancing removal efficiencies and others suggesting minimal contribution compared to unplanted systems. For example, Beral et al. (2023) found that plants contributed significantly to the removal of total phosphorus (TP) and orthophosphate (PO_4^{3-}) compared to unplanted systems. Similarly, Bratieres et al. (2008) reported that the presence of vegetation enhanced TP and PO_4^{3-} removal, with plants featuring more extensive roots such as *Carex appressa* being the highest performers. However, the difference between species was not of great practical significance as TP was relatively high (>77%) across planted and unplanted systems. The authors attributed this to filtration processes in the filter

media as TP was found to be mainly particulate bound in the influent. Nonetheless, The authors recommended that careful plants selection *Carex appressa* has the potential to improve TP removal in the long-term (Bratieres et al. 2008).

Similar findings were reported by Barrett et al. (2013) where the presence of vegetation was found to improve TP removal although the selection of species in that study did not significantly affect the removal performance. Conversely, a study by Read et al. (2008) demonstrated that the presence of plants had no significant effect on TP removal except for one species (*Carex appressa)* out of 20 tested species. However, the difference in the removal of total dissolved phosphorus (TDP) and filterable reactive phosphorus (FRP, a measure of PO_4^{3-})—which are more bioavailable—was statistically significant in all except one species (*Leucophyta*). This suggests that phosphorus interacts differently with plant species depending on its bioavailability. The study attributed the variation in performance to differences in root structure and morphology, affecting pollutant uptake, soil properties, and microbial community composition.

Most of the studies on bioretention plants were conducted on regional species, such as Australia, which may perform very differently in a temperate climate such as the UK. Detailed studies on plant-related processes in bioretention systems remain limited, especially on species native to the UK. Therefore, it is essential to conduct experiments on native species operating under specific UK conditions and clarify how vegetation influences pollutant removal processes, to identify the conditions under which plants provide measurable benefits. Direct comparisons between planted and unplanted systems are crucial for isolating the contributions of vegetation with seasonal variations, yet such studies remain limited (Dagenais et al. 2018).

2.3.1.3 Design guidelines for species selection

There are various factors to consider when selecting plants for bioretention systems, most of which are site-specific and require careful design considerations. These factors include the local climate, availability of plants locally, moisture conditions of the bioretention system, maintenance requirements, and more. Although many plants are recommended in bioretention design guidelines, research on plant selection, particularly regarding empirical evidence from UK native species is lacking. Current guidelines for plant selection in

bioretention systems include the following key design criteria (Bray et al. 2012; Payne et al. 2015; Woods-Ballard et al. 2015):

- Amenity: Ornamental plants with rich textures, such as ornamental grasses, are well-suited to bioretention systems such as rain gardens. Consideration of the system's location is important during the plant selection process; for instance, a vibrant planting scheme with flowering plants is recommended for urban environments.
- Seasonality: Perennial plants that survive winter and bloom again under favourable conditions require less maintenance and can provide colour throughout the season in urban environments.
- Soil moisture content: This is an important factor in the plant selection process to ensure plant survival and adequate functionality. For bioretention designs, plants should tolerate occasional droughts and short-term inundation. Plants that are less tolerable to occasional flooding should be avoided, particularly near the inlet. Plants positioned towards the middle of the bioretention system may experience drier conditions.
- Height: Similarly, short plants are suitable around the edges of the system, while taller plants are more appropriate for the middle. Their deeper root systems can benefit from the deeper soil media bed that is typically found in the centre of a bioretention system.
- Nativity: Native plants are valuable for providing biodiversity and wildlife habitats. Therefore, it is recommended to select species native to the specific site that are affordable and available in local nurseries.
- Plant density and growth rate: Plant sizing and density should be considered when installing a rain garden. A mix of densely packed plant species is recommended to prevent erosion and weed invasion, creating a stable and thriving bed with a robust, thick root system, which will reduce maintenance requirements. The Rain Garden Guide suggest a typical planting density of 6-12 plants/m^2 in 2-3 clumps, depending on the plant type and size (Bray et al. 2012).
- Pollutant removal and tolerance of expected pollution load: Bratieres et al. (2008) and Muerdter et al. (2018) suggest using plants with extensive, dense root systems featuring fine hair-like structures to maximise pollutant capture potential, particularly for nutrient removal.

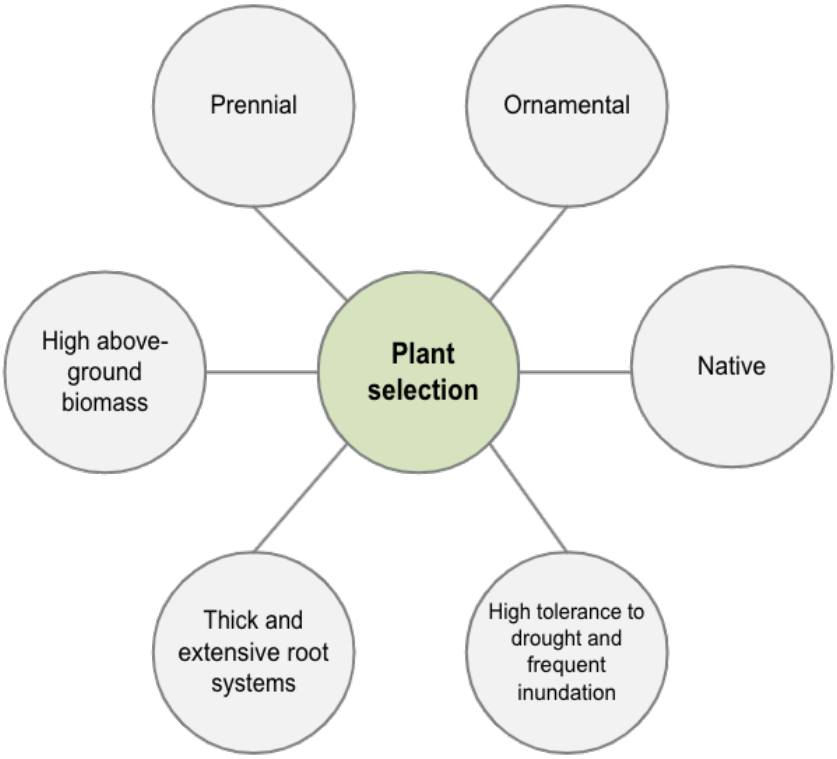

Figure 2.7 Plant selection criteria based on design manuals.

2.3.2 Saturated zones

Saturated zones (SZ) in bioretention systems, created by upturned underdrain elbows or raised outlet pipes (Figure 2.8) play a critical design feature for improving the removal of stormwater pollutants, including nutrients and metals while improving system resilience during dry periods (Muerdter et al. 2018). By maintaining a permanently damp layer at the bottom of the biofilter, SZs support microbial processes such as nitrification (conversion of ammonia to nitrate) and denitrification (converting nitrate into nitrogen gas), buffer against plant water stress, and retain stormwater between inflow events. Bioretention systems differ from wetlands in their dynamic moisture conditions and free-draining design (no drainage restrictions), which results in lower organic content and fluctuating redox potential (Payne et al. 2014b).

Unlike wetlands, which maintain stable anoxic conditions that promote denitrification, bioretention systems experience prolonged drying and oxygenated inflows, potentially limiting nitrate removal. While rapid drying in conventional biofilters can enhance phosphorus removal (less studied compared to nitrogen), prolonged drying reduces nitrogen

and phosphorus retention. Conventional biofilters also dry faster than those with SZs, leading to soil cracking and preferential flow paths, which can release bioavailable nutrients upon re-wetting (Zinger et al. 2021). Carbon sources such as wood chips and straws are often added in the SZ to support denitrification (Payne et al. 2014b).

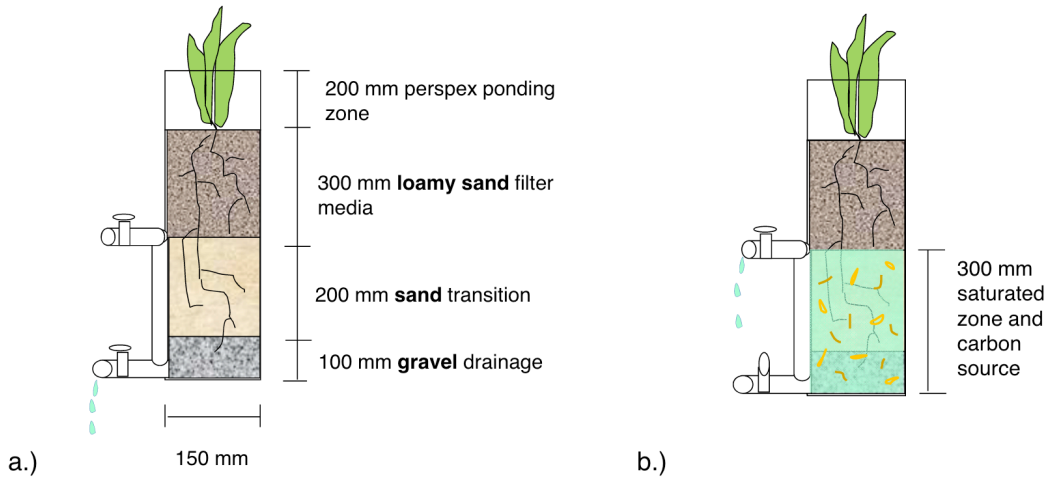

Figure 2.8 Design configuration of bioretention column experiments by Payne et al. (2014b), showing a) non-saturated design, b) saturated zone with carbon source (image: Payne et al.).

Previous studies by (Payne et al. 2014b; Payne et al. 2014a; Payne et al. 2018) and Zhang et al. (2011) demonstrate that SZs generally enhance total nitrogen (TN) removal by maintaining anaerobic conditions and providing a carbon source for microbial activity. Payne et al. (2014b) compared the effects of SZ in vegetated and non-vegetated systems. The study showed that during wet periods, vegetated systems with SZs achieved TN reductions of 87% outperforming non-saturated designs (75%). The study highlights that the effect of SZ was less significant in high-performing plants, which was attributable to the rapid microbial processes occurring before drying between events—a process that is minimal during frequent dosing.

Zinger et al. (2021) compared free-draining and SZ designs under varying antecedent dry weather periods (ADWP) for up to 7 weeks of drying. The study demonstrates that SZ systems maintained higher hydraulic conductivity (20%) and significantly improved TSS removal efficiency (98%) during extended dry periods, reducing the risk of media cracking and fine particle migration, which can cause clogging in free-draining designs.

These effects diminished after 4 weeks of drying, when moisture content was found to be similar across all designs. Payne et al. (2014) noted a similar observation. Following a dry period of 15 days, SZs mitigated performance declined, with saturated vegetated systems reducing TN by 12% to 78%, compared to non-saturated designs, which often increased TN concentrations. This highlights the critical role of SZs in maintaining biofilter functionality during extended dry periods by preserving soil moisture and supporting plant and microbial activity.

In terms of plant response, SZs play a nuanced role, with species-specific responses influencing system performance. Payne et al. (2018) observed that SZs did not uniformly affect plant characteristics; some species exhibited increased root mass and fine roots in SZs, while others thrived in free-draining conditions. High-performing species, with extensive root systems and high total biomass, showed less dependency on SZs for nutrient removal, likely due to efficient nitrogen assimilation. In contrast, low-to-mid-performing species benefited significantly from SZs, particularly during dry periods.

Despite the demonstrated benefits of SZs, their impact on phosphorus removal remains unclear, with some studies reporting enhanced TP removal (Zhang et al. 2011; Wu et al. 2017) and others showing no significant effect (Barrett et al. 2013), or increased TP leaching (Dietz and Clausen 2006). Previous studies by Lucas (2015) and Kiiza (2017) on constructed wetlands utilised a tidal vertical flow regime, in which water was held in the system for a set period of time, known as residence time, to enhance denitrification processes, followed by rapid draining to re-introduce anaerobic conditions and oxygen transfer. The studies found that the systems achieved TP removal efficiencies of 71-83% (Lucas 2015), and 67% (Kiiza 2017).

This approach balanced the benefits of extended residence time such as enhanced pollutant removal and adsorption, with periodic aeration to prevent prolonged anaerobic conditions, which could reduce phosphorus removal (Dietz and Clausen 2006; Wu et al. 2017; Xiong et al. 2019). However, these studies did not investigate the interaction between saturation and different plant species, which requires further investigation to identify optimal combinations of operational conditions.

2.3.3 Substrate media composition and amendment

The performance of bioretention systems is heavily influenced by the characteristics of the substrate media, and similar to vegetation, it also possesses a dual functionality in impacting the hydrological and the treatment performance of bioretention systems (Chen et al. 2021). Therefore, the selection of an appropriate bioretention medium is of critical importance, as it sustains plant health, infiltration rates, pollutant removal efficiency, and system structural stability, all of which are dependent upon media type and depth (Vijayaraghavan 2016; Premarathna et al. 2023).

Over the past two decades, bioretention media design has evolved significantly, shifting from basic volume reduction and limited pollutant removal to comprehensive stormwater treatment for reuse (Tirpak et al. 2021). Particle size distribution is a critical factor influencing the physical properties of bioretention media, including surface area, bulk density, and pore size distribution. These properties, in turn, affect hydraulic conductivity, maintenance frequency, and pollutant removal. For example media with a higher percentage of fine particles like silt and clay provides higher surface area which is beneficial for pollutant removal (Hatt et al. 2008; Logsdon 2008), however, they have greater tendency to clog the media and cause system failure (Hatt et al. 2008; Li and Davis 2008c). A balance between coarse and fine particles is essential to optimise hydraulic performance while maintaining efficient pollutant removal.

2.3.3.1 Typical bioretention media

Current design guidelines of bioretention media typically recommend a well-graded soil with varying proportions, typically sand-based with consistency varying from sand, sandy loam, to loamy sand. The soil grading varies across geographical jurisdictions depending on the locally available soil. For example, the UK SuDS manual and the Australian FAWB recommends a media consistency of fines (> 30%), medium sand (30-65%), and coarse sand (50-60%) to maintain a saturated hydraulic conductivity between 100 mm/h and 300 mm/h (FAWB 2009; Woods-Ballard et al. 2015). Example grading is presented in Table 2.3. On the other hand, typical bioretention soil composition in tropical climates such as Singapore involves a higher percentage of clay due to the regional catchment characteristics, with design guidelines ranging from clay (5-30%), silt (5-60%) and sand (20-75%) (Lim and Lu 2016).

Table 2.3 Example grading of a bioretention filter medium as outlined in the SuDS Manual (Woods-Ballard et al. 2015).

Sieve size (mm)	% passing
6 – 2	100
2 – 0.6	90 – 100
0.6 – 0.2	40 – 70
0.2 – 0.063	5 – 20
> 0.063	< 5

Another influential factor is the organic fraction of the bioretention media, which is vital in sustaining plant and microbial health. Organic Matter Content (OMC) contributes to pollutant removal, including, nutrients (Reddy et al. 2014b), heavy metals (Mohanty et al. 2018), and organic pollutants (Ulrich et al. 2017b), through organic complexation and biodegradation. However, OMC can also leach nutrients into the effluents (Bratieres et al. 2008; Sun et al. 2020), necessitating careful selection and testing of organic amendments (FAWB 2009; Tirpak et al. 2021). To minimise this, the SuDS manual recommends the OMC in the bioretention media in the range of 3-5% by volume (Woods-Ballard et al. 2015).

Typical loam sand media and topsoil have proven to be effective in removing suspended solids (Li and Davis 2008b), and particulate metals and phosphorus (Hatt et al. 2007b; Hatt et al. 2007a; Bratieres et al. 2008), through mechanical filtration, settling and sedimentation processes (Hatt et al. 2007a; Hatt et al. 2008; LeFevre et al. 2015), but their performance is variable in capturing dissolved pollutants, which are a major concern as they constitute a significant percentage of urban runoff and are more mobile and bioavailable (LeFevre et al. 2015).

The leaching of dissolved phosphorus from bioretention media have been demonstrated in several studies and remains a persistent concern (Bratieres et al., 2008; Iqbal et al., 2015; Jacklin et al., 2021b; LeFevre et al., 2015). Typical substrate media also demonstrated high potential for clogging, significantly reducing the lifespan of bioretention systems (Li and Davis 2008b; Le Coustumer et al. 2012).

2.3.3.2 Media amendment for enhanced performance

Given the diverse requirements for bioretention systems, including effective treatment of dissolved pollutants, resilience during extreme weather events, no single material can fulfil all necessary criteria. Consequently, a combination of organic and inorganic materials is typically used to create substrates with specific properties (Vijayaraghavan et al. 2021). Recent research has focused on enhancing media performance by incorporating additives to improve hydraulic conductivity, water retention, and pollutant removal. A wide range of amendments, including vermiculite (Bratieres et al. 2008), zeolite (Li et al. 2020), fly ash (Hermawan et al. 2021), perlite (Jacklin et al. 2021b), and biochar (Ashoori et al. 2019), have been explored to enhance bioretention media performance.

Studies have demonstrated that amended media can significantly improve the removal of heavy metals (Sun et al. 2020; Spahr et al. 2022), and nutrients (Bock et al. 2015; El Hanandeh et al. 2018; Rahman et al. 2020) compared to traditional filter media. However, the adoption of these amendments in practice has been limited due to factors such as high costs, inconsistent performance, and regulatory constraints (Tirpak et al. 2021; Vijayaraghavan et al. 2021). Further research and regulatory support are needed to facilitate the widespread adoption of these advanced materials in bioretention design.

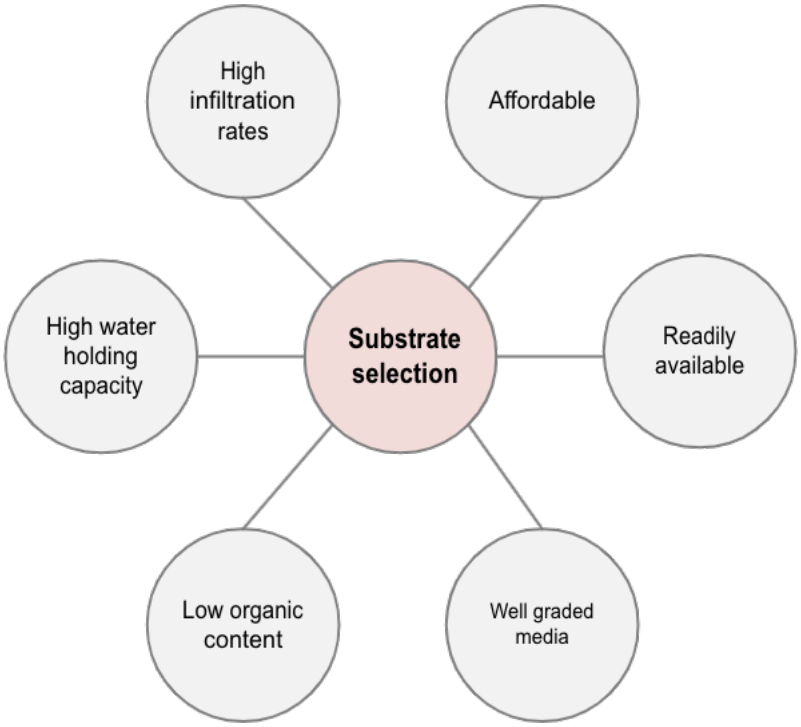

Figure 2.9 Selection of substrate characteristics for bioretention systems.

2.3.4 Biochar

One material that has shown significant potential for bioretention application due to its affordability, and high sorption capacity for a wide range of pollutants is biochar. A carbon-rich material produced via thermochemical processes such as the pyrolysis or gasification of plant-based or waste biomass in closed environments with little to no oxygen (Uchimiya et al. 2011; Yao et al. 2012; Reddy et al. 2014a). Its ubiquitous presence in the environment, constituting up to 35% of soil organic carbon, makes it a prominent carbonaceous geo-sorbent in soils and sediments (Uchimiya et al. 2011). It has garnered significant attention for its multifunctional applications as both a by-product of biofuel production and a sustainable soil amendment for water treatment (Reddy et al. 2014a; Biswal et al. 2022).

2.3.4.1 Properties of biochar

Biochar has unique physicochemical and biological properties including high surface area, high porous structure, surface functional groups, hydrophobic surfaces, and high mineral and ash content, enabling its application in enhancing soil fertility, sequestering carbon, and water treatment (Melo et al. 2013; Tian et al. 2014; Mohanty et al. 2018). Its ability to support biofilm development, plant growth and microbial activity, further enhances its potential as amendment material in bioretention design (Mohanty et al. 2018; Boehm et al. 2020; Biswal et al. 2022). The properties of biochar are governed by pyrolysis parameters such as temperature, feedstock type, and production conditions (Agrafioti et al., 2013; Mohanty et al., 2018).

Biochar is typically produced at pyrolysis temperatures ranging from 300 to 800°C. It has been shown that higher temperatures (e.g. 500-700 °C) increase porosity, surface area, carbon content, and aromatic structure and stability (Agrafioti et al. 2013; Biswal et al. 2022), However, they decrease biochar yields, water sorption capacity and cation exchange capacity (CEC) (Agrafioti et al. 2013). Whereas, low pyrolysis temperatures (e.g., 250-350 °C) may result in a higher CEC due to preserved surface functional groups and volatile organic matter on the biochar (Agrafioti et al. 2013; Mohanty et al. 2018). The production processes also influence the yield of biochar, for example slow pyrolysis typically yields higher quantities of biochar compared to fast pyrolysis or gasification (Biswal et al. 2022).

Feedstock composition is another critical factor that determines biochar properties, as biochar retains the pore structure and the chemical properties of its source material. Highly dense structures, such as those derived from hardwood, tend to have lower porosity and smaller surface area than softwood-derived biochar (Mohanty et al. 2018). On the other hand, biochar derived from industrial wastewater such as sewage sludge contains high metal content giving it excellent adsorption capacity for heavy metals, while nutrients-rich biochar such as manure-based biochar may affect nutrients retention differently depending on its cation and anion exchange capacities (Mukome et al. 2013; Mohanty et al. 2018).

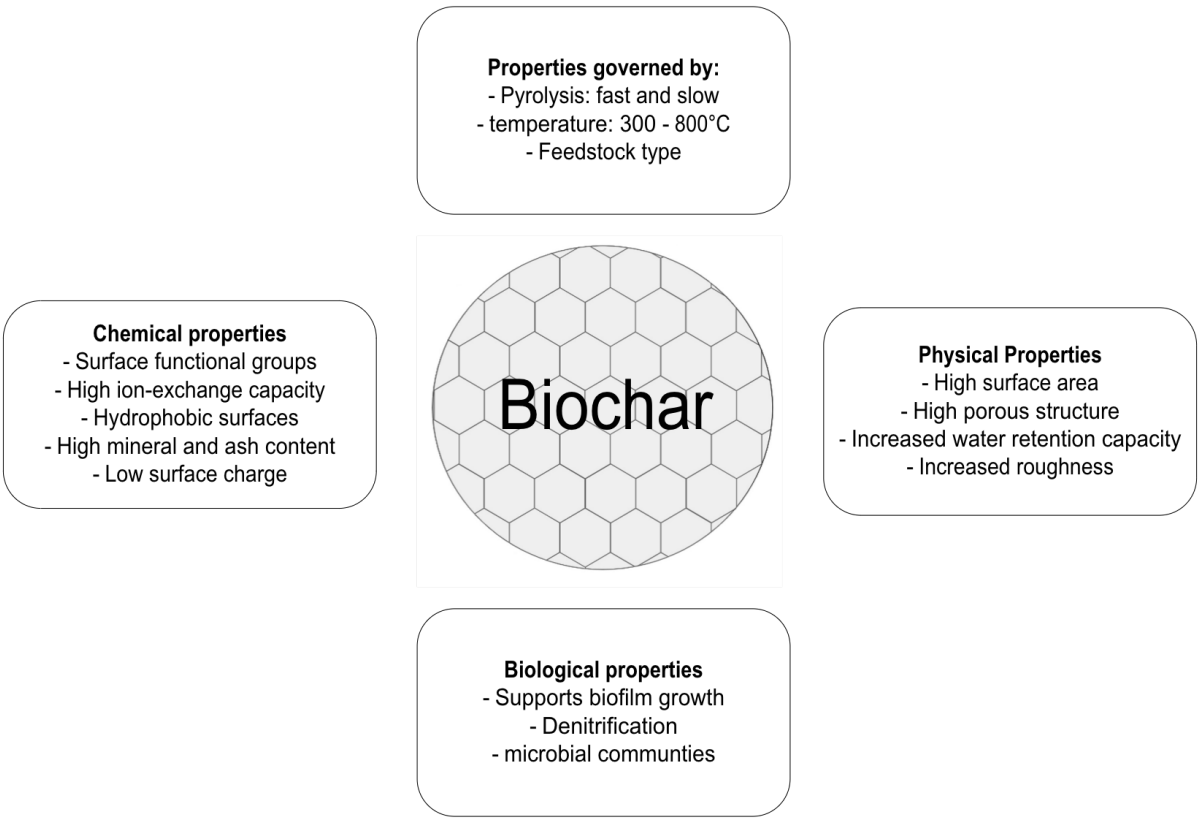

Figure 2.10 Physical, chemical and biological properties of biochar, and key parameters affecting its properties.

2.3.4.2 Biochar pollutant removal

While biochar properties show promise for water treatment, research has shown that its effectiveness in removing pollutants depends on its properties, pollutant characteristics and treatment conditions (Mohanty et al. 2018). As a results, the optimal pyrolysis temperature is determined by the intended application of the biochar due to its synergistic properties. For example studies on biochar removal of microplastics showed that biochar produced at higher

pyrolysis temperatures (e.g. 700) was more effective in trapping emerging pollutants such as microplastics through biocahr's porous structure and Van der Waals forces (Wang et al. 2020; Hsieh et al. 2022; Ahmad et al. 2023).

In contrast, higher temperatures may compromise metal and nutrient retention due to reduced CEC and surface functional groups, which are preserved in lower temperatures, despite resulting in smaller surface area (Mohanty et al. 2018; Jagadeesh and Sundaram 2023). Similarly, Biochar high in ash content can increase the effluent pH which favours metal removal (Mohanty et al. 2018).

The particle size of biochar also affects removal performance. Researchers have demonstrated that biochar with finer particles exhibits higher removal rates for *E. coli* (Mohanty and Boehm 2014), and nutrients removal (McCrum et al. 2017), owing to the larger surface area provided by its finer particles. However, other studies have reported no significant effect of biochar properties, including particle size and feedstock type, on phosphorus removal (Bock et al. 2015). Biochar particle size and feedstock composition can also affect the hydraulic conductivity of the media, which can in turn affect treatment performance. Biochar particles have internal pores, which increase its water holding capacity and hydraulic conductivity. However, some bioretention studies have reported that biochar addition to substrate media decreased the hydraulic conductivity, depending on the particle size distribution and feedstock type (Mohanty et al. 2018).

2.3.4.3 Applications in stormwater treatment

Recent studies in stormwater applications have demonstrated biochar's effectiveness in adsorbing nutrients (Iqbal et al. 2015; Ashoori et al. 2019; Rahman et al. 2020), organic and microbial contaminants (Mohanty et al. 2014; Ulrich et al. 2017a; Ulrich et al. 2017b), and heavy metals (Reddy et al. 2014a; Cairns et al. 2020; Hasan et al. 2020; Sun et al. 2020).

2.3.4.3.1 Heavy metal removal

The removal of heavy metals by biochar involves multiple abiotic processes, including physical sorption, electrostatic interactions, precipitation, complexation, ion-exchange, and chemical reduction; the relative significance of each mechanism depends on the specific metal and biochar characteristics (Biswal et al. 2022). The metal retention capacity of biochar

is influenced by biocahr's surface area, pH conditions, and the presence of surface functional groups (C-O groups), which give biochar a negative surface charge, creating adsorption sites for effective metal binding, while acidic groups can aid in electrostatic interactions and support surface complexation with metal cations (Uchimiya et al. 2011; Reddy et al. 2014a; Sun et al. 2020).

A study by Hasan et al. (2020) explored the removal mechanisms of heavy metals by pinewood biochar, and biochar modified by nanoscale-zerovalent iron (BC-nZVI), in a series of batch and column experiments using highly concentrated synthetic stormwater solutions (2.5-60 mg/L). The study revealed that BC-nZVI significantly improved dissolved metal ions (Cd and Zn) removal by 43-50% and 42-57% respectively, compared to unmodified biochar. The transformation of surface functional groups (C-O and -COOH) to (C-O-Fe) iron oxides on the surface functional groups enhanced reduction reactions through increased adsorption sites for Zn and Cd ions.

However, there was no significant difference (≈ 1%) in Cu removal between modified and unmodified biochar, due to Cu's high affinity to sorbents. The study concluded that the primary removal mechanisms of heavy metals in biochar is primarily governed by chemisorption processes such as surface complexation and reduction reactions (Hasan et al. 2020). However, the study was performed under constant flow rates for 195 days, which are unusual for bioretention unsaturated conditions.

Another column study by Sun et al. (2020) investigated heavy metal removal by forestry-wood derived biochar, in intermittent wetting and drying cycles to simulate bioretention unsaturated conditions. They found that biochar was highly effective in removing heavy metals, particularly Zn (51.6-100% removal). The study reported that the removal efficiency was further enhanced by the co-existence of kaolinite in the synthetic stormwater solutions, providing an abundance of metal adsorption sites. The study highlighted that metal removal efficiencies generally improved and stabilised with subsequent cycles, and that the removal efficiencies depended on biochar properties and the co-existence of organic and inorganic colloids (e.g. kaolinite and humic acid), with heavy metals in the stormwater mixture (Sun et al. 2020).

2.3.4.3.2 Phosphorus removal

Studies showed less efficient and more variable removal of phosphorus compared to heavy metals and other nutrients such as nitrogen, with some studies reporting net leaching of phosphorus in biochar columns (Yao et al. 2012; Iqbal et al. 2015; Kuoppamäki et al. 2021). Biochar retention capacity for phosphorus, especially phosphate (PO_4^{3-}), is governed by abiotic mechanism such as adsorption, precipitation and complexation, which are largely impacted by pH and the presence of anions (e.g. sulphate bicarbonate) and cations (e.g. metal oxides) (Biswal et al. 2022). The anionic nature of phosphate allows it to form complexes and precipitates with positively charged metals co-existing in stormwater, as well as surface functional groups in biochar with electrostatic attraction shifting to repulsion under alkaline conditions. However, this mechanism is limited in biochar due to its typically low anion exchange capacity which reduce its adsorption capacity for phosphate (El Hanandeh et al. 2018; Biswal et al. 2022).

A pilot-scale study by Ulrich et al. (2017) reported that although biochar (pinewood) amended media in vegetated systems removed 60% of total dissolved phosphorus (TDP), they were less efficient than sand filters, which consistently removed TDP to below the limits of detection. Nonetheless, the study highlights promising results for biochar removal of trace organic contaminants. Similarly, a study by Kuoppamäki et al. (2021) reported that biochar (spruce wood) amendment was the least efficient in TP removal with 52% removal rate, compared to other investigated media. However, the removal rate measured in this study was related to the high TP loading in the influent, which was almost entirely in particulate state. The study mentioned that the addition of biochar resulted in increased dissolved phosphorus leaching compared to the stormwater input, suggesting that biochar was a source of phosphate in the effluent, which was supported by a leaching test. The study also highlighted that vegetation had minimal interaction on TP removal (Kuoppamäki et al. 2021).

To counter leaching issues, studies have investigated modifying biochar with metal-oxides such as iron-oxides (Xiong et al. 2019) and magnesium-oxides (Zhao et al. 2021), to promote phosphate removal through complexations with positively charged metal oxides. For example, a column study conducted by Xiong et al. (2019) showed that iron-coated biochar (derived from rice husk) was more effective in total phosphorus removal (93.7%) compared to unmodified biochar (57.4%).

However, the study highlighted that the introduction of a saturated zone may have compounded the effects of TP leaching in the unmodified biochar filters due to induced anaerobic conditions which possibly remobilised and leached particulate P from the filters (Xiong et al., 2019).

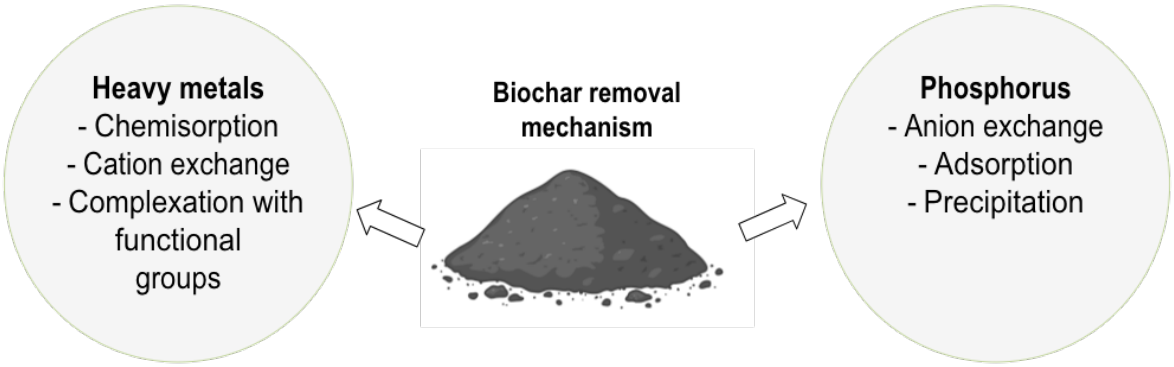

Figure 2.11 Key removal mechanisms of heavy metals and phosphorus governed by biochar.

The persistent challenge of dissolved pollutants bypassing standard sand filters remains a concern in bioretention systems. Whilst biochar-amended media show promise for enhancing their removal, the current evidence base is fragmented by a limited number of studies that accurately simulate the design characteristics and hydrological conditions of bioretention systems. Consequently, the effects of biochar amendment on system performance are not yet fully understood, owing to the complex, synergistic properties of biochar and its interactions with bioretention design components.

Further research is needed to isolate these variable effects under controlled conditions to inform practical application. Moreover, most existing studies assess pollutant removal in isolation rather than in combined synesthetic solutions and often fail to differentiate between the dissolved and particulate forms typically present in real stormwater. Recognising this distinction is crucial, as each form interacts uniquely with the filter media, engaging complex removal mechanisms, which is fundamental to designing more effective bioretention systems.

2.4 Fate and management of captured pollutants

Although bioretention systems are widely adopted as a stormwater control measure, there is relatively limited research on the long-term performance of these systems, particularly regarding the fate of pollutants captured over their life cycle (Dechesne et al. 2005; Guo et al. 2018). While the spatial distribution and fate of pollutants within bioretention media have started to be quantified (Li and Davis 2008a; Johnson and Hunt 2016), significant gaps remain in understanding the potential for pollutants to accumulate to toxic levels or re-mobilise in infiltrated runoff and pose environmental risks to groundwater and receiving water bodies, which necessitates further investigation (Li and Davis 2008a; Johnson and Hunt 2016).

Recent research has shifted focus towards understanding the internal mechanisms and soil profiles within bioretention systems, particularly the leaching phenomena in the filter media over extended periods (Shao et al. 2018). There is a notable gap in the literature concerning how the soil composition within bioretention systems evolves over time under the influence of stormwater accumulation (Jenkins et al. 2010). This knowledge is essential for estimating pollutant enrichment over the long term and for planning appropriate maintenance activities (Tedoldi et al. 2016).

2.4.1 Accumulation of heavy metals in bioretention media

Pollutants such as heavy metals, commonly referred to as potentially toxic elements (PTE), do not degrade over time, posing significant environmental and human health risks, through pathways such as hand-to-mouth ingestion of contaminated bioretention media, which raises concens related to the management, maintenance, and disposal of bioretention media (Jones and Davis 2013; Johnson and Hunt 2016). Studies indicate that heavy metals are predominantly captured within the upper layers of bioretention media, typically within the top 10-30 cm, with the highest accumulation occurring near the inlet (Hatt et al. 2008; Davis et al. 2009; Jones and Davis 2013; Johnson and Hunt 2016; Al-Ameri et al. 2018).

For instance, Li and Davis (2008) observed that heavy metals and sediments accumulated primarily within the top 10-20 cm of the media. This top-heavy accumulation pattern is attributed to two primary mechanisms: (1) the rapid settling, straining, and depth filtration of

particulate-bound metals (2) the effective capture of dissolved metals through sorption processes (Read et al. 2008; Jones and Davis 2013; LeFevre et al. 2015). Li and Davis (2008) suggested that a shallower depth design between 20-40 cm is sufficient for effective retention if metals are the target pollutants. Laboratory-scale (Hatt et al. 2008; Lim et al. 2015; Wu et al. 2017) and field-scale studies (Hossain et al. 2008; Jones and Davis 2013; Al-Ameri et al. 2018) have corroborated these findings, demonstrating similar metal distribution profiles.

Despite this general trend, captured metals can remobilise resulting in variations in soil profiles, and the mechanisms governing these variations remain poorly understood, complicating the prediction of metal behaviour in bioretention media (Li and Davis 2008a). A comprehensive review by Tedoldi et al. (2016) examined the accumulation and transport of pollutants, including heavy metals, in SuDS filter media. The review highlighted that heavy metal distribution profiles and surface concentrations were not correlated with system operating time or traffic intensity in roadside systems. Conversely, Al-Ameri et al. (2018) reported that metal accumulation levels were strongly correlated with catchment characteristics such as urban density, bioretention to catchment area ratio and current and past land use. However, no significant increase in metals concentrations were observed in the 8-year study period (Al-Ameri et al. 2018).

Metal mobility within the soil column is influenced by the presence and quantity of key solid-phase constituents, including mineralogical clays, iron (Fe), aluminium (Al), and manganese (Mn) oxides, soil organic matter, and carbonates. Additionally, physicochemical interactions such as dissolution, oxidation, reduction, chemisorption, interactions with surfactants in runoff, changes in soil pH, organic matter degradation, at the solid/water interface play a critical role in metal accumulation and mobilisation (LeFevre et al. 2015; Johnson and Hunt 2016; Tedoldi et al. 2016).

High rainfall events may also contribute to the mobilisation of heavy metals. For example, Shao et al. (2018) noted that suspended solids remobilisation was particularly pronounced during high inflow events, with a positive correlation between inflow velocity and sediment release rates. However, sediment release rates declined more rapidly than inflow velocity during the later stages of rainfall events, suggesting the existence of a critical threshold below which remobilisation was unlikely (Shao et al. 2018).

Further research is needed to better understand the long-term fate of heavy metals in bioretention systems and to develop strategies for mitigating their environmental and health risks.

2.4.2 Performance monitoring and maintenance strategies

Despite the widespread popularity of bioretention systems as a mitigating strategy against the impacts of stormwater runoff, challenges related to their long-term performance and maintenance remain an area requiring further research (Shao et al., 2018). Research has shown that the hydraulic performance of bioretention systems is inevitably compromised without regular maintenance and inspections (Blecken et al. 2017; Yin et al. 2021). A key issue is the accumulation of fine-grained sediments, primarily silt and clay, in the surface layer, which leads to clogging and reduced infiltration rates. This is particularly pronounced near the inlet, increasing the risk of overflow and the discharge of untreated runoff (Virahsawmy et al. 2014).

To optimise maintenance plans, the distribution of captured pollutants across the soil media—from the surface layer to the filter bed and inlet to inlet—must be understood as it plays a critical role in determining maintenance needs and subsequent costs in restoring the functionality and extending the lifespan of the system. Maintenance tasks such as removing the top 5-10 cm of media, which was demonstrated to retain a significant proportion of incoming sediments, especially near inlets are essential to sustain infiltration rates and reduce environmental risks (Dechesne et al. 2005; Davis et al. 2009). In extreme cases, partial or complete excavation of the filter bed may be necessary to address severe clogging or pollutant build-up exceeding regulatory limits (Komlos and Traver 2012).

The choice of filter media also influences maintenance requirements. Coarse media, such as gravel, are effective at removing coarse sediments but less so for dissolved pollutants. These systems are prone to clogging as fine sediments migrate and form low-permeability layers at the filter base, necessitating complete media replacement and incurring avoidable costs (Kirk et al. 2006; Andrew and Vesely 2008). In contrast, fine media, such as soil, offer better pollutant removal through mechanisms like sorption, ionic adhesion, and precipitation. Clogging in fine media systems typically occurs at the surface, making it easier to manage through scraping (Hatt et al. 2008; Jenkins et al. 2010; Yergeau and Obropta 2013).

Vegetation further enhances performance by creating preferential flow pathways, alleviating surface clogging, and improving infiltration rates (Virahsawmy et al. 2014). However, other factors, such as media compaction, biofilm formation, and organic matter decomposition, can also reduce hydraulic capacity over time, necessitating adaptive maintenance strategies (Andrew and Vesely 2008; Shuster et al. 2017).

The environmental impacts of bioretention systems, including construction, maintenance, and disposal, should be considered during decision-making. Life-cycle assessment (LCA) is a suitable method for quantifying these impacts, though data on the disposal stage remain limited, as most systems are still operational (Andrew and Vesely 2008; Xu et al. 2019). Research by Andrew and Vesely (2008) on the life-cycle cost suggests that smaller, well-designed bioretention systems can achieve significant life-time savings while meeting treatment efficiency expectations. However, challenges persist in evaluating SuDS maintenance due to the lack of comprehensive spatial and temporal data, particularly for water and soil quality monitoring (Asleson et al. 2009; Xu et al. 2019).

2.4.2.1 In-situ monitoring

Traditional monitoring methods, which rely on discrete grab samples and laboratory analysis, often yield low-resolution data that are difficult to interpret and may not adequately support management decisions (Asleson et al. 2009; Pellerin et al. 2016). Moreover, they are often hindered by the high cost and logistical challenges associated with conventional laboratory methods, such as Atomic Absorption Spectrophotometry (AAS) and Inductively Coupled Plasma Mass Spectrometry (ICP-MS).

Advances in remote sensing and in-situ monitoring offer promising solutions. High-frequency, real-time data collection can provide detailed insights into soil and water quality and quantity, enabling better design and maintenance strategies (Kalnicky and Singhvi 2001; Pellerin et al. 2016). For instance, Abbott and Comino-Mateos (2003) used in-situ sensors to monitor permeable pavements, demonstrating the potential for continuous data collection to improve system evaluation. Similarly, in-situ portable X-ray fluorescence (pXRF) technologies offer a rapid, non-destructive, and cost-effective solution for in-situ soil quality measurements, enabling real-time decision-making for preliminary risk assessments (Venvik and Boogaard 2020; Lenormand et al. 2022).

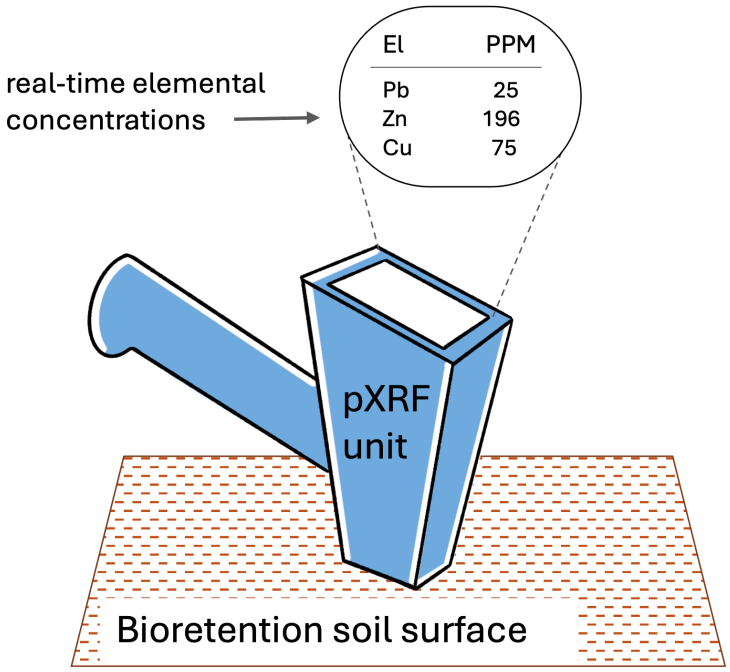

Figure 2.12 Rapid in-situ assessment of heavy metal concentrations in bioretention systems.

The pXRF technique facilitates high-resolution contamination mapping and can serve as a decision-support tool to identify hotspots, guide targeted remediation, and ensure adherence to soil screening thresholds (Radu and Diamond 2009; Venvik and Boogaard 2020; Lenormand et al. 2022). Whilst pXRF is commonly deployed in highly metal-polluted sites, including mining areas, and landfills (Kalnicky and Singhvi 2001), its application to map heavy metal distribution in SuDS remains rarely explored. Recent studies using in-situ monitoring via pXRF to map heavy metals distribution on the surfaces of infiltration basins and swales include; Boogaard et al. (2024), Lenormand et al. (2022), and Venvik and Boogaard (2020). These studies demonstrated the suitability of pXRF for qualitive risk assessment of field-scale SuDS.

However, a recognised limitation is that pXRF data are often less accurate than traditional laboratory methods, as its performance is contingent upon soil matrix characteristics, such as particle size and moisture content, necessitating tailored calibration protocols for reliable quantification (Kalnicky and Singhvi 2001; Lenormand et al. 2022). Consequently, its strength lies in identifying hotspots and guiding where to conduct the limited number of subsequent, more accurate laboratory tests.

In summary, while bioretention systems are effective in stormwater management, their long-term performance depends on addressing maintenance challenges, improving monitoring techniques, and integrating life-cycle considerations into design and operation. High-resolution data and advanced technologies, such as remote sensing and in-situ monitoring, hold significant potential to enhance system performance and inform maintenance strategies.

2.5 Summary

This review has examined the challenges of urban stormwater pollution, and critically assessed key bioretention design elements, with a particular emphasis on the role of vegetation, and biochar amendment in bioretention systems. It has also addressed critical issues related to the long-term fate and management of captured pollutants. While bioretention systems have proven benefits, the effectiveness and longevity of these systems depend on proper design and ongoing maintenance. This synthesis has identified the following knowledge gaps:

1. While vegetation is recommended to improve infiltration and pollutant removal, their performance is highly variable depending on species selection, different climate regions, and saturation conditions. There is a critical lack of empirical data for UK-native species, even those recommended in national design manuals.
2. While the potential of biochar amendments is well-recognised, its practical application in bioretention systems is hindered by a fragmented understanding of its effectiveness, due to the inherent complexity of biochar's synergistic properties, which vary widely with feedstock type and production conditions. More research on its removal mechanisms under unsaturated conditions, particularly the distinction between particulate and dissolved pollutants, when treating complex stormwater mixtures is required to guide its effective application.
3. The long-term spatial accumulation of pollutants, especially heavy metals, in bioretention systems is a significant concern that is poorly integrated into maintenance guidelines. Studies have shown that heavy metals accumulate predominantly in the upper layers of bioretention systems, posing potential health risks and regulatory breach if not properly managed. Cost-effective monitoring strategies are needed to quantify accumulation patterns and inform targeted maintenance.

To address these gaps, this research establishes the following main objectives:

1. To investigate the influence of selected UK-native plant species on the hydrological and treatment performance of bioretention systems, and to evaluate their interaction with saturation conditions.
2. To determine the effects of biochar amendments on enhancing the removal of stormwater pollutants and provide mechanistic insights into distinct removal mechanisms.
3. To examine the spatial accumulation of heavy metals in bioretention media, identify contamination hotspots through rapid in-situ mapping, and evaluate the impact of system age and proximity to the inlet on accumulation levels.

Chapter 3. Materials and Methods

This chapter details the laboratory column experiments designed to investigate the effects of two key design variables (vegetation and biochar amendments) on bioretention system performance, and the long-term accumulation of heavy metals in the biofilter media. To effectively manage the complexity of these variables and practical resource constraints, a dual experimental approach was implemented, consisting of a large-scale and a small-scale column setup.

1. The large column setup was designed to evaluate the influence of mature vegetation and controlled drainage configurations on pollutant removal and system hydrology. Its size was specifically chosen to accommodate well-established root systems and approximate field-scale conditions.
2. The small column setup was designed to isolate and evaluate the effectiveness of biochar amendments within the filter media for enhancing pollutant retention. This highly controlled environment was essential for a precise examination of the biochar's inherent removal mechanisms, free from the confounding biological processes present in the vegetated systems.

This isolated approach was essential for two main reasons:

1. Biochar performance is highly dependent on properties governed by feedstock type and pyrolysis conditions, leading to widely variable characteristics. The smaller, more manageable bench-scale setup (requiring less media, biochar, and space) provided a resource-efficient method to screen biochar efficiency before committing to its use in larger, more complex systems. This preliminary step was critical for selecting appropriate biochar types for future integrated studies.
2. Investigating complex interactions between plant species, drainage configurations, and multiple biochar types simultaneously, would have introduced significant confounding factors, making it difficult to attribute any observed effects to a single variable. Isolating the biochar variable in the small columns allowed for a controlled assessment of its specific contribution to pollutant retention. Therefore, the experiment specific procedures (e.g., media preparation, dosing method, inclusion of microplastics) were optimised for its distinct objectives under controlled conditions.

Consequently, direct interaction effects between specific plant species and biochar amendments were beyond the scope of this research. Both setups employed core methodological principles (e.g., synthetic stormwater composition, key analytical and statical procedures). However, their specific configurations were designed to address separate but complementary research questions regarding bioretention design.

3.1 Site description

The large column experiment was conducted in an open car park near the Characterisation Laboratories for Environmental Engineering Research (CLEER), School of Engineering, Cardiff University (51°29'01.9"N, 3°10'12.5"W). The area experiences a maritime climate characterised by mild, often cloudy, wet, and windy weather. The daily average temperatures range between 19-22°C in summer and 5-6°C in winter. During the experimental period (2023-2024), the average air temperature was 17°C in summer and 5°C in winter (Met Office [no date][a]).

Figure 3.1 Location of large bioretention columns at Cardiff University, School of Engineering.

3.2 Synthetic stormwater

Laboratory studies of bioretention columns typically use synthetic or semi-synthetic stormwater to minimise variations in inflow concentrations while simulating realistic compositions. Various methods exist for creating a synthetic stormwater mix, depending on the target concentrations and study objectives. For instance, Bratieres et al. (2008) used semi-synthetic stormwater of two different compositions to investigate the impact of influent concentrations (typical concentrations and twice the typical concentrations) on the nutrient removal efficiency of different biofilter media and plant species. Another study that provided a performance comparison between synthetic and natural stormwater, concluded that the use of synthetic stormwater is both realistic and comparable to figures observed in the field (Limouzin et al. 2011).

The application of semi-synthetic stormwater for testing biofilters in laboratory settings has been validated at the field scale, as confirmed by Hatt et al. (2009), who examined the hydrological and pollutant removal performance of field-scale biofilters. In all studies, semi-synthetic stormwater was prepared by mixing natural sediments in deionised water or dechlorinated tap water, with any deficiencies in pollutant concentrations in the natural sediments supplemented using chemical additives to achieve the target concentrations.

In this study, Synthetic stormwater was used for all column experiments to ensure consistent influent quality and composition, minimising variability inherent in natural stormwater. This approach provided essential experimental control while avoiding logistical challenges associated with collecting and storing natural runoff (Hatt et al. 2007a; Bratieres et al. 2008).

3.2.1 Pollutant loading

Stormwater quality data reported in the *Nationwide Urban Runoff Program* (Cole et al. 1984), and Duncan (1999), were used as a guide for determining the base composition of the synthetic stormwater. These reports provide average values of typical pollutants found in highly urbanised catchments. The reported values were compared with the compositions of synthetic stormwater used in previous bioretention studies, and adjustments were made as necessary.

The pollutants targeted in this study were selected because they are classified as *priority pollutants*, as detailed in Section 2.1.1. Additionally, the selection was influenced by the availability of appropriate analytical methods. Synthetic stormwater was prepared using analytical-grade compounds to achieve the desired concentrations, following established methodologies by Bratieres et al. (2008) and Hatt et al. (2007a).

Table 3.1 Target stormwater composition and dosing materials.

Pollutant	Target concentration (mg/l)	Typical runoff concentrations (mg/L)[a]	Dosed with	Setup
TSS	190	144-155	Kaolin clay	Both
Zn	2.7	0.23-0.32	Zinc chloride - $ZnCl_2$	Both
Pb	1.2	0.093-0.14	Lead nitrate - $Pb(NO_3)_2$	Both
Cu	0.6	0.059-0.062	Copper sulphate - $CuSO_4$	Both
TP	0.39	0.32	Dipotassium hydrogen phosphate - K_2HPO_4	Both
MPs	200	Vary widely[b]	PMMA microbeads (ThermoFisher Scientific, 50-200µm particles)	Small columns

[a] Pollutant concentration ranges (geometric means) of stormwater quality data reported by Cole et al. (1984) and Duncan (1999), for highly urbanised catchments.
[b] Concentrations typically reported in particles/L and vary widely depending on particle size range (e.g. 1500-6000 particles/L reported by Wang et al. (2022).

Table 3.1 lists the ingredients used to achieve the desired stormwater composition including the following target pollutants:

1. Total suspended solids (TSS): kaolin clay replaced natural sediments to maintain consistent concentrations and uniform suspension stability during the dosing procedure.
2. Heavy metals (Zn, Pb, Cu): concentrations were elevated to approximately ten times typical urban runoff levels. The rationale behind this was to ensure reliable detection within the analytical instrument limits. These exaggerated concentrations also enabled investigation of long-term accumulation levels beyond the study timeframe, as one dosing event simulated the metal load of 10 storm events, supporting the study's objective to assess the prolonged accumulation of heavy metals in bioretention media.

3. Total Phosphorus (TP): was maintained at 0.39 mg/L, reflecting typical urban levels in highly urbanised catchments.
4. Microplastics: lab-grade PMMA microbeads (50–200µm) were used in the stormwater mix for the small columns to examine its retention mechanism. Despite fibres being the most abundant type of microplastic in urban environments (Wright et al. 2020), lab-grade microbeads were chosen to facilitate microscopic identification and minimise contamination from surrounding environments. Their distinctive spherical shape is easily detectable and distinguishable from other particles under the microscope. The smooth, spherical shape of the chosen microbeads also represents a conservative scenario for soil infiltration, as they tend to escape more easily through pores compared to irregularly shaped microplastics (Wang et al. 2020). Their uniform shape allows for smoother movement through the soil with minimal resistance and clogging. Conversely, fibrous particles experience greater resistance due to their irregular shape, which limits their mobility. It is acknowledged that the target concentration for microplastics (200 mg/L) may not reflect typical field conditions. However, this concentration was selected to facilitate weighing and to increase the likelihood of microscopic detection.

3.2.2 Dosing volume

A bioretention system should be sized at a minimum of 2% of the contributing catchment area (FAWB 2009). The *SuDS Manual* recommends that the surface area of a typical bioretention system should be within the range of 2-4% of its catchment area (Woods-Ballard et al. 2015). In this study, the catchment size was calculated based on 2.5% of the surface area of the biofilter columns to minimise overloading the biofilter surface. The loading volume was calculated based on the average annual rainfall and typical rainfall patterns data for the catchment to be drained.
This simplified approach was established previously in the column trials conducted by Bratieres et al. (2008) and Lucas (2015), and is recommended by FAWB (2009).

The UK Met Office climate data for the period 1991–2020 (Met Office [no date][b]) were used to estimate the average volume of stormwater that the systems should handle under field conditions. Assuming a biofilter size of 2.5% of its impervious catchment area, the average dosing volume was calculated using the equation adapted from Jacklin et al. (2021a) below:

$$V_d = \frac{A_s}{A_r} \times \text{P} \times PR \quad (3.1)$$

Where

V_d = dosing volume (L)
A_s = biofilter surface area (m^2)
A_r = treatment area to catchment area ratio (%)
P = precipitation event rainfall (mm)
PR = percentage runoff (%)

In urban areas, impermeable surfaces increase runoff volume and peak discharge into stormwater biofilters. However, infiltration and evapotranspiration reduce runoff. To account for these losses, an imperviousness of 75% was assumed for the effective contributing proportion (i.e., the percentage of runoff from surfaces that directly drain into the drainage system) as the recommended value in the *SuDS Manual* (Woods-Ballard et al. 2015).
Data from the Met Office's Cardiff climate station (Table 3.2), on average annual rainfall and rainy days were used to calculate rainfall depth per event, following the methodology of Lucas (2015):

$$Percipatation\ event\ rainfall = \frac{average\ annual\ rainfall}{number\ of\ rainy\ days} = \frac{1203.3}{153.4} = 7.8\ mm \quad (3.2)$$

Table 3.2 Cardiff average rainfall data for the climate period 1991-2020 (Met Office).

Month	Rainfall (mm)	Days of rainfall ≥1 mm (days)
January	126.97	15.6
February	92.97	12
March	85.29	12.29
April	72.07	10.73
May	78.45	11.17
June	73.54	10.37
July	83.58	11.23
August	104.82	12.4
September	86.31	11.8
October	129.05	15.03
November	130.65	15.6
December	139.58	15.17
Annual total	**1203.28**	**153.39**

The Met Office defines a 'rainy day' as any calendar day recording ≥1 mm of precipitation, including events ranging from light drizzle to extreme storms, the latter occurring more frequently in winter. This mean-based calculation (7.8 mm × 153 days ≈ 1,203 mm annual rainfall) conserves total annual rainfall volume while accounting for seasonal intensity variations, with December averaging 9.2 mm per rainy day compared to 7.1 mm in June. The 7.8 mm value serves as a moderate-intensity benchmark that appropriately balances frequent low-volume events with rare high-intensity storms, representing Cardiff's rainfall characteristics (Table 3.2).

3.2.3 Dosing frequency

Climate statistics for the period 1991-2020 indicate that Cardiff experiences rainfall on approximately 153 days per year (Table 3.2), equating to an average of three days per week. Although the exact number of rainy days varies annually and seasonally, Cardiff maintains relatively stable precipitation frequency (10-15 rainy days/month) throughout the year. Therefore, it was decided to maintain a consistent dosing frequency of three times per week to simplify the variable matrix and maintain controlled experimental conditions.

3.3 Experimental design

3.3.1 Large column experiments (vegetation effects)

3.3.1.1 Column setup

Six biofilter columns were recycled and reconstructed from previous PhD projects (Lucas 2015; Kiiza 2017; Bosnina 2021), to investigate the effects of vegetation on pollutant removal and system hydrology. All columns were constructed using high-density polyethylene (HDPE), as shown in Figure 3.2. The HDPE pipes, manufactured by Asset International Ltd (Lucas 2015), had a height of 1000 mm and an internal diameter of 400 mm. The bottom of each column was sealed with an HDPE cover, forming the bed of the biofilter. A main drainage valve was installed below the base of each column, positioned at the centre of the sealed end. This configuration enabled controlled saturation conditions by switching between valve closure and free drainage configurations (Figure 3.3). Each column was placed on a steel frame and fitted with a shower head at the top to simulate rainfall (Figure 3.2).

This design aimed to prevent scouring of the biofilter surface during stormwater dosing (Woods-Ballard et al. 2015) and to enable precise control over rainfall intensity and duration using control valves. The structure was connected to a 400 L mixing tank, where synthetic stormwater was prepared before each dosing event and applied to the system via an automatic feeder using a submersible pump.

Figure 3.2 Experimental setup of large bioretention columns used to investigate the effects of vegetation on pollutant removal and system hydrology.

3.3.1.2 Media configuration

For an effective bioretention system design, the SuDS manual recommends a three-layer configuration, ordered from top to bottom as shown in Figure 3.3:

1. Layer 1 - filter layer: this layer, 200 - 500 mm deep, consists of sand-based soils with adequate permeability and organic matter to promote healthy plant growth. In temperate climate such as the UK, a hydraulic conductivity of 100 - 300 mm/hr is recommended.
2. Layer 2 - transition layer: at least 100 mm deep, this layer's purpose is to prevent fine particles from migrating from the filter layer into the drainage layer, potentially clogging the underdrain pipe (Bratieres et al. 2008).
3. Layer 3 - drainage layer: this layer, typically at least 100 mm deep, should consist of material with significantly higher permeability than the filter media. Its role is to facilitate efficient water flow from the filter media to the drainage pipe, considering factors such as underdrain pipe diameter, minimum pipe cover, and any additional storage requirements for attenuation as per the SuDS manual (Woods-Ballard et al. 2015).

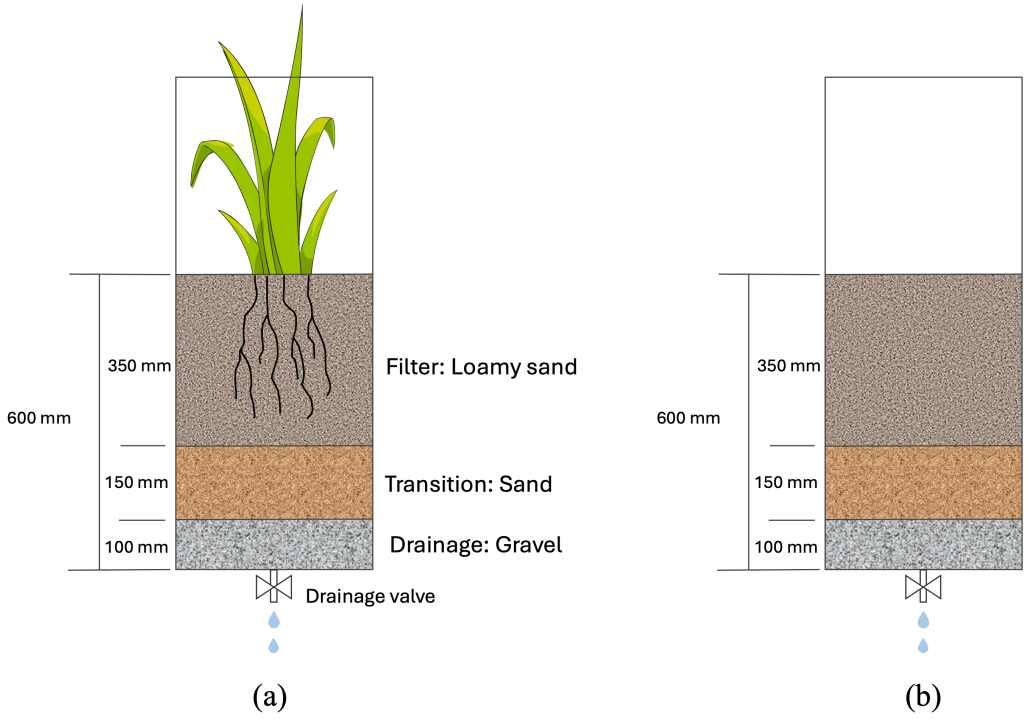

Figure 3.3 Schematic cross-sections of bioretention configurations, (a) vegetated columns, (b) non-vegetated columns.

3.3.1.3 Selection of media type and depth

The selection of filter media was based on a review of recommended types (Section 2.3.3). The FAWB suggests using loamy sand for the filter medium due to its proven high efficiency in pollutant removal and promotion of plant growth, as supported by various studies (Hatt et al. 2007a; Bratieres et al. 2008; Read et al. 2008; FAWB 2009). Additionally, loamy sand is readily available and cost-effective, also important factors in media selection. Similarly, sand and gravel is recommended by the FAWB for the transition and drainage layers respectively, due to their higher permeability compared to loamy sand, along with their affordability and availability (FAWB 2009). Therefore, in this study, loamy sand was chosen for the filter layer and gravel for the drainage layer, while sand was chosen for the transition layer. Several studies that investigated similar configurations and media types include Hatt et al., 2007a; Jacklin et al., 2021a; Payne et al., 2014b; and Zinger et al., 2021.

In terms of the filter media depth, the FAWB recommends a deeper filter layer for plant root establishment and improved overall performance. Although, in a study conducted by Bratieres et al. (2008), they found that biofilters with shallower media depths initially performed significantly better, as plant roots in shallower depths occupied more soil, the removal efficiency of deeper filters increased at a faster rate as the systems matured. The authors attributed this temporal improvement in removal performance to differences in the expansion rate of plant root systems and uptake capacities among species (Bratieres et al. 2008; Read et al. 2008). Other studies have indicated that shallower filter depths are sufficient for heavy metal removal (Hatt et al. 2008; Li and Davis 2008c; Jones and Davis 2013), which are the primary pollutants of concern in this study.

Consequently, the depth of the filter medium was set to 350 mm, representing the mean value of the recommended range in the SuDS manual. The transition layer and the drainage layer were set to 150 mm and 100 mm respectively, making the total depth of the filter media in each column be 600 mm, which exceeds the minimum depth suggested by the FAWB for adequate establishment of plant roots. Each layer of the filter media was compacted using a flat circular plate during installation to prevent the migration of fine particles between layers, as recommended in the SuDS manual (Woods-Ballard et al. 2015). Starting from the bottom gravel layer, the column was gradually filled and compacted every 50-100 mm to ensure uniform compaction.

3.3.1.4 Selection of plants

Three plant types were selected in this study following the design guidelines described in Section 2.3.1.3: sedges, rushes, and grass. Despite belonging to different plant families, they share several common characteristics that align them with similar ecological groups and visual forms. *Juncus effusus*, also known as Soft Rush, has been investigated in a couple of biofilter column studies and have demonstrated high removal efficiency for nutrients and heavy metals both in temperate (Beral et al. 2023) and arid climates (Jacklin et al. 2021a).

While, *Carex pendula*, a type of sedge, was highly efficient in wastewater remediation containing high lead concentrations (Yadav et al. 2011). *Phalaris arundinacea 'Variegata Picta'*, also known as Ribbon Grass or Reed Canary Grass, is an ornamental grass valued for its dense foliage. Studies have shown that it can improve stormwater infiltration, water-holding capacity, and the retention of particulate pollutants, such as suspended solids and microplastics (MPs) (Kuoppamäki et al. 2021). Table 3.3 lists the selected plant species in this study. The first two species, *Carex* and *Juncus*, are also listed in the recommended species for UK rain garden design in the Rain Garden Guide (Bray et al. 2012).

All plants were nursery-grown and were purchased in packs of three per species during the growing season of 2023. A hole about twice the size of the potted root, was excavated for each plant in the designated biofilter and the potted soil was gently shaken to loosen the roots and ensure adequate contact with the filter medium. The plants were placed in the hole, and the soil was pressed firmly around the root so that the stems were at the same level as the biofilter surface. To assess the impact of vegetation, three vegetated columns were compared to three non-vegetated columns, which served as controls.

Table 3.3 Selected plant species.

Scientific name	Common name	Family	Broad plant type
Carex pendula	Pendulous sedge	*Cyperaceae*	sedges
Juncus effusus	Soft rush	*Juncaceae*	rushes
Phalaris arundinacea 'Variegata Picta'	Ribbon grass	*Poaceae*	grass

a)

b)

c)

Figure 3.4 Types of species and planting arrangement of a) *Juncus effusus,* b) *Carex pendula,* c) *Phalaris arundinacea.* Pictures were taken on day of planting in April 2023 prior to the start of experiments.

3.3.1.5 Drainage configuration

To evaluate the interaction effect of residence time and saturation dynamics with vegetation and pollutant removal, the systems were tested under two distinct drainage experiments:

1. **Closed-valve experiment:** this design simulated intermittent saturation via a manually regulated bottom valve, closed for 24 hours post-dosing to retain stormwater and extend residence time, which has shown to generally improve pollutant removal (Lucas 2015; Woods-Ballard et al. 2015). This mimicked a temporary saturated zone to promote anaerobic processes such as denitrification and metal adsorption (Hatt et al. 2007b; Blecken et al. 2010). In UK climates, a retention period of 36 ± 12 hours, up to a maximum of 48 hours, is considered sufficient to

achieve 80-90% removal efficiency of priority urban stormwater pollutants in detention ponds and wetlands (Mulhall and Revitt 2003; Shutes et al. 2005; Lucas 2015). A lower limit of 24 hours was used in the closed-valve experiment to accommodate the dosing and sampling schedule. After 24 hours, the valve was opened to drain the effluent and reintroduce aerobic conditions. The closed-valve configuration extended residence time, which balanced the benefits of a saturated zone with periodic aeration for enhanced pollutant removal and adsorption as discussed in Section 2.3.2.

2. **Free-draining design experiment:** conducted separately after the closed-valve experiments, this design featured a permanently open valve, allowing unrestricted drainage by gravity within hours of dosing, which served as a conventional bioretention baseline for pollutant removal efficiency without saturation enhancement.

Table 3.4 Media configurations and investigated variables in large column experiments.

Layer	**Media type**	**Layer depth (mm)**
Filter Layer	Loam	350
Transition Layer	Sand	150
Drainage Layer	Gravel	100
Total depth		600
Variables		
Vegetation	3x vegetated (1x *Carex pendula*, 1x *Juncus effusus*, 1x *phalaris arundinacea 'Variegata Picta'*), and 3x non-vegetated.	
Drainage configurations	Closed valve, and free-draining.	

3.3.1.6 Dosing procedure

The biofilters were planted in April 2023, with one plant species per column in the vegetated configurations and watered twice weekly with tap water for 16 weeks prior to synthetic stormwater dosing and testing. This period was essential to allow plant establishment, hydraulic compaction, and system maturity (Hatt et al. 2007b).

The required dosing volume for each event was calculated based on Equation (3.1), as follows:

$$V_d = \frac{\pi\left(\frac{0.4}{2}\right)^2}{0.025} \times\ 7.8\ \times 0.75 = 29.4\ L$$

This amount was rounded up to facilitate the calculation of stock solutions. Therefore, 30 litres of synthetic stormwater were administered per dose per column, allowing for runoff bypass in excess of the design storm.

Prior to each experiment, the appropriate quantities of stock solutions were combined and dissolved in 240 litres of dechlorinated tap water to minimise chlorine interference and avoid influencing the biological community. This was achieved by neutralising the tap water with sodium thiosulphate (1 mg/L), as recommended by FAWB (2009). The stock solutions were replenished every five weeks to facilitate accurate chemical measurements.
The synthetic stormwater was mixed continuously in a 400 L tank for 10 minutes to ensure uniform dispersion and adsorption of pollutants onto particles in the mixture (FAWB 2009). The electric paddle mixer used featured an 80 cm-long metal propeller with three blades. The mixer was secured to the circular opening at the top of the tank, ensuring stability and vigorous mixing of the entire contents.

Despite using a consistent synthetic stormwater recipe and maintaining continuous mixing, fluctuations in influent concentrations were observed both during the dosing event and from week to week. These fluctuations were expected due to the presence of larger particle-size fractions in the clay sediments, which were difficult to keep in suspension within the tank. Despite efforts to maintain suspension using a submersible pump and rigorous mixing, suspended particles gradually settled, leading to a decline in total suspended solids (TSS) concentrations—a phenomenon also observed by Milandri et al. (2012). This issue was mitigated by increasing the pump system's flow rate while monitoring TSS concentrations throughout the dosing event, ensuring that all columns received the required dose before a significant change (>10%) in concentration was recorded. In general, variability in pollutant concentrations in stormwater is inherent, and the observed concentration range falls within typical reported values (Duncan 1999), allowing for performance testing across a range of concentrations (Hatt et al. 2007a).

All dosing events were carried out on dry days to minimise synthetic stormwater dilution from natural rainfall and to avoid safety hazards associated with electrical equipment. Initially, synthetic stormwater was applied to the columns three times per week. However, this process gradually introduced a problem with sampling as infiltration rates in the columns began to decline under the three-times-per-week dosing schedule due to formation of cake layers (discussed in Chapter 4). This resulted in prolonged ponding of stormwater on the biofilter surface by the time of the next dose, particularly in non-vegetated systems. To ensure representative effluent sample collection, the dosing schedule was reduced from three to once per week. Similarly, sampling runs were restricted to once per week.

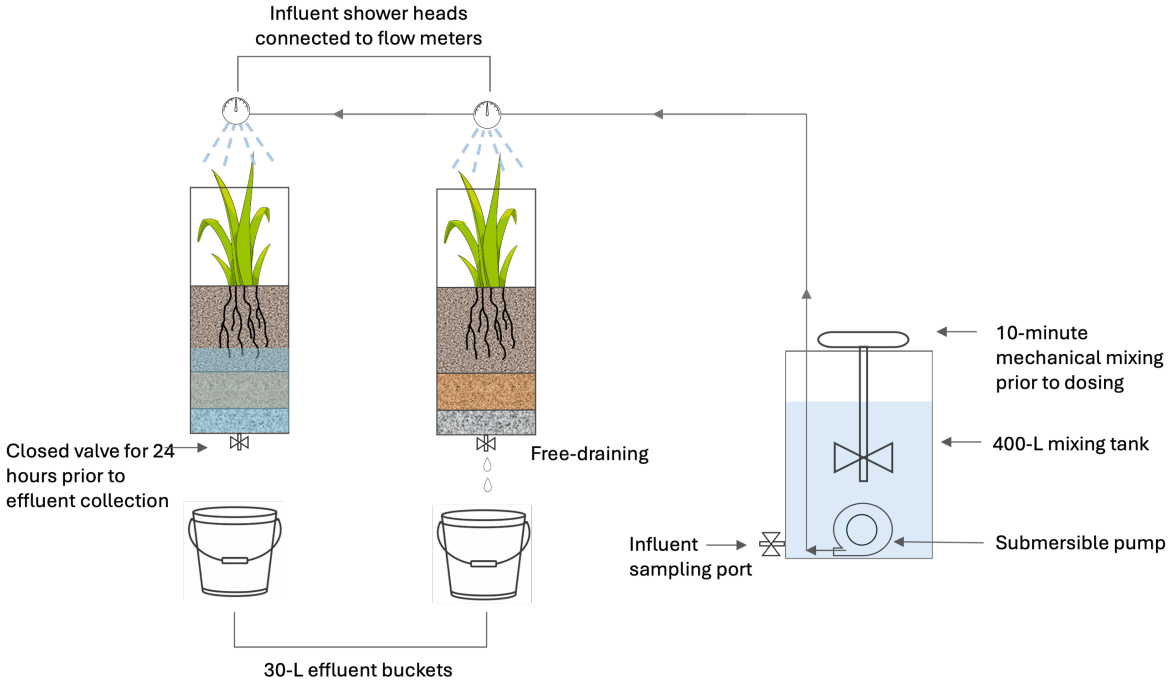

Figure 3.5 Schematic of columns dosing procedures. Synthetic stormwater was mixed via a mechanical mixer for 10-minutes in a mixing tank prior to pumping. In the closed-valve experiments, drainage valves remined shut for 24 hours prior to effluent collection. Whereas valves remained open to allow water to drain freely in the free-draining experiments.

3.3.1.7 Method development

The initial 13 weeks of the experiments involved a method development phase. During this phase, various inflow concentrations for heavy metals were tested, some significantly exceeding target levels. While the removal efficiency results from this phase were excluded from the final analysis due to inconsistencies in inflow concentrations and sampling protocols, the accelerated loading of heavy metals aligns with the study's objective of

investigating long-term heavy metal accumulation in bioretention media. For completeness, the data from this developmental phase are presented alongside the full experimental datasets in Appendix B. During the method development phase, total suspended solids (TSS) were monitored in situ by taking grab samples from the influent to measure changes in concentrations throughout the dosing process, which may have occurred due to the settling of solids. Whenever a significant increase in TSS concentrations was recorded, the automatic feeder was paused, and an additional round of mechanical mixing was carried out. This ensured that particle suspension remained uniform throughout the dosing event. It was found that keeping the dosing event between 30 and 40 minutes in total did not significantly affect TSS concentration rates. This involved dosing two columns simultaneously at a rate of 2-3 L/min. The order of dosing for each pair of columns was alternated every week to maintain consistent pollutant loading across the weeks.

3.3.1.8 Experimental duration

The systems received continuous weekly dosing with synthetic stormwater for a total of 61 weeks to simulate long-term operation and investigate heavy metal accumulation and hydrological performance. The experiment was terminated at this point due to severe clogging, which significantly reduced the infiltration capacity.

Water quality sampling to assess pollutant removal efficiency was conducted during three distinct experimental phases. The duration and purpose of these sampling phases are summarised as follows:

1. Method development (13 weeks): the initial sampling phase focused on stabilising influent concentrations and sampling protocols. The water quality data from this phase were excluded from statistical analysis of removal efficiencies (further details in Section 3.3.1.7).
2. Closed-valve experiments (21 weeks): this core sampling phase investigated performance under enhanced conditions. As described in Section 3.3.1.5, the drainage valve was closed for 24 hours after dosing to create a temporary saturated zone and extend hydraulic residence time.
3. Free-draining experiments (8 weeks): this final sampling phase provided a baseline for comparison (Section 3.3.1.5). The outlet valve was left permanently open to allow immediate drainage, simulating a conventional bioretention system without a saturated zone.

It is important to note that while water sampling was confined to these specific phases, the weekly dosing schedule continued throughout the entire 61-week period between them to maintain consistent long-term loading on the systems.

Table 3.5 Summary of experimental sampling phases.

Phase	Duration	Purpose
Method development	13 weeks	Stabilisation of sampling protocols and influent concentrations (excluded from statistics).
Closed-valve experiments	21 weeks	Assess removal with extended residence time.
Free-draining experiments	8 weeks	Establish a baseline for removal comparison without saturation enhancement.

3.3.1.9 Water sampling

A 300 mL composite sample of the influent was collected from a tap located at the bottom of the mixing tank near the submersible pump at the beginning, middle, and end of each dosing event in a clean polyethylene bottle. In the closed-valve experiments, each dose of stormwater was retained within the column for 24 hours before release to allow sufficient time for the biotreatment process to occur. In contrast, in the free-draining experiments, the valve was left open to allow water to drain freely from the column without restrictions.
In both cases, effluents were collected in 30 L buckets prewashed with phosphate-free detergents.

During the method development phase, a composite effluent sample was created by collecting 10 mL every 2 L of outflow as recommended in FAWB (2009). This method became impractical as declining infiltration rates made it difficult to collect samples proportionally across the entire 30 L drainage volume. During this period, different effluent sampling protocols were tested, including single grab sampling after the effluent rates stabilised and composite sampling at different time and volume intervals. It was found that collecting the entire drained volume and then taking a sub-sample from it provided the most representative measure of effluent quality.

This method captured more representative TSS amounts than the other approaches which correlated more accurately with metal concentrations in the effluents. Therefore, the entire drainage volumes were allowed to accumulate in 30 L buckets, usually overnight, before sample collection. At this point, the effluent was thoroughly mixed by hand for two minutes using a stirrer, and a 500 mL subsample was collected from each bucket in acid-washed, polyethylene bottles and transported to the laboratory. Influent and effluent lab samples were collected in 40 mL polyethylene vials, acidified with nitric acid to preserve the samples, and stored at <4°C for further analysis. Operational consistency was ensured through standardised dosing, sampling, and equipment handling.

3.3.1.10 Soil sampling

Soil grab samples were obtained from the biofilters to assess changes in heavy metal concentrations and their vertical accumulation in the biofilter media. The initial sampling, conducted prior to the application of synthetic stormwater treatment, established baseline soil background concentrations. Between 25 and 50 grams of soil were collected from the surface directly beneath the centre of the shower heads using fresh plastic scoops rinsed with deionised water, after the experiments concluded.

Subsurface samples were extracted from the same locations using a hand soil auger (15×30 cm) to obtain core samples from a depth of approximately 12-15 cm below the surface. Each soil sample was placed in a labelled zip bag and transported to the laboratory for heavy metal determination using X-ray fluorescence (XRF) spectrometry analysis. Sample preparation followed the instrument protocol manual supplied by the manufacturer (*Innov-X Systems Olympus* mobile XRF analyser).

The soil samples were transferred into clean containers and oven-dried at 40°C for 48 hours. The dried samples were then sieved through a >2mm mesh to screen out debris and organic matter. The sieved soil was subsequently crushed and passed through a 200µm sieve to ensure homogeneity before being placed into XRF cups. The samples were analysed for multiple elemental concentrations, and results were obtained for target metals (Zn, Cu, Pb). To maintain quality assurance, the instrument was calibrated using a standard check sample (316) provided by the manufacturer.

3.3.2 Small column experiments (biochar effects)

3.3.2.1 Media configuration

Two types of biochar: Sewage Sludge Biochar (SSB) and Rice Husk Biochar (RHB), pyrolysed at 550°C, were used as filter amendment in this experiment. The biochar was obtained from the UK Biochar Research Centre (standard biochar set) (UKBRC [no date]). The aim was to produce a sand-biochar mixture as homogeneous as possible to provide greater control over the experiment.

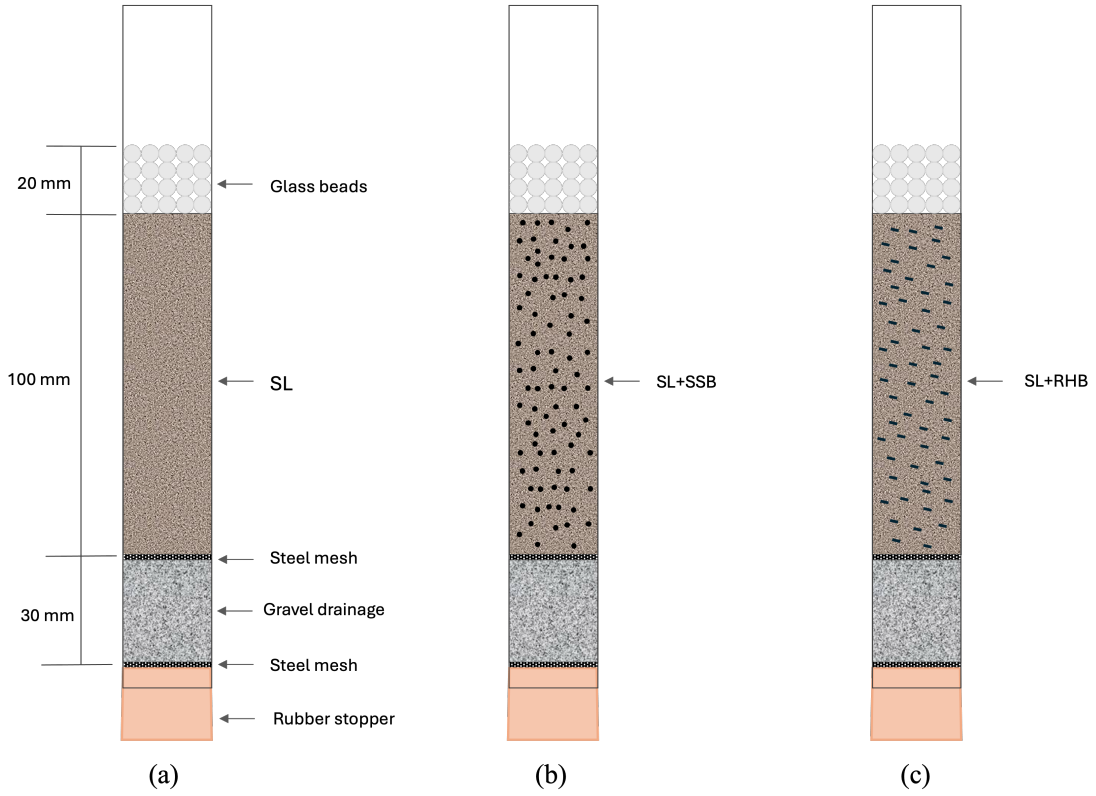

Figure 3.6 Schematic cross-sections of filter media configurations, (a) sandy loam control (SL), (b) sandy loam mixed with sewage sludge biochar SL+SSB, (c) sandy loam mixed with rice husk biochar (SL+RHB).

First, the dry mass of biochar was lightly ground to match the particle size grading of typical loamy sand/sandy loam media, as recommended in the SuDS manual, and to achieve relatively consistent bulk densities during packing. Initially, each of the two biochar types and the loam was sieved separately to achieve the filter media grading described in Table 3.6. However, the amount of RHB particles retained on the 2-0.6mm sieve size was insufficient for the experiment's requirements.

Consequently, it was decided to target a single particle size range, and the 0.6-0.2mm sieve size range (medium sand) was chosen for this study as it retained the largest percentage of particles based on the SuDS manual grading outlined in Table 3.6.

Table 3.6 Example grading of a bioretention filter medium as outlined in the SuDS Manual (Woods-Ballard et al. 2015). Thick borders represent sieve-size range chosen for this study.

Sieve size (mm)	% passing
6 – 2	100
2 – 0.6	90 – 100
0.6 – 0.2	40 – 70
0.2 – 0.063	5 – 20
> 0.063	< 5

A mixture of sandy loam (90% w/w) and biochar (10% w/w) was used to fill the columns. The performance of biochar can be affected by amendment ratio. While some studies have amended biofilters with high quantities (up to 33% w/w), these have been associated with negative effects, such as increased phosphate leaching when increasing biochar from 15% to 30% (McCrum et al. 2017).

In contrast, filter media amended with a lower amount of biochar (≤10% w/w) is frequently reported in other studies (Tian et al. 2016; Rahman et al. 2020; Sun et al. 2020; Biswal et al. 2022). Therefore, a rate of 10% (w/w) was selected for this study to leverage the documented benefits of biochar amendment while mitigating the risk of nutrient leaching associated with higher amendment ratios.

The mixture was thoroughly blended for 15 minutes using a food blender at a slow speed to prevent crushing the biochar particles. The resultant filter media are described in Table 3.7 as follows: 90% Sandy Loam + 10% Sewage Sludge Biochar (SL+SSB), 90% Sandy Loam + 10% Rice Husk Biochar (SL+RHB), and 100% Sandy Loam (SL) as the control.

Table 3.7 Media configurations and tested variables in biochar effects experiments.

Layer	**Media type**	**Layer depth (mm)**
Top layer	Glass beads (5 mm)	20
Filter layer	Tested variable	100
Transition layer	Replaced by a steel mesh	-
Drainage layer	Gravel (2 - 4 mm)	30
Bottom layer	Steel mesh	-
Variables		
Media type	3x Sandy Loam (90% w/w d.b.) + Sewage Sludge (10% w/w d.b.), abbreviated as SL+SSB. 3x Sandy Loam (90% w/w d.b.) + Rice Husk (10% w/w d.b.), abbreviated as SL+RHB. 3x 100% Sandy Loam (control), abbreviated as SL.	

3.3.2.2 Column setup

The three filter media were dry-packed into plexiglass columns (ID = 2.6 cm, column ID: particle size ratio > 40 to prevent boundary effects), following a layer configuration typical of bioretention columns as described in Section 3.3.1.2. In this specific setup, the transition layer was replaced with a steel mesh to prevent clogging in the drainage layer. The filter layer depth was set to 10 cm, while the drainage layer depth was set to 3 cm, maintaining the same layer-depth ratio used in the large column setup (Figure 3.6). Gravel (4-2 mm) was washed and used for the drainage layer. Another steel mesh layer was placed at the bottom of the column to hold the overlying gravel in place. The top and bottom openings of the column were fitted with rubber stoppers, each with a 5-mm opening to facilitate water flow.

A 2-cm layer of glass beads (5 mm in size) was placed at the top of the filter media to promote uniform flow distribution and minimise preferential flow paths. The columns were gradually packed to the specified heights with a known mass using a vibrating table to ensure consistent and uniform compaction. Each filter medium was tested in triplicate to ensure reliability and reproducibility (Figure 3.7).

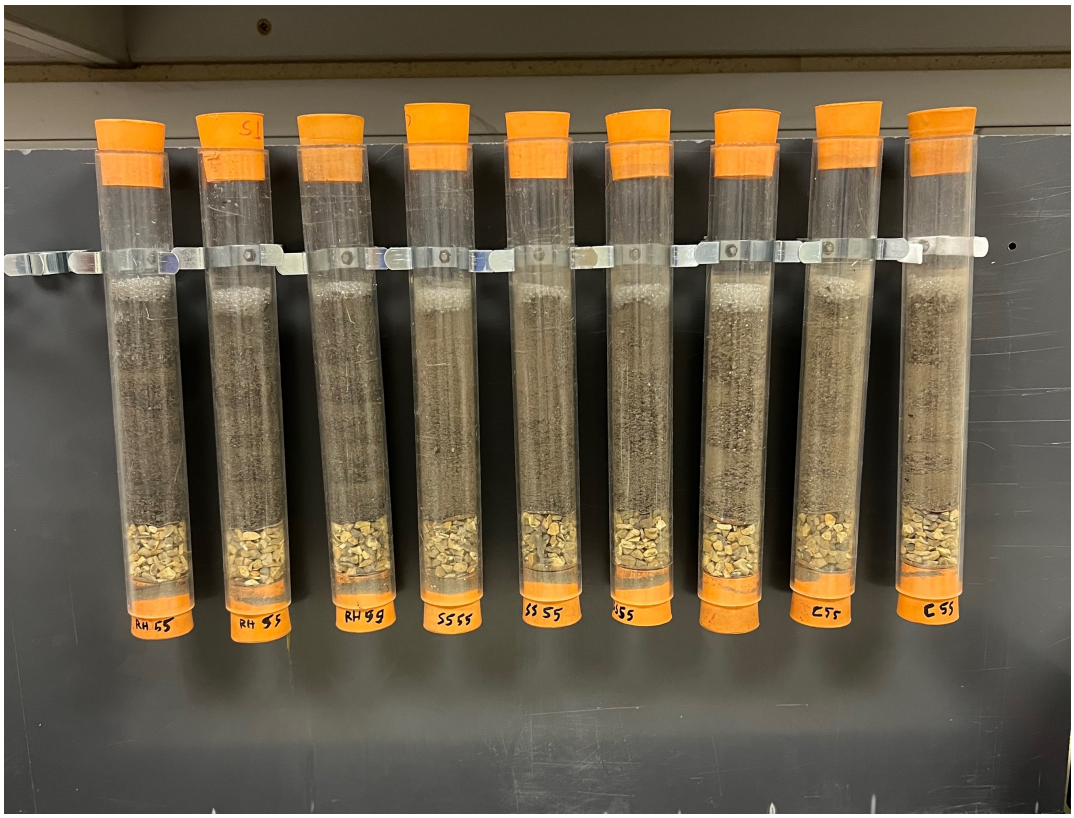

Figure 3.7 Plexiglass columns with layered filter media, drainage gravel, and top glass beads, prepared for the bioretention study.

3.3.2.3 Dosing procedure

Prior to each dosing event, the synthetic stormwater solution was prepared at least three hours in advance and mixed continuously using a magnetic stirrer, sometimes overnight, to allow constituents to stabilise and reach background concentrations.

This approach better represented field conditions, as it has been shown that synthetic stormwater undergoes significant decay during the first three hours of mixing before reaching equilibrium (Milovanovic et al. 2023). Synthetic stormwater was mixed in a single batch of deionised water and thoroughly stirred with a magnetic stirrer, to ensure uniform distribution of constituents. The total dosing volume was determined using Equation 3.1.

$$V_d = \frac{\pi\left(\frac{26}{2}\right)^2}{0.025} \times 7.8 \times 0.75 \approx 120\ mL$$

The final dosing volume was rounded down to 120 mm, to facilitate the dilution and weighing of chemicals and other constituents.

The dosing frequency was kept at 3 times per week as described in Section 3.2.3. Bioretention studies typically extend over several months of stormwater dosing, generally from 6 to 18 months. Such long-term durations allow sufficient time for key phenomena to emerge, such as pollutant breakthrough and filter conditioning (discussed in Chapter 4). However, the purpose of this study was to investigate biochar effects on pollutant retention capacity while differentiating between pollutant and dissolved removals, which is essential before long-term investigations. Subsequently, the 2-week period provided sufficient time for the objective of this study. Other studies with similar timeframes include Sun et al. (2020) and Xiong et al. (2019). In total, there were six dosing events, with 3 doses per week.

Prior to stormwater dosing, the pore volume was measured gravimetrically by subtracting the column's dry weight from its saturated weight. The columns were repeatedly flushed with deionised water to the equivalent of 26 pore volumes to wash away any fines mobilised during the packing process (Reddy et al. 2014a; Mohanty and Boehm 2015). Initially, the experimental design involved the use of a peristaltic pump and tubing to convey the stormwater to each column at a controlled flow rate. However, it was observed that this setup significantly reduced the inflow concentrations of microplastics (MPs), as MP particles adhered to the inner walls of the tubing, leading to wall breakage (Figure 3.8).

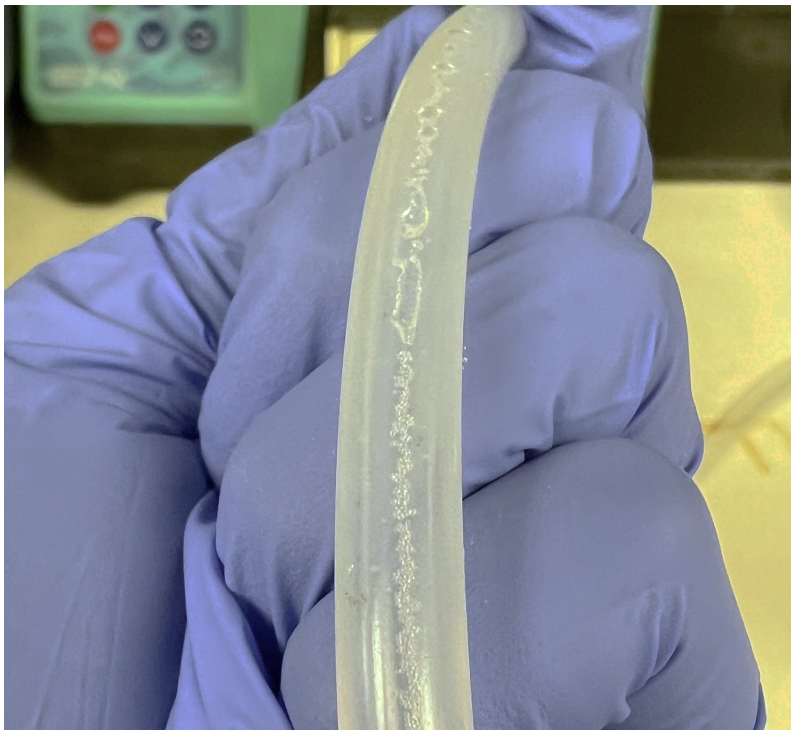

Figure 3.8 Peristaltic pump tubing showing microplastic adhesion, which significantly reduced inflow concentrations and caused tube damage, prompting a switch to manual dosing.

Figure 3.9 A column during test trial dosing, showing temporary ponding on the filter surface due to varying infiltration rates.

Consequently, the use of the pump was discontinued, and the synthetic solution was manually injected into each column using a pipette in 10-mL batches at 2-minute intervals. Although this pulse-batch flow method represented extreme rainfall patterns, the intermittency also simulated variations that occur within a single rain event. The 2-minute interval between flows was calculated based on the modified rational method equation for peak flow rates, as described in the SuDS manual (Woods-Ballard et al. 2015), as shown in Equation 3.3, giving:

$$Q = 16.7\ C\ i\ A \qquad (3.3)$$

Where

Q = design event peak rate of runoff (L/s)
C = non-dimensional runoff coefficient which is dependent on the catchment characteristics
i = rainfall intensity for the design return period (mm/hr)
A = total catchment area being drained (m^2)
16.7 = conversion factor to address units in L/s

For simplicity, a runoff coefficient value of 0.6 was used, and the rainfall intensity was assumed to be constant at 35 mm/hr (Woods-Ballard et al. 2015).

The total area to be drained was calculated based on the biofilter surface area (ID = 26 mm), which represents 2.5% of its total catchment area. This yielded an event peak inflow rate (Q) of approximately 7 mL/min.

It takes approximately 16 minutes to inject 120 mL into the system, with around 2-minute intervals between each pulse. However, this timing was not always achievable with pulse-batch dosing, as repeated dosing occasionally resulted in a ponding layer accumulating on the surface of some columns, due to the varying infiltration rates of the different filter media (Figure 3.9).

In such instances, longer intervals were necessary to allow sufficient time for water to percolate through the column before the subsequent 10-mL dose. This procedure was repeated until the entire 120 mL of synthetic solution had been injected into each column. Effluents were collected in acid-washed borosilicate jars at the base of each column after the water was allowed to drain freely until flow ceased.

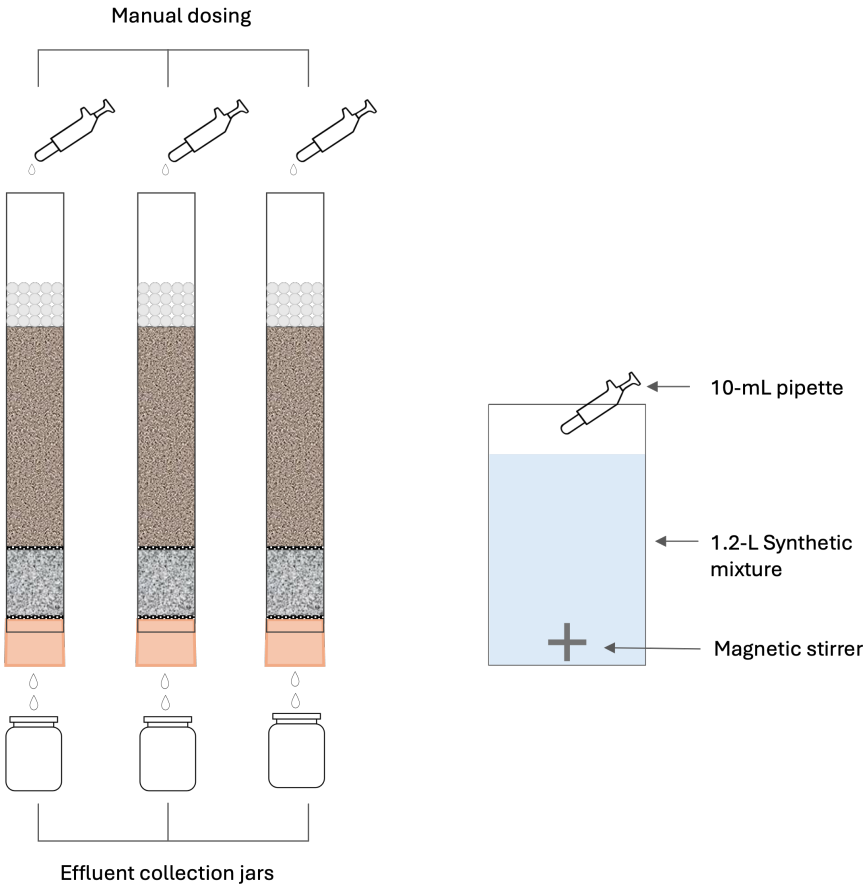

Figure 3.10 Schematic of the manual dosing procedure using a pipette for 10-mL batch dosing.

3.3.2.4 Water sampling

Influent sampling was conducted immediately prior to each dosing event, assuming that background concentrations had stabilised after ≥ 3 hours from preparation. Similarly, effluent samples were collected immediately after outflow ceased. Each effluent container was thoroughly mixed using a magnetic stirrer to ensure uniform distribution of constituents. Samples were taken using a syringe and 0.45µm filter paper, then stored in fresh 60-mL polypropylene containers preserved with nitric acid and maintained at <4°C for laboratory analysis.

3.3.3 Laboratory analysis

Influent and effluent samples were analysed for total suspended solids (TSS), pH, electrical conductivity (EC), temperature, phosphorus (P), zinc (Zn), lead (Pb), copper (Cu), and microplastics (MPs). Basic parameters such as TSS, pH, EC, and temperature were measured immediately after sampling the influents and effluents to minimise storage requirements. TSS was measured using Hach DR 900 photometric method, while pH, temperature, and EC were measured using the Mettler Toledo S47 SevenMulti instrument.

Dissolved and total metals and phosphorus (Zn, Pb, Cu, P) were determined using ICP-OES (inductively coupled plasma optical emission spectrometry - PerkinElmer®). Speciation analysis was conducted on influent and effluent samples to elucidate the removal mechanisms of dissolved and particulate pollutants.

Samples for microplastics (MPs) determination were conducted using a 1-mL pipette, placed on labelled petri dishes, and left to air dry overnight. The number of MP beads in each sample was visually counted using a VHX digital microscope at x100 magnification.
Each MPs sample was analysed in six replicates, and the average count was recorded. Blanks were analysed to ensure the reliability of the method. The detection limits for each analytical method are provided in Table 3.8.

Table 3.8 Detection limits of analytical methods.

Element	Analytical method	units	Detection limit
Pb	ICP-OES	µg/L	21
Cu	ICP-OES	µg/L	5
Zn	ICP-OES	µg/L	2
TP	ICP-OES	µg/L	27
MPs	Optical microscopy	Particles/L	500

3.3.3.1 Media characterisation tests

The filter media was characterised prior to experimentation for particle size distribution and hydraulic conductivity in accordance with the BS1377: Part2: 1990 and BS1377: Part5: 1990 standard tests respectively. The results are presented in Appendix A. The physicochemical properties of biochar were obtained from the manufacturer and are presented in Table 3.9.

The Cation Exchange Capacity (CEC) of the filter media was obtained using elemental data from XRF analysis. The instrument quantified key elements, including Ca, Ti, V, Cr, Fe, Cu, Sr, and Zr, which were used as predictors in a multiple linear regression model (Equation 3.4) derived from Sharma et al. (2015).

$$CEC = 17.2507 - (3.6514E-4 * Ca) - (3.4957E-3 * Ti) + (7.0977E-2 * Cr) + (5.9759E-4 * Fe) + (0.1479 * Cu) - (6.2096E-2 * Sr) + (5.6551E-3 * Zr) \quad (3.4)$$

This model was selected due to its robust performance in predicting soil CEC ($R^2 = 0.908$) using only elemental data, providing a cost-effective and efficient alternative for soil CEC determination without the need for time-consuming laboratory methods.

The resulting value of 15.2 cmol/kg for loamy sand aligns with reported values in the literature (e.g. 17 cmol/kg by Bratieres et al. (2008). Elemental data are provided in Table A.3 in the appendices.

3.3.3.2 Scanning Electron Microscopy

The Scanning Electron Microscope (SEM) analysis for biochar morphology and removal mechanism, was conducted using a Carl Zeiss Sigma HD Field Emission Gun SEM, with a beam energy of 10kV. The samples were taken from the top 2-cm layer near the inlet of used filters, and air dried for 72 hours to remove any moisture before being placed on SEM holders for imaging. The results are presented and discussed in Chapter 5.

Table 3.9 Physicochemical characteristics of tested biochar.

Properties	**Rice Husk Biochar**	**Sewage Sludge Biochar**
Pyrolysis temperature (°C)	550	550
pH	9.71	8.17
CEC (cmol/kg)[a]	16.17	48.40
BET surface area[b] (m^2/g)	44.8	18.5
C_{tot} (wt% d.b.)[c]	48.69	29.53
H (wt% d.b.)	1.24	1.33
O (wt% d.b.)	2.47	6.5
O:C_{tot} (molar ratio)	0.04	0.17
Total P (mg/kg d.b.)	0.10	2.29
Total N (wt% d.b.)	1.04	3.75
Zn (mg/kg d.b.)	23.58	835.69
Cu (mg/kg d.b.)	5.40	255.22
Pb (mg/kg d.b.)	bdl[d]	201.19
Polycyclic Aromatic Hydrocarbons (EPA16) (mg/kg d.b.)	0.21	3.76

[a] Measurement derived from XRF elemental analysis using Equation (3.3.) described in Section 3.3.3.
[b] Measurement derived from Brunauer, Emmett and Teller (BET) theory of surface area, using analysis of 0.5-1mm particle size sample via N^2 gas adsorption-desorption isotherms at 77 K. Values taken from (Melia et al. 2019) using UKBRC standard biochar samples similar to those used in this study.
[c] d.b. = dry basis.
[d] bdl = below detection limit.

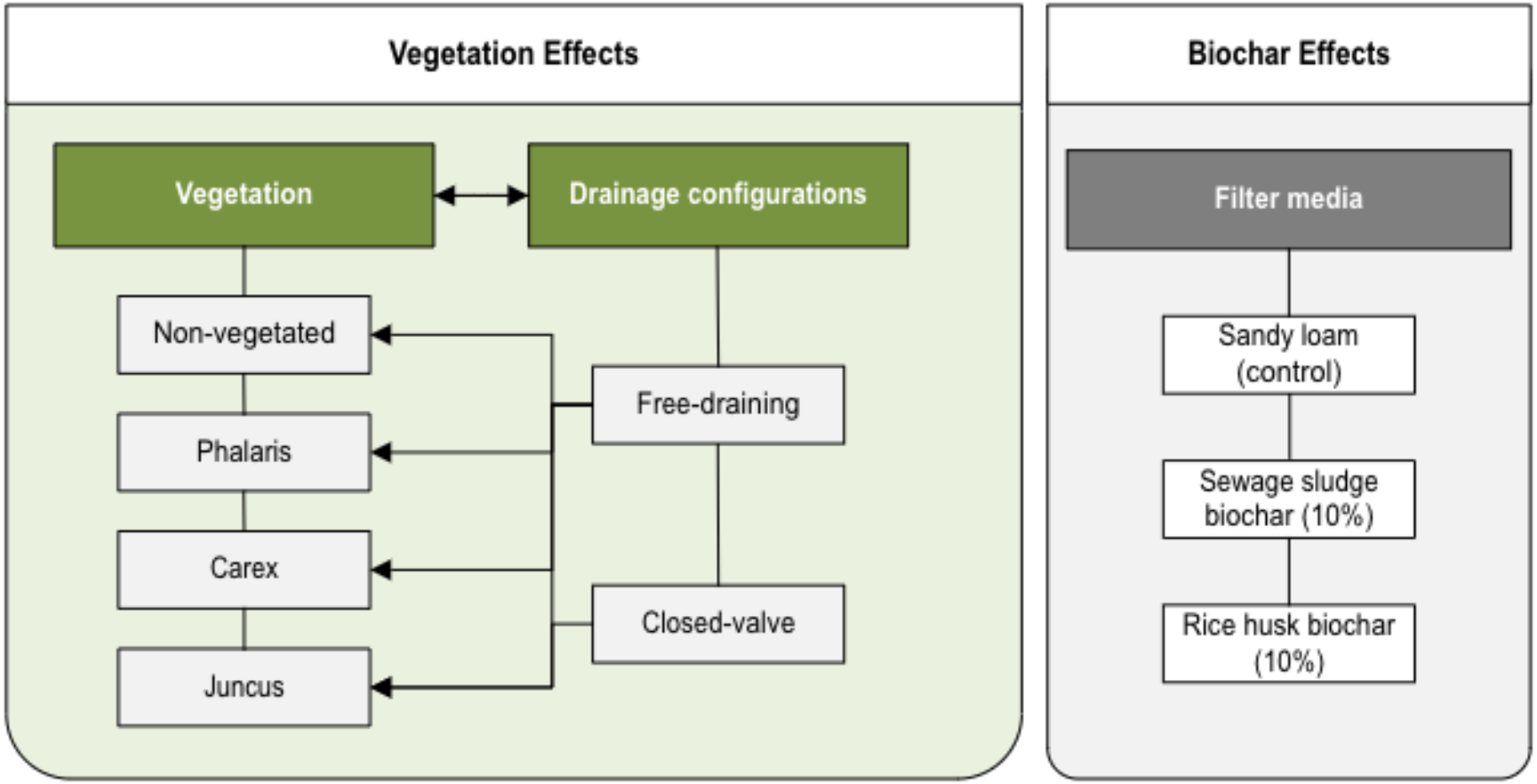

Figure 3.11 Summary of experimental variables. The large-column study tested the individual and interactive effects of vegetation and drainage configurations. The small-column study isolated biochar amendment effects under highly controlled conditions.

3.4 Statistical analysis

3.4.1 Common statistical approaches and their limitations

In studies evaluating the performance of bioretention systems, hypothesis testing often employs general linear models (GLMs), such as analysis of variance (ANOVA), to compare treatment effects on pollutant removal (Read et al. 2008; Zhang et al. 2011; Milandri et al. 2012; Chandrasena et al. 2014; Payne et al. 2018; Zinger et al. 2021). However, this experimental design involves repeated measurements of effluent pollutant concentrations from individual columns over several weeks, introducing temporal dependencies within each experimental unit (i.e., column). Traditional ANOVA assumes independence of observations—an assumption that is violated in this context due to repeated sampling from the same columns.

This violation is rarely addressed in bioretention studies. Among the few studies that do consider this issue, different workarounds have been employed. For example, Bratieres et al. (2008) accounted for repeated measures by treating time as a categorical variable (e.g., T1-T5) to capture temporal trends, as sampling occurred at fixed intervals in their study. Another common but suboptimal workaround, reported by Limouzin et al. (2011) involves aggregating repeated measurements (e.g., averaging pollutant removal percentages per column across time and replicates). While this method simplifies analysis, it disregards temporal variability and risks biased interpretations by ignoring within-subject correlations (Muhammad 2023).

Repeated measures ANOVA partially addresses this issue by modelling correlations between measurements from the same column. However, far fewer bioretention studies utilised repeated measures ANOVA, including those by Bock et al. (2015), Bratieres et al. (2008) Kuoppamäki et al. (2021), Mehmannavaz et al. (2001), and Pritchard et al. (2018). Repeated measures ANOVA requires strict assumptions, including sphericity (equal variances across time points) and balanced data (equal observations per column). These assumptions are often unmet in environmental studies, particularly in long-term research where missing data or unequal sampling intervals are common. Excluding columns with incomplete data (complete case analysis) reduces statistical power and introduces bias, especially in small-sample experiments typical of bioretention research (Muhammad 2023).

Additionally, repeated measures ANOVA treats time as a categorical variable, limiting its ability to model continuous temporal trends.

3.4.2 Linear mixed models

Linear mixed models (LMMs) overcome these limitations by explicitly modelling both fixed effects (experimental factors of interest) and random effects (sources of variability, such as differences between columns). Unlike ANOVA-based methods, LMMs accommodate unbalanced designs, missing data, and diverse covariance structures (e.g., autoregressive or unstructured), better reflecting the temporal correlation inherent in repeated measurements (Seltman 2012; Muhammad 2023). LMMs use maximum likelihood (ML) or restricted maximum likelihood (REML) estimation, enabling robust inference even with incomplete data. This contrasts with ANOVA, which relies on balanced designs for optimal performance (SPSS 2005).

In this study, two independent variables (2 × 2 levels) were tested: (1) vegetation presence (vegetated vs. non-vegetated columns) and (2) drainage configuration (closed-valve vs. free-draining configurations). The dependent variable (pollutant removal %) was measured repeatedly over several weeks for each column. LMMs are particularly suited to this design due to the nature of repeated measures and temporal correlation, as measurements from the same column are inherently correlated.

This was accounted for in the LMM by including column IDs as a random intercept, modelling within-column variability while adjusting for temporal correlation. Since the sampling intervals were not equal due to limitations imposed by weather conditions and other logistical constraints over the course of the experimental period, the dataset contained unbalanced data and missing observations. Unlike repeated measures ANOVA, LMMs retain experimental units with missing or irregularly spaced measurements, maximising statistical power. The model evaluated fixed effects (vegetation, drainage configuration, their interaction, and time) while controlling for random column-specific effects (column ID). This approach prevents confounding column-level variability with treatment effects.

Statistical analyses were conducted using IBM® SPSS Statistics, version 29.0.2.0 (20). The LMM input included:

- Fixed effects: vegetation presence (vegetated/non-vegetated), drainage configuration (closed-valve/free-drainage), their interaction effect, and time (weeks). Time was treated as a continuous variable to assess temporal trends in pollutant removal.
- Random effects: column ID was included as a random intercept to account for repeated measurements and inherent variability between columns.
- Covariance structure: an unstructured covariance structure was selected to allow the model to freely estimate correlations between measurements.

The effect of biochar amendment on pollutant removal was analysed similarly. The column ID was set as the random effects, while the repeated measures (time in days) and the filter media type were set as the fixed effects.

Hypothesis testing for fixed effects was performed using Type III F-tests and corresponding *p*-values, with the significance threshold $\alpha = 0.05$. Model assumptions, including normality of residuals and homoscedasticity, were verified using Shapiro-Wilk tests and residual plots respectively. In cases where model residuals were found to be non-normally distributed, the test was repeated using transformed values of the raw data (pollutant removals).
The pollutant removal efficiency of each column was calculated using the following formula:

$$Reomval\ (\%) = \frac{Inf_C - Eff_c}{Inf_C} \times 100 \quad (3.5)$$

Where Inf_C and Eff_c represent the respective influent and effluent concentrations.

In cases of leaching, the net increase was calculated as the difference between effluent and influent concentrations, normalised by influent concentrations, using the following equation:

$$Net\ leaching\ (\%) = \frac{Eff_c - Inf_C}{Inf_C} \times 100 \quad (3.6)$$

Correlation analysis was conducted to investigate possible correlations between dependent variables (pollutant removals and other parameters). Spearman's rank correlation was used as most of the data was found to be non-normally distributed (Payne et al. 2014a).

Chapter 4. Effects of Vegetation on the Performance of Bioretention Systems

This chapter details the core experimental study on the performance of bioretention systems in removing stormwater pollutants, including suspended solids, heavy metals (zinc, lead, and copper), and total phosphorus. This work represents the first study investigating the performance of native plant species under UK climate conditions. The research supports the thesis aim of enhancing bioretention design by evaluating how vegetation and extended residence time influence treatment and hydrological performance, while also examining the resulting spatial accumulation of heavy metals within the filter media.

The main objectives of this chapter are to:

1. Isolate and quantify the effects of vegetation by comparing vegetated and non-vegetated systems.
2. Assess and compare the efficiency of three UK-native plant species in enhancing system performance.
3. Evaluate the interaction effect of extended residence time on treatment performance and hydrology.
4. Examine the long-term spatial accumulation of heavy metals in the filter media.

4.1 Overall removal performance

4.1.1 Total suspended solids removal

Table 4.1 provides a summary of the statistics for TSS influent and effluent concentrations, as well as the calculated removal efficiencies of the bioretention columns in the analysed experiments. The results show that all columns achieved high mean removal of TSS in the closed-valve and the free-draining designs. TSS removal ranged from 85% to 92% in the closed-valve design, which is comparable with values found in the literature (87% to 99%) and considered successful in studies with similar column configurations (Hatt et al. 2007b; Hatt et al. 2007a; Bratieres et al. 2008; Barrett et al. 2013; Lucas 2015). The TSS removal efficiency was, on average, 5% lower in the free-draining design, where values ranged from 82% to 89%, suggesting a possible effect of extended residence time on pollutant removal.

A graphical presentation of the results, showing the variability of the measured TSS data, can be seen in the boxplots in Figure 4.1.

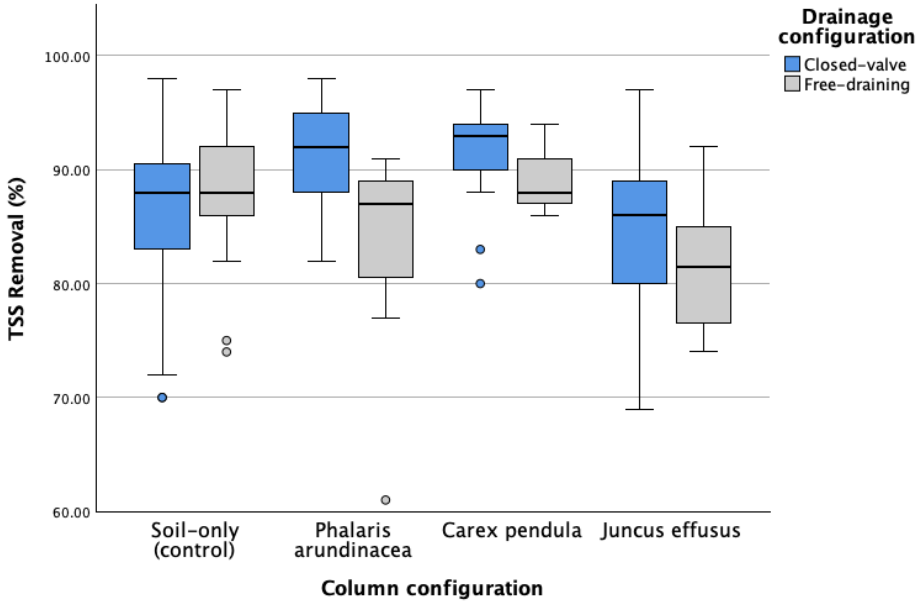

Figure 4.1 TSS removal efficiencies of non-vegetated controls and planted treatments under closed-valve and free-draining configurations. The box extends to the 1st and 3rd quartiles, and the whiskers show 1.5 times the interquartile range (IQR). Black lines represent the median values, while individual data points represent outliers. Longer whiskers indicate greater variability.

The performance of the *Carex* treatment was the best in TSS removal (89-91.5%), with the least variability in the dataset (SD, 2.98-4.49), while the *Juncus* treatment displayed the highest variability (SD, 5.98-7.69) and has the lowest mean removal efficiencies (81.5-85%), as detailed in Table 4.1. Similarly, the non-vegetated configurations showed a wide data spread in the closed-valve design, but there was no significant difference in the mean removal efficiencies between the free-draining and the closed-valve designs in the non-vegetated columns. The control and *Juncus* treatments exhibited greater spread in TSS removal efficiency in the closed-valve configuration, as indicated by the longer whiskers in Figure 4.1. Whereas the *Phalaris* treatment displayed wide variability in performance in the free-draining experiments. However, the spread of data within the 25th and 75th percentiles is relatively small across all configurations and falls within similar observations by Hatt et al. (2007a).

Table 4.1 General performance of bioretention columns showing mean concentrations and removal efficiencies in the closed-valve and free-draining experiments. SD are shown in parentheses.

Mean influent concentrations									
TSS (mg/L)		Zn (mg/L)		Pb (mg/L)		Cu (mg/L)		TP (mg/L)	
171 (34.75)		2.55 (0.26)		0.99 (0.26)		0.53 (0.04)		0.94 (0.21)	
Mean effluent concentrations and removal efficiencies									
Drainage		Closed valve				Free draining			
Vegetation		None	*Phalaris*	*Carex*	*Juncus*	None	*Phalaris*	*Carex*	*Juncus*
TSS	Concentrations (mg/L)	22 (12)	15 (9)	13 (6)	25 (14)	17 (8)	24 (11)	16 (4)	27 (7)
	Removal (%)	86.66 (6.97)	91.29 (4.47)	91.53 (4.49)	85.00 (7.95)	88.09 (5.80)	83.13 (9.93)	89.00 (2.98)	81.50 (5.98)
Zn	Concentrations (mg/L)	0.18 (0.13)	0.07 (0.05)	0.04 (0.03)	0.05 (0.02)	0.27 (0.22)	0.13 (0.22)	0.13 (0.21)	0.15 (0.21)
	Mean removal (%)	93.10 (5.06)	97.38 (2.09)	98.11 (1.50)	98.11 (0.86)	90.13 (7.72)	95.46 (7.65)	95.50 (7.31)	94.89 (7.11)
Pb	Concentrations (µg/L)	<20 (0.0)	<20 (0.0)	<20 (0.0)	<20 (0.0)	40 (0.0)	40 (0.0)	50 (0.0)	40 (0.0)
	Removal (%)	>98 (0.38)	>98 (0.40)	>98 (0.40)	>98 (0.40)	96.47 (3.52)	96.59 (4.11)	96.24 (3.87)	96.40 (3.56)
Cu	Concentrations (µg/L)	<5 (0.0)	<5 (0.0)	<5 (0.0)	<5 (0.0)	<10 (0.0)	<5 (0.0)	<5 (0.0)	<5 (0.0)
	Removal (%)	>99 (0.04)	>99 (0.04)	>99 (0.04)	>99 (0.04)	>99 (1.25)	>99 (0.12)	>99 (0.12)	>99 (0.12)
TP	Concentrations (mg/L)	0.94 (0.36)	0.98 (0.19)	0.67 (0.12)	0.65 (0.04)	0.59 (0.13)	0.85 (0.07)	0.54 (0.03)	0.58 (0.06)
	Removal (%)	17.5 (24.7)	9.2 (6.7)	38.3 (7.0)	38.8 (9.6)	25.4 (15.4)	-8.9(19.0)	31.46 (7.1)	26.7 (12.4)

The primary removal mechanism of total suspended solids (TSS) in bioretention systems is mechanical filtration through sedimentation and straining processes (Hatt et al. 2007b). As sediment-laden runoff flows through bioretention systems and passes through the filter media, larger particles, such as sand and debris, are strained at the media surface, while smaller particles settle by gravity through sedimentation and are typically trapped in larger pores within the upper layer of the filter media. In contrast, finer particles, such as silt and clay, are more difficult to remove through sedimentation, as they remain suspended in water for longer due to their small size and may easily pass through larger pore spaces in the filter media.

A particle size distribution analysis of the primary filter media used in this study (loamy sand) showed that approximately 79% of the filter media consisted of particles smaller than 600µm, 39% were smaller than 212µm, and about 5% were smaller than 63µm (Table A.1 in the Appendices). This heterogeneous mixture increased the likelihood of stratification within the filter media (Li and Davis 2008b). On the other hand, a particle size distribution analysis of the infiltrating particles (kaolin clay) used in this study showed that their size ranged from 1.2 to 32µm. Given this small size range, the clay particles could potentially pass through the larger pore spaces within the loamy sand. According to Li and Davis (2008a), the dominant removal mechanisms of suspended solids in bioretention media can be inferred from the ratio of the particle size of the filter media (d_m) to that of the infiltrating particles (d_p). A low ratio suggests surface straining with cake layer formation, whereas a high ratio shifts the process towards depth filtration or other physical and chemical separation methods.

The loamy sand media used in the present study had a particle size distribution skewed towards coarser grains (15.87% at 300µm, 15.61% at 212µm), and also contained a notable fraction of finer particles (5.10% ≤ 63µm as shown in Table A.1). The large size ratio between the median particle size (d_{50}) of loamy sand and kaolin clay (≈ 300µm and 9µm, respectively, giving $d_m/d_p \approx 33.3$) initially suggests that the dominant removal mechanism should be depth filtration as per the theory of Li and Davis (2008a). In this process, colloidal particles such as kaolin clay are transported through the porous medium via physicochemical filtration. Particles are brought to the surface of filter grains (collectors) through three primary mechanisms: interception, gravitational sedimentation, and Brownian diffusion. Interception occurs when a particle following a fluid streamline contacts the collector due to its finite size. Gravitational sedimentation, causes denser particles to settle onto the collector

surface; and Brownian diffusion, governs the motion of smaller particles, enabling contact with collector grains through random motion (Tufenkji and Elimelech 2004).

However, with repeated dosing in this study, a white cake layer was observed on the surface of the filter media, indicating kaolin clay accumulation (Figure 4.2). Despite the relatively high d_m/d_p ratio and the coarser grains of the filter media, cake layers formed on the media surfaces in all columns. This may be attributed to the high surface area and swelling potential of kaolin clay when wetted, which promoted gradual accumulation near the media surface (Li and Davis 2008b). Over time, these particles clog pores and form a low-permeability cake layer, shifting the dominant removal mechanism from depth filtration to surface straining. This observation aligns with Li and Davis's (2008a) findings, where cake formation of kaolin clay (d_{50} < 1µm) occurred in one out of two trials in bioretention media (d_{50} = 570µm). Even in media with coarse grains, the finer kaolin particles are prone to forming this impermeable layer on the media surface, restricting deeper penetration and increasing reliance on cake filtration.

Li and Davis (2008a) suggested that a media depth of 5-20 cm is sufficient for TSS capture, given its limited penetration. However, they emphasised the trade-off that fine sediments, such as clay, are critical drivers of clogging, as their small size and cohesive nature enhance pore blockage. This phenomenon is further explored in Section 4.2.3.

Figure 4.2 Cake layer formation decreased permeability rates and increased ponding time particularly in non-vegetated systems.

4.1.2 Heavy metals removal

Table 4.1 provides a summary of heavy metals removal. The results show that all column configurations effectively and consistently removed > 90% of heavy metal concentrations in the effluents. Lead and copper concentrations were mostly below the detection limits. These results are comparable to studies of similar bioretention column configurations, where heavy metals removal was considered highly successful (Hatt et al. 2007a; Hatt et al. 2007b; Read et al. 2008; Barrett et al. 2013; Lucas 2015; Jacklin et al. 2021a; Jacklin et al. 2021b).

4.1.2.1 Zinc removal

The mean removal efficiencies of Zn achieved in this study ranged from 93% to 98% in the closed-valve design, which is comparable to values found in the literature and considered successful in similar studies (>70%). Columns with the free-draining design achieved slightly lower performance, with removal efficiencies ranging from 90% to 96% (Figure 4.3). Similar to TSS removal, this difference in performance also highlights the effect of the extended residence time on Zn removal. This difference in performance was expected, as other studies have highlighted the importance of a saturated zone and longer contact time in improving the performance of biofilters in Zn and Cu removal (Blecken et al. 2010; Zhang et al. 2011), which is further discussed in Section 4.2.2.

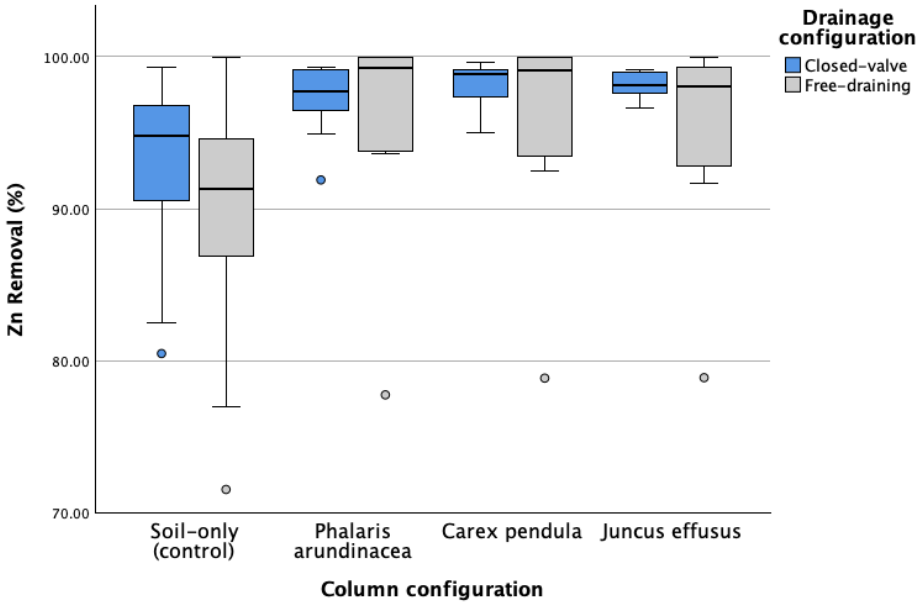

Figure 4.3 Zn removal efficiencies of non-vegetated controls and planted treatments under closed-valve and free-draining configurations. Black lines represent the median values, while individual data points represent outliers.

A partitioning analysis of Zn composition showed that, on average, about 86% of Zn in the influents and 89% of Zn in the effluent were dissolved. This suggests that the filter media was highly effective in removing both particulate and dissolved Zn. Given that Zn in the influent was predominantly in the dissolved form, the main removal mechanisms were likely adsorption, filtration, and precipitation within the media (Muerdter et al. 2018; Jacklin et al. 2021a). It is possible that most of the dissolved Zn in the influent was removed through adsorption onto the filter media surfaces. Given the moderate CEC of loamy sand (15.2 cmol/kg), the fine content (5.10% ≤ 63µm) and the Organic Matter Content (12%) can provide adsorption sites effectively removing dissolved Zn from the water.

On the other hand, physical filtration and surface straining likely contributed to the overall removal by capturing particulate-bound Zn in the small media pores (Hatt et al. 2007b). The cake layer and the fine sand content in the upper filter layers were more likely to have captured most of the Zn in the influent (refer to Section 4.3 for more details). Filtration of particulate-bound Zn was likely a secondary mechanism but still contributed to overall Zn removal where Zn adhered to suspended particles.

4.1.2.2 Lead removal

The biofilter columns effectively reduced Pb concentrations in the effluent to below the detection limit (i.e. < 20µg/L) for all closed-valve trials. However, a few concentrations were detected during the initial weeks of the free-draining experiment before declining to below the detection limits as shown in Figure 4.4 below. Overall, the columns were highly effective in removing Pb, with 96% to > 98% removal. This rate aligns with values found in other studies with similar column configurations (Hatt et al. 2007a; Hatt et al. 2007b; Read et al. 2008; Lucas 2015).

The partitioning analysis revealed that Pb in both influent and effluent samples was almost entirely particulate-bound, indicating that the predominant removal mechanism for Pb was filtration and surface straining. Consequently, Pb was effectively removed alongside TSS particles, as described earlier in Section 4.1.1. Given that Pb was present solely in particulate form, it was most likely captured through cake filtration in the upper layers of the filter (detailed in Section 4.3).

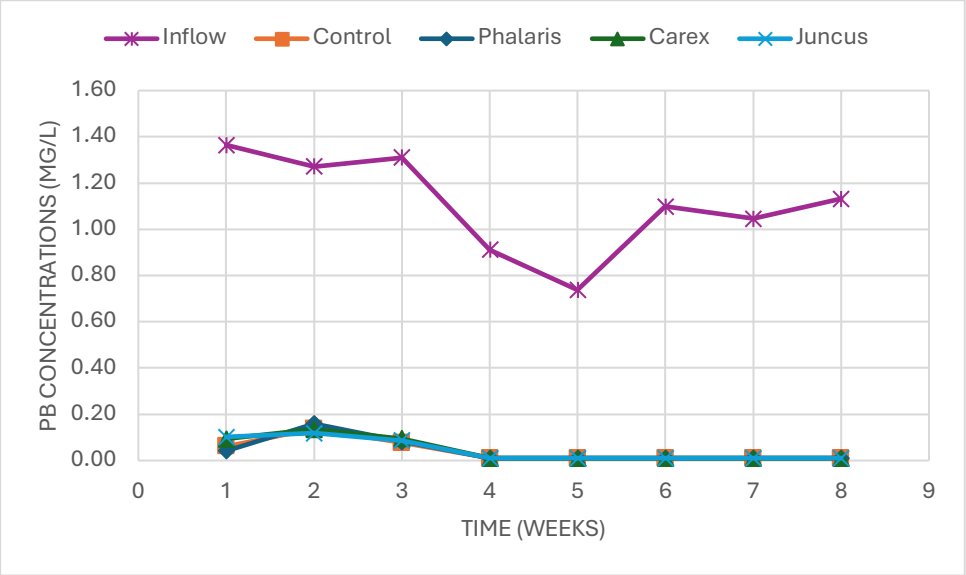

Figure 4.4 Effluent Pb concentrations in the free-draining treatments over 8 consecutive weeks. Concentrations from week 4-8 were below the detection limit in all columns.

4.1.2.3 Copper removal

Similarly, apart from a single reading detected in a free-draining trial (Figure 4.5), all Cu was effectively removed from all columns in all trials, reducing concentrations to below the detection limit (< 5µg/L). Despite 29% of Cu in the influents being present in dissolved form, all columns effectively reduced particulate and dissolved Cu concentrations to below the detection limit. The primary removal mechanisms were likely a combination of physical filtration for particulate-bound Cu and adsorption for dissolved Cu. Filtration and surface straining played the main role by capturing the 71% of particulate-bound Cu in the upper layers of the filter media. As water percolated down the column, the fine content in the loamy sand media likely had sufficient adsorption capacity to attract dissolved copper ions (Cu^{2+}), effectively removing them from the water as it percolated down the column.

The results showed no significant differences between design variables (vegetation or residence time), which is attributable to the high affinity of Cu to adsorbents such as clay particles and organic matter (Hasan et al. 2020; Furén et al. 2023). It is important to note that the pollutant loading in this study was 10 times the typical concentrations found in urban runoff and in synthetic stormwater used in similar studies. Despite the high concentrations, all columns performed consistently well in metals removal.

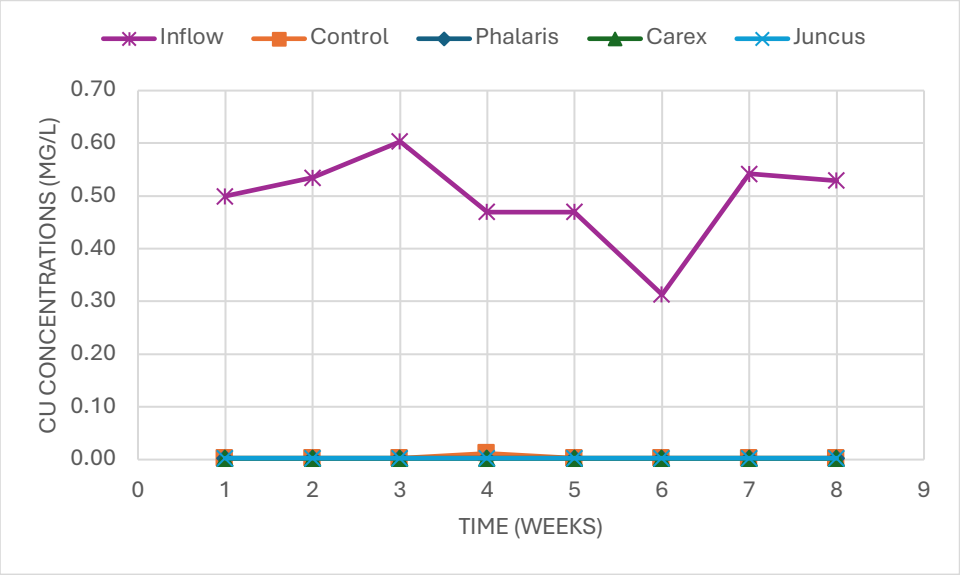

Figure 4.5 Effluent Cu concentrations in the free-draining treatments over 8 consecutive weeks. All concentrations were below the detection limit in all columns except one observation in week 4 in a non-vegetated control.

4.1.3 Total phosphorus removal

Table 4.1 shows that the biofilter columns performed poorly in total phosphorus removal compared to other pollutants, with mean removal efficiencies ranging from 9% to 39% in the closed-valve experiment. Mean TP removal rates in vegetated columns were even lower in the free-draining experiment, with the *Phalaris* treatment showing a net production of 9%, indicating consistent leaching of TP into the effluent and highlighting the possibility of biofilters being a source of phosphorus. Figure 4.6 shows the removal rate of TP in consecutive trials. The graphs illustrate that non-vegetated columns had the highest removal rate variability in the closed-valve trials, which was mainly caused by a drop in influent concentrations around week 32, leading to a 15-fold increase in average removal rates.

This demonstrates that removal performance might be significantly affected by the pollutant strength in non-vegetated columns. It is also possible that this variability in performance is a result of the leaching of TP during the first weeks of dosing, which stabilised with time, as noted in a similar study by Jacklin et al. (2021a), where TP removal improved with repeated dosing. In contrast, the removal rate in the *Juncus* column showed a slight decrease over time. In both experiments, the vegetated columns slightly outperformed the non-vegetated columns in TP removal, except for the *Phalaris* column (Figure 4.7).

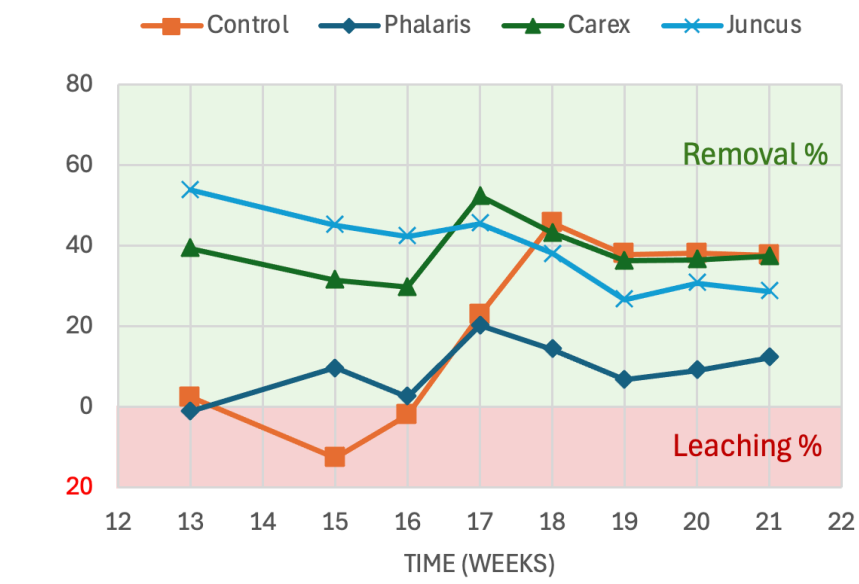

a)

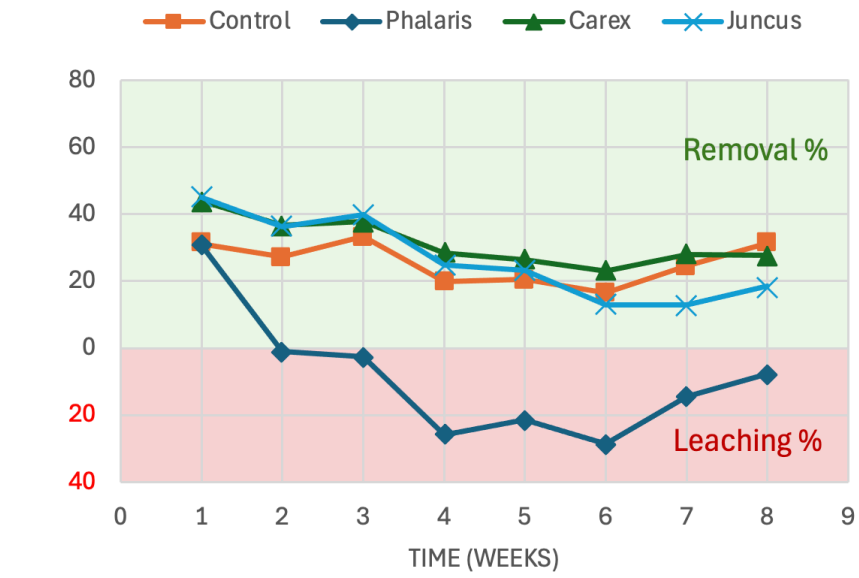

b)

Figure 4.6 Variations of TP removal in a) the closed-valve and b) the free-draining experiments over 8 consecutive weeks.

This highlights the complex interactions between the type of vegetation, residence time, and phosphorus removal dynamics in bioretention systems. A partitioning analysis of phosphorus in the influent showed that about 66% was particulate-bound, while only 18% was in particulate form in the effluent, suggesting good retention of particulate P and possible leaching of dissolved P from the filter media itself as a primary source of dissolved P in the effluents. In the free-draining design with shorter residence time, the primary removal mechanism for particulate phosphorus was likely physical filtration by the filter media

(Bratieres et al. 2008). The presence of root systems and root expansion in vegetated columns could have altered the pore distribution and media structure, creating preferential flow paths for particulate phosphorus to bypass filtration near root zones, which can reduce the efficiency and uniformity of physical filtration in vegetated columns. This effect was minimal in soil-only configurations with less heterogeneous flow paths (Li et al. 2020; Zinger et al. 2021). This is also evident in a performance comparison between the *Juncus* column and non-vegetated columns, where TSS removal was lower in the former (82-85%) than in the latter (87-88%).

Excessive organic matter might have contributed to the net release of phosphorus in the *Phalaris* columns, which experienced plant die-off and exudates, leading to the leaching of dissolved phosphorus (Bratieres et al. 2008). This problem can be mitigated with extended residence time, as evidenced by Table 4.1, where the *Phalaris* treatment leached 8.9% in the free-draining trials but removed 9.2% in the closed-valve trials.

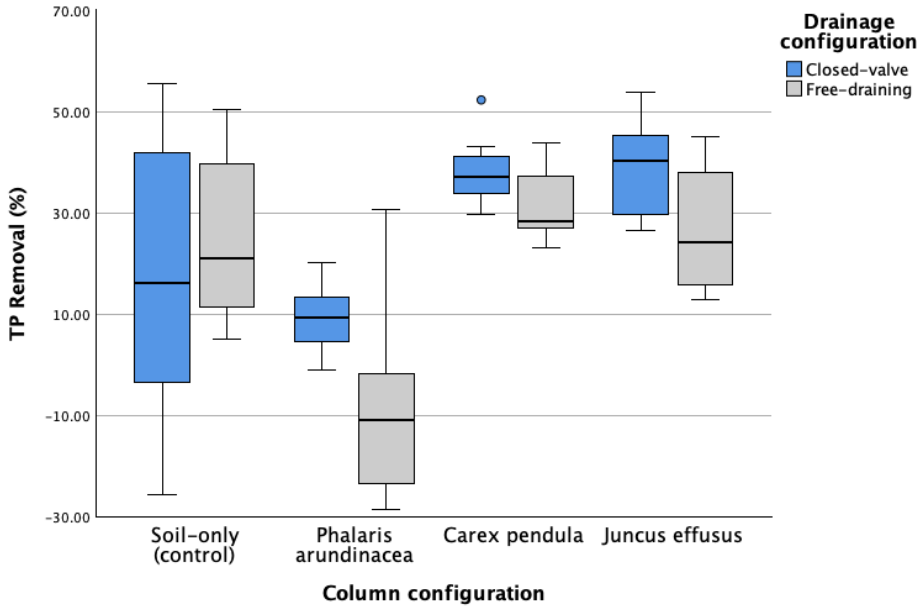

Figure 4.7 TP removal efficiencies of non-vegetated controls and planted treatments under closed-valve and free-draining configurations. Black lines represent the median values, while individual data points represent outliers.

4.2 Effects of design variables on system performance

4.2.1 Vegetation

4.2.1.1 Effect of vegetation on TSS removal

Figure 4.8 displays the variations in TSS removal in the closed-valve experiment. On average, a slightly downward trend can be observed in the vegetated columns, and a slightly upward trend in the non-vegetated columns. However, the relatively small values of the coefficient of determination (R^2 = 0.1–0.2) suggests that the variability in the data does not have a strong correlation with time over the 20-week period. When evaluating the overall effect of vegetation, the results from the Linear Mixed Model (LMM) presented in Table 4.2, showed that the presence of vegetation had no significant effect on TSS removal (p = 0.504). Although the removal efficiency of suspended solids was slightly higher on average in the vegetated columns (89%) compared to the non-vegetated columns (87%), this difference appears to be insignificant in practical terms. This finding agrees with similar studies where no significant difference was observed with the presence of vegetation (Read et al. 2009; Barrett et al. 2013; Jacklin et al. 2021b).

However, different species performed better than others in removing suspended solids, with average removal rates of 93%, 91%, and 88% for *Carex*, *Phalaris*, and *Juncus*, respectively. Average effluent concentrations were found to be the highest in the *Juncus* column (25 mg/L), with high variability in the dataset (SD ± 14 mg/L). It is important to highlight that the limited number of columns used in this study restricted hypothesis testing to the presence of vegetation effect alone and prevented a statistically robust assessment of species selection effects. Increasing the number of replicates per species would enhance the reliability and reproducibility of the results.

Table 4.2 Linear Mixed Model showing effects of design variables on pollutants removal in bioretention columns (α = 0.05).

Effect	**p-value**		
	TSS	Zn	TP
Vegetation (vegetated, non-vegetated)	0.504	0.059	0.704
Drainage (closed-valve, free-draining)	0.435	0.070	0.810
Vegetation x drainage[a]	0.588	0.859	0.469

[a] interaction effects between vegetation and drainage configurations.

The variability among non-vegetated columns was also relatively high (22 ± 12 mg/L), despite having a replicated design. Efforts were made to achieve replicated columns as much as possible during the mixing and packing process of the filter media; however, it is possible that some columns had higher percentages of fines than others, which might explain the variability in performance in the non-vegetated columns. Hatt et al. (2007b) argued that this variability can be attributed to what they referred to as the "conditioning" of the filter media, where higher suspended solids concentrations were typically observed in the early stages of the experiment as a result of settling and washing out of fines in the media. They showed that filters with high levels of suspended solids tended to increase removal efficiencies over time, as the supply of fines in the media was exhausted with repeated flushing. Other studies have confirmed that TSS removal efficiency increases with time (Li et al. 2020; Jacklin et al. 2021a).

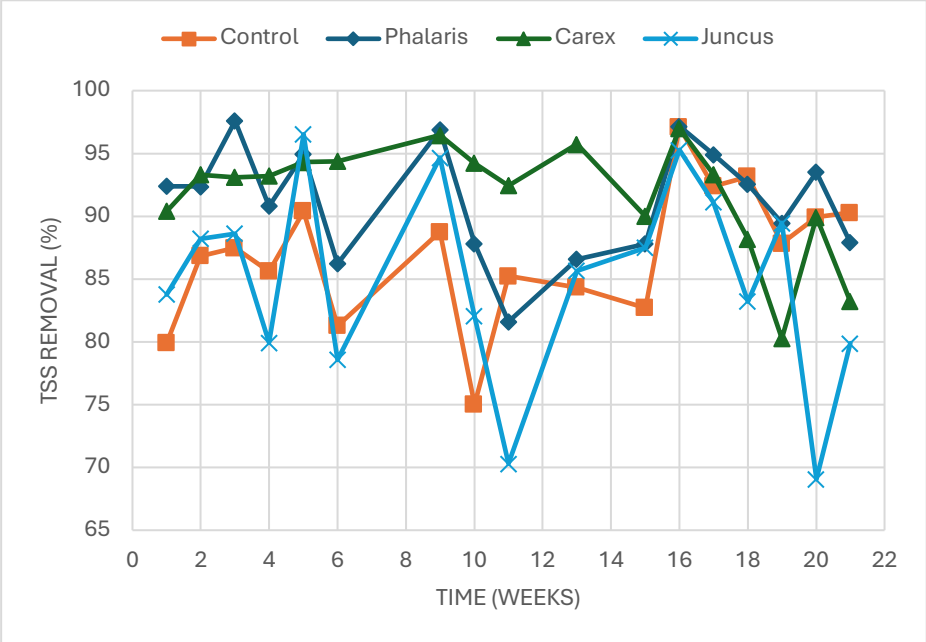

Figure 4.8 TSS removal variations in the closed-valve experiment over 21 weeks of dosing.

This trend was difficult to be observed in this study, as data from the early weeks of the experiments were used for method development and were not included in the analysis, while the data that were included did not show a strong correlation with time (Figure 4.8). However, this trend was observed in the biochar column study, which are discussed in Chapter 5. Overall, *Carex* had the highest and least variable removal rate of suspended solids (SD ± 4%), followed by *Phalaris*, soil-only controls, and lastly *Juncus*.

A possible explanation for the observed difference in TSS removal efficiencies between *Carex* and *Juncus*, despite having similar biomass, may be explained in two ways. Firstly, it can be attributed to differences in rhizome structure, root morphology, and distribution. *Juncus effusus* are clump-forming plants with stout rhizomes and a dense root system. Similarly, *Carex pendula* forms thick clumps but tends to have more fibrous and extensive, hair-like roots as shown in Figure 4.9 (Bratieres et al. 2008). Secondly, the spreading rhizomatic structure of *Carex pendula* could have provided more surface area and promoted more uniform water distribution and slower flow rates, which prevented preferential flow paths, resulting in better suspended solids retention.

On the other hand, channelling and preferential flow paths can become more prominent in the clumpier, compact rhizomes and root structure of *Juncus effusus* when the filter media is subjected to unsaturated conditions, such as in bioretention systems. This might lead to the formation of large pores (particularly during prolonged drying periods) and faster water percolation. This was supported by measurements of the outlet discharge rates presented in Table 4.3. The mean discharge rate in the *Carex* column was 48.3 (±9.0) mL/min, while the *Juncus* column had a mean rate of 66.3 (±18.4) mL/min, supporting the possibility of flow paths occurring in the *Juncus* column. This likely contributed to the migration of fine particles from the top filter layer along the flow paths, resulting in less surface straining and reduced TSS retention in the *Juncus* column (Li et al. 2020; Zinger et al. 2021).

Similarly, the *Phalaris* column showed signs of channelling, based on the relatively high discharge rate (84.3 mL/min). However, the TSS removal remained as high as the *Carex* column, with a mean removal of 91%, which might have resulted from the accumulation of biofilms and decomposed organic matter on the *Phalaris* biofilter surface, preventing the migration of fines down the column. Section 4.2.3 below discusses the clogging phenomenon observed in the columns and the effect of vegetation on hydraulic conductivity.

Figure 4.9 Comparative root structure of *Juncus effusus* (left, thick roots) and *Carex pendula* (right; fibrous structure). Differences in roots may have promoted preferential flow paths in *Juncus*, or uniform filtration in *Carex*.

Table 4.3 Mean discharge rates measured from outlet pipes of bioretention columns after 61 weeks of operation, showing effect of plants on enhancing hydraulic conductivity. Measurements were taken immediately after discharge began until discharge ceased or up to 12 hours of drainage.

Column	**Mean discharge rate (mL/min)**
Soil-only (control)	2.9 (±0.4)
Phalaris	84.3 (±18.3)
Carex	48.3 (±9.0)
Juncus	66.3 (±18.4)

4.2.1.2 Effect of vegetation on heavy metals removal

Vegetation columns were on average 5% more efficient in Zn removal than non-vegetated systems in both drainage experiments, with slight variations between treatments (Figure 4.10). However, these variations were not statistically significant on average. This was likely due to the relatively high overall removal rate, the rapid sedimentation and precipitation occurring within the first few centimetres of the soil media, and the probable adsorption of dissolved metals. This aligns with the findings of this study, in which Zn was predominantly present in dissolved form (Read et al. 2008; Read et al. 2009; Al-Ameri et al. 2018; Muerdter et al. 2018).

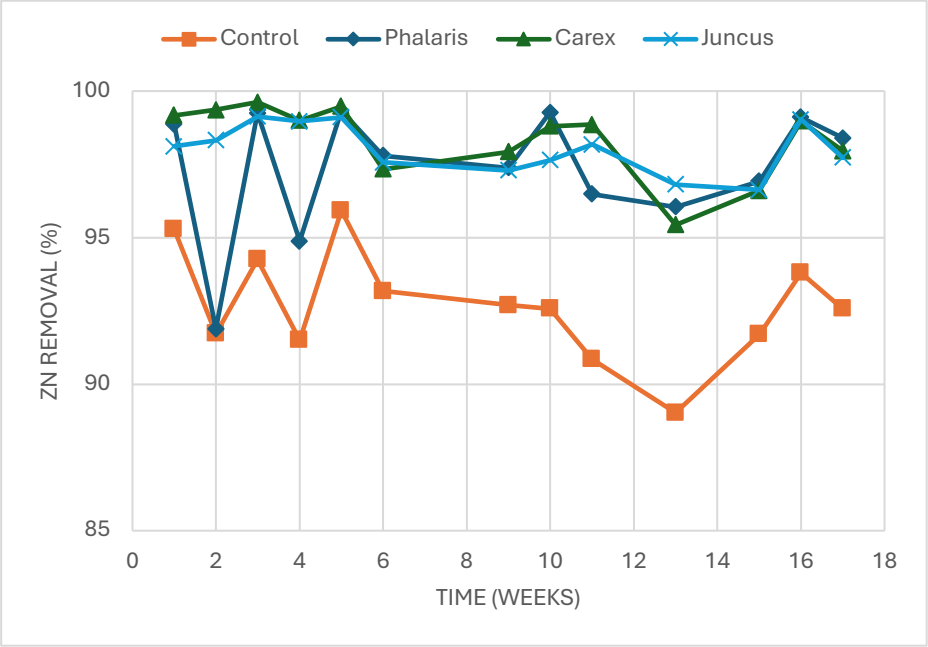

Figure 4.10 Zn removal variations in the closed-valve experiments over 17 weeks of dosing.

Table 4.2 shows the results from the LMM, as with TSS, the presence of vegetation had no significant effect on metals removal ($p = 0.059$). This is consistent with observations in similar studies, where both vegetated and non-vegetated biofilters were found to be highly effective in removing heavy metals, and significant differences in effluent concentrations between vegetated and non-vegetated configurations were rare (Hatt et al. 2007b; Read et al. 2008; Read et al. 2009). Similarly, there was no difference in Pb and Cu removal efficiencies between vegetated and non-vegetated systems, indicating that the removal of both Pb and Cu is independent of the presence of vegetation or the type of plants, and that they can be predominantly removed through the soil media (Read et al. 2008; Read et al. 2009).

This was evident in Figure 4.4 and Figure 4.5, where Pb and Cu concentrations in all effluent samples were below the detection limits, except for a few observations in the free-draining design.

Certain heavy metals are required by plants only in trace amounts, and they are significantly less crucial than nutrients, as demonstrated by analysis of plant tissues where their concentrations were found to be generally low (Read et al. 2009). Sun and Davis (2007) found that 88-97% of Cd, Cu, Pb, and Zn were adsorbed by the filter media, with only 0.5- 3.3% being taken up by plants. They argued that an increase in plant biomass could enhance metal uptake.

Similar findings were reported by Beral et al. (2023), who showed that while analysis of trace elements such as Cr, Cu, Ni, and Pb in plant tissues was below detection limits, plants with high biomass, such as *Juncus*, accumulated more Zn and Manganese (Mn) in their shoots than the cumulative mass of Zn and Mn in the effluents over the course of the experiment, suggesting that *Juncus* uptake of Zn and Mn was supplied from both the substrate and the influent loadings.

It is difficult to confirm these findings since plant tissue was not analysed in this study. However, the difference observed in the average removal rates shown in Table 4.1 between the vegetated columns (95-98%) and non-vegetated columns (90-93%) suggests possible plant uptake of dissolved Zn. Conversely, the difference between species with varying biomass was marginal (<1%), making it difficult to establish a strong correlation between plant traits and Zn removal. This finding is consistent with Read et al. (2009).

The significance of these results lies in the relatively high concentrations of heavy metals in the influent. For instance, a breakthrough analysis by Hatt et al. (2011) which experimented with influent concentrations five times the typical stormwater levels in soil-only columns without the effect of vegetation, concluded that while Zn breakthrough occurred, it was less likely for Pb and Cu to break through during the operational life of the filter (>10 years for biofilters sized 2-3% catchment area, or with ≥ 500mm-deep filter layer). This finding was corroborated in this study where each dosing event corresponded to the pollutant loading of ten storm events under field conditions, only Zn was consistently observed in the effluent.

This suggests that even with a relatively shallow filter media depth (350 mm), all columns were highly effective in removing Pb and Cu, irrespective of plant presence or species selection, with no indication of metal saturation. However, the presence of vegetation showed improvement in the removal efficiency of dissolved Zn by 4% and 5% in the free-draining and closed-valve experiments, respectively, reinforcing the potential role of vegetation in optimising treatment performance of dissolved metals.

4.2.1.3 Effect of vegetation on TP removal

TP removal in vegetated systems was on average 6% higher than non-vegetated systems in the closed-valve design. However, there was substantial variability observed between treatments, particularly in the free-draining design (Figure 4.6). This variability led to a high p-value (> 0.704) for the effect of vegetation, as determined by the LMM. Although this agrees with a study by Read et al. (2008), which found no significant differences among plant species and soil-only controls, the overall removal rates in this study (21%) do not compare favourably with the relatively high removal (>70%) rates reported by Read et al. (2008) and other studies in the literature. It is worth noting that the mean TP influent concentration achieved in this study (0.95 mg/L) was relatively higher than those found in other studies (0.4-0.7 mg/L), which may have contributed to the lower removal rates.

Another factor that could play a significant role in the low mean removal efficiency of TP in the columns is the high Organic Matter Content (OMC) in the loamy sand media (12%), which exceeded the OMC of 4% reported by Read et al. (2008) and the recommended SuDS guidelines of 3-5%. While the high organic content was crucial for plant growth and survival, the trade-off was the relatively large amount of TP leaching from the media. Indeed, Bratieres et al. (2008) demonstrated that the addition of organic matter to the filter media can lead to the release of phosphate (PO_4^{3-}) during breakdown reactions, resulting in increased phosphate leaching from the system, as also noted by Read et al. (2008) and Jacklin et al. (2021a). This was demonstrated in the *Phalaris* column, where plant stress and die-off due to frequent inundation caused a consistent net release of TP into the effluent in the free-draining design, as shown in Figure 4.6.

This outcome is unsurprising, as *Phalaris* had a smaller biomass, a thinner root system, and lower tolerance to stormwater inundation compared to *Carex* and *Juncus*. However, longer residence time tended to improve TP retention, even in the *Phalaris* column (Figure 4.6).

This highlights the potential role of extended residence time and species selection in enhancing TP removal. On average, *Carex pendula* was the best performer in terms of TP removal, followed by *Juncus effusus*, non-vegetated controls, and *Phalaris arundinacea*. This confirms the findings of Read et al. (2008), and aligns with the recommendations of Bratieres et al. (2008) to use plants with morphological characteristics similar to *Carex appressa*, a species native to Australia that has been shown to achieve >77% TP removal. Bratieres et al. (2008) attributed the high performance of *Carex* species to their extensive, hair-like root systems, which could satisfy up to 60% of the plant's phosphorus demand.

Although *Carex pendula* (the plant native to the UK used in this study) achieved high TSS and metal removal comparable to the studies mentioned above, it was less effective in TP removal, with mean removals of 38% in the closed-valve design and 31% in the free-draining design (Table 4.1), compared to 70% measured in other studies (Bratieres et al. 2008), but within the upper range (-81-63% for orthophosphate) reported by Jacklin et al. (2021a). This relatively poor performance was likely influenced by the leaching of organic matter from the substrate media and pollutant loading rather than the presence of this species.

Overall, the results of this study are consistent with findings by Bratieres et al. (2008) and Read et al. (2008) which highlight that there was no significant difference between vegetated and non-vegetated systems, due to the particulate form of phosphorus found in the influent, which was likely removed by filtration processes.

4.2.2 Effect of residence time on pollutant removal

Although there were removal enhancement of TP and TSS in the closed-valve experiment with extended residence time, particularly in vegetated columns (Table 4.1), the effect was not statistically significant. Table 4.2 shows the results from the LMM for the effect of design variables on pollutant removal. As can be seen, the high p-values (>0.05) for the effect of drainage configurations (closed-valve, free-draining) suggest that the extended residence time of 24 hours had no significant effect on pollutant removal overall. There was also no significant interaction effect between the tested variables (i.e., the interaction between the presence of vegetation and drainage design). These results agree with similar studies, where the presence of a saturated zone was investigated and found not to have a practical influence on TSS and heavy metals removal (Blecken et al. 2010; Barrett et al. 2013).

These results are unsurprising, given the very high removal rates of heavy metals as noted by Blecken et al. (2010). Additionally, the water quality parameters investigated in this study, apart from Zn, were predominantly particulate-bound, as determined by the partitioning analysis of the influents. Given that the primary removal mechanism for particulates in bioretention systems is filtration and straining (Hatt et al. 2007b; Kuoppamäki et al. 2021), it was expected that residence time will play a minor role in particulate removal. However, it was expected to observe the residence time effect on TP removal as previously documents by Wu et al., (2017) and Zhang et al. (2011).

The lack of significant difference between the two drainage experiments is likely to arise from two sources: the relatively high variability within each column configuration (not only between different plant species but also within non-vegetated configurations), particularly in terms of TP removal. The second source could be the short timeframe during which the effect of residence time was investigated (8 weeks), resulting in a smaller sample size with fewer observations that might not have been sufficient to detect a true effect at the 95% confidence level.

Although residence time appeared to have no significant overall impact, it is important to note that this outcome applies only to the limited range of pollutants investigated in this study (TSS, heavy metals, and TP). The results might differ if nitrogen species were analysed. Additionally, the existing data on TP removal are inconsistent and the sample size is relatively small, warranting long-term investigation.

4.2.3 Hydrological performance and clogging

Evidence of clogging was observed in this study. After six weeks of synthetic stormwater dosing, the non-vegetated controls began to show signs of clogging, with prolonged ponding and detention times (Figure 4.2). This necessitated a change in the dosing schedule, reducing dosing events from three times per week to once per week to allow more time for water infiltration, as explained in Chapter 3. The concentration of suspended solids was kept close to typical concentrations, as urban runoff rich in fine sediments (<6 mm in diameter) has been shown to accelerate clogging and system failure, including frequent overflows, prolonged ponding, reduced treatment capacity, and potential aesthetic and public health concerns (Hatt et al. 2008; Li and Davis 2008b; Le Coustumer et al. 2012; Lim et al. 2015).

Indeed, sediment accumulation is a primary driver of clogging. In the field, such conditions exacerbate watercourse degradation and may encourage mosquito breeding due to prolonged standing water (Muerdter et al. 2018; Jacklin et al. 2021a).

A field study by Le Coustumer et al. (2009) assessing the long-term hydraulic performance of stormwater bioretention systems found that approximately 40% failed to meet design expectations for hydraulic conductivity. Similarly, Le Coustumer et al. (2012) demonstrated that biofilters tend to clog over time, with average hydraulic conductivity decreasing by a factor of 3.6 over 72 weeks of testing. Their findings highlighted the role of design configuration in enhancing both the performance and longevity of biofilters.

Key factors influencing pollutant removal efficiency and the rate of clogging include vegetation type, media depth, system size relative to its catchment, soil composition, and sediment load (Le Coustumer et al. 2012). The size of a bioretention system relative to its catchment area is particularly influential. Smaller systems are prone to clogging more quickly, whereas larger systems tend to sustain higher hydraulic conductivity over time, with rates of up to 50 cm/h even after 10 months of operation (Barrett et al. 2013).

The sediment composition also contributes to clogging. In this study, the use of kaolin clay (1.2 to 32μm) led to the formation of cake layers on the filter media surface, causing pore blockage and reduced permeability, consistent with the observations of Li and Davis (2008). Another important factor that may have contributed to the clogging observed in this study was the small size of the outlet pipes (~10 mm), which, although facilitating longer contact times, makes them more susceptible to clogging (Sileshi et al. 2010).

Prolonged residence time can heighten the risk of clogging due to the accumulation of suspended solids, biological growth, and sedimentation within the media. Extended residence times facilitate the settling of fine particles and the accumulation of organic materials, promoting microbial activity that can result in bioclogging (Zhu et al. 2020). This process reduces the hydraulic conductivity of the system, which affects its overall efficiency, particularly in vertical flow systems similar to this study design.

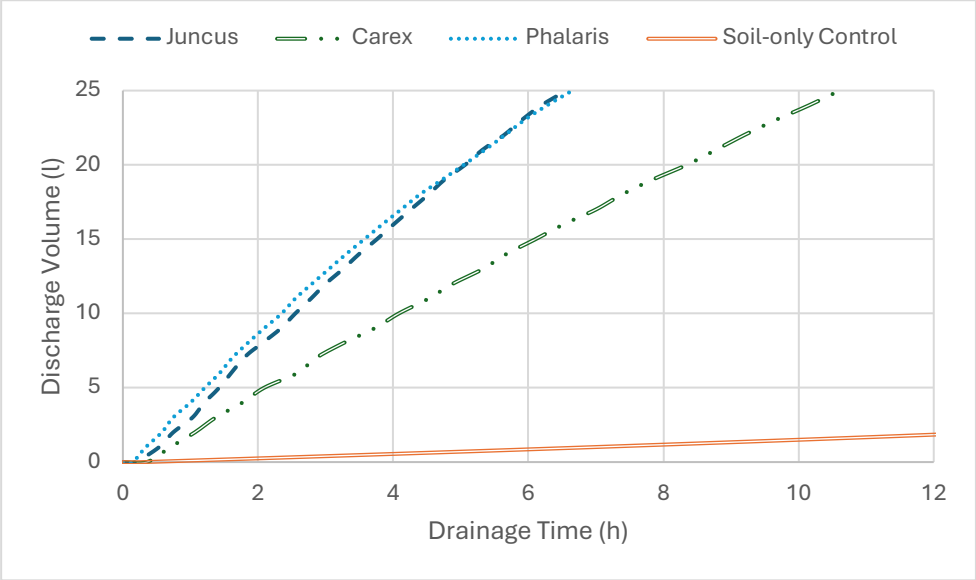

Figure 4.11 Measurements of discharge volumes of bioretention columns over 12 hours of drainage after 61 weeks of operation, showing the effect of planted treatments on maintaining the hydraulic conductivity of the systems.

While longer residence times may enhance pollutant removal, especially for soluble zinc, there is a trade-off with the increased risk of clogging. This was particularly significant in non-vegetated columns. Figure 4.11 shows the outflow rates of columns after 61 weeks of operation. As can be seen, the vegetated columns had a significantly higher conductivity by the end of the experiment than the non-vegetated controls, highlighting the importance of vegetation in improving the long-term hydraulic performance of biofilters.

This confirms the findings of similar studies in the literature (Bratieres et al. 2008; Read et al. 2009; Le Coustumer et al. 2012; Barrett et al. 2013). These studies also highlighted media and species selection as key factors for performance and sustainability. For example, plants with thick root systems, capable of forming extensive macropores within the media, are particularly effective in maintaining hydraulic conductivity and preventing clogging (Read et al. 2009; Muerdter et al. 2018), while plants with finer roots showed no such beneficial effects (Le Coustumer et al. 2012). Conversely, soil penetration by roots, particularly in vertical flow conditions with intermittent wetting and drying such as in bioretention systems, can cause micro-crack formation and disrupt the retention of fine particles (Li et al. 2020; Zinger et al. 2021). This was observed in the high TSS concentrations in the effluent of the *Juncus* configuration, as discussed in Section 4.2.1.1.

Other trade-offs reported in bioretention studies of plants with denser roots include the formation of preferential flow paths, which can reduce nitrate removal (Muerdter et al. 2018). Therefore, bioretention design should carefully consider plant species, root depth relative to media depth, vegetation density, and optimised residence time, alongside outlet pipe design, to ensure balanced and sustainable performance (Le Coustumer et al. 2012; Muerdter et al. 2018).

4.3 Accumulation of heavy metals in the media

Following the conclusion of the experiment, grab samples of soil were collected from the surface (0-3 cm) and the subsurface (12-15 cm) and compared with samples taken prior to the application of any synthetic stormwater treatment, which served as a baseline for soil background concentrations. The results from the XRF analysis of the three metals investigated (Zn, Pb, Cu) are presented in Figure 4.12. The data indicate that substantial accumulation of metals occurred in the surface layer relative to the subsurface layers. For example, Pb concentrations in the surface layer reached 3,321 mg/kg in the vegetated columns (Table 4.4), whereas subsurface Pb levels were only 184 mg/kg.

Similar trends were observed for Cu (surface: 1,408 mg/kg; subsurface: 146 mg/kg) and Zn (surface: 4,743 mg/kg; subsurface: 588 mg/kg). Non-vegetated systems exhibited comparable accumulation, although the surface concentrations were lower (e.g., Pb: 2,556 mg/kg at the surface versus 183 mg/kg in the subsurface). This is supported by a paired t-test which revealed significant differences between the surface and subsurface groups ($p < 0.05$).

It is important to note that the relatively high concentrations observed in this study are attributable to the high influent loading. As described in Chapter 3, the synthetic stormwater recipe used had average concentrations approximately 10 times higher than those in typical runoff in the field, to simulate accelerated dosing within the timeframe of the study. As a result, 1 storm even had heavy metal influent loading equivalent of 10 storm events.

Table 4.4 Mean heavy metals concentrations at the surface and subsurface layers of bioretention columns after 61 weeks of operation and baseline concentrations.

Configuration	Pre-treatment (baseline)	Surface (0-3 cm)	Sub-surface (12-15 cm)
	Pb concentrations (mg/kg)		
Vegetated	28	3321	184
Non-Vegetated	48	2556	183
	Cu concentrations (mg/kg)		
Vegetated	26	1408	146
Non-Vegetated	27	1451	102
	Zn concentrations (mg/kg)		
Vegetated	60	4743	588
Non-Vegetated	65	3999	404

A visual representation of the accumulation levels, grouped by configuration, is provided in Figure 4.12. Compared with baseline levels—represented in the boxplots by the horizontal lines—the mean increase in heavy metal concentrations in the surface layer over the course of the experiment was by factors of 86, 54 and 70 for Pb, Cu and Zn, respectively, while concentrations in the subsurface layers increased by factors of 5.2, 4.7 and 8 for Pb, Cu and Zn, respectively. This vertical trend is consistent with the findings of Jones and Davis (2013), who reported that the majority of metals accumulate in the top 5-10 cm of bioretention media, followed by a rapid drop to baseline concentrations with increasing depth due to filtration and sorption processes.

The dominance of surface-layer retention can be attributed to cake layer formation, which increased surface straining, particularly for Pb, which was found to be almost entirely particulate-bound. The surface cake layers may also have provided adsorption sites for dissolved Cu and Zn via cation exchange and complexation (Hasan et al. 2020; Furén et al. 2023). Subsurface layers showed minimal metal accumulation, indicating limited downward migration, with Pb and Cu concentrations in the subsurface being ≤10% of those at the surface, and Zn reaching a slightly higher proportion (≤12%).

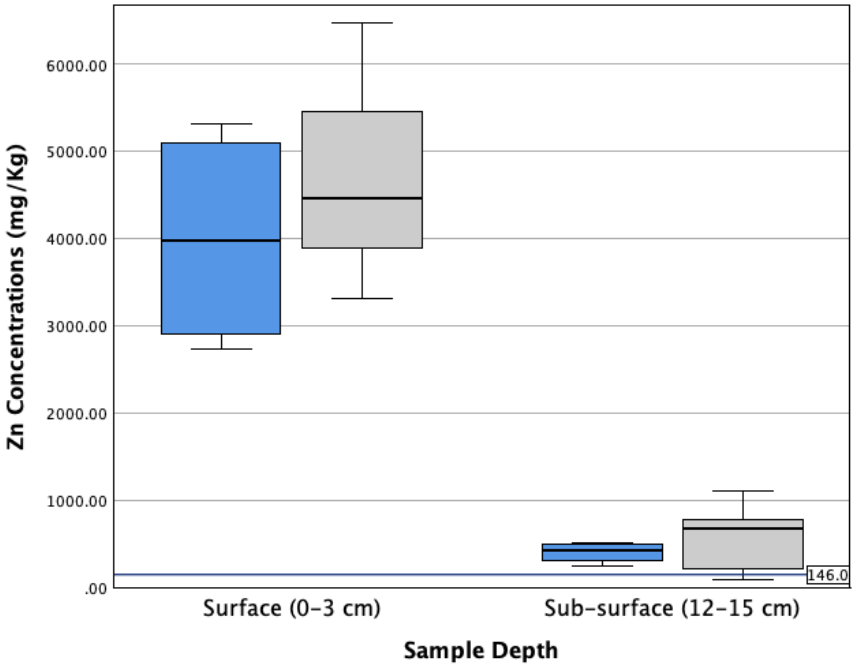

a)

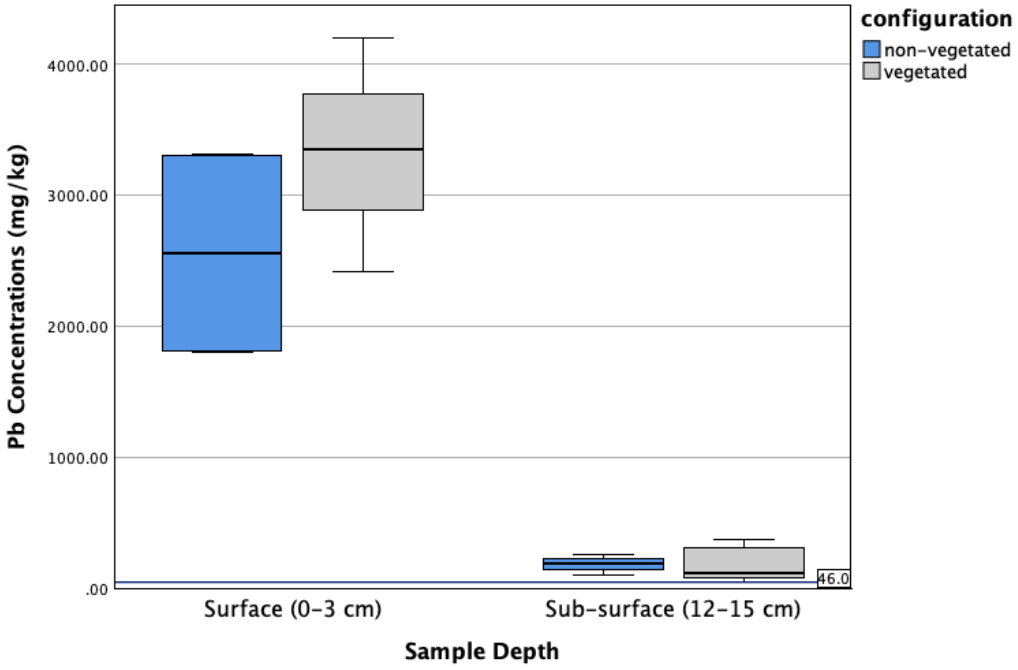

b)

Figure 4.12 Accumulation of heavy metals at the surface and subsurface layers of bioretention columns for a) Zn, b) Pb and c) Cu accumulation. The horizontal lines refer to pre-treatment soil baseline levels.

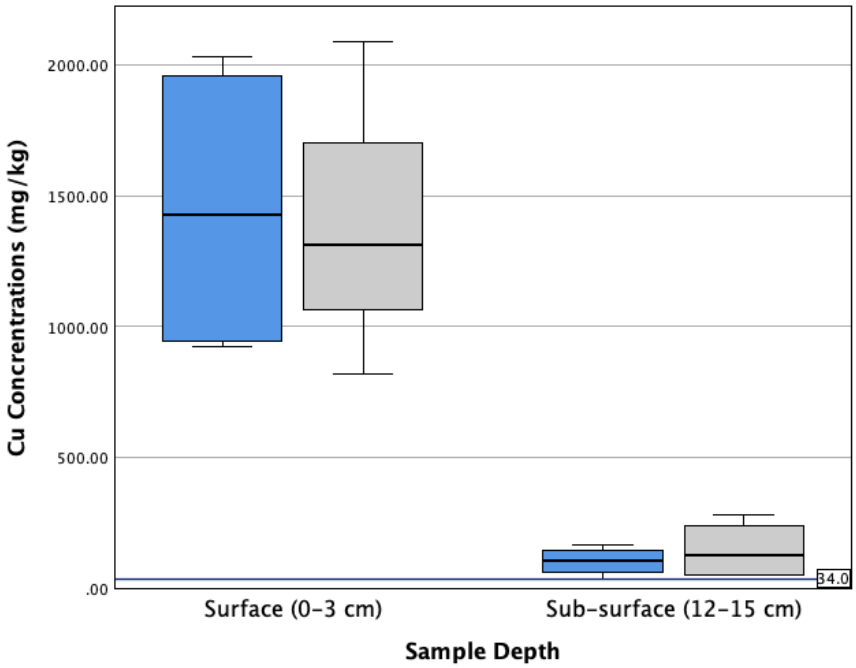

c)

Figure 4.12 continued**.**

This observation aligns with Hatt et al. (2011), who noted that dissolved Zn, being relatively more mobile, was the first metal to break through a 6-cm filter column, equivalent to approximately 9-15 years of operation under typical stormwater loading. However, the study observed that after the equivalent of 12-15 years of operation, metals such as Cd, Cu and Zn had accumulated in the filter to levels exceeding soil guideline values for ecological and human health risks, leading to the classification of the soil as contaminated and necessitating special disposal procedures.

In this study, the cumulative mass of heavy metals received by each column was 13.3 g, 4.4 g, and 2.4 g for Zn, Pb, and Cu, respectively. This mass loading is equivalent to 10.5, 7.9, and 8.5 years of operational exposure in the field for each metal. The majority of the applied pollutants were captured within the cake layer formed on the biofilter surface. This accumulation of metals in the bioretention media in this study raises significant contamination concerns that could breach regulatory thresholds for contaminant lands, necessitating a field investigation to validate these concerns, and highlight targeted maintenance needs to ensure regulatory compliance. Without routine maintenance, surface heavy metal concentrations may exceed regulatory thresholds within 10-15 years of operation (Hatt et al. 2011). The threshold values for contaminated soil vary between jurisdictions, as will be further explored in Chapter 6.

4.4 Conclusions

This chapter focused on the role of vegetation in enhancing the performance of bioretention systems. The key findings are as follows:

1. Vegetated systems maintained hydraulic conductivity and significantly reduced the risk of clogging, whereas non-vegetated systems experienced significant clogging after 61 weeks of operation, leading to system failure. The formation of cake layers contributed to decreased infiltration rates in non-vegetated systems.
2. Plants and extended residence time improved overall removal (particularly dissolved Zn and TP), however, their effects on pollutant removal were statistically insignificant. The particulate nature of most tested pollutants, apart from Zn, resulted in effective capture (>90% for metals, 82-92% for TSS) through filtration within the cake layer and substrate media. On the other hand, TP removal was more variable between treatments.
3. Species exhibited variable performance, involving notable trade-offs:
    a. *Juncus effusus* exhibited the highest infiltration rates which created preferential flow paths for particle migration, reducing TSS removal efficiency.
    b. *Phalaris* proved unsuitable for bioretention design as it experienced decomposition under frequent inundation, exhibiting net phosphorus leaching, particularly in free-draining trials.
    c. *Carex pendula* optimally balanced infiltration rates and pollutant retention.
4. Bioretention designs should consider planting species, such as *Carex pendula* to effectively balance treatment and hydraulic functions for efficient long-term bioretention performance.

Chapter 5. Effects of Biochar Amendments on Pollutant Removal in Bioretention Systems

5.1 Introduction

A primary aim of this research was to enhance the design of bioretention systems by evaluating media amendments for improved pollutant removal performance. As established in Chapter 4, pollutants like dissolved zinc and phosphorus were consistently detected in the effluents of all treatments using typical loam media. Biochar amendments have emerged as a promising solution to this challenge; however, as identified in the literature review, a fragmented understanding of its practical application in bioretention systems persists due to biochar synergistic properties. Notably, there is a lack of data distinguishing its removal mechanisms for particulate and dissolved pollutants, particularly when treating complex pollutant mixtures representative of real stormwater under unsaturated conditions.

This chapter evaluates the efficiency of two biochar types as amendments to standard bioretention media in removing stormwater pollutants and highlights the removal mechanisms by differentiating between particulate and dissolved pollutants.
Using lab-scale filtration columns under unsaturated conditions, the performance of biochar-amended media is compared against a pure sandy loam control.

By measuring the removal efficiencies of heavy metals (Zn, Cu, Pb), phosphorus, suspended solids, and microplastics (MPs), and differentiating between particulate and dissolved phases, this chapter provides the mechanistic insight required to guide the effective application of biochar, thereby contributing to the thesis aim of optimising bioretention system design for more robust bioretention performance.

Table 5.1 General performance of filtration columns showing mean concentrations and removal efficiencies by filter media over 6 dosing events. Standard deviations are shown in parentheses.

Mean influent concentrations					
TSS (mg/L)	**Zn (mg/L)**	**Pb (mg/L)**	**Cu (mg/L)**	**TP (mg/L)**	**MPs (particles/L)**
154 (5.72)	2.64 (0.08)	1.08 (0.04)	0.49 (0.06)	0.22 (0.05)	19611 (5031)

Mean effluent concentrations and removal efficiencies				
Pollutant		**Filter media[a]**		
		SL	**SL+SSB**	**SL+RHB**
TSS	Concentrations (mg/L)	46 (12)	64 (20)	74 (28)
	Removal (%)	70.32 (7.76)	58.41 (12.84)	52.10 (18.75)
Zn	Concentrations (µg/L)	46 (30)	31 (29)	28 (25)
	Mean removal (%)	98.28 (1.25)	98.87 (1.19)	99.00 (0.98)
Pb	Concentrations (µg/L)	89 (49)	107 (44)	164 (72)
	Removal (%)	90.69 (4.38)	89.17 (3.91)	83.61 (6.99)
Cu	Concentrations (µg/L)	bdl[b]	bdl	bdl
	Removal (%)	>99 (0.06)	>99 (0.06)	>99 (0.06)
TP	Concentrations (mg/L)	0.32 (0.10)	1.36 (0.18)	0.71 (0.24)
	Removal (%)	-49.84 (53.71)	-533.80 (159.61)	-230.94 (124.63)
MPs	Concentrations (particles/L)	bdl	bdl	bdl
	Removal (%)	98.63 (0.42)	98.54 (0.78)	98.63 (0.42)

a SL= 100% sandy loam (control), SL+SSB = 90% sandy loam + 10% sewage sludge biochar (w/w), SL+RHB = 90% sandy loam + 10% rice husk biochar (w/w).
b bdl= below detection limit (Cu <5 µg/L, MPs <500 particles/L).

5.2 Total suspended solids removal

Table 5.1 summarises the mean pollutant concentrations and removal efficiencies by filter media type. The mean removal efficiency of TSS ranges from 70% in the sandy loam (SL) controls to 58% and 52% in the sewage sludge biochar (SL+SSB) and the rice husk biochar (SL+RHB) amended columns, respectively. Mean effluent concentrations were 46, 64, and 74 mg/L in the SL, SL+SSB, and SL+RHB columns, respectively, indicating that the addition of biochar resulted in a significant decrease in TSS removal efficiency. These findings differ from previously reported results in the literature, where biochar amendments were observed to retain, on average, ≥ 86% of suspended solids (Kuoppamäki et al., 2021; Ouedraogo et al., 2023; Reddy et al., 2014), which is comparable to TSS removal rates observed in the large columns in Chapter 4 (82–92%), and similar studies utilising sandy filter media (Hatt et al. 2007a; Hatt et al. 2007b; Bratieres et al. 2008).

Other bioretention studies by Buates et al. (2024) and Mitchell et al. (2023), have demonstrated that biochar amendments significantly improve the removal of TSS and turbidity compared to sand-only controls. However, with reported amendment ratios ranging from 4% (w/w) to 20% (v/v), the differences in measurement units (weight versus volume) make direct comparisons between studies challenging. Figure 5.1 shows boxplots of TSS removal efficiencies grouped by filter media over the course of the experiment (6 dosing events), where each filter medium has 3 replicates (n=3).

As can be seen from Figure 5.1, the mean TSS removal efficiencies indicated by the black horizonal lines in the SL+SSB, and SL+RHB filters were significantly lower than the SL control filters, resulting in higher amounts of fines in the effluents of biochar-amended filters. This observation can be partially explained by the hydraulic conductivity test results (see Table A.4 in the appendices), which revealed that the SL+RHB filters exhibited the highest coefficient of permeability ($K= 6.5\times10^{-3}$cm/s), followed by SL ($K= 2.1\times10^{-3}$cm/s) and SL+SSB ($K= 1.1\times10^{-3}$cm/s). The higher hydraulic conductivity of the SL+RHB filters increased water flow rate and reduced the retention time available for sedimentation and filtration, leading to higher effluent concentrations of suspended solids. This could be mitigated by increasing the filter depth, or by layering the biochar as a discrete (or 'sandwich') layer within the filter media rather than a mixed sand-biochar layer, as demonstrated by Xiong et al. (2019).

A similar observation was reported by Hasan et al. (2021), where a discrete biochar layer resulted in higher retention of particulate arsenic (As) due to increased contact time necessary for physical adsorption compared to a heterogenous biochar-sand mixture.

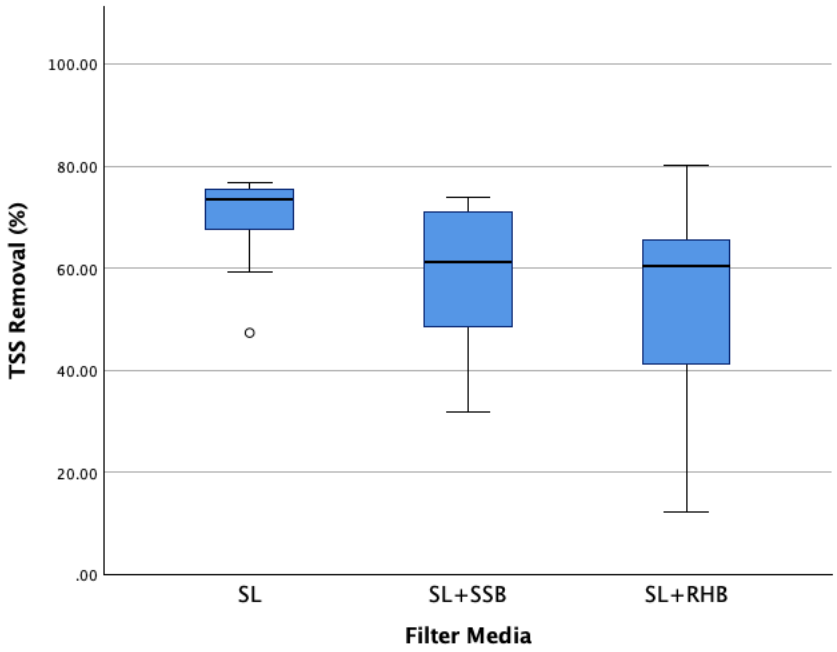

Figure 5.1 TSS removal efficiencies by filter media across six dosing events, with each filter medium tested in triplicate (n=3). SL: 100% Sandy Loam (control), SL+SSB: 90% Sandy Loam amended with 10% Sewage Sludge Biochar, and SL+RHB: 90% Sandy Loam amended with 10% Rice Husk Biochar (w/w).

On the other hand, the SL+SSB filters used in this study also leached significantly higher amounts of TSS in the effluents than pure sand filters (SL), despite exhibiting a lower K value than sand. This may be attributed to the resuspension and mobilisation of biochar particles. A similar trend was observed by Iqbal et al. (2015), where the addition of biochar to a compost mix (1:3 v/v) contributed to the leaching of significant amounts of suspended particles compared to pure filters (100% biochar and 100% compost filters). The mixing process may have introduced more fines into the filters compared to pure SL media, where no mixing took place. Another study by Reddy et al. (2014) showed that washed biochar successfully reduced particle leaching to below the detection limit compared to unwashed biochar (<40 mg/L).

Although a similar media preparation and pretreatment, as detailed in Section 3.3.2.2, was followed in this study to flush away fines, more fines may have been introduced during mixing and packing, particularly in the biochar-amended media, as biochar was more susceptible to crushing than sand, despite careful efforts to prevent this during column packing. Mohanty and Boehm (2015) studied the effect of weathering on the mobilisation of biochar particles in biochar-amended media. They found that the mobilisation of biochar particles, which was shown to increase under dry-wet conditions and lower temperatures, is similar to colloid mobilisation, which can be attributed to an increase in shear forces from air-water flow, thin water film expansion, and stagnant water zones reconnecting with flowing water.

Furthermore, it was noted that the lower density of biochar, compared to other suspended solids such as clay and sand, increased the likelihood of it being washed away from the filters. This might explain the higher mean and more variable concentrations of TSS (74 ±28 mg/L) found in the effluents of the lower-density SL+RHB filter columns. These results strongly correlated with particulate Pb removal which will be discussed in Section 5.3.2.

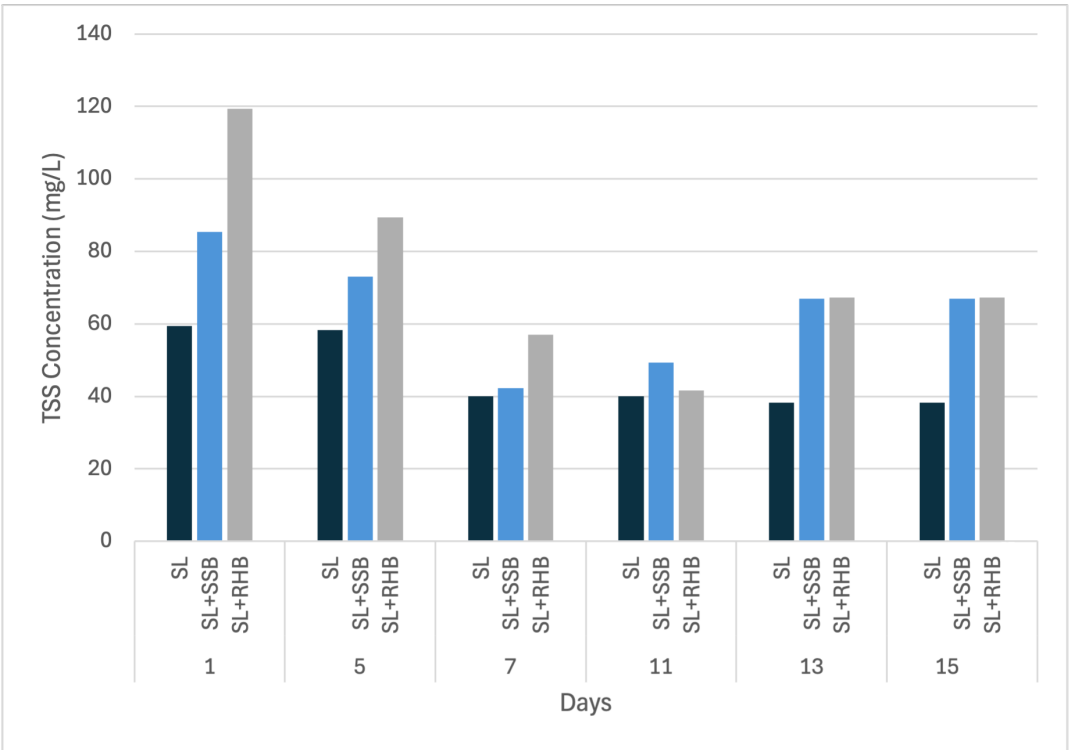

Figure 5.2 Mean TSS effluent concentrations over 15 days of dosing. Bars clustered on the x-axis by filter media. Data points represent the means of three replicates.

Although TSS removal rates were low initially, all columns showed improvement with repeated dosing. Figure 5.2 shows that mean TSS concentrations in the effluents tended to decrease and stabilise with time, particularly in the SL controls. This trend was also observed by Mohanty and Boehm (2015) and Reddy et al. (2014), where they found that suspended solids concentrations in the effluent decreased with successive dry-wet cycles. This is also consistent with the 'conditioning' of filters as described by Hatt et al. (2007b), where higher sediment concentrations were observed in the early stages of dosing, and depleted with time as fines settled out and their supply was exhausted. Therefore, based on trends seen in Figure 5.2, it is expected that TSS concentrations will follow the same trend in a longer experimental timeframe, which will subsequently increase the average removal rates to a level comparable with similar studies, as was demonstrated in the large columns in Chapter 4.

5.3 Heavy metals removal

All media configurations were effective in removing metals from the effluents, achieving removal rates ranging from 98-99%, 84-91%, and >99% for Zn, Pb, and Cu, respectively. Biochar-amended columns improved the removal of Zn but decreased Pb removal compared to non-amended filters. Cu concentrations in the effluents were below the detection limit (<5 µg/L) across all filter treatments, regardless of biochar amendment. Overall, the average removal performance of heavy metals fell within the upper limit of the 24-100% range reported in the literature (Hasan et al. 2020; Sun et al. 2020; Hasan et al. 2021; Spahr et al. 2022; Buates et al. 2024).

The variability in performance for each metal removed in this study can be attributed to the distinct physical and chemical behaviours of individual metals and their interactions with the properties of biochar and sand. Table 5.1 summarises the mean influent and effluent concentrations and the mean removal efficiencies achieved by each filter medium.

5.3.1 Zinc removal

Figure 5.3 shows the mean removal rates of Zn in the tested filter media, which range from 98-99%, outperforming those achieved in comparable studies (Reddy et al. 2014a; Hasan et al. 2020; Sun et al. 2020; Hasan et al. 2021; Buates et al. 2024). All filter media treatments were highly effective, removing ≥ 94% of the total zinc concentrations from the treated

synthetic stormwater. The addition of biochar showed improvement in total Zn retention, with SL+RHB exhibiting the highest average removal rate of 99%, followed by SL+SSB (98.9%) and the SL controls (98.3%). These values outperform the removal rates observed in the large column experiment (see Section 4.1.2.1), possibly due to the lower hydraulic conductivity as demonstrated by the coefficient of permeability in Table A.4. It is also possible that the synthetic stormwater preparation in this study (≥3 hours of mixing), to stabilise the solution, created more adsorption sites for Zn with colloidal kaolinite particles, as reported by (Sun et al. 2020), which resulted in a higher removal efficiency compared to the large column study.

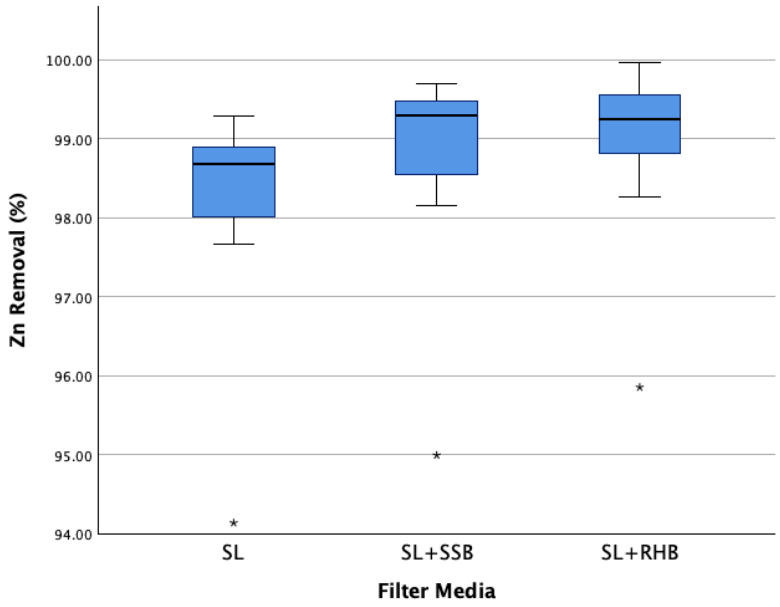

Figure 5.3 Zn removal efficiencies by filter media across six dosing events, with each filter medium tested in triplicate (n=3). SL: 100% Sandy Loam (control), SL+SSB: 90% Sandy Loam amended with 10% Sewage Sludge Biochar, and SL+RHB: 90% Sandy Loam amended with 10% Rice Husk Biochar (w/w).

Figure 5.4, shows variations in effluent Zn concentrations over the duration of the experiment. As can be seen, the addition of biochar resulted in significant decreases in dissolved Zn concentrations (represented by the patterned bars). As 95% of Zn in the inflow was in dissolved form according to the speciation analysis, the dissolved fractions in the effluents for SL+RHB, SL+SSB filters were approximately half those found in the control filters (20%, 26%, and 51% SL+RHB, SL+SSB respectively), indicating higher adsorption sites of dissolved Zn in the biochar treatments.

This effect was confirmed by the LMM (results summarised in Table 5.2), suggesting a significant difference between SL+RHB and sand only controls in dissolved Zn removal (p=0.009).

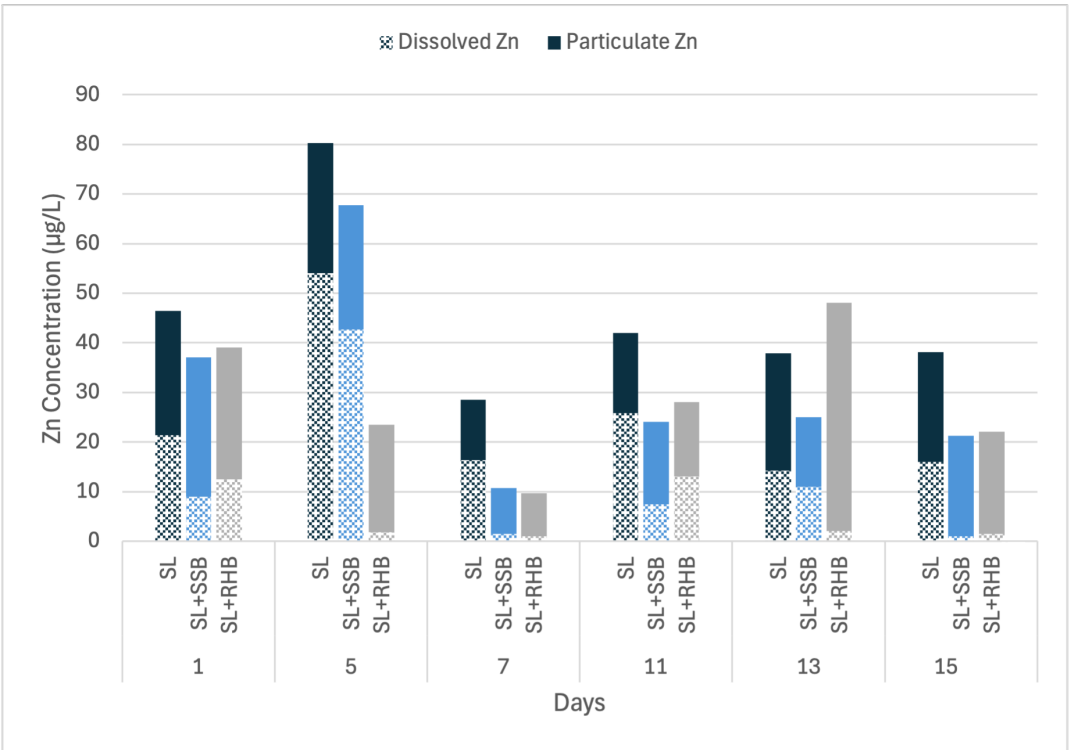

Figure 5.4 Zn effluent concentrations over 15 days of dosing. Bars clustered on the x-axis by filter media. Stacked bars represent dissolved fraction (patterned bars), and particulate fraction (solid bars). Data points represent the means of three replicates.

The higher removal rates in biochar-amended columns can be attributed to the physicochemical properties of biochar and its synergistic interactions with Zn complexes and ions. These interactions drive the removal mechanisms of Zn, including physical adsorption, chemisorption, and precipitation reactions (Cairns et al. 2020; Hasan et al. 2020). Physical adsorption is likely greater in biochar-amended media due to their porous structure and fine particle composition, which increase the surface area and provide more adsorption sites for Zn compared to SL (Hasan et al. 2021). This was demonstrated by the high mean removal rate of the SL+RHB media (99%), reflecting the greater surface area of RHB compared to the surface areas of other media (Table 3.9).

The higher removal efficiency in biochar-amended media can also be explained by the presence of surface functional groups such as carboxylic, hydroxyl, and phenolic groups,

which play an integral role in binding metal ions to the biochar surface (Uchimiya et al. 2011). These functional groups enhance the chemisorption process by forming complexes with positively charged Zn ions, providing stable immobilisation and effectively removing them from flowing water (Hasan et al. 2020). This was likely the predominant removal mechanism for dissolved Zn in biochar-amended media, as demonstrated by the dissolved and particulate Zn fractions shown in Figure 5.4.

The ability of these functional groups to form complexes with Zn ions is also influenced by the pH of the synthetic solution. Higher pH levels deprotonate the surface functional groups, further increasing their metal retention capacity (Uchimiya et al. 2011). The synthetic solution used in this study had pH levels between 5.1 and 6.9, enabling functional groups to bind effectively with positively charged Zn ions (Hasan et al. 2020). The pH levels in the effluents increased to between 7.7 and 7.9 due to the alkaline pH of biochar (Table 3.9). This alkaline condition decreased surfaces potential and the number of protons competing with Zn ions for binding spots during the filtration process, contributing to the overall removal of Zn (Lim et al. 2015; Cairns et al. 2020; Sun et al. 2020).

Despite the significant effect of biochar-amendment on dissolved Zn removal, the overall difference of total Zn removal between biochar-amended filters and sand-only controls was not practically significant, as suggested by the LMM ($p = 0.080$), given the high removal rates of total Zn across all treatments (>98%). However, as Zn is more mobile and likely to bypass filtration in biorientation systems compared to other heavy metals, as demonstrated in Chapter 4, biochar amendments, particularly with rice husk biochar, show higher potential for minimising dissolved Zn leaching.

Table 5.2 Linear mixed model showing effects of filter media on pollutant removal and a pairwise comparison using Bonferroni post-hoc test ($\alpha = 0.05$).

Effect	**p-value**				
	TSS	TZn	DZn	Pb	TP
Filter media	<0.001	0.080	0.011	<0.001	<0.001
SL x SL+SSB	0.028	0.256	0.226	1.000	<0.001
SL x SL+RHB	<0.001	0.104	0.009	<0.001	<0.001
SL+SSB x SL+RHB	0.436	1.000	0.620	0.007	<0.001

5.3.2 Lead removal

It was observed that Pb removal was lower compared to Zn removal, with mean efficiencies of 91%, 89%, and 83% in the SL, SL+SSB, and SL+RHB treatments, respectively. Nonetheless, these rates were higher than those reported by Reddy et al. (2014) at 75% and Spahr et al. (2022) at 80%, but lower than those reported by Hasan et al. (2021) at 98-100%. Conversely, this study showed that the addition of biochar tended to decrease Pb removal efficiency compared to SL controls. This trend was also observed by Buates et al. (2024) and Hasan et al. (2021), where sand-only filters performed slightly better on average than biochar-amended filters in Pb retention. The LMM results in Table 5.2 showed that there was a significant difference between the two types of biochar in Pb removal ($p = 0.007$), where SL+SSB media performed better on average (89% mean removal) than SL+RHB media (84% mean removal), which can be explained by the lower hydraulic conductivity of the SL+SSB filters, promoting filtration and sedimentation processes. The partitioning analysis of Pb concentrations in the influents and effluents supported this explanation, as it revealed that Pb was almost entirely particulate-bound, indicating that physical filtration played a major role in Pb retention.

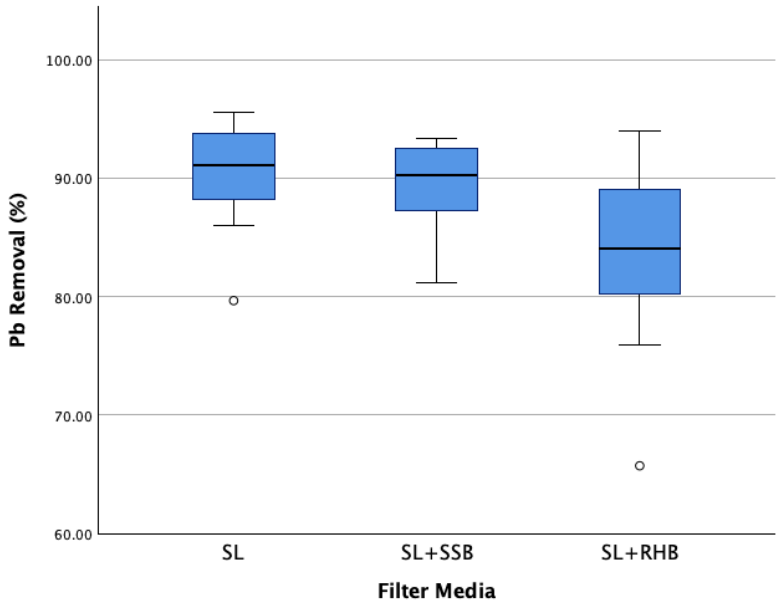

Figure 5.5 Pb removal efficiencies by filter media across six dosing events, with each filter medium tested in triplicate (n=3). SL: 100% Sandy Loam (control), SL+SSB: 90% Sandy Loam amended with 10% Sewage Sludge Biochar, and SL+RHB: 90% Sandy Loam amended with 10% Rice Husk Biochar (w/w).

A closer look at Figure 5.2 and Figure 5.6 suggests a possible correlation between TSS and Pb removal, as control filters outperformed biochar-amended filters in both cases. A Spearman's rank correlation analysis (summarised in Table 5.3) showed that the correlation between TSS and Pb removals was strong ($R^2 > 0.6$) and statistically significant ($p < 0.05$) in the biochar-amended filters. Similarly, Xiong et al. (2022) reported strong linear correlations between the concentrations of TSS and heavy metals in the effluent. The effect of TSS removal on the particulate-bound Pb was more prominent in the biochar-amended columns compared to the SL controls, suggesting a possible secondary factor influencing Pb retention.

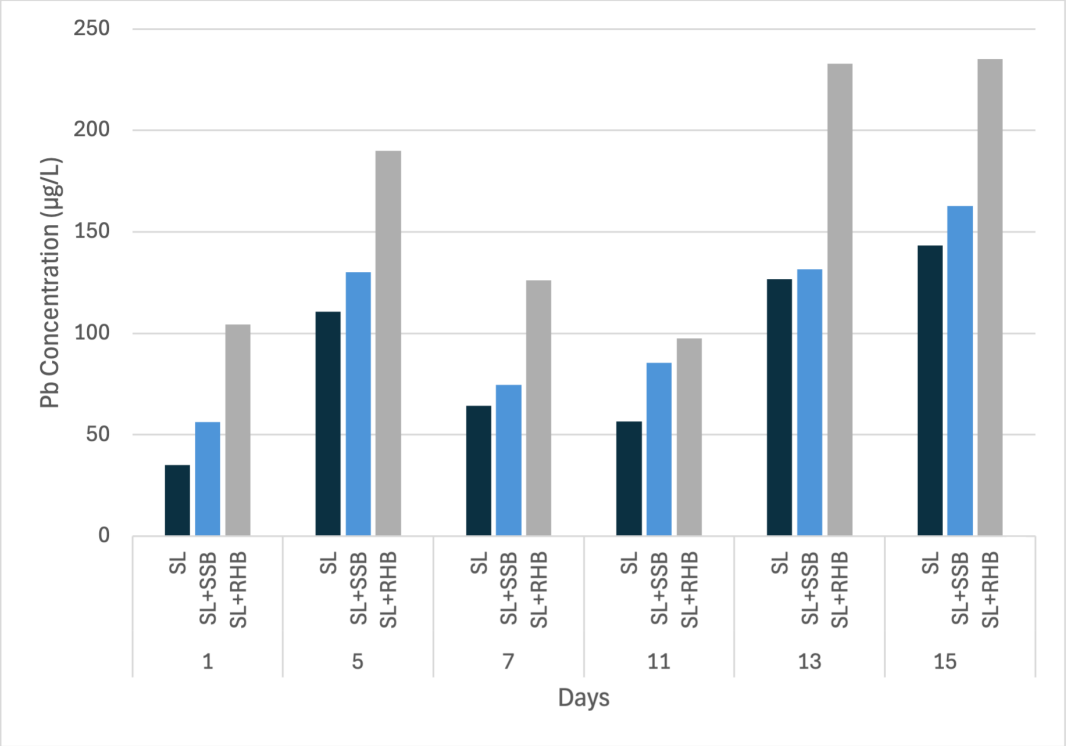

Figure 5.6 Pb effluent concentrations over 15 days of dosing. Bars clustered on the x-axis by filter media. Data points represent the means of three replicates.

A closer examination of pollutant concentrations in successive dosing events indicated that the concentrations of Pb in the effluent increased during the last two dosing events (days 13 and 15 in Figure 5.6) in all filter media treatments, including the SL columns, despite TSS concentrations gradually decreasing and stabilising with time. This is explained by the weak correlation between TSS and Pb (R^2=0.084) in the SL media in Table 5.3. Hasan et al. (2021) reported that Pb removal efficiency decreased towards the end of the study (~200 days), while Cairns et al. (2020) reported that Pb started to decrease and desorb from biochar media columns after two weeks of dosing, before it recovered towards the end of the study period

(36 days). However, the Pb investigated in the above studies was in dissolved form, contrary to the particulate nature of Pb observed in this study.

It is possible that repeated dosing caused resuspension and remobilisation of Pb-coated particles, as more Pb accumulates and coats the surfaces of biochar particles. Consequently, a larger proportion of the suspended particles in the effluents became enriched in Pb towards the end of the experiment. This is consistent with the decreased removal rates of TSS in the SL+RHB media, as discussed in Section 5.2.

Rice husk biochar had a lower density and a higher surface area than sandy loam and sewage sludge biochar, which provides more surface area for Pb-particle collision and increases the likelihood of remobilisation and leaching during wetting and drying due to its lower particle density. However, this remains a hypothesis. Given the objective of this study to assess removal efficiency and mechanism, definitive time trends in Pb retention could not be conclusively established, and longer-term investigations are needed to explore Pb removal trends and stability over time.

Table 5.3 Spearman's rank correlation analysis between TSS removal and other pollutants removal factored by filter media.

media	Element	Spearman's ρ	p-value
SL	Zn	-0.071	0.800
	Pb	0.084	0.766
	TP	-0.075	0.790
SL+SSB	Zn	**0.679**	**0.005**
	Pb	**0.652**	**0.008**
	TP	0.284	0.304
SL+RHB	Zn	0.373	0.170
	Pb	**0.670**	**0.006**
	TP	-0.023	0.934
Overall	Zn	0.036	0.812
	Pb	**0.601**	**<0.001**
	TP	0.450	0.002

5.3.3 Copper removal

Similar to the large column study discussed in Chapter 4, all filter media treatments were successful (>99%) in reducing copper from mean influent concentrations of 0.5 ± 0.06 mg/L to below the detection limit of 5 µg/L in the effluents during all six dosing events. This aligns with the high removal rates observed in similar biochar column studies (Hasan et al. 2020; Sun et al. 2020; Hasan et al. 2021). Therefore, the addition of biochar in this study had no significant advantage than the SL controls, despite the relatively high influent concentrations (0.6 mg/L, 10 times typical runoff concentrations). Similarly, Hasan et al. (2020) investigated biochar-amended sand filters in removing copper from highly concentrated synthetic stormwater (2.5 mg/L) and found that biochar-amended sand media did not significantly enhance the removal efficiency (99.6%) compared to sand-only media (99.2%). The authors attributed this high removal of copper to its strong sorption affinity for the filter media and lower influent concentrations compared to other metals used in their study.

A partitioning analysis of the influents in this study showed that 87% of copper was in dissolved form, suggesting that adsorption was likely the dominant removal mechanism. Although the biochar had a higher surface area, providing more adsorption sites for metals than sandy loam, a property that is strongly correlated with the abundance of oxygenated functional groups (Reddy et al. 2014a), no Cu breakthrough was observed in any of the treatments, including SL controls, within the timeframe of this study, even at the relatively high influent concentrations. This finding is consistent with the large-column study, which had a considerably longer experimental duration, yet Cu did not show any signs of breakthrough. However, other pilot-scale studies have shown that biochar amendment can further enhance Cu removal compared to non-amended media (Spahr et al. 2022; Buates et al. 2024).

5.3.4 Phosphorus removal

All filter media were found to leach significant amounts of total phosphorus (TP) that far exceeded the synthetic stormwater concentrations (Figure 5.7). The biochar-amendment filters leached considerably more TP compared to the sand-only controls ($p < 0.001$). Results in the literature regarding phosphorus removal performance vary widely, from 20% to 94%, depending on the column setup and the biochar type (Reddy et al. 2014b; Bock et al. 2015;

Nabiul Afrooz and Boehm 2017; El Hanandeh et al. 2018; Xiong et al. 2019). Other studies have shown that biochar was not as effective in TP retention due to leaching of phosphorus from the biochar itself (Yao et al. 2012; Iqbal et al. 2015; Kuoppamäki et al. 2016). The two biochar types used in this study were also rich in phosphorus content (0.1% and 2.3% in SSB and RHB, respectively, as shown in Table 3.9), which might explain the high phosphorus content in the effluents of biochar-amended filters.

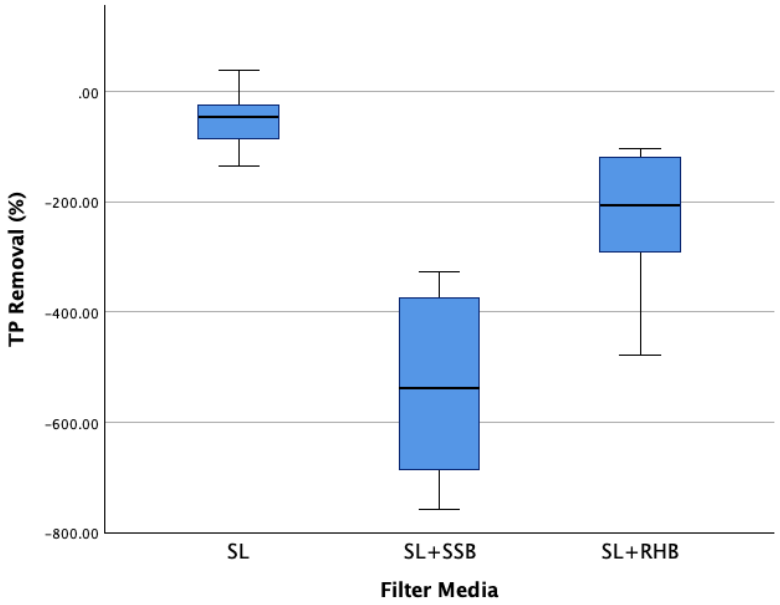

Figure 5.7 TP leaching in filter media across six dosing events, with each filter medium tested in triplicate (n=3). SL: 100% Sandy Loam (control), SL+SSB: 90% Sandy Loam amended with 10% Sewage Sludge Biochar, and SL+RHB: 90% Sandy Loam amended with 10% Rice Husk Biochar (w/w).

Table 5.1 shows that mean effluent concentrations were 0.32, 0.71, and 1.36 mg/L in the SL, SL+RHB, and SL+SSB, respectively, while mean influent TP concentrations were 0.22 mg/L. This shows net TP leaching of 46%, 228%, and 518% from the SL, SL+RHB, and SL+SSB filters, respectively. It is important to note that these relatively high leaching percentages were normalised by the mean influent loading (0.22 mg/L) achieved in this study as a baseline concentration, which is relatively low compared to other studies.

Figure 5.8 shows that more than 70% of TP detected in the effluents was in dissolved form. Conversely, the majority of TP in the influents was particulate-bound (72%), suggesting that physical filtration played a major role in the removal of influent TP, and that the main source of TP in the effluents was the phosphorus content in the filter media itself rather than the

influent loading. For example, the SL+SSB filter media, which leached the highest amount of TP in the effluents (1.36 mg/L on average), achieved about 74% of particulate P removal, higher than the 51% and 37% achieved by SL+RHB and SL, respectively. The SL+SSB filters outperformed the SL+RHB despite having a smaller surface area, which could be attributed to the lower coefficient of permeability (K= 1.1×10^{-3} cm/s) and the higher metal content in the sewage sludge biochar that might have promoted particulate P removal through physical adsorption and sedimentation processes (Xiong et al. 2019).

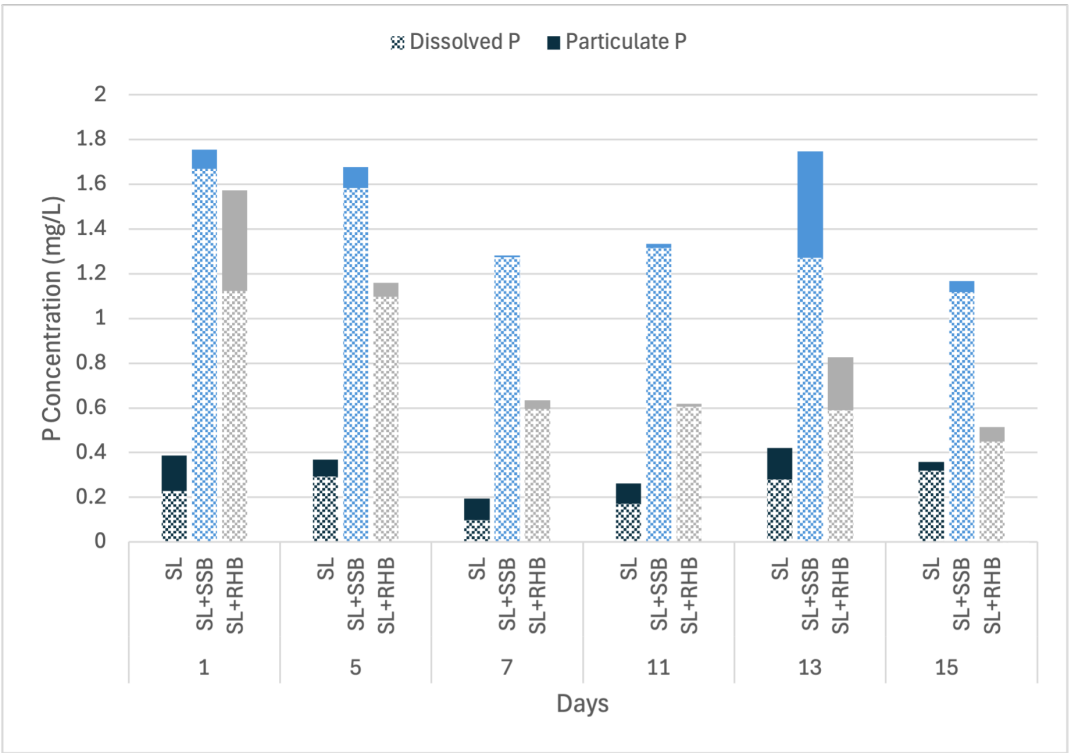

Figure 5.8 Phosphorus effluent concentrations over 15 days of dosing. Bars clustered on the x-axis by filter media. Stacked bars represent dissolved fraction (patterned bars), and particulate fraction (solid bars). Data points represent the means of three replicates.

Although both the biochar-amended filters and the sand-only controls resulted in increased TP leaching in the effluents, the difference among the biochar-amended filters was statistically significant ($p < 0.001$), with SL+SSB filters leaching almost twice the amount of TP in the effluents relative to SL+RHB filters. This highlights the importance of biochar feedstock selection in limiting TP leaching.

The poor performance of biochar in the retention of phosphorus is unsurprising, as biochar has been widely reported to have a poor adsorption capacity for phosphate compared to total nitrogen (Nabiul Afrooz and Boehm 2017; Biswal et al. 2022). Yao et al. (2012) recommended that the sorption capacity of biochar for nutrients should be determined through laboratory batch sorption experiments before full-scale applications. Others have recommended the use of simple sand filters if phosphorus is the primary pollutant of concern . An optimum solution is to modify the biochar with metals or metal oxides, such as iron, which have been shown to significantly improve metals and nutrient retention (Xiong et al. 2019; Hasan et al. 2020; Biswal et al. 2022).

Phosphorus retention in biochar is primarily governed by a combination of abiotic mechanisms, including adsorption, precipitation, and complexation with functional groups and metal oxides and hydroxides (Liu and Davis 2014; Xiong et al. 2019; Biswal et al. 2022). Adsorption involves dissolved phosphate ions (PO_4^{3-}) binding to positively charged sites on biochar and sand, a process influenced by surface charge and pH, with lower pH enhancing electrostatic attraction and higher pH causing repulsion (Biswal et al. 2022). Precipitation occurs when phosphate reacts with cations such as Mg^{2+}, Ca^{2+}, and Al^{3+} to form insoluble compounds, such as aluminium phosphate and calcium phosphate, which are particularly effective in alkaline conditions (Nabiul Afrooz and Boehm 2017; El Hanandeh et al. 2018).

Phosphate may also interact with oxygen-containing functional groups, such as carboxyl and hydroxyl groups, which provide exchange sites on the biochar surfaces for phosphate ions. However, biochar's low anion exchange capacity can limit this mechanism, and phosphorus is predominantly removed by other mechanisms (El Hanandeh et al. 2018). Additionally, organic compounds, such as polycyclic aromatic hydrocarbons (PAHs), can form organo-phosphorus complexes, contributing to phosphorus removal (Biswal et al. 2022). This mechanism was more likely to contribute to particulate phosphorus removal in sewage sludge biochar, as it contained higher amounts of PAHs than rice husk biochar, as shown in Table 3.9.

As mentioned above, metal oxides, particularly iron oxides, have been shown to enhance phosphorus retention by forming complexes with phosphate, making iron-modified biochar valuable amendments for nitrogen and phosphorus removal (Iqbal et al. 2015; Xiong et al. 2019).

Recent studies highlight the potential of engineered biochar, such as nano-metal oxide-biochar composites (NMOBCs), to enhance phosphorus retention through surface precipitation and electrostatic attraction between anionic phosphate and positively charged metal oxides, such as magnesium oxide (Zhao et al. 2021). Overall, phosphorus removal efficiency in biochar-amended media is determined by the interplay of these factors and mechanisms, with materials rich in iron and magnesium, or modified biochar, demonstrating the greatest potential (Iqbal et al. 2015; Xiong et al. 2019).

5.3.5 Microplastics removal

All treatments, including the SL controls and both biochar-amendment media demonstrated exceptionally high removal efficiency for MPs. Influent concentrations of approximately 20,000 particles/L were reduced to levels below the analytical detection limit (<500 particles/L) in the effluents, corresponding to removal rates of >98%.

The microscopic imaging analysis for MPs removal in water samples was carried out only on the 1st, 4th, and 6th dosing events due to cost constraints. It was expected that breakthrough would be more likely towards the end of the experimental period as the columns became more saturated with MP particles. However, no particles were observed in the effluents of the first or final dosing events. It was also hypothesised that biochar amendment would result in higher retention of MPs compared to the sand-only controls. Contrary to the initial hypothesis, the addition of biochar did not yield a statistically significant improvement in MP removal compared to the soil-only controls.

This high and uniform removal efficiency across all media types is attributed primarily to physical filtration (straining) as the dominant removal mechanism. Given the large size of the MP beads (50-200µm) used in this study, relative to the inter-particle pores of the filter media (200-600µm), they acted as a highly effective sieve. This conclusion is supported by the Scanning Electron Microscope (SEM) analysis of the used filter media. The analysis revealed that retained MP particles were observed in both lodged and dislodged states within the filter media, rather than being adsorbed onto particle surfaces (Figure 5.9). The images suggest that surface interaction mechanisms played a minimal role under these experimental conditions.

Previous studies reported enhanced retention in biochar-amended media for smaller plastic particles. For instance, Wang et al. (2020) study of 10µm spheres, showed that their removal in biochar was enhanced through morphologically-controlled mechanisms characterised as 'trapped' and 'entangled' within the abundant honeycomb structures and complex internal porosity of hardwood and corn straw biochar used in their study. While the dominant removal mechanism in pure sand filters was classified as ‘stuck’, a mechanism in which MP particles were retained between the gaps of sand particles that were smaller than the MP particles. In other words the sand filters acted as a sieve for MP particles (Wang et al. 2020). Similarly, studies on nanoplastics (0.02µm) showed strong adsorption to biochar surfaces due to greater influence of electrostatic interactions in the nano-scale (Tong et al. 2020a; Tong et al. 2020b).

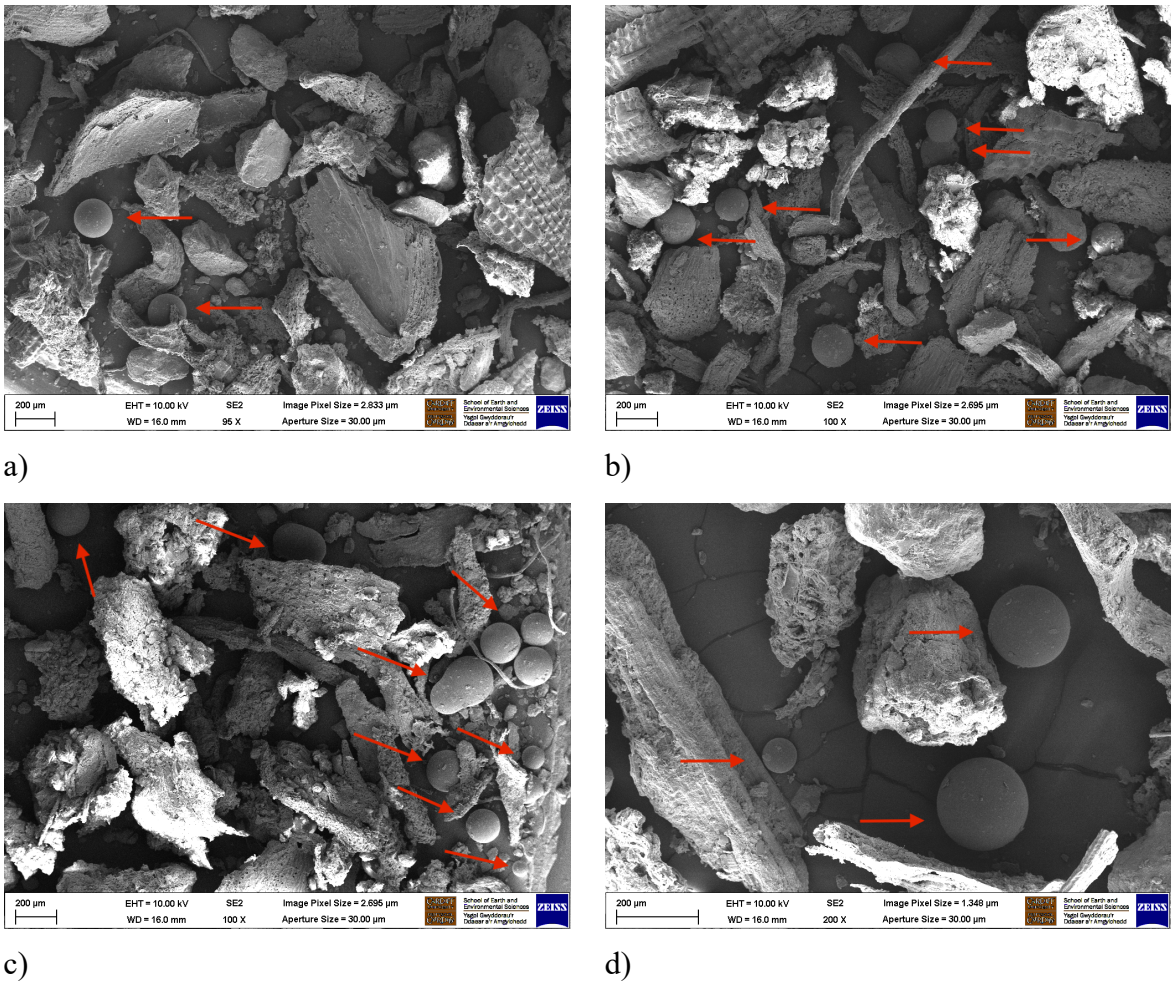

Figure 5.9 SEM images of retained PMMA beads in SL+ RHB (a, b), and SL+SSB (c, d) samples. The particles were retained by physical straining between filter media pores. This was the typical retention mechanism observed.

In contrast, the MP beads used in the present study (50-200µm) were considerably larger, thus the dominant removal mechanism was physical straining, a mechanism for which the sandy loam control was already highly effective. Consequently, the processes of morphological entrapment and surface interactions—the primary mechanisms for biochar-enhanced removal—had no significant advantage in this system.

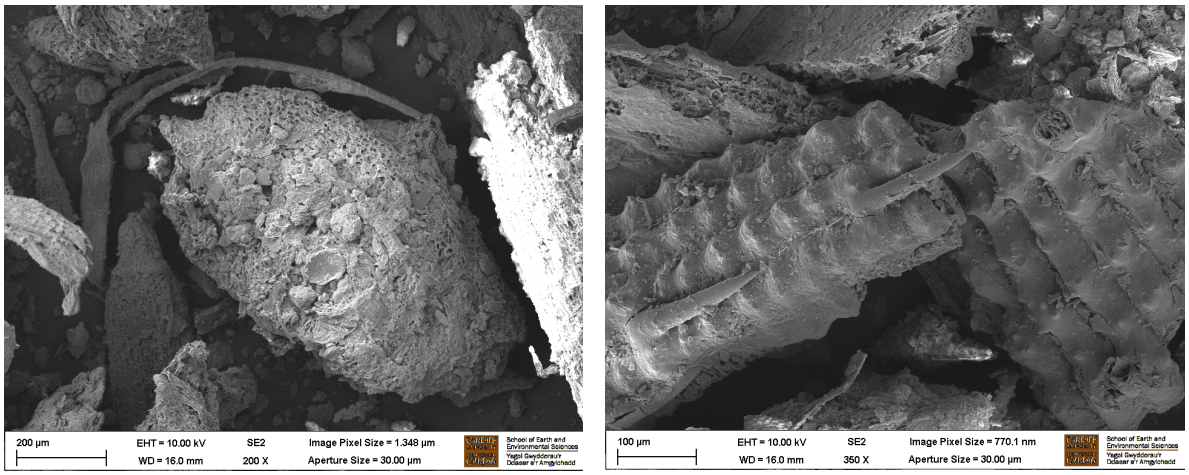

a) b)

Figure 5.10 SEM images showing morphology of a) sewage sludge biochar, b) rice husk biochar.

While the unique morphology of biochar, such as the internal honeycomb structures found in wood-derived types, can enhance the retention of smaller MPs through entrapment mechanism (Wang et al. 2020), the biochar used in this study differed significantly. The sewage sludge biochar exhibited a rough, nodular morphology (Figure 5.10-a), and the rice husk biochar was characterised by flat, ridged structures (Figure 5.10-b). These distinct morphologies might have resulted in a reduced capacity for the internal entrapment of smaller MP particles compared to other types of biochar cited in the literature (Wang et al. 2020; Hsieh et al. 2022).

Furthermore, the relatively low influent MP concentration (12,000 particles/L) reduced the probability of observing surface adsorption sites, further explaining the lack of observed difference between treatments. It was observed that a greater number of particles were retained in the top 0-2cm of the SL+SSB columns, which can be attributed to the lower conductivity of the SL+SSB filters compared to other treatment. However, the 10cm filter depth was sufficient for effective removal in all filters.

In conclusion, for the removal of microplastics ≥ 50µm, the physical filtration capacity of a typical sandy loam media is itself highly effective. The addition of biochar, while beneficial for other pollutants such as dissolved Zn, did not significantly affect MP retention for this size range. This finding is consistent with a recent pilot-scale study by Johansson et al. (2024), which also reported high MP removal in bioretention systems regardless of biochar amendment.

5.4 Conclusions

This chapter evaluated the effects of biochar amendment on enhancing pollutant removal in bioretention systems. The study provided new mechanistic insights for biochar-amended filter design by distinguishing the removal of dissolved and particulate pollutants in a complex synthetic stormwater mixture. The key findings are summarised as follows:

1. Biochar amended (particularly rice husk biochar) enhanced dissolved Zn removal ($p=0.009$), compared to pure sandy filters due to increased surface area, but reduced TSS and Pb particle removal efficiencies, this was explained by:
    a. The higher conductivity in rice husk biochar filters, which decreased contact time, limiting sedimentation and filtration of suspended solids and particulate-bound Pb.
    b. Biochar particle resuspension and mobilisation during wetting-drying cycles further contributed to reduced TSS and Pb efficiency in biochar amended media.
2. Biochar amendment significantly contributed to net phosphorus leaching, primarily from biochar's inherent phosphorus content.
3. Sewage sludge biochar leached the highest dissolved P but captured particulate P most effectively, possibly due to its lower conductivity and high metal content.
4. All filters showed substantial MPs retention (particle size ≥ 50µm) through physical straining, regardless of biochar amendment.
5. To effectively harness biochar's potential in bioretention systems, targeted optimisation (including metal-oxide modification, media layering, and standardised washing protocols) requires further investigation to mitigate phosphorus leaching and suspended solids release.

Chapter 6. Field Assessment of Heavy Metal Accumulation in Bioretention Systems

6.1 Introduction

Bioretention systems are highly effective at capturing heavy metal, particularly in the top 5-10 cm layer of the filter media as demonstrated in Chapter 4, and other similar studies (Read et al. 2008; Hatt et al. 2011; Jacklin et al. 2021b). However, the prolonged accumulation of these elements risks breaching regulatory thresholds for contaminated land, potentially necessitating costly disposal measures. Consequently, effective SuDS management requires proactive monitoring and maintenance strategies to mitigate environmental risks and ensure regulatory compliance. Systematic, large-scale monitoring of SuDS, particularly in urban areas, is constrained by the significant costs and time demands associated with traditional soil sampling and laboratory analysis. The pXRF technique provides a cost-effective and rapid assessment tool that enables wider area coverage and hotspot identification for preliminary risk assessment (Venvik and Boogaard 2020; Boogaard et al. 2024).

This study provides insights into heavy metal accumulation patterns within operational bioretention systems at two urban sites in Cardiff, UK. It identifies contamination hotspots and evaluates the influence of system-specific factors, such as distance from the inlet and biofilter age, on metal distribution, while contextualising the findings through comparison with soil screening values. These critical concerns remain rarely researched; to the author's knowledge, this constitutes the first investigation of its kind conducted on operational bioretention systems in the UK, despite their national-scale implementation.

Building on previous research (Jones and Davis 2013; Al-Ameri et al. 2018; Venvik and Boogaard 2020; Lenormand et al. 2022), this study employed two complementary approaches: traditional grab sampling for ex-situ analysis and an in-situ pXRF for rapid, real-time contaminant mapping. The findings will support improved bioretention design and maintenance to mitigate heavy metal accumulation risks.

6.2 Materials and methods

6.2.1 Site description

The selection criteria for the study sites were based on the operational age of the bioretention systems, as older systems were expected to exhibit elevated levels of heavy metals. Accordingly, two study sites with differing operational durations and land uses were selected for this investigation. The first study site was situated in a residential area on the western side of the River Taff in Grangetown, Cardiff (51°28′11.0"N, 3°10′56.0"W). This area underwent a SuDS retrofit as part of the *Greener Grangetown* project, which was successfully completed in 2018.

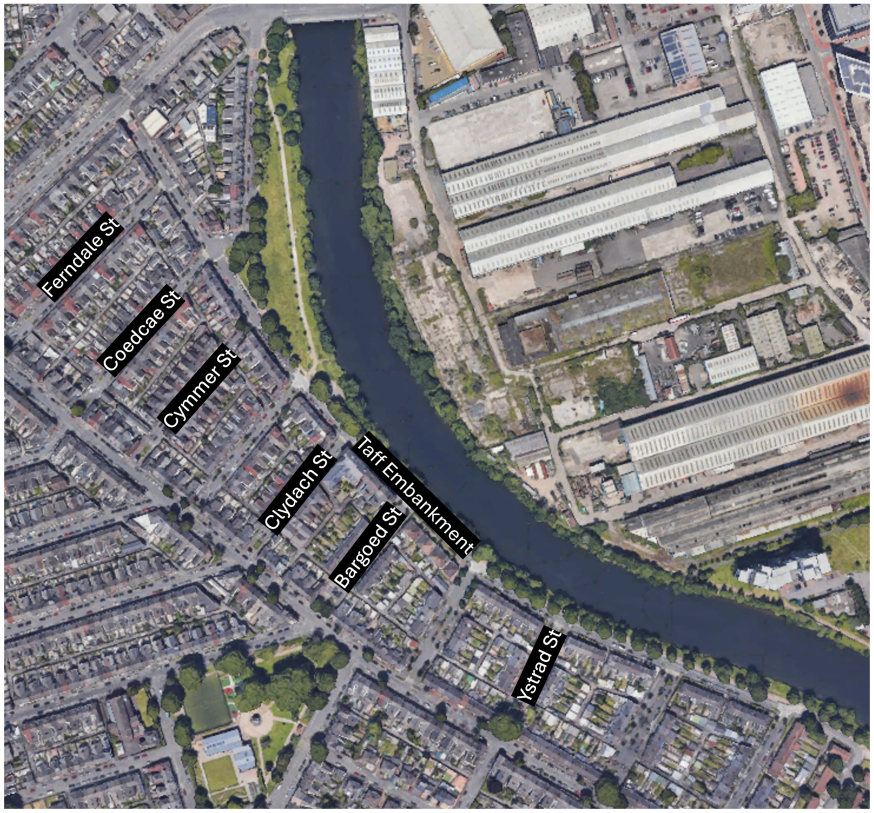

Figure 6.1 Ariel view showing the extent of Greener Grangetown project and the streets where the selected biofilters were located (image: Google Earth).

The project spans approximately 12 hectares, covering 12 streets, and serves around 1,150 residents and 500 properties. It incorporates 108 rain gardens planted with native vegetation and 130 stand-alone trees (JNCC 2021; Green Blue Urban [no date]). *Greener Grangetown* is widely recognised as an award-winning initiative and a leading example of SuDS implementation in Wales (JNCC 2021; Cardiff News Room [no date]).

For this study, eight biofilters were selected within the site, all featuring vegetation cover and sandy filter media. These biofilters were distributed across seven adjacent streets, encompassing the majority of the project's extent. The streets included are Bargoed Street, Coedcae Street, Clydach Street, Cymmer Street, Ferndale Street, Taff Embankment, and Ystrad Street.

Table 6.1 Locations of selected biofilters for the field investigation in Cardiff urban area.

Biofilter #	Site	Street name	Year of implementation	Land use
1	Grangetown	Ferndale St	2018	Residential
2	Grangetown	Taff Embankment	2018	Residential
3	Grangetown	Taff Embankment	2018	Residential
4	Grangetown	Coedcae St	2018	Residential
5	Grangetown	Clydach St	2018	Residential
6	Grangetown	Cymmer St	2018	Residential
7	Grangetown	Bargoed St	2018	Residential
8	Grangetown	Ystrad St	2018	Residential
9	City Centre	Station Terrace	2024	Commercial
10	City Centre	Station Terrace	2024	Commercial
11	City Centre	Station Terrace	2024	Commercial

The second site was recently retrofitted with bioretention systems as part of the Canal Quarter and Cardiff East regeneration scheme, located on the eastern side of Cardiff City Centre (51°28′57.8″N, 3°10′16.2″W). The land use in this area is described as mixed, encompassing apartment buildings, hospitality venues, restaurants, retail spaces, and offices (Cardiff News Room 2022). The scheme was completed during the first quarter of 2024, within the timeframe of this study, and was selected to provide post-construction comparison data relative to the more mature systems in Grangetown. Although a direct comparison with *Greener Grangetown* was not feasible due to differences in land uses, the data collected from this site offer valuable insights into the heavy metal concentrations in the soil media during the early stages of a bioretention system's lifecycle.

For this site, three biofilters located on Station Terrace were selected, bringing the total number of surveyed biofilters to 11, as outlined in Table 6.1. For simplicity, the land use of the Station Terrace biofilters was categorised as commercial in this study.

6.2.2 Ex-situ sampling and analysis

To evaluate the effect of biofilter age on the accumulation levels of heavy metals, grab soil sampling was conducted on the selected biofilters following the sampling protocol adopted by Al-Ameri et al. (2018). Briefly, for biofilters with a surface area of less than 10 m², one surface and one subsurface sample were collected near the inlet. For biofilters with surface areas ranging from 10 to 50 m², three surface and three subsurface samples were collected from evenly distributed locations across the biofilters, based on their distance from the inlet. For biofilters exceeding 50 m^2, one additional surface and one additional subsurface sample were taken for every additional 100 m^2.

Surface samples were collected from the top 0-3 cm layer of the biofilter surface using acid-washed plastic scoops. Any surface mulch, such as fallen leaves, litter, or organic/inorganic material, was removed to expose the underlying soil media. Subsurface samples were taken from the same locations using a hand soil auger (15×30 cm) to extract core samples at a depth of approximately 12-15 cm below the surface. Each soil sample (≈ 50 g) was placed in a sealed sampling bag, labelled with the time and location of the collection point, and transported to the laboratory for preparation for X-ray fluorescence (XRF) spectrometry analysis.

Sample preparation for XRF analysis followed a method similar to that described in the G-BASE survey by the British Geological Survey (Brown 2004) and adhered to the testing protocol recommended by the manufacturer (Innov-X Systems Olympus mobile XRF analyser). The soil samples were placed in clean containers and oven-dried at 40°C for 48 hours. The dried samples were sieved through a >2-mm mesh to remove debris and organic matter. The sieved material was then crushed and passed through a 200µm sieve to create a more homogeneous matrix, before being placed in XRF cups.

The samples were analysed for several elemental concentrations, including the target metals (Zn, Cu, and Pb). Chromium (Cr) was also found in high concentrations in the analysed samples and was subsequently added to the list of target pollutants. The instrument was calibrated using a standard check sample (316) provided by the manufacturer to ensure quality assurance.

6.2.3 In-situ measurements with pXRF

Field portable X-ray fluorescence (pXRF) analysers provide a rapid, non-invasive, and in situ method for detecting heavy metals in soils, sediments, and other environmental samples, making them an effective tool for real-time monitoring and decision-making at contaminated sites (Venvik and Boogaard 2020; Boogaard et al. 2024). Compared to conventional laboratory methods, such as atomic absorption spectrophotometry (AAS) or inductively coupled plasma mass spectrometry (ICP-MS), in-situ pXRF measurements can significantly reduce the time, costs, and logistical challenges associated with sample collection, transport, preparation, and analysis. Additionally, they offer reliable results for preliminary risk assessments and compliance with regulatory frameworks, such as the Water Framework Directive (Radu and Diamond 2009; Venvik and Boogaard 2020).

This technology has been widely applied in urban environments, mining areas, and landfills, and it holds significant potential for the rapid mapping of heavy metal accumulation levels in bioretention systems. It provides higher resolution for identifying contamination hotspots and areas requiring remediation (Kalnicky and Singhvi 2001; Lenormand et al. 2022).
While pXRF has many advantages, careful attention to sampling and preparation is critical to ensuring data quality and reliability of measurements.

pXRF analysers are typically less sensitive than laboratory methods and have higher limits of detection (Kalnicky and Singhvi 2001). Moisture content significantly influences readings; samples with a moisture content exceeding 20% can produce biased results (Bruker [no date]). Additionally, the physical matrix of the soil, including particle size and sample heterogeneity, can affect the accuracy of the results. Soil and sediment samples are inherently non-uniform, which may lead to variability between measurements (Kalnicky and Singhvi 2001; Bruker [no date]).

While pXRF has its limitations, it is important to note that the primary objective of this survey was to provide a quick, non-rigorous screening method for the preliminary assessment of heavy metal contamination levels in bioretention systems and to quickly identify any hotspots for potential remediation. Despite its limitations, pXRF is sufficient for this purpose, as demonstrated in similar studies and other environmental applications (Kalnicky and Singhvi 2001; Radu and Diamond 2009; Venvik and Boogaard 2020; Lenormand et al. 2022; Boogaard et al. 2024).

In-situ measurements of topsoil were conducted on selected biofilters using the pXRF analyser (Bruker S1 TITAN, TRACER 5) with the GeoExploration application (Oxide3phase method) pre-programmed into the instrument. Measurements were performed on dry days, with at least 48 hours having elapsed since the last rain event, to minimise potential bias arising from moisture content. To ensure the validity of the in-situ results, grab samples were collected from each site and prepared in the laboratory (dried and sieved) following the procedure described in Section 6.2.2.

The results were then compared to the pXRF readings. pXRF measurements from most Grangetown biofilters were excluded from the analysis due to significant discrepancies (>50%) between in-situ and laboratory measurements. These discrepancies were attributed to high silt and clay contents in the topsoil, which resulted in higher moisture content and reduced accuracy.

A systematic grid using x, y coordinates (x = length, y = width) was employed to spatially distribute the sampling points for each biofilter. The aim was to cover as much of the biofilter surface as possible, producing reliable results in a time-efficient manner. The variation with distance from the inlet was also considered. Since the surveyed biofilters are typically less than 3 m wide (vertical distance from the inlet), the grid points were spaced 1 metre apart in the x-direction (horizontal distance) and 0.5 metres in the y-direction (vertical distance), totalling approximately two samples per square metre. Sample spacing was kept as regular as possible, with adjustments made to work around vegetation where necessary.

At each grid point, the pXRF was placed against the flat topsoil so that the detector window touched the soil surface to activate the trigger sensor, after removing any surface mulch, leaves, or litter.

Duplicate measurements, and sometimes multiple measurements from different positions, were taken at each sampling point, with the average reading calculated to improve representativeness and minimise particle bias and physical matrix effects (Kalnicky and Singhvi 2001; Bruker [no date]).

Figure 6.2 In-situ measurement of elemental composition using pXRF on a biofilter surface located on Station Terrace.

Although the shooting time of the pXRF can also influence the results, as longer shooting times produce more reliable measurements, a compromise was made to maximise area coverage while minimising fieldwork duration. The shooting time was therefore set to the minimum of 60 seconds per measurement. The pXRF was calibrated prior to each sampling trip using the standard reference material (SRM) sample (CS-M2) and validated against the calibration certificate provided by the manufacturer to ensure quality assurance. The detection limits of the pXRF instrument are presented in Table 6.2. To facilitate statistical analysis, readings below these limits were treated as half of the detection limit.

Table 6.2 Detection limits of the Bruker S1 TITAN, TRACER 5 pXRF.

Element	Units	Detection limit
Pb	mg/kg	5
Cu	mg/kg	3
Zn	mg/kg	3

6.2.4 Statistical analysis

All data analyses were conducted using SPSS Statistics, version 29.0.2.0 (20). Heavy metal concentrations, grouped by site, were presented in box-and-whisker plots against Normal Background Concentrations (NBCs) as a reference, which are discussed in detail in Section 6.3.4.1. Since most datasets were found to be non-normally distributed, the non-parametric Wilcoxon Signed Ranks test was performed on paired samples (surface and subsurface groups) to assess differences in metal concentrations between depths. Similarly, the non-parametric Mann-Whitney U Test was employed to compare differences in metal accumulation between the two study sites. All statistical tests were performed with a confidence level of 95% ($\alpha = 0.05$).

6.3 Results and discussion

6.3.1 Overall metals concentrations

Table 6.3 provides summary statistics of the concentrations of heavy metals in biofilters at the investigated sites. Except for Cr, metal concentrations were generally higher ($p < 0.05$ for Zn and Pb) at the surface level (0-3 cm), with values ranging from 15-69 mg/kg for Cu, 18-340 mg/kg for Pb, and 69-583 mg/kg for Zn, compared to the sub-surface level (12-15 cm), where concentrations ranged from 16-63 mg/kg for Cu, 15.2-296 mg/kg for Pb, and 67-421 mg/kg for Zn.

This suggests that heavy metal accumulation in bioretention systems tended to decrease with depth, supporting the findings from Chapter 4, where the majority of heavy metals were retained in the top 0-3 cm layers of the columns. However, in this field study, the differences in Cu and Cr accumulation between the surface and sub-surface layers were statistically insignificant, as differences between the medians were marginal (Table 6.3). Overall, the results align with similar field investigations conducted by Al-Ameri et al. (2018) and Furén et al. (2023), which reported comparable findings with median concentrations ranging from 21-29, 16-30, 84-170, and 9 mg/kg for Cu, Pb, Zn, and Cr respectively.

Similarly, in 4 out of the 11 sampled biofilters with surface areas > 10 m², metals (Pb, Zn, and Cr) were more concentrated at the inlets and tended to decrease with increasing distance towards the biofilter centre. However, this trend was not observed for Cu concentrations. In some biofilters, metal concentrations were higher in the middle of the biofilter than at the inlet, suggesting the presence of preferential flow paths for stormwater entering the biofilter (Heal et al. 2009; Al-Ameri et al. 2018).

It is also plausible that higher inflow rates resulted in the scouring and redeposition of sediments, which are often enriched in heavy metals as they tend to bind to suspended particles, from the inlet to more central locations (Hatt et al. 2007b; Al-Ameri et al. 2018; Guo et al. 2021). This scenario was more likely in biofilters with more than one inlet, as was the case in the sampled biofilters in this study. Moreover, in Station Terrace, biofilters were designed with diffused inlets, where water ingress occurred from all directions to promote a more uniform distribution of stormwater runoff, as shown in Figure 6.3 (a).

In such cases, the in-situ mapping with the pXRF, detailed in Section 6.3.3, provided valuable insights and a rapid assessment of the spatial distribution of heavy metals on the surfaces of bioretention systems.

Table 6.3 Summary statistics of heavy metal concentrations at surface and subsurface layers of surveyed biofilters grouped by site.

Pb Concentrations (mg/kg)								
Site	Surface				Subsurface			
	Mean	Min	Max	Median	Mean	Min	Max	Median
Station Terrace	46.83	18	208	20.2	17.59	15.2	20.9	16.6
Grangetown	78.46	30.5	340	46.55	57.34	24.3	296	38.95
Cu Concentrations (mg/kg)								
Site	Surface				Subsurface			
	Mean	Min	Max	Median	Mean	Min	Max	Median
Station Terrace	29.86	15	59	23	27.29	16	63	22
Grangetown	39.06	26	69	38	38.00	25	58	35
Zn Concentrations (mg/kg)								
Site	Surface				Subsurface			
	Mean	Min	Max	Median	Mean	Min	Max	Median
Station Terrace	99.14	69	173	89	80.14	67	96	76
Grangetown	222.69	137	583	169	189.06	130	421	157
Cr Concentrations (mg/kg)								
Site	Surface				Subsurface			
	Mean	Min	Max	Median	Mean	Min	Max	Median
Station Terrace	23.84	13.4	38.8	21.2	30.86	24.4	40.8	28.5
Grangetown	50.81	34	95	46.5	50.69	22.3	118	49.5

(a) (b)

Figure 6.3 biofilter inlet design, (a) diffused inlet in Station Terrace biofilters, (b) centralised inlet in Greener Grangetown biofilters.

6.3.2 Effect of biofilter age on accumulation levels

The results of this study revealed significant differences in the accumulation levels of heavy metals in biofilters between the Grangetown and Station Terrace sites, largely attributable to the differing ages of the systems. The Grangetown biofilters, implemented in 2018 as part of the Greener Grangetown project, consistently showed higher concentrations of Pb, Zn, and Cr compared to the Station Terrace biofilters, which were only a few weeks old at the time of the survey.

This trend was evident in both the surface (0-3 cm) and subsurface (12-15 cm) soil layers. For Pb, the Grangetown biofilters exhibited significantly higher concentrations at both depths, with the median surface concentration at Grangetown measuring 46.55 mg/kg, compared to 20.2 mg/kg at Station Terrace. A similar trend was observed in median concentrations in the subsurface layers (39 and 16.6 mg/kg in Grangetown and Station terrace respectively). Zn concentrations followed a similar pattern, with the Grangetown biofilters showing a surface mean of 222.69 mg/kg, compared to 99.14 mg/kg at Station Terrace, and the subsurface levels reflecting the same disparity.

These findings suggest that Zn, although more mobile than Pb—as demonstrated in the column experiments in Chapter 4 and confirmed by Furén et al. (2023)—can still accumulate over time if attached to particles, as sediments enter and are filtered in the top layer of the biofilter media (Guo et al. 2021; Furén et al. 2023). Similarly, Cr concentrations were higher at Grangetown across both layers, with a mean surface concentration of 50.81 mg/kg, compared to 23.84 mg/kg at Station Terrace. These levels demonstrate evidence of gradual Cr accumulation over time, consistent with the behaviour of persistent particulate-bound metals.

In contrast, Cu concentrations showed minimal differences between the two sites, as indicated by the Mann-Whitney U Test ($p > 0.05$). This suggests that Cu accumulation was possibly governed by distinct transport or retention mechanisms, such as the formation of Cu-organic matter complexes or binding to clay particles (Furén et al. 2023), which were less influenced by biofilter age. Nonetheless, the difference in median Cu concentrations between Grangetown (38 mg/kg) and Station Terrace (23 mg/kg), although statistically insignificant, indicates some accumulation over time.

The findings from this field investigation differ from those of the column study in Chapter 4 regarding the magnitude of concentration differences between surface and subsurface layers. For instance, the column study showed Cu concentrations approximately 11.5 times higher in the surface layer than in the subsurface. In contrast, the Grangetown biofilters exhibited no significant difference in median Cu concentration between these layers. This discrepancy is largely attributed to the formation of cake layers in the column study, which acted as a sieve and provided sufficient adsorption sites for Cu, limiting its downward migration. It is also important to note that the high mean concentrations observed in the column study represent a conservative scenario for highly sediment-laden inlets, which is not representative of typical median field conditions.

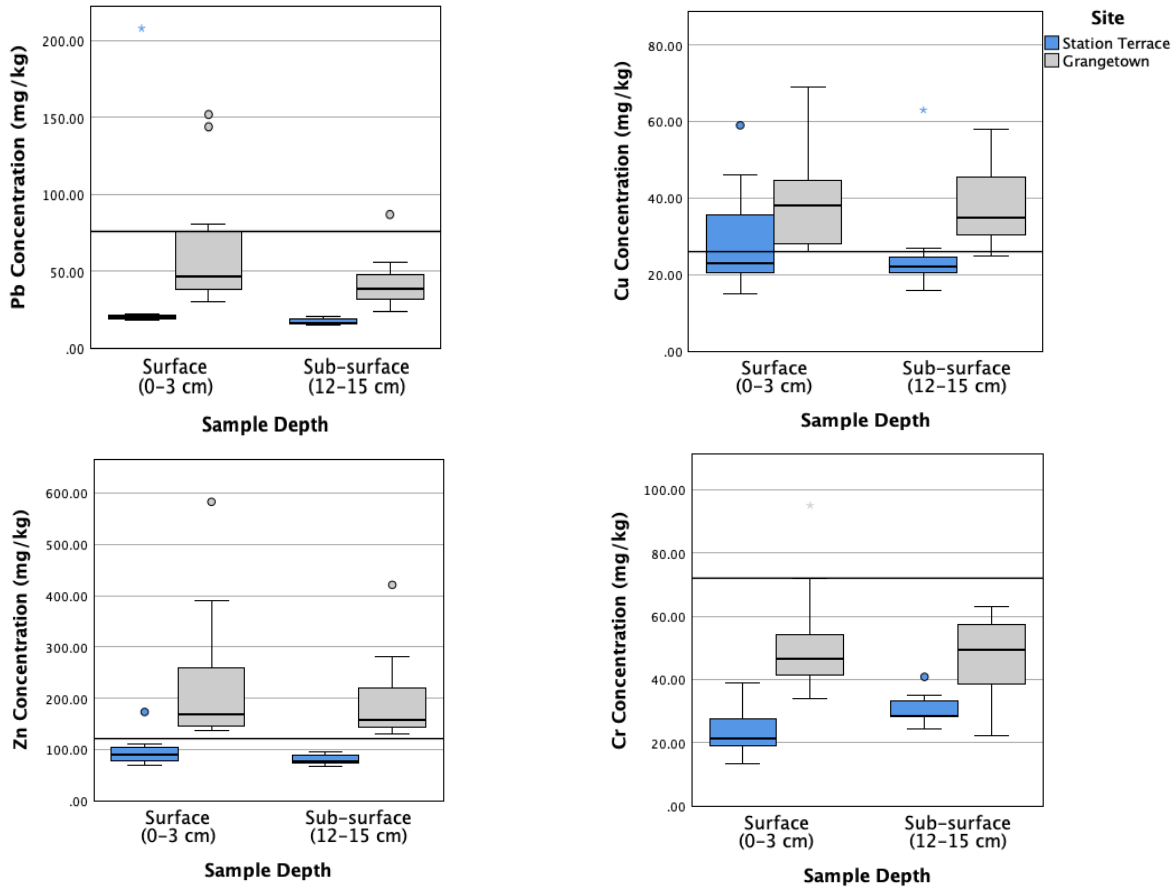

Figure 6.4 Heavy metal concentrations at the surface and subsurface layers of 12 biofilters at two sites. The black horizontal lines refer to Normal Background Concentrations (NBCs) of topsoil in Cardiff.

The higher concentrations of heavy metals in the older Grangetown biofilters highlight the cumulative effect of prolonged filtration of urban stormwater runoff on heavy metal accumulation. These biofilters have received higher amounts of pollutants over their 6-year operational period, resulting in a progressive build-up of heavy metals in the filter media. In contrast, the newly constructed systems at Station Terrace have not had sufficient time to accumulate heavy metals to the same extent, as evidenced by their generally lower concentrations.

Nevertheless, the median concentrations at both study sites were below the Normal Background Concentrations (NBCs, shown as reference black lines in Figure 6.4 for Pb and Cr. The NBCs represent the median concentrations of topsoil in Cardiff's G-BASE dataset (discussed later in Section 6.3.4.1). On the other hand, the median concentrations for Zn and Cu exceeded the NBCs in the Grangetown biofilters, while the median concentrations in the Station Terrace biofilters were slightly below the NBC levels.

Although these systems were designed to receive stormwater runoff, the results showed that at least 75% of the data obtained from Grangetown were below the NBCs for Pb and Cr, even after 6 years of operation. This is somewhat unsurprising, as the urban G-BASE survey was conducted in 1994 (Brown 2004), prior to the ban on leaded petrol in the UK in 2000 (Hwang et al. 2016). Consequently, a decline in Pb accumulation levels today compared to the NBCs was expected.

6.3.3 In-situ measurement with pXRF

The spatial distribution of heavy metals (Zn, Cu, and Pb) across biofilter surfaces at two urban sites in Cardiff was examined using in-situ pXRF measurements. The analysis focused on one biofilter at Station Terrace and one at Grangetown (Ferndale Street), as these demonstrated the least discrepancies between in-situ and ex-situ measurements. Other biofilters were excluded due to the lack of reliability of the pXRF measurements. The results revealed differences in metal accumulation patterns between the two sites, which can be attributed to variations in biofilter design, inlet configuration, and system age.

At Station Terrace, the biofilter had a surface area of 22.1 m², featuring a diffused inlet design where water infiltrated from all edges, as can be seen in Figure 6.3 (a), with the highest inflow rates occurring along the traffic-facing edge (denoted by the black diagonal lines in Figure 6.5, and Figure 6.6). In contrast, the Grangetown biofilter (Ferndale Street), with a surface area of 7.68 m², was constructed in 2018 and had a concentrated inlet design, where stormwater flow was directed to three specific points as can be seen in Figure 6.5 and Figure 6.6. These differences in inlet configuration influenced the spatial distribution of metals within the biofilters.

To demonstrate the spatial variations in metal concentrations across the biofilter surface, heatmaps were plotted using a colour scheme with a scale in 50 mg/kg increments, to highlight hotspots and accumulation patterns, rather than to compare with contamination thresholds. This approach was chosen as contamination thresholds far exceed most of the measured values as will be discussed in Section 6.3.4.2. In the Station Terrace biofilter, Pb concentrations were generally below the instrument detection limit of 5 mg/kg and were treated as half of the detection limit, as shown in Figure 6.5.

The concentrations tended to increase around the edges, particularly towards the traffic-facing edge. Pb concentrations ranged from as low as 2.5 mg/kg on the footway side to 24 mg/kg near the corner edge.

Zn concentrations showed a relatively uniform distribution, with values ranging from 35 mg/kg in the centre of the biofilter to 340 mg/kg near the footway corner edge (Figure 6.5). This spatial pattern reflects the influence of the diffused inlet design, where stormwater was distributed more evenly across the biofilter edges. On average, the traffic-facing edge exhibited higher concentrations, likely due to higher inflow rates from the traffic side, while lower concentrations were observed towards the middle and footway-facing edges of the biofilter.

Cu concentrations (Figure 6.6) followed a similar trend but with more gradual gradients, ranging from 10 mg/kg towards the centre of the biofilter to 50 mg/kg near the traffic-facing edge. Interestingly, Cu concentrations in the Grangetown biofilter, constructed in 2018, were generally lower than those in the Station Terrace biofilter, as demonstrated in Figure 6.6, despite the difference in biofilter age. This observation aligns with the Mann-Whitney U Test results from the grab samples discussed in Section 6.3.2, which revealed that biofilter age had no significant effect on Cu concentrations.

However, the distribution of Cu in the Grangetown biofilter was more localised, with higher levels near inlets and a maximum value of 25.5 mg/kg near one of the traffic-facing inlets, supporting the conclusion that concentrated inflow paths increase sediment deposition and metal accumulation near centralised inlets. This effect was more pronounced with Zn concentrations, as seen in Figure 6.5 (ii), where areas near the three inlets exhibited the highest concentrations.

Similarly, Pb distribution in the Grangetown biofilter, shown in Figure 6.5 (i), reflected more heterogeneous patterns due to its centralised inlet design, with concentrations reaching up to 256 mg/kg near the traffic side. These concentrations far exceeded those in the Station Terrace biofilter, reflecting prolonged accumulation of Pb on the biofilter surface, which may necessitate remedial actions.

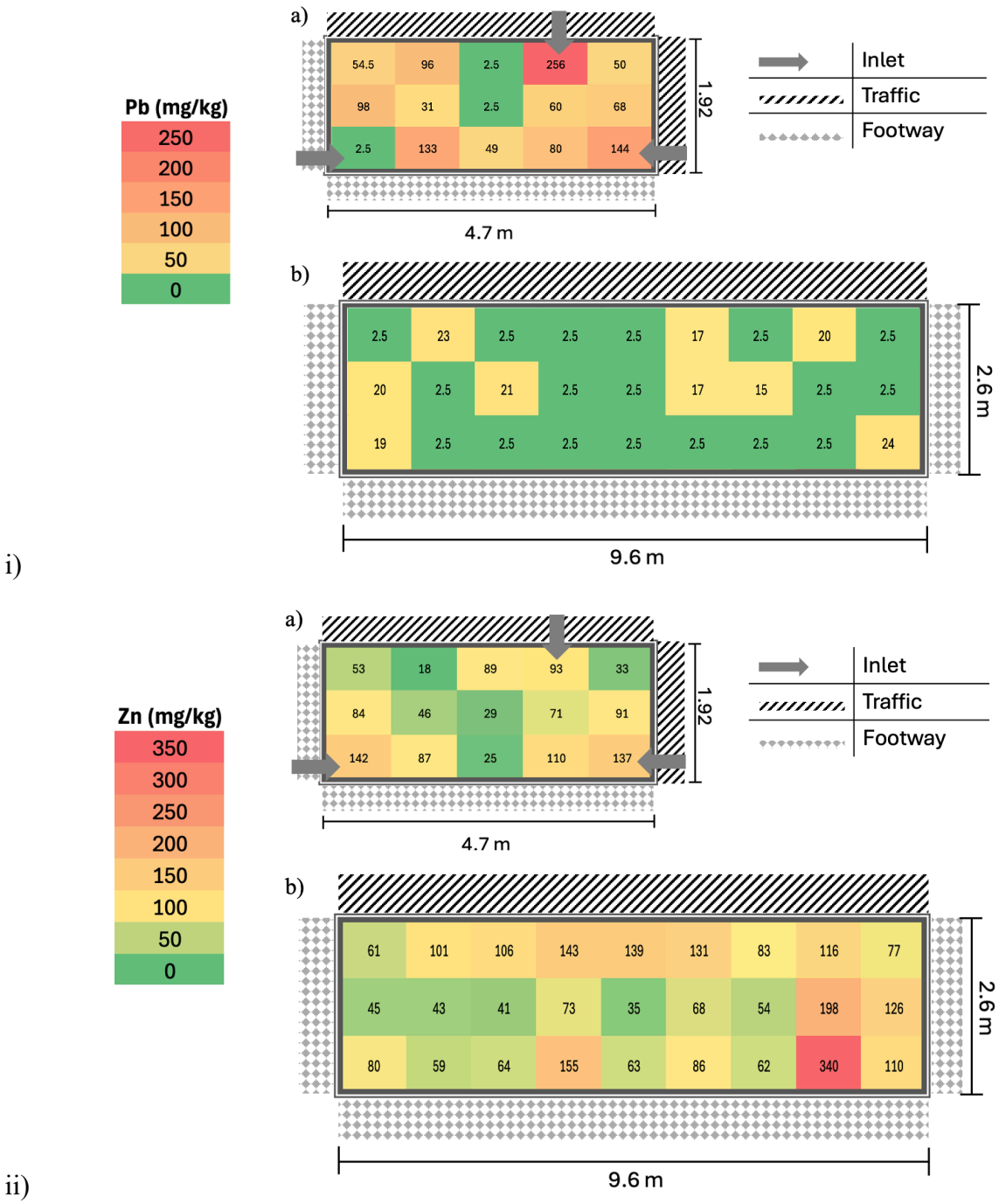

Figure 6.5 Heat maps showing i) Pb, and ii) Zn spatial distribution in two biofilters, a) Ferndale St., Grangetown, and b) Station Terrace, Cardiff City Centre. Diagonal lines represent traffic edge, while the diamond pattern represent pedestrian footways. The Ferndale St. biofilter had centralised inlet design demonstrated by the 3 arrows, while Station Terrace had diffused inlet design.

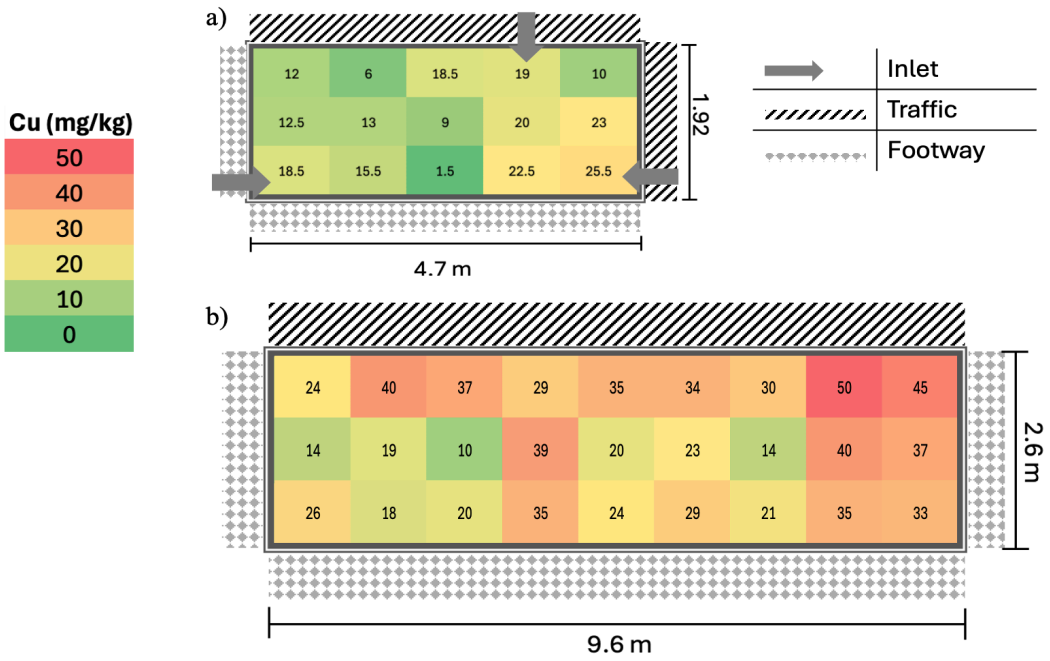

Figure 6.6 Heat maps showing Cu spatial distribution in two biofilters, a) Ferndale St., Grangetown, and b) Station Terrace, Cardiff City Centre. Diagonal lines represent traffic edge, while the diamond pattern represent pedestrian footways. The Ferndale St. biofilter had centralised inlet design demonstrated by the 3 arrows, while Station Terrace had diffused inlet design.

6.3.4 Comparison of concentrations to soil quality guidelines

To understand the necessary maintenance requirements for bioretention systems in relation to the associated risks of heavy metal accumulation in the soil media, it is important to compare the findings to soil quality guidelines, specifically within the UK regulatory context. Since the introduction of Part 2A of the Environmental Protection Act 1990 in the UK, which established a legal framework for identifying and managing contaminated land in England and Wales (Defra 2012), the British Geological Survey was commissioned to conduct a systematic survey of the geochemistry of UK soils, known as the Geochemical Baseline Survey of the Environment (G-BASE) programme. This programme provides comprehensive mapping of inorganic soil contaminants in urban centres across the UK (Ander et al., 2013a). The primary datasets include G-BASE rural, G-BASE urban, and the National Soil Inventory (NSI), which focus on topsoil (0-15 cm) and capture both natural (parent material) and anthropogenic contributions to soil chemistry (Ander et al. 2013a; Ander et al. 2013b).

6.3.4.1 Normal background concentrations

The G-BASE survey, conducted in 1994, provides data on elemental concentrations in urban soils and stream sediments. The purpose of these datasets is to offer an overview of typical background concentrations (Brown 2004), later referred to as Normal Background Concentrations (NBCs), which are influenced by three main factors: the underlying parent material (natural soil), non-ferrous metalliferous mineralisation and mining activities, and urbanisation or industrialisation (Ander et al., 2013a). These factors contribute to varying pollutant concentrations across different regions. The results for the NBCs from the G-BASE survey for topsoil in the Cardiff urban area are presented in Table 6.4.

Although the NBCs provide a baseline for what level of contamination is considered normal (median concentrations) in respective regions, they do not offer insights into the environmental implications or whether the soil is considered contaminated. The Environment Agency has developed frameworks and screening tools to address the ecological and toxicological risks arising from soil contamination.

Such tools include Soil Guideline Values (SGVs), which are scientifically based, non-statutory benchmarks developed using the Contaminated Land Exposure Assessment (CLEA) model, based on Health Criteria Values (HCVs) among other factors, to assess the potential long-term health risks to humans from chemical contamination in soil under general land-use scenarios (Cole and Jeffries 2009).

SGVs serve as conservative "trigger values" in the second stage of land contamination risk assessment for tolerable exposure levels. Exceeding an SGV does not indicate significant harm, only that further detailed investigation is necessary (Cole and Jeffries 2009). They do not address short-term or non-human risks, nor do they dictate remediation standards. SGVs exist for some but not all elements; certain priority pollutants, such as Pb, Cu, Zn, and Cr (the main pollutants investigated in this study), do not have published SGVs or toxicological reports in the UK as of 2024. Other risk assessment tools, such as the Generic Assessment Criteria (GAC), which was developed by CL:AIRE and followed the same protocols developed for SGVs, focus on organic pollutants in soils (CL:AIRE 2010).

It is important to consider the main functions of the bioretention system when deriving contamination thresholds to be applied in the context of SuDS maintenance and remediation. For example, if the system primarily serves to protect downstream ecosystems by retaining pollutants within the soil matrix, it may accommodate higher thresholds than if its primary function is to provide wildlife habitats (Ander et al., 2013a). Land use is another important factor to consider, as different land uses exhibit varying contamination levels. For instance, the results from the G-BASE report discussed earlier showed that, within the Cardiff survey domain, stream sediment concentrations from rural areas were generally slightly higher than those in urban topsoil. This was attributed to the natural composition of the underlying bedrock, such as the Coal Measures, which contain naturally higher levels of elements like nickel (Ni) and vanadium (V). In contrast, elements such as arsenic (As), Cu, and Pb were higher in urban areas, likely due to human activities such as vehicle emissions and fossil fuel combustion (Brown 2004).

6.3.4.2 Soil screening levels

A new technical tool used to identify contaminated land in a more general and pragmatic manner, using higher threshold values, is the Category 4 Screening Levels (C4SLs), which were developed by Defra and Natural Resources Wales to enable local authorities to identify land that poses a low risk to human health and requires no further assessment. These levels apply to four general land uses: residential, commercial, allotments, and public open spaces, and were derived for six key substances, including Pb (Harries et al. 2014). Unlike Soil Guideline Values (SGVs), which represent minimal risk, C4SLs define a slightly higher but still precautionary level of risk.

This distinction ensures that C4SLs reflect land that falls under Category 4 (Human Health), where contamination levels are low enough to be considered suitable for use without significant possibility of harm (Harries et al. 2014). Although they serve as technical tools to guide decision-making, C4SLs are not legal thresholds for declaring contaminated land under Part 2A. The figures in Table 6.4 present the soil screening values for Pb concentrations in residential and commercial land uses according to the C4SLs. For the remaining pollutants (Zn, Cu, and Cr), threshold values were obtained from the National Environment Protection Council's Health Investigation Levels (HILs), adopted in Australia (NEPC 2013), as these follow similar classifications and deterministic models used to derive the C4SLs.

Both C4SLs and HILs are defined as values below which the possibility of harm is unlikely, and no further site assessment may be required.

Table 6.4 Comparison of median and 95th percentile of measured concentrations of biofilters in residential (Grangetown) and commercial (Station Terrace) sites, to normal background concentrations and soil screening levels.

	Measured concentrations (mg/kg)				**NBCs[a]**	**Soil screening levels[b] (mg/kg)**	
	Residential		Commercial		Urban	Residential[c]	Commercial[d]
	50th	95th	50th	95th	50th		
Cu	25	59	30	77	26	7000	250000
Pb	36	183	2.5[e]	33	76	130-330	1100-6000
Zn	131	327	95	339	121	8000	400000
Cr	48	103	28	NA[f]	72	100	3000

a Median normal background concentrations of topsoil from Cardiff G-BASE urban data (Brown 2004).
b Soil screening levels for Pb were obtained from C4SLs (Harries et al. 2014), while screening levels for the other three metals were obtained from the NEPC's HILs in Australia (NEPC 2013).
c C4SLs classification of standard residential land without consumption of homegrown produce, where a child is the critical receptor of toxic intake (Harries et al. 2014).
d C4SLs classification of commercial land, where an adult is the critical receptor of toxic intake (Harries et al. 2014).
e Median concentration was below the detection limit and were calculated as half the detection limit.
f Sample size insufficient to calculate the 95th percentile.

Table 6.4 compares the average calculated 95th percentile of heavy metal concentrations measured in the surveyed biofilters to the soil screening levels for health risks, as described above. Soil screening levels vary significantly between residential and commercial land uses (Grangetown and Station Terrace respectively, which were the main study sites presented in Table 6.1). Although Pb accumulation levels in the column study (2556-3321 mg/kg) fell within the range of soil screening levels for commercial land use (1100-6000 mg/kg) after an equivalent of 8 years of operation, concentrations in the field biofilters were significantly lower. As can be seen from Table 6.4, the median and 95th percentiles of all the measured metal concentrations across all biofilters fell substantially below the screening levels. This indicates that, regarding heavy metal accumulation, operational bioretention systems are likely to require less frequent routine maintenance than the conservative scenario represented by the column experiment.

All measured Zn and Cu concentrations in all biofilters were significantly below the HILs for both residential and commercial lands (Figure 6.7). In contrast, the 95th percentile of Pb concentrations fell within the C4SLs for residential land (183 mg/kg, which is higher than the lower limit of 130 mg/kg but below the upper limit of 330 mg/kg). These values were observed in the biofilters located in Grangetown's residential area. Of the eight surveyed biofilters in Grangetown, only one biofilter at the junction of Clydach Street had a Pb concentration that exceeded the C4SLs (340 mg/kg > 330 mg/kg) near the inlet. This inlet received runoff from a drainage channel (Figure 6.8).

Similarly, the Cr concentration observed at this sampling point exceeded the Australian HILs for residential land (100 mg/kg). This supports the conclusion that metal deposition and accumulation increased over time near centralised inlets. As discussed earlier, exceeding the C4SLs or the HILs does not necessarily imply a significant possibility of harm to human health, only that the possibility of harm may or may not exist, and further assessments may be required (Harries et al. 2014).

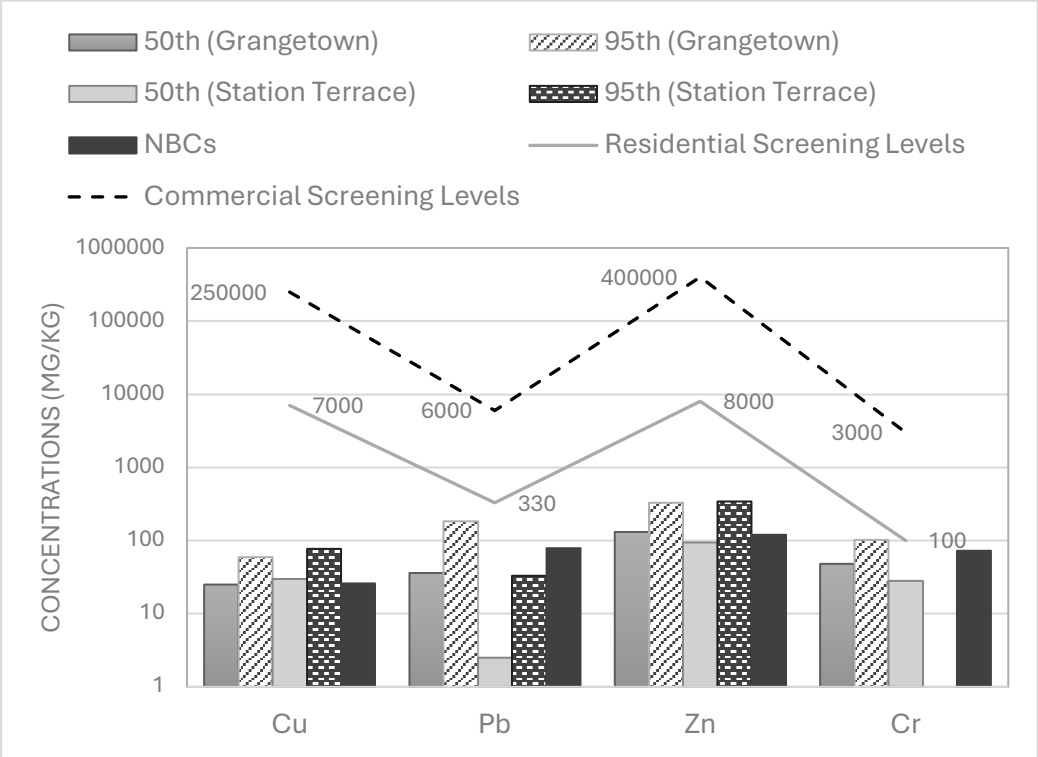

Figure 6.7 Measured 50th and 95th percentiles of heavy metal concentrations in residential (Grangetown) and commercial (Station Terrace) biofilters, compared to urban Normal Background Concentrations (NBCs), and soil screening values (upper limits).

6.3.5 Maintenance requirements

The results from this field investigation showed that one biofilter exhibited Pb and Cr concentrations that exceeded the soil screening values for Pb and Cr, within the first 6 years of operation, posing potential contamination concerns. This risk can be significantly reduced through regular maintenance protocols, such as scraping the top 5-10 cm layer of the biofilter soil, where a significant proportion of metals are retained, while ensuring regulatory compliance indefinitely (Jones and Davis 2013).

Routine maintenance, such as removing mulch, addressing litter and organic matter buildup, and maintaining even inflow distribution, could also reduce the reliance on extensive sampling and analysis of media, which may be impractical on a larger scale. As suggested by the results from Chapter 4, and supported by other studies, clogging from sediment deposition is more likely to necessitate remediation before the system reaches metal saturation (Li and Davis 2008b; Le Coustumer et al. 2009; Hatt et al. 2011; Jones and Davis 2013; Al-Ameri et al. 2018). While risks from breaching soil screening levels, as shown by the pXRF survey, were limited to hotspots near the inlets rather than affecting the entire system, which helps reduce the amount of media replacement and associated maintenance costs (Jones and Davis 2013).

Figure 6.8 Channel inlet configuration of the biofilter located at the junction of Clydach St., Grangetown.

6.4 Conclusions

This field study investigated the accumulation of heavy metals in biofilters at two urban sites in Cardiff, UK. The aim was to gain a practical understanding of heavy metal accumulation patterns and identify contamination hotspots through rapid in-situ mapping to aid practitioners in targeted maintenance planning. The investigation was carried out using traditional grab sampling and in-situ pXRF measurements. The study findings are summarised as follows:

1. Heavy metals primarily accumulated in the top 0-3 cm layer of biofilter surface, and concentrations increased with biofilter age.
2. Accumulation levels in the surface layers were within the following ranges, Cu: 15-69, Pb: 18-340, Zn, 69-583, and Cr, 13-95 mg/kg.
3. Inlet design influenced heavy metal distribution, as centralised inlets were observed to create contaminated hotspots near inflow points (particularly in channel inlet design), while diffused inlets distributed heavy metals more evenly across the biofilter surface.
4. All Zn and Cu concentrations were significantly below the soil screening values. One observation near a channel inlet exhibited Pb and Cr concentrations that exceeded soil screening levels for residential lands (Pb: 330 mg/kg, Cr: 100 mg/kg), posing potential contamination concern, which can be reduced indefinitely through regular maintenance (e.g. scraping of the top 5-10 cm layer).
5. Bioretention design should prioritise diffuse inlet configurations, and pXRF monitoring in future investigations to inform targeted maintenance interventions.

Chapter 7. Conclusion

This research aimed to enhance the design and maintenance of bioretention systems by evaluating specific design configurations using native plants and biochar amendments for improved performance, and by generating new insights into metal accumulation patterns through in-situ monitoring for targeted maintenance. This chapter synthesises the key findings, their implications for bioretention design and maintenance, and recommendations for future research. The research was carried out through laboratory column experiments and field investigation, contributing empirical insights to optimise bioretention design and assessment.

The investigation into design components was conducted through laboratory column studies. A large-scale column experiment was conducted to evaluate the influence of UK-native vegetation (*Phalaris, Carex, Juncus*), and drainage configurations under conditions that approximated field environments while accommodating mature root systems. Concurrently, the effects of biochar amendments (sewage sludge and rice husk biochar) were evaluated using a controlled bench-scale study to isolate their impacts and discern their removal mechanisms.

To address the maintenance aspect of the research aim, the long-term accumulation of heavy metals was investigated. This was achieved by analysing the filter media from aged laboratory columns to establish depth profiles, complemented by a field investigation of operational bioretention systems in Cardiff, UK. The application of in-situ pXRF analysis enabled rapid contaminant mapping and hotspot identification, which was used to evaluate the impact of system-specific factors, such as age and inlet design, on accumulation patterns and to inform targeted maintenance strategies.

7.1 Summary of key findings

TSS, heavy metals, and MPs (≥ 50µm), were successfully removed from designed columns with average removal rates ranging from 80% to ≥ 99%. No copper breakthrough was observed despite the application of an accelerated pollutant load equivalent to ten times typical stormwater concentrations. In contrast, phosphorus removal was more variable, with efficiencies ranging from 53% removal to significant net leaching, depending on the specific design variable.

7.1.1 Effects of design variables on bioretention performance

7.1.1.1 Effect of vegetation

Vegetated systems were 2-5% more efficient on average than non-vegetated systems in TSS and Zn removal, particularly dissolved Zn. Similarly extending the residence time through controlled-valve design increased the removal efficiency by 2-5% for TSS and Zn. Despite that, the overall impact of vegetation and residence time on pollutant treatment was statistically insignificant given the high overall removal rates. Most of the tested pollutants (TSS, Pb, Cu) were predominantly in particulate form, as a results, they were successfully removed through cake and depth filtration processes within the cake layer and substrate media, respectively. The cake layer also provided sufficient adsorption sites for dissolved Zn as demonstrated in their significant accumulation levels in the surface layers, contributing to the overall removal efficiencies. On the other hand, TP removal was more variable with removal efficiencies ranging from 39% to -9%. Vegetation enhanced TP removal, particularly in closed-valve design, however, the removal performance was variable depending on plant species.

The presence of vegetation was proven significant in preventing system clogging. Vegetated systems maintained hydraulic conductivity while non-vegetated systems clogged after 61 weeks of operation. It was observed that the formation of cake layers on biofilter surfaces contributed to prolonged ponding and reduced infiltration rates over time eventually causing system failure. This was prevented by the presence of roots in vegetated systems, which helped maintain infiltration rates over time.

Notably, bioretention performance was variable among plant species, with performance trade-offs in species selection. Plants with thick roots like *Juncus effusus* exhibited the highest infiltration rates which compromised TSS removal and increased particle migration, possibly due to channelling. Species like *Phalaris* proved unsuitable for bioretention design due to susceptibility to frequent inundation, resulting in net phosphorus leaching from plant exudates. *Carex pendula*, with its extensive fibrous root system, consistently outperformed other designs in all pollutant removals. Therefore, bioretention system design should prioritise selecting species such as *Carex pendula*, for optimum hydraulic performance and treatment efficiency over extended operational periods.

7.1.1.2 Effect of biochar amendments

The study of biochar amendment revealed that biochar with large surface area such as rice husk biochar improved dissolved Zn ($p=0.009$) when amended in traditional sandy loam filters. On the other hand, biochar-amendment reduced the removal efficiency of suspended solids (by 12-18%), and lead-bound particles (2-7%) compared to sand controls, especially in rice husk biochar filters. This was partially attributed to the higher conductivity of rice husk biochar filters increasing water flow, which reduced contact time necessary for sedimentation and filtration processes, resulting in higher concentrations of suspended particles in the effluents. It was also speculated that the lighter-density particles of biochar undergone resuspension and mobilisation during repeated wetting and drying in unsaturated conditions, contributing to the reduced removal efficiency of biochar-amended filters. Further investigation is required to understand this mechanism.

On the other hand, all filters exhibited significant net phosphorus leaching, particularly biochar amendment filters (1.36 and 0.71 mg/L in the effluents of sewage sludge and rice husk biochar filters respectively). More than 70% of phosphorus detected in the effluent was in dissolved form, indicating that the leaching was from the phosphorus content inherent in the biochar itself rather than the influent loading. This was particularly pronounced in sewage sludge biochar, which leached the highest amount of dissolved phosphorus. Despite that, it performed the best at capturing particulate phosphorus compared to sand and rice husk biochar, possibly due to its lower conductivity and high metal content, which promoted particulate phosphorus removal.

In summary, this study demonstrated that biochar amendments offer targeted pollutant removal benefits, however, selection and design must be optimised for overall treatment performance. Biochar, particularly rice husk biochar, is recommended for amendment prioritising dissolved zinc removal, due to its high surface area. However, careful design considerations must be made to minimise leaching of phosphorus, suspended solids and associated lead particles. Such considerations include increased filter depth, media layering, standardised washing procedures and biochar modification with metal oxide to promote phosphorus retention, especially in sewage sludge biochar.

7.1.2 Accumulation of heavy metals in bioretention media

Analysis of heavy metal accumulation within the bioretention media in the column study revealed significant accumulation in the surface layer (0-3 cm), with limited downwards migration. These results confirmed that metal retention predominantly occurred within the top 3-5cm layer, likely due to surface straining and cake filtration mechanisms. Similarly, the field assessment at two bioretention sites in Cardiff urban areas revealed that heavy metals primarily accumulated in the top 0-3 cm layer of the biofilter surface, with the following ranges: Cu: 15-69, Pb: 18-340, Zn: 69-583, and Cr: 13-95 mg/kg.

Biofilter age influenced accumulation levels, with older systems demonstrating higher heavy metal concentrations. Similarly, accumulation levels tended to decrease with depth and distance from the inlet. The pXRF technique provided rapid hotspot identification and insights into the influence of inlet design on the spatial distribution of heavy metals on the biofilter surface. The survey showed that diffused inlets resulted in a more even distribution along the biofilter edges, while centralised inlets created contaminated hotspots near inflow points. A couple of these points approached soil screening levels for Pb and Cr in residential land (Pb: 330; Cr: 100 mg/kg), while those that exceeded the screening levels were confined to a small area near a centralised inlet receiving runoff from a drainage channel, posing potential contamination concerns and requiring further investigation.

This risk can be significantly reduced through routine maintenance such as scraping of the top 5-10 cm layer, especially near centralised inlets and drainage channels, as well as by integrating a diffuse inlet design, which exhibited more even distribution of heavy metals across the biofilter surface.

The pXRF technique enables practitioners to proactively identify ongoing hotspots, while prioritising targeted maintenance intervention to ensure heavy metal concentrations are kept below soil screening levels indefinitely.

7.2 Limitations and recommendations for future studies

Although this study offers valuable insights into the design, monitoring and maintenance in bioretention systems, the following practical limitations must be acknowledged:

1. The large column study employed a limited number of columns, which confined hypothesis testing to the presence of vegetation only. Increasing the number of replicates would yield a statistically robust evaluation of species selection effects.
2. The relatively small sample size for TP data in the vegetation study (8 weeks) and variability in influent concentrations may have obscured vegetation and residence time interaction effects. Longer-term evaluation would provide enhanced assessment of interaction effects on TP removal trends.
3. pXRF provided rapid in-situ measurements; however, its accuracy was influenced by soil matrix effects, such as moisture content which resulted in significant discrepancies between in-situ and laboratory measurements, particularly in Grangetown biofilters with high silt and clay content, a standardised calibration protocols that account for variations in soil composition, and moisture content would improve the reliability of measurements.

Future research should explore the following directions building on this study's findings:

1. Investigating vegetation effects using a more complex mixture of pollutants that represent the full spectrum of urban stormwater, including nitrogen species, hydrocarbons and microplastics to examine dynamic interactions and complex removal mechanisms.
2. Investigating variable residence times (e.g. six and twelve hours) to optimise redox conditions for concurrent metal and nutrient removal. Analysis of plant tissues, tracer tests and mass balance may also provide insights into pollutant uptake, and other removal mechanisms.
3. The performance of biochar-amended filters can vary considerably with differences in feedstock type, pyrolysis temperature, production conditions, and amendment ratio. Future research can explore a broader range of biochar amendment ratios, and

modifications (e.g. metal oxide-modified biochar) for optimised phosphorus removal. The optimised biochar can be used to investigate its interaction effects with vegetation and saturation dynamics in pilot-scale bioretention systems.

4. Future research can draw comparison data from this field study and assess the change over time on the surveyed biofilters. Moreover, examining how influent pollutant loading and changing rainfall patterns affect metal accumulation, speciation and mobility can clarify transport mechanisms and accumulation patterns.

References

Abbott, C.L. and Comino-Mateos, L. 2003. In-situ hydraulic performance of a permeable pavement sustainable urban drainage system. *Water and Environment Journal* 17(3), pp. 187–190. doi: 10.1111/j.1747-6593.2003.tb00460.x.

Agrafioti, E., Bouras, G., Kalderis, D. and Diamadopoulos, E. 2013. Biochar production by sewage sludge pyrolysis. *Journal of Analytical and Applied Pyrolysis* 101, pp. 72–78. doi: 10.1016/j.jaap.2013.02.010.

Ahmad, M. et al. 2023. Scavenging microplastics and heavy metals from water using jujube waste-derived biochar in fixed-bed column trials. *Environmental Pollution* 335, p. 122319. doi: 10.1016/j.envpol.2023.122319.

Al-Ameri, M., Hatt, B., Le Coustumer, S., Fletcher, T., Payne, E. and Deletic, A. 2018. Accumulation of heavy metals in stormwater bioretention media: A field study of temporal and spatial variation. *Journal of Hydrology* 567, pp. 721–731. doi: 10.1016/j.jhydrol.2018.03.027.

Alyaseri, I., Zhou, J., Morgan, S.M. and Bartlett, A. 2017. Initial impacts of rain gardens' application on water quality and quantity in combined sewer: field-scale experiment. *Frontiers of Environmental Science & Engineering* 11(4), p. 19. doi: 10.1007/s11783-017-0988-5.

Ander, E.L., Cave, M.R. and Johnson, C. 2013a. *Normal background concentrations of contaminants in the soils of Wales. Exploratory data analysis and statistical methods*. British Geological Survey. p. 144. Available at: https://nora.nerc.ac.uk/id/eprint/501566/ [Accessed: 7 July 2024].

Ander, E.L., Johnson, C.C., Cave, M.R., Palumbo-Roe, B., Nathanail, C.P. and Lark, R.M. 2013b. Methodology for the determination of normal background concentrations of contaminants in English soil. *Science of The Total Environment* 454–455, pp. 604–618. doi: 10.1016/j.scitotenv.2013.03.005.

Andrew, R.M. and Vesely, É.-T. 2008. Life-cycle energy and CO2 analysis of stormwater treatment devices. *Water Science and Technology* 58(5), pp. 985–993. doi: 10.2166/wst.2008.455.

Aryal, R.K., Murakami, M., Furumai, H., Nakajima, F. and Jinadasa, H.K.P.K. 2006. Prolonged deposition of heavy metals in infiltration facilities and its possible threat to groundwater contamination. *Water Science and Technology* 54(6–7), pp. 205–212. doi: 10.2166/wst.2006.584.

Ashoori, N., Teixido, M., Spahr, S., LeFevre, G.H., Sedlak, D.L. and Luthy, R.G. 2019. Evaluation of pilot-scale biochar-amended woodchip bioreactors to remove nitrate, metals, and trace organic contaminants from urban stormwater runoff. *Water Research* 154, pp. 1–11. doi: 10.1016/j.watres.2019.01.040.

Asleson, B.C., Nestingen, R.S., Gulliver, J.S., Hozalski, R.M. and Nieber, J.L. 2009. Performance assessment of rain gardens 1. *JAWRA Journal of the American Water Resources Association* 45(4), pp. 1019–1031. doi: 10.1111/j.1752-1688.2009.00344.x.

Atchison, D., Potter, K. and Severson, L. 2006. *Design guidelines for stormwater bioretention facilities*. United States: Water Resources Institute.

Badruzzaman, M., Pinzon, J., Oppenheimer, J. and Jacangelo, Joseph.G. 2012. Sources of nutrients impacting surface waters in Florida: A review. *Journal of Environmental Management* 109, pp. 80–92. doi: 10.1016/j.jenvman.2012.04.040.

Bąk, J. and Barjenbruch, M. 2022. Benefits, inconveniences, and facilities of the application of rain gardens in urban spaces from the perspective of climate change: A review. *Water* 14(7), p. 1153. doi: 10.3390/w14071153.

Barrett, M.E., Limouzin, M. and Lawler, D.F. 2013. Effects of media and plant selection on biofiltration performance. *Journal of Environmental Engineering* 139(4), pp. 462–470. doi: 10.1061/(ASCE)EE.1943-7870.0000551.

Beral, H., Dagenais, D., Brisson, J. and Kõiv-Vainik, M. 2023. Plant species contribution to bioretention performance under a temperate climate. *Science of The Total Environment* 858, p. 160122. doi: 10.1016/j.scitotenv.2022.160122.

Berndtsson, J.C. 2010. Green roof performance towards management of runoff water quantity and quality: A review. *Ecological Engineering* 36(4), pp. 351–360. doi: 10.1016/j.ecoleng.2009.12.014.

Bertrand-Krajewski, J.-L. et al. 2008. Priority pollutants in stormwater: the ESPRIT project.

Birch, H., Mikkelsen, P.S., Jensen, J.K. and Lützhøft, H.-C.H. 2011. Micropollutants in stormwater runoff and combined sewer overflow in the Copenhagen area, Denmark. *Water Science and Technology* 64(2), pp. 485–493. doi: 10.2166/wst.2011.687.

Biswal, B.K., Vijayaraghavan, K., Tsen-Tieng, D.L. and Balasubramanian, R. 2022. Biochar-based bioretention systems for removal of chemical and microbial pollutants from stormwater: A critical review. *Journal of Hazardous Materials* 422, p. 126886. doi: 10.1016/j.jhazmat.2021.126886.

Blecken, G.-T., Hunt, W.F., Al-Rubaei, A.M., Viklander, M. and Lord, W.G. 2017. Stormwater control measure (SCM) maintenance considerations to ensure designed functionality. *Urban Water Journal* 14(3), pp. 278–290. doi: 10.1080/1573062X.2015.1111913.

Blecken, G.-T., Zinger, Y., Deleti, A. and Viklander, M. 2010. Effect of retrofitting a saturated zone on the performance of biofiltration for heavy metal removal: preliminary results of a laboratory study. In: *Inovatech* 2010, 27/06/2010-01/07/2010. Graie.

Bock, E., Smith, N., Rogers, M., Coleman, B., Reiter, M., Benham, B. and Easton, Z.M. 2015. Enhanced nitrate and phosphate removal in a denitrifying bioreactor with biochar. *Journal of Environmental Quality* 44(2), pp. 605–613. doi: 10.2134/jeq2014.03.0111.

Boehm, A.B. et al. 2020. Biochar-augmented biofilters to improve pollutant removal from stormwater: can they improve receiving water quality? *Environmental Science: Water Research & Technology* 6(6), pp. 1520–1537. doi: 10.1039/D0EW00027B.

Boogaard, F.C., Venvik, G. and Roest, A.H. 2024. Stormwater quality and long-term efficiency capturing potential toxic elements in sustainable urban drainage systems: Is the soil quality of bio-swales after 10-20 years still acceptable? *Sustainability* 16(7), p. 2618. doi: 10.3390/su16072618.

Bosnina, M. 2021. *Characterising and modelling pollutant dynamics in urban stormwater constructed wetlands*. PhD Thesis, Cardiff University.

Bratieres, K., Fletcher, T.D., Deletic, A. and Zinger, Y. 2008. Nutrient and sediment removal by stormwater biofilters: A large-scale design optimisation study. *Water Research* 42(14), pp. 3930–3940. doi: 10.1016/j.watres.2008.06.009.

Bray, B., Gedge, D. and Grant, G. 2012. *Rain Garden Guide*. UK: Thames Water, Environment Agency, CIRIA.

Brown, J.N. and Peake, B.M. 2006. Sources of heavy metals and polycyclic aromatic hydrocarbons in urban stormwater runoff. *Science of The Total Environment* 359(1–3), pp. 145–155. doi: 10.1016/j.scitotenv.2005.05.016.

Brown, S.E. 2004. *Geochemical baseline data for the urban area of Cardiff*. UK: British Geological Survey. p. 66. Available at: https://nora.nerc.ac.uk/id/eprint/7014/ [Accessed: 5 July 2024].

Bruker. [no date]. *Is my Handheld XRF analyzer working*. Available at: https://www.bruker.com/en/products-and-solutions/elemental-analyzers/handheld-xrf-spectrometers/is-my-handheld-xrf-analyzer-working.html [Accessed: 21 May 2024].

Buates, J., Sun, Y., He, M., Mohanty, S.K., Khan, E. and Tsang, D.C.W. 2024. Performance of wood waste biochar and food waste compost in a pilot-scale sustainable drainage system for stormwater treatment. *Environmental Pollution* 348, p. 123767. doi: 10.1016/j.envpol.2024.123767.

Cairns, S., Robertson, I., Sigmund, G. and Street-Perrott, A. 2020. The removal of lead, copper, zinc and cadmium from aqueous solution by biochar and amended biochars. *Environmental Science and Pollution Research* 27(17), pp. 21702–21715. doi: 10.1007/s11356-020-08706-3.

Cardiff News Room. 2022. *Work to start on Churchill Way to bring back the dock feeder canal*. Available at: https://www.cardiffnewsroom.co.uk/releases/c25/28406.html [Accessed: 15 May 2024].

Cardiff News Room. [no date]. *Greener Grangetown project completion marked by Welsh Environment Minister*. Available at: https://cardiffnewsroom.co.uk/releases/c25/20034.html?utm_source=chatgpt.com [Accessed: 23 July 2020].

Carey, R.O., Hochmuth, G.J., Martinez, C.J., Boyer, T.H., Dukes, M.D., Toor, G.S. and Cisar, J.L. 2013. Evaluating nutrient impacts in urban watersheds: Challenges and research opportunities. *Environmental Pollution* 173, pp. 138–149. doi: 10.1016/j.envpol.2012.10.004.

Chandrasena, G.I., Pham, T., Payne, E.G., Deletic, A. and McCarthy, D.T. 2014. E. coli removal in laboratory scale stormwater biofilters: Influence of vegetation and submerged zone. *Journal of Hydrology* 519, pp. 814–822. doi: 10.1016/j.jhydrol.2014.08.015.

Chen, S.S. et al. 2021. Designing sustainable drainage systems in subtropical cities: Challenges and opportunities. *Journal of Cleaner Production* 280, p. 124418. doi: 10.1016/j.jclepro.2020.124418.

CL:AIRE. 2010. *The EIC/AGS/CL:AIRE Soil Generic Assessment Criteria for Human Health Risk Assessment*. UK: Contaminated Land: Applications in Real Environments. Available at: https://claire.co.uk/projects-and-initiatives/39-generic-assessment-criteria-gac/108-generic-assessment-criteria-gac.

Clar, M., Laramore, E. and Ryan, H. 2012. Rethinking bioretention design concepts. pp. 119–127. doi: 10.1061/41007(331)11.

Cole, R.H., Frederick, R.E., Healy, R.P. and Rolan, R.G. 1984. Preliminary findings of the priority pollutant monitoring project of the nationwide urban runoff program. *Water Pollution Control Federation*. pp. 898–908.

Cole, S. and Jeffries, J. 2009. *Using Soil Guideline Values*. UK: Environment Agency. Available at: https://www.gov.uk/government/publications/contaminated-soil-assessing-risks-on-human-health [Accessed: 28 February 2024].

Dagenais, D., Brisson, J. and Fletcher, T.D. 2018. The role of plants in bioretention systems; does the science underpin current guidance? *Ecological Engineering* 120, pp. 532–545. doi: 10.1016/j.ecoleng.2018.07.007.

Davis, A.P., Hunt, W.F., Traver, R.G. and Clar, M. 2009. Bioretention technology: overview of current practice and future needs. *Journal of Environmental Engineering* 135(3), pp. 109–117. doi: 10.1061/(ASCE)0733-9372(2009)135:3(109).

Davis, A.P., Shokouhian, M., Sharma, H., Minami, C. and Winogradoff, D. 2003. Water quality improvement through bioretention: lead, copper, and zinc removal. *Water Environment Research* 75(1), pp. 73–82. doi: 10.2175/106143003X140854.

Dechesne, M., Barraud, S. and Bardin, J.-P. 2005. Experimental assessment of stormwater infiltration basin evolution. *Journal of Environmental Engineering* 131(7), pp. 1090–1098. doi: 10.1061/(ASCE)0733-9372(2005)131:7(1090).

Defra. 2012. *Environmental Protection Act 1990: Part 2A - Contaminated Land Statutory Guidance*. UK: Department for Environment, Food & Rural Affairs. Available at: https://www.gov.uk/government/publications/contaminated-land-statutory-guidance [Accessed: 28 February 2024].

Delpla, I., Jung, A.-V., Baures, E., Clement, M. and Thomas, O. 2009. Impacts of climate change on surface water quality in relation to drinking water production. *Environment International* 35(8), pp. 1225–1233. doi: 10.1016/j.envint.2009.07.001.

Dietz, M.E. 2007. Low impact development practices: A review of current research and recommendations for future directions. *Water, Air, and Soil Pollution* 186(1–4), pp. 351–363. doi: 10.1007/s11270-007-9484-z.

Dietz, M.E. and Clausen, J.C. 2005. A field evaluation of rain garden flow and pollutant treatment. *Water, Air, and Soil Pollution* 167(1–4), pp. 123–138. doi: 10.1007/s11270-005-8266-8.

Dietz, M.E. and Clausen, J.C. 2006. Saturation to improve pollutant retention in a rain garden. *Environmental Science & Technology* 40(4), pp. 1335–1340. doi: 10.1021/es051644f.

Duncan, H. 1999. *Urban stormwater quality: a statistical overview*. Victoria, Australia: CRC for Catchment Hydrology.

Eckart, K., McPhee, Z. and Bolisetti, T. 2017. Performance and implementation of low impact development: A review. *Science of The Total Environment* 607–608, pp. 413–432. doi: 10.1016/j.scitotenv.2017.06.254.

El Hanandeh, A., Gharaibeh, M. and Albalasmeh, A.A. 2018. Phosphorus removal efficiency from wastewater under different loading conditions using sand biofilters augmented with biochar. *International Journal of Environmental Science and Technology* 15(5), pp. 927–934. doi: 10.1007/s13762-017-1474-0.

Ellis, J.B. and Lundy, L. 2016. Implementing sustainable drainage systems for urban surface water management within the regulatory framework in England and Wales. *Journal of Environmental Management* 183, pp. 630–636. doi: 10.1016/j.jenvman.2016.09.022.

Environment Agency. 2024. *Flood and coastal erosion risk management report: 1 April 2023 to 31 March 2024*. Available at: https://www.gov.uk/government/publications/flood-and-coastal-risk-management-national-report/flood-and-coastal-erosion-risk-management-report-1-april-2023-to-31-march-2024 [Accessed: 13 January 2025].

Environmental Protection Agency [EPA]. [no date]. *The Effects: Human and Animal Health | US EPA*. Available at: https://www.epa.gov/nutrientpollution/effects-human-and-animal-health [Accessed: 17 August 2020].

Eriksson, E. et al. 2007. Selected stormwater priority pollutants: A European perspective. *Science of The Total Environment* 383(1–3), pp. 41–51. doi: 10.1016/j.scitotenv.2007.05.028.

Eriksson, E., Baun, A., Mikkelsen, P.S. and Ledin, A. 2004. Selected stormwater priority pollutants (SSPP): Introduction and database.

European Commission. 2003. *Monitoring under the water framework directive: Guidance document No 7*. Luxembourg: European Communities.

European Commission. 2009. *Guidance on surface water chemical monitoring under the water framework directive: Guidance document No 19*. Luxembourg: European Communities. doi: 10.2779/72701.

European Commission. [no date]. *Water Framework Directive - European Commission*. Available at: https://environment.ec.europa.eu/topics/water/water-framework-directive_en [Accessed: 10 February 2025].

Facility for Advancing Water Biofiltration [FAWB]. 2009. *Stormwater biofiltration systems: adoption guidelines*. Australia: Monash University.

Furén, R. et al. 2023. Concentration, distribution, and fractionation of metals in the filter material of 29 bioretention facilities: A field study. *Environmental Science: Water Research & Technology* 9(12), pp. 3158–3173. doi: 10.1039/D2EW00823H.

Göbel, P., Dierkes, C. and Coldewey, W.G. 2007. Storm water runoff concentration matrix for urban areas. *Journal of Contaminant Hydrology* 91(1–2), pp. 26–42. doi: 10.1016/j.jconhyd.2006.08.008.

Google Earth. 2022. *Greener Grangetwon*. Available at: https://earth.google.com/web/@51.47145988,-3.18285349,10.92949116a,1393.80320145d,35y,-0h,0t,0r/ [Accessed: 24 January 2025].

Green Blue Urban. [no date]. *Urban Tree Planting Projects*. Available at: https://greenblue.com/gb/case-studies/greener-grangetown/ [Accessed: 23 January 2025].

Guo, C., Li, J. and Li, H. 2021. The composition of urban storm-water runoff pollutants in sediment and loess soil in rain garden. *Polish Journal of Environmental Studies* 30(4), pp. 3533–3543. doi: 10.15244/pjoes/127274.

Guo, C., Li, J., Li, H., Zhang, B., Ma, M. and Li, F. 2018. Seven-year running effect evaluation and fate analysis of rain gardens in Xi'an, northwest China. *Water* 10(7), p. 944. doi: 10.3390/w10070944.

Han, Z., Xiong, J., Zhou, J., Wang, Z., Hu, T. and Xu, J. 2024. Microplastics removal from stormwater runoff by bioretention cells: A review. *Journal of Environmental Sciences*, p. S100107422400370X. doi: 10.1016/j.jes.2024.07.007.

Harries, N. et al. 2014. *Development of Category 4 Screening Levels for Assessment of Land Affected by Contamination*. UK: Contaminated Land: Applications in Real Environments. Available at: https://claire.co.uk/projects-and-initiatives/category-4-screening-levels [Accessed: 7 July 2024].

Hasan, M.S., Geza, M., Vasquez, R., Chilkoor, G. and Gadhamshetty, V. 2020. Enhanced heavy metal removal from synthetic stormwater using nanoscale zerovalent iron-modified biochar. *Water, Air, & Soil Pollution* 231(5), p. 220. doi: 10.1007/s11270-020-04588-w.

Hasan, M.S., Vasquez, R. and Geza, M. 2021. Application of biochar in stormwater treatment: experimental and modeling investigation. *Processes* 9(5), p. 860. doi: 10.3390/pr9050860.

Hatt, Deletic, A. and Fletcher, T.D. 2007a. Stormwater reuse: designing biofiltration systems for reliable treatment. *Water Science and Technology* 55(4), pp. 201–209. doi: 10.2166/wst.2007.110.

Hatt, Fletcher, T.D. and Deletic, A. 2007b. The effects of drying and wetting on pollutant removal by stormwater filters. In: *NOVATECH 2007. 6th International Conference on sustainable techniques and strategies for urban water management*. Lyon, France, pp. 1057–1064.

Hatt, B.E., Fletcher, T.D. and Deletic, A. 2008. Hydraulic and pollutant removal performance of fine media stormwater filtration systems. *Environmental Science & Technology* 42(7), pp. 2535–2541. doi: 10.1021/es071264p.

Hatt, B.E., Fletcher, T.D. and Deletic, A. 2009. Hydrologic and pollutant removal performance of stormwater biofiltration systems at the field scale. *Journal of Hydrology* 365(3–4), pp. 310–321. doi: 10.1016/j.jhydrol.2008.12.001.

Hatt, B.E., Steinel, A., Deletic, A. and Fletcher, T.D. 2011. Retention of heavy metals by stormwater filtration systems: breakthrough analysis. *Water Science and Technology* 64(9), pp. 1913–1919. doi: 10.2166/wst.2011.188.

Heal, K.V., Bray, R., Willingale, S.A.J., Briers, M., Napier, F., Jefferies, C. and Fogg, P. 2009. Medium-term performance and maintenance of SUDS: a case-study of Hopwood Park Motorway Service Area, UK. *Water Science and Technology* 59(12), pp. 2485–2494. doi: 10.2166/wst.2009.288.

Hermawan, A.A., Teh, K.L., Talei, A. and Chua, L.H.C. 2021. Accumulation of heavy metals in stormwater biofiltration systems augmented with zeolite and fly ash. *Journal of Environmental Management* 297, p. 113298. doi: 10.1016/j.jenvman.2021.113298.

Holvoet, K.M.A., Seuntjens, P. and Vanrolleghem, P.A. 2007. Monitoring and modeling pesticide fate in surface waters at the catchment scale. *Ecological Modelling* 209(1), pp. 53–64. doi: 10.1016/j.ecolmodel.2007.07.030.

Hossain, M.A., Furumai, H., Nakajima, F. and Kasuga, I. 2008. Accumulated sediments within soakaways in an old infiltration facility: source or sink for heavy metals?

Hsieh, L., He, L., Zhang, M., Lv, W., Yang, K. and Tong, M. 2022. Addition of biochar as thin preamble layer into sand filtration columns could improve the microplastics removal from water. *Water Research* 221, p. 118783. doi: 10.1016/j.watres.2022.118783.

Huber, M., Welker, A. and Helmreich, B. 2016. Critical review of heavy metal pollution of traffic area runoff: Occurrence, influencing factors, and partitioning. *Science of The Total Environment* 541, pp. 895–919. doi: 10.1016/j.scitotenv.2015.09.033.

Hwang, H.-M., Fiala, M.J., Park, D. and Wade, T.L. 2016. Review of pollutants in urban road dust and stormwater runoff: part 1. Heavy metals released from vehicles. *International Journal of Urban Sciences*, 20(3), pp. 334–360. doi: 10.1080/12265934.2016. 1193041.

Iqbal, H., Garcia-Perez, M. and Flury, M. 2015. Effect of biochar on leaching of organic carbon, nitrogen, and phosphorus from compost in bioretention systems. *Science of The Total Environment* 521–522, pp. 37–45. doi: 10.1016/j.scitotenv.2015.03.060.

Jacklin, D.M., Brink, I.C. and Jacobs, S.M. 2021a. Efficiencies of indigenous South African plant biofilters for urban stormwater runoff water quality improvement with a focus on nutrients and metals. *Journal of Water Supply: Research and Technology-Aqua* 70(7), pp. 1094–1110. doi: 10.2166/aqua.2021.187.

Jacklin, D.M., Brink, I.C. and Jacobs, S.M. 2021b. Urban stormwater nutrient and metal removal in small-scale green infrastructure: exploring engineered plant biofilter media

optimisation. *Water Science and Technology* 84(7), pp. 1715–1731. doi: 10.2166/wst.2021.353.

Jacobson, C.R. 2011. Identification and quantification of the hydrological impacts of imperviousness in urban catchments: A review. *Journal of Environmental Management* 92(6), pp. 1438–1448. doi: 10.1016/j.jenvman.2011.01.018.

Jagadeesh, N. and Sundaram, B. 2023. Adsorption of pollutants from wastewater by biochar: A review. *Journal of Hazardous Materials Advances* 9, p. 100226. doi: 10.1016/j.hazadv.2022.100226.

James, J. 2023. *Written Statement: Securing greater nature, environmental and community benefits through Sustainable Drainage Systems (SuDS) - publication of the Welsh Government's review and the way forward.* Available at: https://www.gov.wales/written-statement-securing-greater-nature-environmental-and-community-benefits-through-sustainable [Accessed: 4 June 2024].

Jang, A., Seo, Y. and Bishop, P.L. 2005. The removal of heavy metals in urban runoff by sorption on mulch. *Environmental Pollution* 133(1), pp. 117–127. doi: 10.1016/j.envpol.2004.05.020.

Jenkins, J.K.G., Wadzuk, B.M. and Welker, A.L. 2010. Fines accumulation and distribution in a storm-water rain garden nine years postconstruction. *Journal of Irrigation and Drainage Engineering* 136(12), pp. 862–869. doi: 10.1061/(ASCE)IR.1943-4774.0000264.

JNCC. 2021. *Greener Grangetown | JNCC - Adviser to Government on Nature Conservation*. Available at: https://jncc.gov.uk/our-work/greener-grangetown/ [Accessed: 26 February 2024].

Johansson, G., Fedje, K.K., Modin, O., Haeger-Eugensson, M., Uhl, W., Andersson-Sköld, Y. and Strömvall, A.-M. 2024. Removal and release of microplastics and other environmental pollutants during the start-up of bioretention filters treating stormwater. *Journal of Hazardous Materials* 468, p. 133532. doi: 10.1016/j.jhazmat.2024.133532.

Johnson, J.P. and Hunt, W.F. 2016. Evaluating the spatial distribution of pollutants and associated maintenance requirements in an 11-year-old bioretention cell in urban Charlotte, NC. *Journal of Environmental Management* 184, pp. 363–370. doi: 10.1016/j.jenvman.2016.10.009.

Jones, P.S. and Davis, A.P. 2013. Spatial accumulation and strength of affiliation of heavy metals in bioretention media. *Journal of Environmental Engineering* 139(4), pp. 479–487. doi: 10.1061/(ASCE)EE.1943-7870.0000624.

Kalnicky, D.J. and Singhvi, R. 2001. Field portable XRF analysis of environmental samples. *Journal of Hazardous Materials* 83(1–2), pp. 93–122. doi: 10.1016/S0304-3894(00)00330-7.

Kiiza, C. 2017. *Design and modelling of pollutant removal in stormwater constructed wetlands*. PhD Thesis, Cardiff University.

Kirk, B., Roseen, R.M. and Etnier, C. 2006. The big picture: evaluating stormwater BMPs through the life cycle lens. *Proc. 5th Annu. Storm Conf.* Available at: https://www.researchgate.net/publication/241764350_The_Big_Picture_-

_Evaluating_Stormwater_BMPs_Through_the_Life_Cycle_Lens [Accessed: 9 February 2025].

Komlos, J. and Traver, R.G. 2012. Long-term orthophosphate removal in a field-scale storm-water bioinfiltration rain garden. *Journal of Environmental Engineering* 138(10), pp. 991–998. doi: 10.1061/(ASCE)EE.1943-7870.0000566.

Kuoppamäki, K., Hagner, M., Lehvävirta, S. and Setälä, H. 2016. Biochar amendment in the green roof substrate affects runoff quality and quantity. *Ecological Engineering* 88, pp. 1–9. doi: 10.1016/j.ecoleng.2015.12.010.

Kuoppamäki, K., Pflugmacher Lima, S., Scopetani, C. and Setälä, H. 2021. The ability of selected filter materials in removing nutrients, metals, and microplastics from stormwater in biofilter structures. *Journal of Environmental Quality* 50(2), pp. 465–475. doi: 10.1002/jeq2.20201.

Kurup, P. et al. 2017. A review of technologies for characterization of heavy metal contaminants. *Indian Geotechnical Journal* 47(4), pp. 421–436. doi: 10.1007/s40098-016-0214-6.

Lamprea, K. and Ruban, V. 2011. Characterization of atmospheric deposition and runoff water in a small suburban catchment. *Environmental Technology* 32(10), pp. 1141–1149. doi: 10.1080/09593330.2010.528045.

Lashford, C. et al. 2019. SuDS & Sponge Cities: A comparative analysis of the implementation of pluvial flood management in the UK and China. *Sustainability* 11(1), p. 213. doi: 10.3390/su11010213.

Le Coustumer, S., Fletcher, T.D., Deletic, A., Barraud, S. and Lewis, J.F. 2009. Hydraulic performance of biofilter systems for stormwater management: Influences of design and operation. *Journal of Hydrology* 376(1–2), pp. 16–23. doi: 10.1016/j.jhydrol.2009.07.012.

Le Coustumer, S., Fletcher, T.D., Deletic, A., Barraud, S. and Poelsma, P. 2012. The influence of design parameters on clogging of stormwater biofilters: A large-scale column study. *Water Research* 46(20), pp. 6743–6752. doi: 10.1016/j.watres.2012.01.026.

Lee, G.F. and Jones-Lee, A. 2004. Urban stormwater runoff water quality issues. In: Lehr, J. H. and Keeley, J. eds. *Water Encyclopedia*. 1st ed. Wiley, pp. 432–437. doi: 10.1002/047147844X.sw1602.

Lee, J.H. and Bang, K.W. 2000. Characterization of urban stormwater runoff. *Water research*, 34(6), pp. 1773–1780.

LeFevre, G.H., Paus, K.H., Natarajan, P., Gulliver, J.S., Novak, P.J. and Hozalski, R.M. 2015. Review of dissolved pollutants in urban storm water and their removal and fate in bioretention cells. *Journal of Environmental Engineering* 141(1), p. 04014050. doi: 10.1061/(ASCE)EE.1943-7870.0000876.

Lenormand, É., Kustner, C., Combroux, I., Bois, P. and Wanko, A. 2022. Diagnosing trace metals contamination in ageing stormwater constructed wetlands by portable X-ray Fluorescence Analyzer (pXRF). *Science of The Total Environment* 844, p. 157097. doi: 10.1016/j.scitotenv.2022.157097.

Li, H. and Davis, A.P. 2008a. Heavy metal capture and accumulation in bioretention media. *Environmental Science & Technology* 42(14), pp. 5247–5253. doi: 10.1021/es702681j.

Li, H. and Davis, A.P. 2008b. Urban particle capture in bioretention media. I: Laboratory and field studies. *Journal of Environmental Engineering* 134(6), pp. 409–418. doi: 10.1061/(ASCE)0733-9372(2008)134:6(409).

Li, H. and Davis, A.P. 2008c. Urban particle capture in bioretention media. II: Theory and model development. *Journal of Environmental Engineering* 134(6), pp. 419–432. doi: 10.1061/(ASCE)0733-9372(2008)134:6(419).

Li, Y., Deletic, A. and McCarthy, D.T. 2020. Copper-zeolite integrated stormwater biofilter for nutrient removal – the impact of intermittent wetting and drying conditions. *Blue-Green Systems* 2(1), pp. 352–363. doi: 10.2166/bgs.2020.016.

Lim, H.S., Lim, W., Hu, J.Y., Ziegler, A. and Ong, S.L. 2015. Comparison of filter media materials for heavy metal removal from urban stormwater runoff using biofiltration systems. *Journal of Environmental Management* 147, pp. 24–33. doi: 10.1016/j.jenvman.2014.04.042.

Lim, H.S. and Lu, X.X. 2016. Sustainable urban stormwater management in the tropics: An evaluation of Singapore's ABC Waters Program. *Journal of Hydrology* 538, pp. 842–862. doi: 10.1016/j.jhydrol.2016.04.063.

Limouzin, M., Lawler, D.F. and Barrett, M.E. 2011. *Performance Comparison of Stormwater Biofiltration Designs*. Center for Research in Water Resources, The University of Texas at Austin.

Lisenbee, W.A., Hathaway, J.M., Burns, M.J. and Fletcher, T.D. 2021. Modeling bioretention stormwater systems: Current models and future research needs. *Environmental Modelling & Software* 144, p. 105146. doi: 10.1016/j.envsoft.2021.105146.

Liu, J. and Davis, A.P. 2014. Phosphorus speciation and treatment using enhanced phosphorus removal bioretention. *Environmental Science & Technology* 48(1), pp. 607–614. doi: 10.1021/es404022b.

Logsdon, G.S. 2008. *Water filtration practices: Including slow sand filters and precoat filtration*. American Water Works Association.

Lucas, R. 2015. *Design and experimental assessment of stormwater constructed wetland systems*. PhD Thesis, Cardiff University.

Lucke, T., Drapper, D. and Hornbuckle, A. 2018. Urban stormwater characterisation and nitrogen composition from lot-scale catchments: New management implications. *Science of The Total Environment* 619–620, pp. 65–71. doi: 10.1016/j.scitotenv.2017.11.105.

Luo, X., Yu, S., Zhu, Y. and Li, X. 2012. Trace metal contamination in urban soils of China. *Science of The Total Environment* 421–422, pp. 17–30. doi: 10.1016/j.scitotenv.2011.04.020.

Maniquiz-Redillas, M.C. and Kim, L.-H. 2016. Evaluation of the capability of low-impact development practices for the removal of heavy metal from urban stormwater runoff. *Environmental Technology* 37(18), pp. 2265–2272. doi: 10.1080/09593330.2016.1147610.

McCrum, M.J., Heyvaert, A.C. and Schmidt, C.A. 2017. *Evaluation of pinyon-juniper biochar as a media amendment for stormwater treatment*. Nevada: Nevada Division of State Lands. Available at: https://lands.nv.gov/uploads/documents/3._Evaluation_of_P-J_biochar_final_report_.pdf [Accessed: 20 Feb 2025].

Mehmannavaz, R., Prasher, S.O., Markarian, N. and Ahmad, D. 2001. Biofiltration of residual fertilizer nitrate and atrazine by *rhizobium meliloti* in saturated and unsaturated sterile soil columns. *Environmental Science & Technology* 35(8), pp. 1610–1615. doi: 10.1021/es0015693.

Melia, P.M., Busquets, R., Hooda, P.S., Cundy, A.B. and Sohi, S.P. 2019. Driving forces and barriers in the removal of phosphorus from water using crop residue, wood and sewage sludge derived biochars. *Science of The Total Environment* 675, pp. 623–631. doi: 10.1016/j.scitotenv.2019.04.232.

Melo, L.C.A., Coscione, A.R., Abreu, C.A., Puga, A.P. and Camargo, O.A. 2013. Influence of pyrolysis temperature on cadmium and zinc sorption capacity of sugar cane straw-derived biochar. *BioResources* 8(4), pp. 4992–5004. doi: 10.15376/biores.8.4.4992-5004.

Met Office. [no date][a]. *Cardiff Bute Park*. Available at: https://www.metoffice.gov.uk/pub/data/weather/uk/climate/stationdata/cardiffdata.txt [Accessed: 8 July 2024].

Met Office. [no date][b]. *UK Climate Averages*. Available at: https://www.metoffice.gov.uk/research/climate/maps-and-data/uk-climate-averages/gcjszmp44 [Accessed: 23 January 2022].

Milandri, S., Winter, K., Chimphango, S., Armitage, N., Mbui, D., Jackson, G. and Liebau, V. 2012. The performance of plant species in removing nutrients from stormwater in biofiltration systems in Cape Town. *Water SA* 38(5), pp. 655–662. doi: 10.4314/wsa.v38i5.2.

Miller, J.D. and Hutchins, M. 2017. The impacts of urbanisation and climate change on urban flooding and urban water quality: A review of the evidence concerning the United Kingdom. *Journal of Hydrology: Regional Studies* 12, pp. 345–362. doi: 10.1016/j.ejrh.2017.06.006.

Milovanovic, I., Herrmann, I., Hedström, A., Nordqvist, K., Müller, A. and Viklander, M. 2023. Synthetic stormwater for laboratory testing of filter materials. *Environmental Technology* 44(11), pp. 1600–1612. doi: 10.1080/09593330.2021.2008516.

Mitchell, C.J., Jayakaran, A.D. and McIntyre, J.K. 2023. Biochar and fungi as bioretention amendments for bacteria and PAH removal from stormwater. *Journal of Environmental Management* 327, p. 116915. doi: 10.1016/j.jenvman.2022.116915.

Mitchell, G. 2005. Mapping hazard from urban non-point pollution: A screening model to support sustainable urban drainage planning. *Journal of Environmental Management* 74(1), pp. 1–9. doi: 10.1016/j.jenvman.2004.08.002.

Mohanty, S.K. and Boehm, A.B. 2014. *Escherichia coli* removal in biochar-augmented biofilter: Effect of infiltration rate, initial bacterial concentration, biochar particle size, and presence of compost. *Environmental Science & Technology* 48(19), pp. 11535–11542. doi: 10.1021/es5033162.

Mohanty, S.K. and Boehm, A.B. 2015. Effect of weathering on mobilization of biochar particles and bacterial removal in a stormwater biofilter. *Water Research* 85, pp. 208–215. doi: 10.1016/j.watres.2015.08.026.

Mohanty, S.K., Cantrell, K.B., Nelson, K.L. and Boehm, A.B. 2014. Efficacy of biochar to remove Escherichia coli from stormwater under steady and intermittent flow. *Water Research* 61, pp. 288–296. doi: 10.1016/j.watres.2014.05.026.

Mohanty, S.K., Valenca, R., Berger, A.W., Yu, I.K.M., Xiong, X., Saunders, T.M. and Tsang, D.C.W. 2018. Plenty of room for carbon on the ground: Potential applications of biochar for stormwater treatment. *Science of The Total Environment* 625, pp. 1644–1658. doi: 10.1016/j.scitotenv.2018.01.037.

Muerdter, C.P., Wong, C.K. and LeFevre, G.H. 2018. Emerging investigator series: the role of vegetation in bioretention for stormwater treatment in the built environment: pollutant removal, hydrologic function, and ancillary benefits. *Environmental Science: Water Research & Technology* 4(5), pp. 592–612. doi: 10.1039/C7EW00511C.

Muhammad, L.N. 2023. Guidelines for repeated measures statistical analysis approaches with basic science research considerations. *Journal of Clinical Investigation* 133(11), p. e171058. doi: 10.1172/JCI171058.

Mukome, F.N.D., Zhang, X., Silva, L.C.R., Six, J. and Parikh, S.J. 2013. Use of chemical and physical characteristics to investigate trends in biochar feedstocks. *Journal of Agricultural and Food Chemistry* 61(9), pp. 2196–2204. doi: 10.1021/jf3049142.

Mulhall, E. and Revitt, M. 2003. *Protection of the water environment using balancing facilities*. Environment Agency.

Müller, A., Österlund, H., Marsalek, J. and Viklander, M. 2020. The pollution conveyed by urban runoff: A review of sources. *Science of The Total Environment* 709, p. 136125. doi: 10.1016/j.scitotenv.2019.136125.

Nabiul Afrooz, A.R.M. and Boehm, A.B. 2017. Effects of submerged zone, media aging, and antecedent dry period on the performance of biochar-amended biofilters in removing fecal indicators and nutrients from natural stormwater. *Ecological Engineering* 102, pp. 320–330. doi: 10.1016/j.ecoleng.2017.02.053.

National Environment Protection Council [NEPC]. 2013. *Schedule B (1) - Guideline on investigation levels for soil and groundwater*. Australia: National Environment Protection Council. Available at: https://www.nepc.gov.au/sites/default/files/2022-09/schedule-b1-guideline-investigation-levels-soil-and-groundwater-sep10.pdf [Accessed: 7 July 2024].

Nyenje, P.M., Foppen, J.W., Uhlenbrook, S., Kulabako, R. and Muwanga, A. 2010. Eutrophication and nutrient release in urban areas of sub-Saharan Africa: A review. *Science of The Total Environment* 408(3), pp. 447–455. doi: 10.1016/j.scitotenv.2009.10.020.

Odobašić, A., Šestan, I. and Begić, S. 2019. Biosensors for determination of heavy metals in waters. In: Rinken, T. and Kivirand, K. eds. *Biosensors for Environmental Monitoring*. IntechOpen. Available at: https://www.intechopen.com/books/biosensors-for-environmental-monitoring/biosensors-for-determination-of-heavy-metals-in-waters [Accessed: 29 January 2025].

Payne, E. et al. 2014a. Temporary storage or permanent removal? The division of nitrogen between biotic assimilation and denitrification in stormwater biofiltration systems. Virolle, M.-J. ed. *PLoS ONE* 9(3), p. e90890. doi: 10.1371/journal.pone.0090890.

Payne, E., Pham, T., Cook, P.L.M., Fletcher, T.D., Hatt, B.E. and Deletic, A. 2014b. Biofilter design for effective nitrogen removal from stormwater: influence of plant species, inflow hydrology and use of a saturated zone. *Water Science and Technology* 69(6), pp. 1312–1319. doi: 10.2166/wst.2014.013.

Payne, E., Hatt, B., Deletic, A., Dobbie, M., McCarthy, D. and Chandrasena, G. 2015. *Adoption guidelines for stormwater biofiltration systems: Summary report*. Australia: Cooperative Research Centre for Water Sensitive Cities.

Payne, E.G.I., Pham, T., Deletic, A., Hatt, B.E., Cook, P.L.M. and Fletcher, T.D. 2018. Which species? A decision-support tool to guide plant selection in stormwater biofilters. *Advances in Water Resources* 113, pp. 86–99. doi: 10.1016/j.advwatres.2017.12.022.

Pellerin, B.A. et al. 2016. Emerging tools for continuous nutrient monitoring networks: Sensors advancing science and water resources protection. *JAWRA Journal of the American Water Resources Association* 52(4), pp. 993–1008. doi: 10.1111/1752-1688.12386.

Peng, J., Cao, Y., Rippy, M., Afrooz, A. and Grant, S. 2016. Indicator and Pathogen Removal by Low Impact Development Best Management Practices. *Water* 8(12), p. 600. doi: 10.3390/w8120600.

Petrucci, G., Gromaire, M.-C., Shorshani, M.F. and Chebbo, G. 2014. Nonpoint source pollution of urban stormwater runoff: a methodology for source analysis. *Environmental Science and Pollution Research* 21(17), pp. 10225–10242. doi: 10.1007/s11356-014-2845-4.

Pitt, R., Clark, S. and Field, R. 1999. Groundwater contamination potential from stormwater infiltration practices. *Urban Water* 1(3), pp. 217–236. doi: 10.1016/S1462-0758(99)00014-x.

Premarathna, K.S.D. et al. 2023. Biofilters and bioretention systems: the role of biochar in the blue-green city concept for stormwater management. *Environmental Science: Water Research & Technology* 9(12), pp. 3103–3119. doi: 10.1039/D3EW00054K.

Pritchard, J. et al. 2018. Benzotriazole uptake and removal in vegetated biofilter mesocosms planted with Carex praegracilis. *Water* 10(11), p. 1605. doi: 10.3390/w10111605.

Radu, T. and Diamond, D. 2009. Comparison of soil pollution concentrations determined using AAS and portable XRF techniques. *Journal of Hazardous Materials* 171(1–3), pp. 1168–1171. doi: 10.1016/j.jhazmat.2009.06.062.

Rahman, M.Y.A., Nachabe, M.H. and Ergas, S.J. 2020. Biochar amendment of stormwater bioretention systems for nitrogen and Escherichia coli removal: Effect of hydraulic loading rates and antecedent dry periods. *Bioresource Technology* 310, p. 123428. doi: 10.1016/j.biortech.2020.123428.

Read, J., Fletcher, T.D., Wevill, T. and Deletic, A. 2009. Plant traits that enhance pollutant removal from stormwater in biofiltration systems. *International Journal of Phytoremediation* 12(1), pp. 34–53. doi: 10.1080/15226510902767114.

Read, J., Wevill, T., Fletcher, T. and Deletic, A. 2008. Variation among plant species in pollutant removal from stormwater in biofiltration systems. *Water Research* 42(4–5), pp. 893–902. doi: 10.1016/j.watres.2007.08.036.

Reddy, K.R., Xie, T. and Dastgheibi, S. 2014a. Evaluation of biochar as a potential filter media for the removal of mixed contaminants from urban storm water runoff. *Journal of Environmental Engineering* 140(12), p. 04014043. doi: 10.1061/(ASCE)EE.1943-7870.0000872.

Reddy, K.R., Xie, T. and Dastgheibi, S. 2014b. Nutrients removal from urban stormwater by different filter materials. *Water, Air, & Soil Pollution* 225(1), p. 1778. doi: 10.1007/s11270-013-1778-8.

Sample, D.J., Grizzard, T.J., Sansalone, J., Davis, A.P., Roseen, R.M. and Walker, J. 2012. Assessing performance of manufactured treatment devices for the removal of phosphorus from urban stormwater. *Journal of Environmental Management* 113, pp. 279–291. doi: 10.1016/j.jenvman.2012.08.039.

Seltman, H.J. 2012. Mixed Models. A flexible approach to correlated data. In: *Experimental design and analysis*. Available at: https://imaging.mrc-cbu.cam.ac.uk/statswiki/FAQ/multilevel?action=AttachFile&do=view&target=SPSSmixed.pdf [Accessed: 14 November 2024].

Shao, Z. et al. 2018. Analysis of the sediment remobilization phenomenon in a rain garden using CSTR theory. *Journal of Water and Climate Change* 9(2), pp. 356–366. doi: 10.2166/wcc.2018.056.

Sharma, A., Weindorf, D.C., Wang, D. and Chakraborty, S. 2015. Characterizing soils via portable X-ray fluorescence spectrometer: 4. Cation exchange capacity (CEC). *Geoderma* 239–240, pp. 130–134. doi: 10.1016/j.geoderma.2014.10.001.

Shuster, W., Darner, R., Schifman, L. and Herrmann, D. 2017. Factors contributing to the hydrologic effectiveness of a rain garden network (Cincinnati OH USA). *Infrastructures* 2(3), p. 11. doi: 10.3390/infrastructures2030011.

Shutes, B., Ellis, J.B., Revitt, D.M. and Scholes, L.N.L. 2005. Constructed wetlands in UK urban surface drainage systems. *Water Science and Technology* 51(9), pp. 31–37. doi: 10.2166/wst.2005.0281.

Sileshi, R., Pitt, R. and Clark, S. 2010. Enhanced biofilter treatment of urban stormwater by optimizing the hydraulic residence time in the media. In: *Watershed Management 2010: Innovations in Watershed Management under Land Use and Climate Change,* pp. 587–597.

Siwiec, E., Erlandsen, A.M. and Vennemo, H. 2018. City greening by rain gardens: Costs and benefits. *Ochrona Srodowiska i Zasobów Naturalnych* 29(1), pp. 1–5. doi: 10.2478/oszn-2018-0001.

Søberg, L.C., Al-Rubaei, A.M., Viklander, M. and Blecken, G.-T. 2020. Phosphorus and TSS removal by stormwater bioretention: Effects of temperature, salt, and a submerged zone and their interactions. *Water, Air, & Soil Pollution* 231(6), p. 270. doi: 10.1007/s11270-020-04646-3.

Spahr, S., Teixidó, M., Gall, S.S., Pritchard, J.C., Hagemann, N., Helmreich, B. and Luthy, R.G. 2022. Performance of biochars for the elimination of trace organic contaminants and metals from urban stormwater. *Environmental Science: Water Research & Technology* 8(6), pp. 1287–1299. doi: 10.1039/D1EW00857A.

Statistical Package for the Social Sciences [SPSS]. 2005. *Linear Mixed-Effects Modeling in SPSS: An Introduction to the MIXED Procedure*. Technical Report, pp. 1–29. Available at: https://imaging.mrc-cbu.cam.ac.uk/statswiki/FAQ/multilevel?action=AttachFile&do=get&target=spssegs.pdf [Accessed: 11 September 2024].

Stuart, M.E., Gooddy, D.C., Bloomfield, J.P. and Williams, A.T. 2011. A review of the impact of climate change on future nitrate concentrations in groundwater of the UK. *Science of The Total Environment* 409(15), pp. 2859–2873. doi: 10.1016/j.scitotenv.2011.04.016.

Sun, X. and Davis, A.P. 2007. Heavy metal fates in laboratory bioretention systems. *Chemosphere* 66(9), pp. 1601–1609. doi: 10.1016/j.chemosphere.2006.08.013.

Sun, Y. et al. 2020. Waste-derived compost and biochar amendments for stormwater treatment in bioretention column: Co-transport of metals and colloids. *Journal of Hazardous Materials* 383, p. 121243. doi: 10.1016/j.jhazmat.2019.121243.

Tedoldi, D., Chebbo, G., Pierlot, D., Kovacs, Y. and Gromaire, M.-C. 2016. Impact of runoff infiltration on contaminant accumulation and transport in the soil/filter media of Sustainable Urban Drainage Systems: A literature review. *Science of The Total Environment* 569–570, pp. 904–926. doi: 10.1016/j.scitotenv.2016.04.215.

Tian, J. et al. 2014. Biochar-amended media for enhanced nutrient removal in stormwater facilities. In: *World Environmental and Water Resources Congress 2014*. Portland, Oregon: American Society of Civil Engineers, pp. 197–208. doi: 10.1061/9780784413548.022.

Tian, J., Miller, V., Chiu, P.C., Maresca, J.A., Guo, M. and Imhoff, P.T. 2016. Nutrient release and ammonium sorption by poultry litter and wood biochars in stormwater treatment. *Science of The Total Environment* 553, pp. 596–606. doi: 10.1016/j.scitotenv.2016.02.129.

Tirpak, R.A., Afrooz, A.N., Winston, R.J., Valenca, R., Schiff, K. and Mohanty, S.K. 2021. Conventional and amended bioretention soil media for targeted pollutant treatment: A critical review to guide the state of the practice. *Water Research* 189, p. 116648. doi: 10.1016/j.watres.2020.116648.

Tong, M., He, L., Rong, H., Li, M. and Kim, H. 2020a. Transport behaviors of plastic particles in saturated quartz sand without and with biochar/Fe3O4-biochar amendment. *Water Research* 169, p. 115284. doi: 10.1016/j.watres.2019.115284.

Tong, M., Li, T., Li, M., He, L. and Ma, Z. 2020b. Cotransport and deposition of biochar with different sized-plastic particles in saturated porous media. *Science of The Total Environment* 713, p. 136387. doi: 10.1016/j.scitotenv.2019.136387.

Tsihrintzis, V.A. and Hamid, R. 1997. Modeling and management of urban stormwater runoff quality: A review. *Water resources management*, 11(2), pp. 136–164. doi:10.1023/A:1007903817943

Tufenkji, N. and Elimelech, M. 2004. Correlation equation for predicting single-collector efficiency in physicochemical filtration in saturated porous media. *Environmental Science & Technology* 38(2), pp. 529–536. doi: 10.1021/es034049r.

Uchimiya, M., Chang, S. and Klasson, K.T. 2011. Screening biochars for heavy metal retention in soil: Role of oxygen functional groups. *Journal of Hazardous Materials* 190(1–3), pp. 432–441. doi: 10.1016/j.jhazmat.2011.03.063.

UK Biochar Research Centre [UKBRC]. [no date]. *Standard Biochars*. Available at: https://www.biochar.ac.uk/standard_materials.php [Accessed: 3 December 2022].

Ulrich, B.A., Loehnert, M. and Higgins, C.P. 2017a. Improved contaminant removal in vegetated stormwater biofilters amended with biochar. *Environmental Science: Water Research & Technology* 3(4), pp. 726–734. doi: 10.1039/C7EW00070G.

Ulrich, B.A., Vignola, M., Edgehouse, K., Werner, D. and Higgins, C.P. 2017b. Organic carbon amendments for enhanced biological attenuation of trace organic contaminants in biochar-amended stormwater biofilters. *Environmental Science & Technology* 51(16), pp. 9184–9193. doi: 10.1021/acs.est.7b01164.

Venvik, G. and Boogaard, F.C. 2020. Portable XRF quick-scan mapping for potential toxic elements pollutants in sustainable urban drainage systems: A methodological approach. Sci, 2(3), p. 64. doi: 10.3390/sci2030064

Verhoeven, J., Arheimer, B., Yin, C. and Hefting, M. 2006. Regional and global concerns over wetlands and water quality. *Trends in Ecology & Evolution* 21(2), pp. 96–103. doi: 10.1016/j.tree.2005.11.015.

Vijayaraghavan, K. 2016. Green roofs: A critical review on the role of components, benefits, limitations and trends. *Renewable and Sustainable Energy Reviews* 57, pp. 740–752. doi: 10.1016/j.rser.2015.12.119.

Vijayaraghavan, K. et al. 2021. Bioretention systems for stormwater management: Recent advances and future prospects. *Journal of Environmental Management* 292, p. 112766. doi: 10.1016/j.jenvman.2021.112766.

Virahsawmy, H.K., Stewardson, M.J., Vietz, G. and Fletcher, T.D. 2014. Factors that affect the hydraulic performance of raingardens: Implications for design and maintenance. *Water Science and Technology* 69(5), pp. 982–988. doi: 10.2166/wst.2013.809.

Wang, C., O'Connor, D., Wang, L., Wu, W.-M., Luo, J. and Hou, D. 2022. Microplastics in urban runoff: Global occurrence and fate. *Water Research* 225, p. 119129. doi: 10.1016/j.watres.2022.119129.

Wang, J., Zhao, Y., Yang, L., Tu, N., Xi, G. and Fang, X. 2017. Removal of heavy metals from urban stormwater runoff using bioretention media mix. *Water* 9(11), p. 854. doi: 10.3390/w9110854.

Wang, Z., Sedighi, M. and Lea-Langton, A. 2020. Filtration of microplastic spheres by biochar: removal efficiency and immobilisation mechanisms. *Water Research* 184, p. 116165. doi: 10.1016/j.watres.2020.116165.

Welsh Government. 2019. *Sustainable Drainage (SuDS) Statutory Guidance*. Welsh Government. Available at: http://gov.wales/sites/default/files/publications/2019-06/statutory-guidance.pdf [Accessed: 12 May 2024].

Woods-Ballard, B., Wilson, S., Udale-Clarke, H. and Illman, S. 2015. *The SUDS Manual*. London: CIRIA.

Wright, S.L., Ulke, J., Font, A., Chan, K.L.A. and Kelly, F.J. 2020. Atmospheric microplastic deposition in an urban environment and an evaluation of transport. *Environment International* 136, p. 105411. doi: 10.1016/j.envint.2019.105411.

Wu, J., Cao, X., Zhao, J., Dai, Y., Cui, N., Li, Z. and Cheng, S. 2017. Performance of biofilter with a saturated zone for urban stormwater runoff pollution control: Influence of vegetation type and saturation time. *Ecological Engineering* 105, pp. 355–361. doi: 10.1016/j.ecoleng.2017.05.016.

Xiong, J., Li, G., Zhu, J., Li, J., Yang, Y., An, S. and Liu, C. 2022. Removal characteristics of heavy metal ions in rainwater runoff by bioretention cell modified with biochar. *Environmental Technology* 43(28), pp. 4515–4527. doi: 10.1080/09593330.2021.1954697.

Xiong, J., Ren, S., He, Y., Wang, X.C., Bai, X., Wang, J. and Dzakpasu, M. 2019. Bioretention cell incorporating Fe-biochar and saturated zones for enhanced stormwater runoff treatment. *Chemosphere* 237, p. 124424. doi: 10.1016/j.chemosphere.2019.124424.

Xu, C., Jia, M., Xu, M., Long, Y. and Jia, H. 2019. Progress on environmental and economic evaluation of low-impact development type of best management practices through a life cycle perspective. *Journal of Cleaner Production* 213, pp. 1103–1114. doi: 10.1016/j.jclepro.2018.12.272.

Yadav, B.K., Siebel, M.A. and Van Bruggen, J.J.A. 2011. Rhizofiltration of a heavy metal (lead) containing wastewater using the wetland plant *Carex pendula*. *CLEAN – Soil, Air, Water* 39(5), pp. 467–474. doi: 10.1002/clen.201000385.

Yang, F., Fu, D., Zevenbergen, C. and Rene, E.R. 2022. A comprehensive review on the long-term performance of stormwater biofiltration systems (SBS): Operational challenges and future directions. *Journal of Environmental Management* 302, p. 113956. doi: 10.1016/j.jenvman.2021.113956.

Yang, Y.-Y. and Toor, G.S. 2017. Sources and mechanisms of nitrate and orthophosphate transport in urban stormwater runoff from residential catchments. *Water Research* 112, pp. 176–184. doi: 10.1016/j.watres.2017.01.039.

Yao, Y., Gao, B., Zhang, M., Inyang, M. and Zimmerman, A.R. 2012. Effect of biochar amendment on sorption and leaching of nitrate, ammonium, and phosphate in a sandy soil. *Chemosphere* 89(11), pp. 1467–1471. doi: 10.1016/j.chemosphere.2012.06.002.

Yergeau, S.E. and Obropta, C.C. 2013. Preliminary field evaluation of soil compaction in rain gardens. *Journal of Environmental Engineering* 139(9), pp. 1233–1236. doi: 10.1061/(ASCE)EE.1943-7870.0000732.

Yin, D. et al. 2021. Sponge city practice in China: A review of construction, assessment, operational and maintenance. *Journal of Cleaner Production* 280, p. 124963. doi: 10.1016/j.jclepro.2020.124963.

Zhang, J., Zhou, F., Chen, C., Sun, X., Shi, Y., Zhao, H. and Chen, F. 2018. Spatial distribution and correlation characteristics of heavy metals in the seawater, suspended particulate matter and sediments in Zhanjiang Bay, China. Hong, Y. ed. *PLOS ONE* 13(8), p. e0201414. doi: 10.1371/journal.pone.0201414.

Zhang, Z., Rengel, Z., Liaghati, T., Antoniette, T. and Meney, K. 2011. Influence of plant species and submerged zone with carbon addition on nutrient removal in stormwater biofilter. *Ecological Engineering* 37(11), pp. 1833–1841. doi: 10.1016/j.ecoleng.2011.06.016.

Zhao, C. et al. 2021. Formation and mechanisms of nano-metal oxide-biochar composites for pollutants removal: A review. *Science of The Total Environment* 767, p. 145305. doi: 10.1016/j.scitotenv.2021.145305.

Zhou, Q. 2014. A review of sustainable urban drainage systems considering the climate change and urbanization impacts. *Water* 6(4), pp. 976–992. doi: 10.3390/w6040976.

Zhu, Y., Ye, P., Xu, S., Zhou, Y., Zhang, Y., Zhang, Y. and Zhang, T. 2020. The influence mechanism of bioclogging on pollution removal efficiency of vertical flow constructed wetland. *Water Science and Technology* 81(9), pp. 1870–1881. doi: 10.2166/wst.2020.246.

Zinger, Y., Prodanovic, V., Zhang, K., Fletcher, T.D. and Deletic, A. 2021. The effect of intermittent drying and wetting stormwater cycles on the nutrient removal performances of two vegetated biofiltration designs. *Chemosphere* 267, p. 129294. doi: 10.1016/j.chemosphere.2020.129294.

Appendices

Appendix A – Media characterisation tests.

Appendix B – Pollutant removal datasets.

Appendix C – Surveyed biofilters.

Appendix A – Media characterisation tests

Table A.1 Particle size distribution analysis for primary filter media used in bioretention columns (loamy sand).

Test Method	**BS1377-2:1990:9.2/9.3/9.4/9.5**				
Soil Description	Loamy sand				
Initial dry mass m_I	237 g		Mass passing during wet sieving $\frac{m_I}{m_4}$	10.77 g	
Riffled and washed m_4	226.23 g		Mass retained in pan	1.52 g	
BS test sieve	Mass retained (g)		Percentage retained $\left(\frac{m}{m_I}\right) X100$	Cumulative retained %	percentage passing %
	Actual	Corrected m			
2 mm	15.89	15.91	6.71	6.71	93.29
1.18 mm	10.08	10.10	4.26	10.97	89.03
600 µm	23.45	23.49	9.91	20.89	79.11
425 µm	20.23	20.48	8.64	29.53	70.47
300 µm	37.56	37.62	15.87	45.40	54.60
212 µm	36.94	37.00	15.61	61.01	38.99
150 µm	44.19	44.26	18.68	79.69	20.31
63 µm	36.01	36.06	15.22	94.90	5.10
Total mass passing 63 µm	12.29	12.31	5.19	100.00	00.00

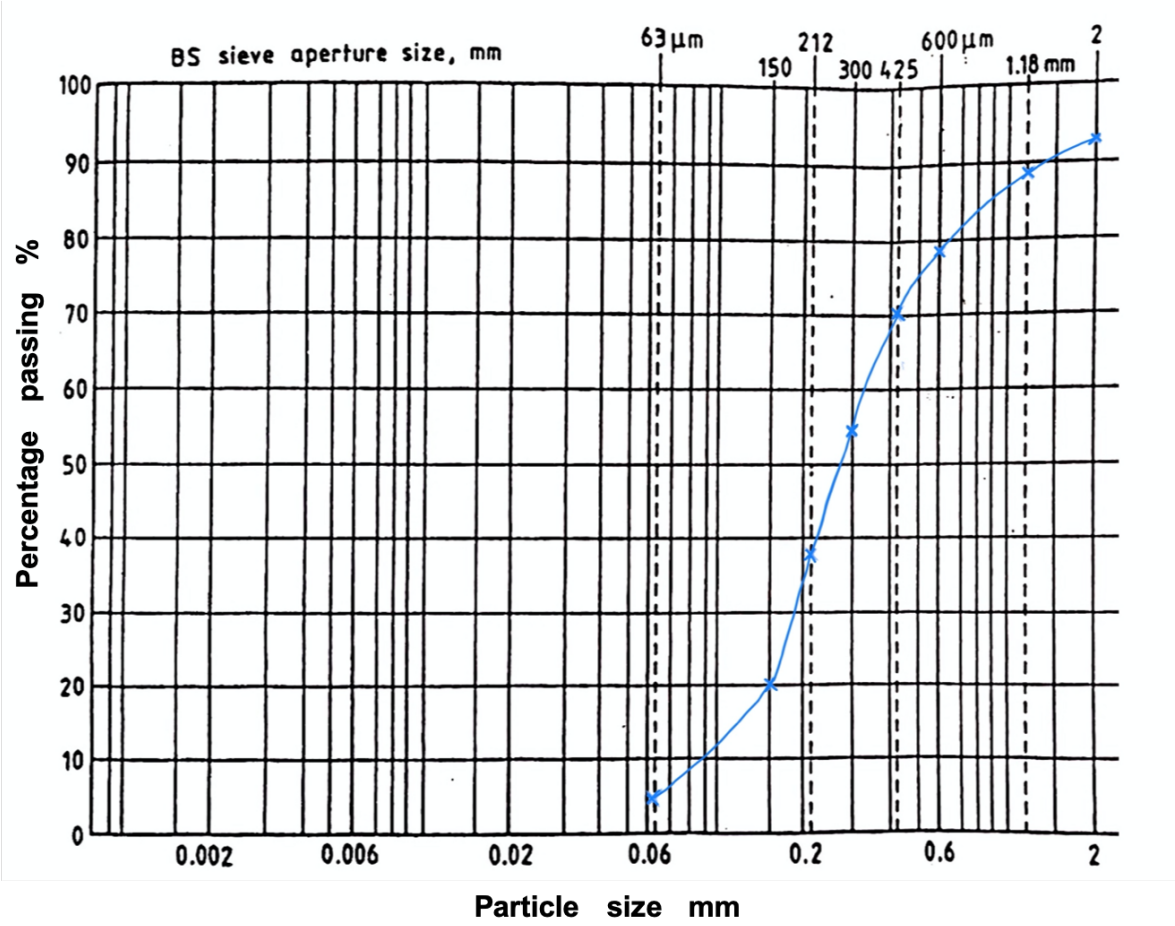

Figure A.1 Particle size distribution graph for primary filter media used in bioretention columns (loamy sand).

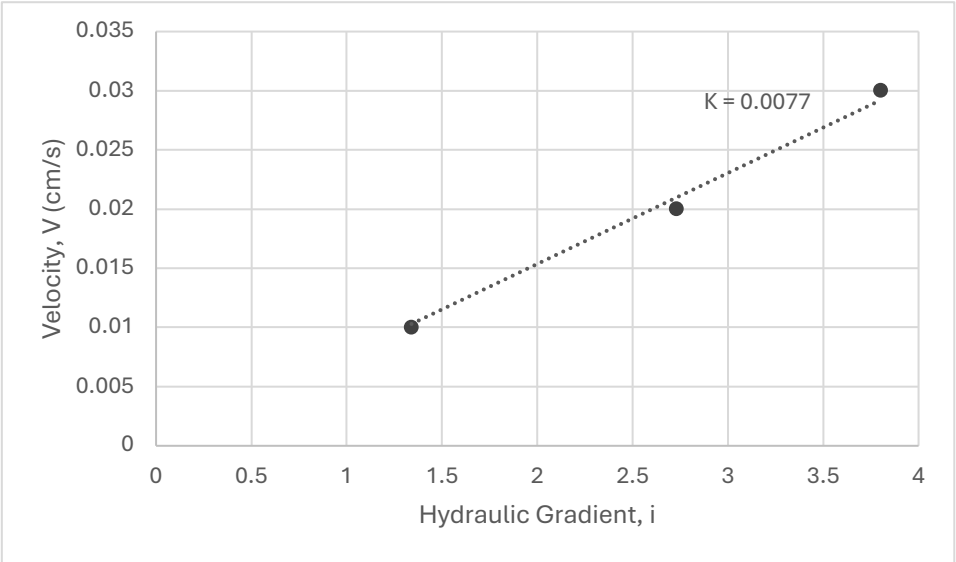

Figure A.2 Coefficient of permeability, K = V/*i* (cm/s). of primary filter media (loamy sand) used in bioretention columns.

Table A.2 Kaolin clay particle size distribution using laser diffraction analysis.

Parameter	Particle Size (µm)
D10	3
D50	9
D90	20
Mean	10

Table A.3 Elemental composition of filter media used in bioretention columns using XRF spectrometry. ND = not detected.

Element	Concentrations (PPM)		
	Loamy sand	**Sewage sludge biochar**	**Rice husk biochar**
Ca	14000	22800	986
Fe	11251	90400	843
K	9683	6347	6330
S	1988	8771	2007
Ti	1396	3692	67
Mn	297	1027	574
Zr	161	139	3
Sr	62	302	34.8
Zn	58	1077	66
Pb	38	227	ND
Cu	24	316	5.4
As	16	ND	9
Cr	12	330	ND
P	ND	12100	ND

Table A.4 Coefficient of permeability of filter media used in biochar column studies. SL: 100% Sandy Loam (control), SL+SSB: 90% Sandy Loam + 10% Sewage Sludge Biochar, and SL+RHB: 90% Sandy Loam + 10% Rice Husk Biochar (w/w). Tests were carried out in accordance with BS1377: Part5: 1990.

Media	**Coefficient of Permeability, K (cm/s)**	**Particle size range (mm)**
SL	2.1×10^{-3}	0.6-0.2
SL+SSB	1.1×10^{-3}	0.6-0.2
SL+RHB	6.5×10^{-3}	0.6-0.2

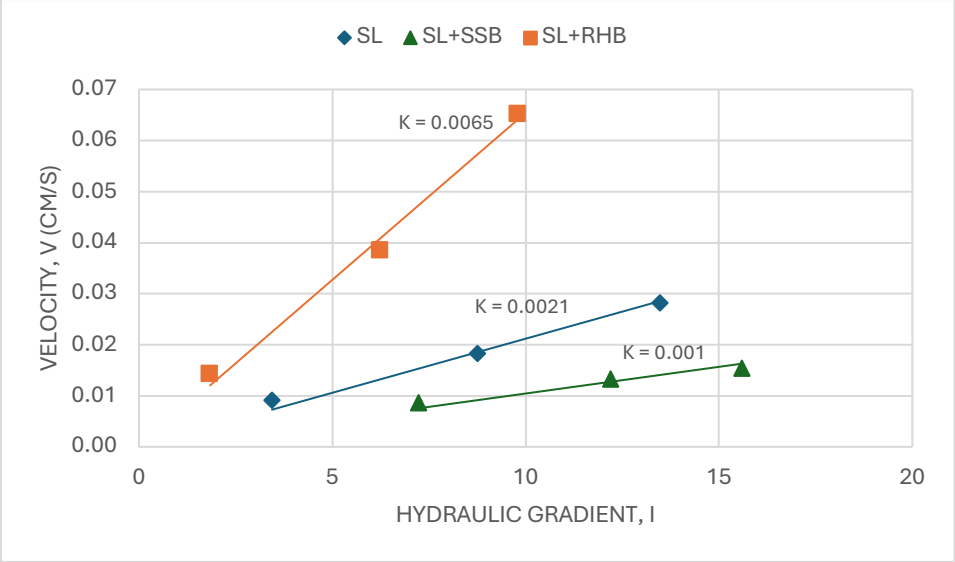

Figure A.3 Coefficient of permeability, K = V/*i* (cm/s). SL: 100% Sandy Loam (control), SL+SSB: 90% Sandy Loam + 10% Sewage Sludge Biochar, and SL+RHB: 90% Sandy Loam + 10% Rice Husk Biochar (w/w).

Appendix B – Pollutant removal datasets

Table A.5 Measured concentrations and removal of TSS in large column experiments.

Total Suspended Solids										
	Weeks	influent (mg/L)	effluent (mg/L)				Removal (%)			
			Control	Phalaris	Carex	Juncus	Control	Phalaris	Carex	Juncus
Method development	1	220	8	7	11	16	96	97	95	93
	2	224	9	12	9	14	96	95	96	94
	3	168	13	11	10	12	92	93	94	93
	4	142	7	4	10	9	95	97	93	94
	5	150	8	7	7	0	95	95	95	100
	6	151	9	6	8	8	94	96	95	95
	7	129	11	6	7	10	92	95	95	92
	8	141	27	31	18	12	81	78	87	91
	9	141	13	12	13	14	91	91	91	90
	10	159	9	5	7	15	94	97	96	91
	11	156	10	4	6	12	93	97	96	92
Closed-valve	1	151	30	12	15	25	80	92	90	84
	2	157	21	12	11	19	87	92	93	88
	3	145	18	4	10	17	87	98	93	89
	4	147	21	14	10	30	86	91	93	80
	5	158	15	8	9	6	90	95	94	97
	6	196	37	27	11	42	81	86	94	79
	9	225	25	7	8	12	89	97	96	95
	10	156	39	19	9	28	75	88	94	82
	11	212	31	39	16	63	85	82	92	70
	13	164	26	22	7	24	84	87	96	86
	15	160	28	20	16	20	83	88	90	88
	16	265	8	8	8	13	97	97	97	95
	17	158	12	8	11	14	92	95	93	91
	18	161	11	12	19	27	93	93	88	83
	19	152	19	16	30	16	88	89	80	89
	20	139	14	9	14	43	90	94	90	69
	21	149	15	18	25	30	90	88	83	80
Free-draining	1	145	22	21	21	38	85	86	86	74
	2	171	19	19	12	25	89	89	93	85
	3	153	18	24	17	31	88	84	89	80
	4	156	14	18	19	24	91	88	88	85
	5	121	14	28	15	30	88	77	88	75
	6	129	25	50	18	28	81	61	86	78
	7	157	10	18	10	13	94	89	94	92
	8	139	12	13	17	23	91	91	88	83

Table A.6 Measured concentrations and removal of Zn in large column experiments. Concentrations below the detection limit were taken as half the limit (0.001 mg/L).

Zn										
	Weeks	influent (mg/L)	effluent (mg/L)				Removal (%)			
			Control	Phalaris	Carex	Juncus	Control	Phalaris	Carex	Juncus
Method development	1	42.520	0.106	0.110	0.046	0.051	99.75	99.74	99.89	99.88
	2	47.621	0.093	0.028	0.054	0.065	99.80	99.94	99.89	99.86
	3	45.523	0.073	0.099	0.081	0.012	99.84	99.78	99.82	99.97
	4	21.602	0.090	0.082	0.053	0.057	99.58	99.62	99.75	99.74
	5	23.047	0.082	0.050	0.042	0.055	99.64	99.78	99.82	99.76
	6	12.727	0.101	0.039	0.028	0.035	99.21	99.70	99.78	99.73
	7	12.151	0.060	0.037	0.017	0.028	99.51	99.70	99.86	99.77
	8	9.705	0.052	0.088	0.059	0.024	99.46	99.10	99.39	99.75
	9	9.794	0.076	0.058	0.009	0.020	99.23	99.41	99.91	99.80
	10	12.072	0.103	0.047	0.001	0.014	99.15	99.61	99.99	99.89
	11	12.476	0.096	0.023	0.003	0.024	99.23	99.81	99.98	99.81
Closed-valve	1	2.418	0.114	0.027	0.020	0.046	95.29	98.87	99.17	98.11
	2	2.178	0.180	0.177	0.014	0.036	91.73	91.89	99.35	98.33
	3	2.275	0.131	0.017	0.009	0.020	94.26	99.25	99.62	99.13
	4	2.468	0.210	0.126	0.025	0.025	91.50	94.88	99.00	98.97
	5	2.896	0.118	0.019	0.015	0.026	95.92	99.33	99.48	99.11
	6	2.765	0.189	0.061	0.074	0.067	93.18	97.80	97.34	97.57
	9	2.935	0.214	0.077	0.061	0.079	92.70	97.38	97.92	97.30
	10	2.881	0.214	0.021	0.034	0.068	92.58	99.27	98.81	97.65
	11	2.300	0.210	0.081	0.026	0.042	90.85	96.49	98.86	98.18
	12	2.525	0.163	0.146	0.030	0.027	93.56	94.23	98.82	98.92
	13	2.278	0.250	0.090	0.104	0.072	89.03	96.05	95.43	96.82
	14	2.487	0.206	0.077	0.085	0.084	91.71	96.92	96.60	96.63
	16	2.576	0.160	0.023	0.026	0.025	93.80	99.11	98.97	99.04
	17	2.332	0.173	0.037	0.048	0.053	92.58	98.40	97.96	97.73
Free-draining	1	1.365	0.706	0.654	0.622	0.621	75.98	77.74	78.84	78.87
	2	1.271	0.331	0.167	0.196	0.218	87.34	93.60	92.51	91.67
	3	1.310	0.284	0.185	0.169	0.185	90.69	93.94	94.47	93.93
	4	0.912	0.204	0.032	0.031	0.071	92.06	98.74	98.77	97.22
	5	0.738	0.153	0.001	0.012	0.029	94.03	99.96	99.52	98.85
	6	1.098	0.194	0.001	0.001	0.019	92.13	99.96	99.96	99.24
	7	1.046	0.082	0.001	0.001	0.001	97.27	99.96	99.96	99.96
	8	1.132	0.105	0.006	0.001	0.016	95.84	99.76	99.96	99.36

Table A.7 Measured concentrations and removal of Pb in large column experiments. Concentrations below the detection limit were taken as half the limit (0.010 mg/L).

Pb										
	Weeks	influent (mg/L)	effluent (mg/L)				Removal (%)			
			Control	Phalaris	Carex	Juncus	Control	Phalaris	Carex	Juncus
Method development	1	5.730	0.010	0.010	0.010	0.010	99.82	99.82	99.82	99.82
	2	6.655	0.010	0.010	0.010	0.010	99.84	99.84	99.84	99.84
	3	5.371	0.010	0.010	0.010	0.010	99.81	99.81	99.81	99.81
	4	6.033	0.010	0.010	0.010	0.010	99.83	99.83	99.83	99.83
	5	5.381	0.010	0.010	0.010	0.010	99.81	99.81	99.81	99.81
	6	4.743	0.010	0.010	0.010	0.010	99.78	99.78	99.78	99.78
	7	3.456	0.010	0.010	0.010	0.010	99.70	99.70	99.70	99.70
	8	4.148	0.010	0.010	0.010	0.010	99.75	99.75	99.75	99.75
	9	4.501	0.010	0.010	0.010	0.010	99.77	99.77	99.77	99.77
	10	4.952	0.010	0.010	0.010	0.010	99.79	99.79	99.79	99.79
	11	5.849	0.010	0.010	0.010	0.010	99.82	99.82	99.82	99.82
Closed-valve	1	0.010	0.010	0.010	0.010	0.010	0.00	0.00	0.00	0.00
	2	0.010	0.010	0.010	0.010	0.010	0.00	0.00	0.00	0.00
	3	0.814	0.010	0.010	0.010	0.010	98.72	98.72	98.72	98.72
	4	0.606	0.010	0.010	0.010	0.010	98.29	98.29	98.29	98.29
	5	0.960	0.010	0.010	0.010	0.010	98.92	98.92	98.92	98.92
	6	1.104	0.010	0.010	0.010	0.010	99.06	99.06	99.06	99.06
	9	1.086	0.010	0.010	0.010	0.010	99.04	99.04	99.04	99.04
	10	0.516	0.010	0.010	0.010	0.010	97.99	97.99	97.99	97.99
	11	0.571	0.010	0.010	0.010	0.010	98.18	98.18	98.18	98.18
	12	0.890	0.010	0.010	0.010	0.010	98.83	98.83	98.83	98.83
	13	1.051	0.010	0.010	0.010	0.010	99.01	99.01	99.01	99.01
	15	1.120	0.010	0.010	0.010	0.010	99.07	99.07	99.07	99.07
	16	1.138	0.010	0.010	0.010	0.010	99.09	99.09	99.09	99.09
	17	1.139	0.010	0.010	0.010	0.010	99.09	99.09	99.09	99.09
Free-draining	1	1.365	0.061	0.043	0.094	0.102	95.54	96.88	93.13	92.54
	2	1.271	0.137	0.159	0.135	0.119	89.19	87.51	89.36	90.65
	3	1.310	0.077	0.082	0.094	0.086	94.13	93.72	92.81	93.41
	4	0.912	0.010	0.010	0.010	0.010	98.86	98.86	98.86	98.86
	5	0.738	0.010	0.010	0.010	0.010	98.59	98.59	98.59	98.59
	6	1.098	0.010	0.010	0.010	0.010	99.05	99.05	99.05	99.05
	7	1.046	0.010	0.010	0.010	0.010	99.01	99.01	99.01	99.01
	8	1.132	0.010	0.010	0.010	0.010	99.08	99.08	99.08	99.08

Table A.8 Measured concentrations and removal of Cu in large column experiments. Concentrations below the detection limit were taken as half the limit (0.003 mg/L).

Cu										
	Weeks	influent (mg/L)	effluent (mg/L)				Removal (%)			
			Control	Phalaris	Carex	Juncus	Control	Phalaris	Carex	Juncus
Method development	1	2.729	0.003	0.003	0.003	0.003	99.90	99.90	99.90	99.90
	2	3.210	0.003	0.003	0.003	0.003	99.92	99.92	99.92	99.92
	3	2.772	0.003	0.003	0.003	0.003	99.91	99.91	99.91	99.91
	4	2.974	0.003	0.003	0.003	0.003	99.91	99.91	99.91	99.91
	5	3.034	0.003	0.003	0.003	0.003	99.91	99.91	99.91	99.91
	6	2.928	0.003	0.003	0.003	0.003	99.91	99.91	99.91	99.91
	7	2.786	0.003	0.003	0.003	0.003	99.91	99.91	99.91	99.91
	8	2.318	0.003	0.003	0.003	0.003	99.89	99.89	99.89	99.89
	9	2.371	0.003	0.003	0.003	0.003	99.89	99.89	99.89	99.89
	10	2.854	0.003	0.003	0.003	0.003	99.91	99.91	99.91	99.91
	11	2.663	0.003	0.003	0.003	0.003	99.90	99.90	99.90	99.90
Closed-valve	1	0.203	0.003	0.003	0.003	0.003	98.52	98.52	98.52	98.52
	2	0.203	0.003	0.003	0.003	0.003	98.52	98.52	98.52	98.52
	3	0.472	0.003	0.003	0.003	0.003	99.45	99.45	99.45	99.45
	4	0.510	0.003	0.003	0.003	0.003	99.49	99.49	99.49	99.49
	5	0.632	0.003	0.003	0.003	0.003	99.59	99.59	99.59	99.59
	6	0.568	0.003	0.003	0.003	0.003	99.54	99.54	99.54	99.54
	9	0.561	0.003	0.003	0.003	0.003	99.54	99.54	99.54	99.54
	10	0.490	0.003	0.003	0.003	0.003	99.47	99.47	99.47	99.47
	11	0.547	0.003	0.003	0.003	0.003	99.52	99.52	99.52	99.52
	12	0.512	0.003	0.003	0.003	0.003	99.49	99.49	99.49	99.49
	13	0.543	0.003	0.003	0.003	0.003	99.52	99.52	99.52	99.52
	15	0.539	0.003	0.003	0.003	0.003	99.52	99.52	99.52	99.52
	16	0.542	0.003	0.003	0.003	0.003	99.52	99.52	99.52	99.52
	17	0.528	0.003	0.003	0.003	0.003	99.51	99.51	99.51	99.51
Free-draining	1	0.500	0.003	0.003	0.003	0.003	99.48	99.48	99.48	99.48
	2	0.535	0.003	0.003	0.003	0.003	99.51	99.51	99.51	99.51
	3	0.603	0.003	0.003	0.003	0.003	99.57	99.57	99.57	99.57
	4	0.470	0.012	0.003	0.003	0.003	99.45	99.45	99.45	97.51
	5	0.470	0.003	0.003	0.003	0.003	99.45	99.45	99.45	99.45
	6	0.313	0.003	0.003	0.003	0.003	99.17	99.17	99.17	99.17
	7	0.542	0.003	0.003	0.003	0.003	99.52	99.52	99.52	99.52
	8	0.529	0.003	0.003	0.003	0.003	99.51	99.51	99.51	99.51

Table A.9 Measured concentrations and removal of TP in large column experiments.

TP										
	Weeks	influent (mg/L)	effluent (mg/L)				Removal (%)			
			Control	Phalaris	Carex	Juncus	Control	Phalaris	Carex	Juncus
Closed-valve	13	1.312	1.281	1.326	0.797	0.605	2.34	-1.07	39.25	53.86
	15	1.126	1.269	1.017	0.771	0.618	-12.69	9.65	31.48	45.07
	16	1.197	1.221	1.167	0.841	0.691	-2.03	2.49	29.73	42.27
	17	1.266	0.976	1.009	0.604	0.692	22.87	20.24	52.26	45.34
	18	1.124	0.611	0.964	0.640	0.696	45.62	14.29	43.09	38.05
	19	0.899	0.559	0.838	0.573	0.660	37.82	6.74	36.26	26.54
	20	0.888	0.550	0.807	0.564	0.616	38.05	9.03	36.51	30.62
	21	0.848	0.530	0.745	0.531	0.605	37.49	12.13	37.41	28.62
Free-draining	1	1.365	0.729	0.735	0.596	0.582	31.19	30.66	43.77	45.09
	2	1.271	0.618	0.859	0.538	0.541	27.29	-1.06	36.71	36.35
	3	1.310	0.526	0.811	0.492	0.476	33.38	-2.66	37.72	39.75
	4	0.912	0.621	0.976	0.555	0.583	19.97	-25.77	28.48	24.87
	5	0.738	0.540	0.826	0.501	0.522	20.54	-21.47	26.32	23.24
	6	1.098	0.567	0.875	0.524	0.592	16.62	-28.68	22.94	12.94
	7	1.046	0.589	0.892	0.562	0.680	24.49	-14.36	27.95	12.82
	8	1.132	0.528	0.829	0.556	0.628	31.43	-7.66	27.79	18.44

Appendix C – Surveyed biofilters

Figure A.4 Station Terrace biofilters.

(a)

(b)

(c)

(d)

(e)

(f)

Figure A.5 Grangetown biofilters. (a) Ferndale St, (b, c) Taff Embankment, (d) Clydach St, (e) Ystrad St, (f) Bargoed St.

(g)

(h)

Figure A.5 Continued. (g) Cymmer St, (h) Coedcae St.